CECE 2018

15th International Interdisciplinary Meeting on Bioanalysis

Conference Proceedings
-
Full Papers

October 15 - 17, 2018
Hotel Continental
Brno, Czech Republic
www.ce-ce.org

Foreword

Welcome to CECE 2018, the 15th International Interdisciplinary Meeting on Bioanalysis. After the CECE 2017 in Veszprém, Hungary, we are back in Brno and our goal remains the same: "bring together scientists from different disciplines who may not meet at other meetings". CECE Junior will follow the two days of invited speaker's lectures and the poster sessions will be open during all three days. The organizers want to thank all invited speakers, sponsors and participants for their continuing support. Please, check our web at www.ce-ce.org for more information about the history, programs, photos and videos from the previous years.

Brno, October 8, 2018

The Medal of Jaroslav Janák

The Medal of Jaroslav Janák for contributions to the development of analytical sciences was established by the Institute of Analytical Chemistry. Named after the inventor of the gas chromatograph (patented in 1952), founder of the institute (1956) and its long-term director, the medal is awarded to scientists who have significantly contributed to the development of separation sciences.

In 2018 the Medal of Jaroslav Janák goes to **Prof. Ludmila Křivánková**. Ludmila Křivánková studied biochemistry at the Masaryk University in Brno and after graduation worked shortly at the Department of Biochemistry. In 1983 she joined the Department of Electromigration Techniques of the Institute of Analytical Chemistry of the Czechoslovak Academy of Sciences. She soon established herself as an internationally recognized expert in capillary isotachophoresis and zone electrophoresis techniques for analyses of trace components in complex biochemical and industrial samples. She is a frequent lecturer at international conferences, author and co-author of numerous textbooks and monographies and published many original scientific publications in international impacted journals. As a successful coordinator of scientific grant projects she was selected into several national and international scientific boards.

She has also been serving as an editor of the journal Electrophoresis (Wiley) for well over a decade. In 2005 she was elected a director of the Institute of Analytical Chemistry. Under her leadership the institute underwent a successful transition into the public research institute (v. v. i.). She was directing the institute for two additional terms until 2017. During her tenure she was instrumental in creation of excellent research conditions in all research directions of the institute. The 2018 Jaroslav Janak Medal goes to Ludmila for her lifetime achievements in separation sciences and promoting of the basic research.

Franta Foret

Program of the CECE 2018

Hotel Continental, Brno, Czech Republic, October 15 – 17, 2018

8:00 – 15:00 **Registration (Monday, Tuesday)**

Monday, October 15

9:00 – 9:20 **Opening remarks and award of the Medal of Jaroslav Janák to <u>Ludmila Křivánková</u>**

9:20 – 9:55 **<u>Jiří Homola</u>**
Institute of Photonics and Electronics of the Czech Academy of Sciences, Prague, Czech Republic
PLASMONIC BIOSENSORS FOR MEDICAL DIAGNOSTICS AND FOOD SAFETY

9:55 – 10:30 **<u>Hans H. Gorris</u>**
University of Regensburg, Institute of Analytical Chemistry, Chemo- and Biosensors, Regensburg, Germany
SINGLE MOLECULE IMMUNOASSAYS BASED ON PHOTON-UPCONVERSION NANOPARTICLES (UCNPs)

10:30 – 11:00 **Coffee break**

11:00 – 11:35 **<u>Yann Astier</u>**
Roche Sequencing Solutions, Pleasanton, CA, USA
EVOLUTION OF THE DIAGNOSTIC-PHARMA RELATIONSHIP TOWARDS HEALTH COORDINATES AND PERSONALIZED TREATMENT

11:35 – 12:10 **<u>Hadar Ben-Yoav</u>**
Ben-Gurion University of the Negev, Israel
INTELLIGENT MULTI-ELECTRODE ARRAYS FOR IN SITU BIOANALYSIS OF BIOFLUIDS

12:10 – 12:45 **<u>Milan Hutta</u>**
Comenius University in Bratislava, Bratislava, Slovakia
HUMIC SUBSTANCES FROM POINT-OF-VIEW OF ANALYTICAL CHEMISTS

12:45 – 14:20	**Lunch break – poster session**
14:20 – 14:55	**Jan Preisler** *Masaryk University, Brno, Czech Republic* MALDI MASS SPECTROMETRY IMAGING AT ACQUISITION RATES ABOVE 100 PIXELS/S
14:55 – 15:30	**Lumir Krejci** *Department of Biology, Faculty of Medicine, Masaryk University, Brno, Czech Republic, National Centre for Biomolecular Research, Faculty of Science, Masaryk University, Brno, Czech Republic, International Clinical Research Center, Center for Biomolecular and Cellular Engineering, St. Anne's University Hospital Brno, Brno, Czech Republic* DNA REPAIR AS A TARGET FOR THERAPY
15:30 – 16:05	**Milos V. Novotny** *Indiana University, Department of Chemistry, Bloomington, IN, USA* CAN HUMAN GLYCOME BE COMPREHENSIVELY COVERED?
16:30 – 18:00	**Invited speaker's visit to the Mendel Museum (http://mendelmuseum.muni.cz/en/)**
19:00	**Conference dinner with the traditional Moravian music**

Tuesday, October 16

09:30 – 10:05	**Andras Guttman** *University of Pannonia, Veszprém, Hungary* AUTOMATED SEQUENCING OF N-LINKED CARBO-HYDRATES
10:05 – 10:40	**Zbyněk Prokop** *Masaryk University, Brno, Czech Republic* DROPLET-BASED ENZYMOLOGY: HIGH-THROUGHPUT ANALYSIS OF NOVEL BIOCATALYSTS
10:40 – 11:10	**Coffee break**

11:10 – 11:45	**Doo Soo Chung** *Seoul National University, Seoul, Korea* LIQUID EXTRACTION SURFACE ANALYSIS COUPLED WITH CAPILLARY ELECTROPHORESIS
11:45 – 12:20	**Iuliana M. Lazar** *Virginia Tech, Biological Sciences, Health Sciences and Carilion School of Medicine, Blacksburg, VA, USA* SPECTROMETRY AND PROTEOMICS AT THE CROSS ROADS OF TECHNOLOGY AND BIOLOGY
12:20 – 14:10	**Lunch break – poster session**
14:10 – 14:45	**Christian G. Huber** *University of Salzburg, Department of Biosciences and Christian Doppler Laboratory for Biosimilar Characterization, Department of Molecular Biology, Salzburg, Austria* MOLECULAR CHARACTERIZATION OF BIO-THERAPEUTIC PROTEINS: CONCEPTS AND CHALLENGES FOR SEPARATION SCIENCE, MASS SPECTROMETRY, AND COMPUTATIONAL BIOLOGY
14:45 – 15:20	**Jiří Fajkus** *Photon Systems Instruments, Drásov, Czech Republic* STATE OF THE ART TECHNOLOGIES FOR PLANT PHENOTYPING
15:20 – 15:55	**Tomasz Bączek** *Medical University of Gdańsk, Department of Pharmaceutical Chemistry, Gdańsk, Poland* COMPARATIVE STUDY ON AMINO ACIDS MEASURED IN PLASMA, CEREBROSPINAL FLUID AND EXHALED BREATH CONDENSATES
15:55 – 16:15	**Csaba Horvath Memorial Lectureship Award** presented by **Ferenc Darvas** *President of the Awards Committee American Chemical Society Hungary Chapter* to **František Foret** *Institute of Analytical Chemistry of the Czech Academy of Sciences, Brno, Czech Republic*

16:15 – 16:30   **Invitation to CECE 2019, Gdańsk, Poland**

16:40   **City walk with invited speakers**

Wednesday, October 17

9:00 – 9:15   **CECE Junior opening**

9:15 – 9:45   **Vladislav Dolnik**
Alcor BioSeparations LLC, Palo Alto, CA, USA
BORATE BUFFERS FOR CZE IN BARE CAPILLARIES

9:45 – 10:00   **Miloš Dvořák**
Institute of Analytical Chemistry of the Czech Academy of Sciences, Brno, Czech Republic
HOLLOW FIBRE-LIQUID PHASE MICROEXTRACTION OF BASIC DRUGS FROM DRIED BLOOD SPOTS

10:00 – 10:15   **Antonín Bednařík**
Central European Institute of Technology (CEITEC), Masaryk University, Brno, Czech Republic
MALDI-MS IMAGING OF C=C POSITIONAL ISOMERS OF LIPIDS ENABLED BY PATERNÒ-BÜCHI PHOTO-DERIVATIZATION

10:15 – 10:30   **Michal Vasina**
Loschmidt Laboratories, Department of Experimental Biology and RECETOX, Faculty of Science, Masaryk University, Brno, Czech Republic
HIGH-THROUGHPUT CHARACTERIZATION OF SUBSTRATE SPECIFICITY OF HALOALKANE DEHALOGENASES BY USING CAPILLARY MICROFLUIDICS

10:30 – 10:45   **Tomas Vaclavek**
Institute of Analytical Chemistry of the Czech Academy of Sciences, Brno, Czech Republic
MICROFLUIDIC DEVICE FOR CELL COUNTING AND ELECTRICAL LYSIS

10:45 – 11:15   **Coffee break**

11:15 – 11:30   **Filip Smrčka**
Department of Chemistry, Faculty of Science, Masaryk University, Brno, Czech Republic
THE UREASE BIOSENSOR BASED ON Eu(III) TERNARY COMPLEX OF DO3A LIGAND

11:30 – 11:45   **Antonín Hlaváček**
Institute of Analytical Chemistry of the Czech Academy of Sciences, Brno, Czech Republic
MEASURING PHOTON-UPCONVERSION LUMI-NESCENCE FROM DROPLETS IN MICROFLUIDIC CHIPS

11:45 – 12:00   **Karolína Kolářová**
Institute of Biophysics of the Czech Academy of Sciences, Brno, Czech Republic
CHARACTERIZATION OF ALLIUM TELOMERE REPEAT BINDING PROTEINS

12:00 – 12:15   **Martin Lyčka**
Mendel Centre for Plant Genomics and Proteomics, Central European Institute of Technology, Masaryk University, Brno, Czech Republic
INTENSITYANALYSER: WEB TOOL FOR ASSESSMENT OF TELOMERE LENGTHS FROM TERMINAL RESTRICTION FRAGMENT ANALYSIS

12:15 – 12:45   **Ctirad Hofr**
LifeB - Laboratory of interaction and function of essential Biomolecules Chromatin Molecular Complexes, CEITEC and NCBR, Faculty of Science, Masaryk University, Brno, Czech Republic
HOW TO TRAIN OUR CELLS TO BECOME YOUNGER – QUANTITATIVE BIOPHYSICS OF HUMAN TELOMERASE AND ITS GUARD SHELTERIN

12:45 – 12:50   **Closing remarks**

12:50   **Lunch break – poster removal**

List of poster presentations

P1   INNOVATION OF DIAGNOSTICS ALGORITHM FOR ACUTE KIDNEY INJURY USING A NEW BIOMARKERS – ESTIMATED REFERENCE RANGE FOR HEALTHY CHILDREN

Katerina Andelova, Zdenek Svagera, Vitezslav Jirik, Michal Hladik

P2   BIOANALYTICAL EVALUATION OF A NOVEL DEXRAZOXANE ANALOGUE JAS-2 AND ITS PRODRUG - IN VITRO AND PILOT IN VIVO STUDIES

Hana Bavlovič Piskáčková, Petra Reimerová, Anna Jirkovská, Veronika Skalická, Petra Brázdová, Martin Štěrba, Petra Kovaříková-Štěrbová

P3   CHARACTERIZATION OF CHOLESTERYL ESTERS USING NANOPARTICLES-ASSISTED DESORPTION MASS SPECTROMETRY

Jakub Bělehrad, Vendula Roblová, Jan Preisler

P4   THE EFFECT OF PREANALYTICAL CONDITIONS ON HUMAN N-GLYCOME

Tereza Dědová, Karina Biskup, Kai Kappert, Dagmar Flach, Rudolf Tauber, Véronique Blanchard

P5   DETERMINATION OF ANIONS IN COFFEE SAMPLES USING CAPILLARY ELECTROPHORESIS

Róbert Bodor, Simona Straňáková, Branislav Žabenský, Marián Masár

P6   GLYCOSYLATION AS A CRITICAL QUALITY ATTRIBUTE (CQA) OF BIOTHERAPEUTICS

Beáta Borza, Márton Szigeti, Ákos Szekrényes, László Hajba, András Guttman

P7   IMPACT OF POST-HARVEST PROCESSING, GEOGRAPHICAL LOCALITY AND PRODUCTION YEAR ON QUALITY OF SELECTED MEDICINAL PLANTS

Lenka Burdejova, Martin Polovka, Jaromir Porizka

P8   SYNTHETIC APPROACHES FOR NEW LABELING TAGS FACILITATING GLYCAN ANALYSIS

Richard Čmelík, Jana Křenková, František Foret

P9   EFFECT OF CAPILLARY LENGTH IN CE-LIF ANALYSIS OF N-GLYCANS: A WALL INTERACTION STUDY

Apolka Domokos, Márton Szigeti, Máté Szarka, András Guttman

P10   A VALIDATION OF NON-INVASIVE METHOD FOR DIAGNOSIS OF CYSTIC FIBROSIS BASED ON ION RATIOS DETERMINED BY CE-C4D

Pavol Ďurč, Júlia Lačná, Věra Dosedělová, František Foret, Lukáš Homola, Eva Pokojová, Miriam Malá, Jana Skřičková, Milan Dastych, Hana Vinohradská, Pavel Dřevínek, Veronika Skalická, Petr Kubáň

P11   EVALUATION OF THE 33 SYNTHESIZED NITROPHENOL-BASED MARKERS OF ISOELECTRIC POINT

Filip Duša, Dana Moravcová, Karel Šlais

P12   IN SITU OPTICAL MONITORING OF SINGLE PARTICLE INTERACTION USING SPR-TIRE

Jan Dvořák, Dušan Hemzal, Tomasz Kabzinski, Karel Kubíček, Josef Humlíček

P13   N-GLYCOMIC ANALYSIS OF SEVERAL ACUTE PHASE GLYCOPROTEINS OF INFLAMMATORY AND MALIGNANT LUNG DISEASE IMPORTANCE

Anna Farkas, Brigitta Mészáros, Zsuzsanna Kovács, Renáta Kun, Eszter Csánky, Miklós Szabó, András Guttman

P14   HIGH EFFICIENCY EVAPORATIVE FLUOROPHORE LABELING OF GLYCANS

Balázs Reider, Márton Szigeti, Csenge Filep, András Guttman

P15   VITAMIN D STATUS AND ITS ASSOCIATION WITH CARDIOMETABOLIC RISK FACTORS IN HEALTHY MEDICATION - FREE SLOVAK POPULATION

Zuzana Gogalova, Maria Konecna, Janka Poracova, Janka Porubska, Marta Mydlarova Blascakova

P16   COMBINATION OF RP-HPLC AND SEC USING MICROBORE SIZE COLUMN FOR CHARACTERIZATION OF HUMIC SUBSTANCES ISOLATED FROM SOIL AND PEAT

Róbert Góra, Milan Hutta, Erik Beňo

P17   PNGASE F PERFORMANCE STUDY FOR IMPROVED GLYCOSYLATION ANALYSIS FROM HUMAN SERUM SAMPLES

Eszter Jóna, Márton Szigeti, András Guttman

P18   HIGH THROUGHPUT GLYCAN ANALYSIS: THE C100HT MULTICAPILLARY ELECTROPHORESIS SYSTEM

László Hajba, Balázs Reider, Beáta Borza, András Guttman

P19   HUMAN TRF1 EXCHANGES TRF2 BOUND TO TIN2 BUT TOLERATES TRF2 IN TPP1 PRESENCE

Tomáš Janovič, Martin Stojaspal, Pavel Veverka, Ctirad Hofr

P20   THE METHOD TO DECREASE IBUPROFEN CONCENTRATION LIMIT IN ELECTROPHORESIS

Lenka Janštová, Jan Pospíchal

P21   DESIGN OF AN ADJUSTABLE CE-MS INTERFACE: ANALYSIS OF APTS-LABELED N-GLYCANS OF BIOPHARMACEUTICAL INTEREST

Gábor Járvás, Márton Szigeti, András Guttman

P22   HEADSPACE IN-TUBE MICROEXTRACTION OF CHLOROPHENOLS FOR CAPILLARY ELECTROPHORESIS-MASS SPECTROMETRY

Sunkyung Jeong, Doo Soo Chung

P23 ADSORPTIVE REMOVAL OF COPPER AND CADMIUM IONS USING FLY ASH RESULTING FROM CFBC TECHNOLOGY

Tomasz Kalak, Ryszard Cierpiszewski

P24 TRIMETHYLSILYL ACETATE-BASED COATINGS FOR BIOAPPLICATIONS

Štěpánka Kelarová, Vojtěch Homola, Michal Kuchařík, Vilma Buršíková

P25 ELECTROPHORETIC QUANTIFICATION OF RAPAMYCIN IN SERUM SAMPLES WITH USING OFF-LINE AND ON-LINE PRECONCENTRATION TECHNIQUES

Piotr Kowalski, Ilona Olędzka, Alina Plenis, Natalia Miękus, Tomasz Bączek

P26 SYNOVIAL FLUID, FORGOTTEN BIOLOGICAL MATERIAL?

Iveta Kozarová, Pavlína Kušnierová, Pavel Walder

P27 UTILIZATION OF WASTE MATERIAL FROM THE WINE PRODUCTION FOR REMOVING COPPER IONS FROM WASTEWATER

Jakub Krikala, Pavel Diviš

P28 DROPLET-BASED MICROFLUIDIC CHIP WITH PASSIVE MIXER FOR ANALYSIS WITH PHOTON-UPCONVERSION NANOPARTICLES

Jana Křivánková, Jan Přikryl, Antonín Hlaváček

P29 ACETONITRILE-ASSISTED ENZYMATIC DIGESTION USED FOR ANALYSIS OF PROTEINS OF CANCER ORIGIN

Markéta Laštovičková, Pavel Bobál, Dana Strouhalová, Janette Bobálová

P30 A MICROFLUIDIC DEVICE FOR MONITORING CELL MIGRATION

Vojtěch Ledvina, Karel Klepárník, Soňa Legartová, Eva Bártová

P31 PLASMA PROTEIN BOUND HYDROPHOBIC METABOLITE RELEASE WITH PROTEINASE K AS A NEW APPROACH TO ENRICH METABOLOME COVERAGE IN UNTARGETED METABOLOMICS

Renata Wawrzyniak, Anna Kosnowska, Szymon Macioszek, Rafał Bartoszewski, Michał J. Markuszewski

P32 DEVELOPMENT OF SEPARATION GEL FOR SDS-CGE-MS

Brigitta Mészáros, Márton Szigeti, András Guttman

P33 EFFICIENT SAMPLE MIXING IN CAPILLARY ELECTROPHORESIS

Lenka Michalcová, Hana Nevídalová, Zdeněk Glatz

P34 NOVEL IONIC LIQUID-BASED EXTRACTION APPROACH FOR THE ISOLATION OF SELECTED NEUROTRANSMITTERS (NTS) FROM RAT BRAIN SAMPLES

Natalia Miękus, Ilona Olędzka, Darya Harshkova, Ivan Liakh, Alina Plenis, Piotr Kowalski, Michał Jaskulski, Tomasz Bączek

P35 CHROMATOGRAPHIC SEPARATION OF AFLATOXIN ANALOGUES

Dana Moravcová, Josef Planeta, Kamila Lunerová, Filip Duša, Jozef Šesták, Oldřich Kubíček, Marie Horká

P36 AFFINITY MICROFLUIDIC CHIP BASED ON PACKED MICROBEADS

Jakub Novotny, Veronika Ostatna, Frantisek Foret

P37 EVALUATION OF EXTRACTION PROCEDURES FOR ISOLATION OF SELECTED BIOGENIC AMINES FROM BIOLOGICAL SAMPLES BEFORE ANALYSIS BY CAPILLARY ELECTROPHORESIS

Ilona Olędzka, Natalia Miękus-Purwin, Piotr Kowalski, Alina Plenis, Marta Rudnicka, Natalia Kossakowska, Tomasz Bączek

P38 OPTIMIZING VOLTAMMETRIC ANALYSIS OF SUDAN I AT PYROLYTIC GRAPHITE ELECTRODES IN AQUEOUS MEDIA: TOWARDS DEVELOPMENT OF ELECTROCHEMICAL ASSAY FOR ACTIVITY OF HYDROXYLASE ENZYMES

Anna Ondráčková, Karolina Schwarzová-Pecková, Miroslav Fojta

P39 HEXAHISTIDINE-BASED TAG FOR CAPILLARY ELECTROPHORESIS-MASS SPECTROMETRY ANALYSIS OF OLIGOSACCHARIDES AND N-LINKED GLYCANS

Jan Partyka, Jana Krenkova, Richard Cmelik, Frantisek Foret

P40 SPECIATION ANALYSIS OF As AND Hg IN BIOLOGICAL MATERIAL

Inga Petry-Podgórska, Tomáš Matoušek, Michaela Migašová, Veronika Zemanová, Milan Pavlík, Jan Kratzer, Daniela Pavlíková

P41 DEVELOPMENT AND VALIDATION OF LC METHOD FOR THE DETERMINATION OF EPIRUBICIN IN HUMAN PLASMA AND URINE. APPLICATION TO A DRUG MONITORING

Alina Plenis, Natalia Treder, Olga Maliszewska, Piotr Kowalski, Ilona Olędzka, Natalia Miękus, Ewa Bień, Małgorzata Anna Krawczyk, Elżbieta Adamkiewicz-Drożyńska, Tomasz Bączek

P42 ARDUINO-BASED PRESSURE-DRIVEN FLOW CONTROLLER FOR DROPLET MICROFLUIDICS

Jan Prikryl, Jana Krivankova, Antonin Hlavacek

P43 CAPILLARY ELECTROPHORETIC METHOD WITH FLUORESCENCE DETECTION AS A PROMISING TOOL FOR SCREENING OF BETA-SECRETASE INHIBITORS

Roman Řemínek, Jan Schejbal, Zdeněk Glatz

P44 RAPID FABRICATION OF MICROEXTRACTION DEVICES FOR DIRECT DETERMINATION OF BASIC DRUGS IN DRIED BLOOD SPOTS

Lenka Ryšavá, Jan Přikryl, Miloš Dvořák, Zdeňka Malá, Pavel Kubáň

P45 N-GLYCOSYLATION MODIFICATION ANALYSIS OF SEVERAL IMPORTANT SERUM GLYCOPROTEINS IN ALZHEIMER'S DISEASE

Zsuzsanna Kovács, Balázs Reider, Dániel Sárközy, András Guttman

P46 ENANTIOSEPARATION AND ESTIMATION OF RACEMIZATION BARRIERS OF SELECTED HELQUATS AND THEIR DERIVATIVES

BY CAPILLARY ELECTROPHORESIS USING SULFATED CYCLODEXTRINS AS CHIRAL SELECTORS

Petra Sázelová, Dušan Koval, Lukáš Severa, Paul E. Reyes-Gutiérrez, Michael Jirásek, Filip Teplý, Václav Kašička

P47 MAXIMIZING EFFICIENCY OF FIELD-AMPLIFIED ELECTROKINETIC INJECTION OF WEAK BASES FOR ENANTIOSELECTIVE CAPILLARY ELECTROPHORESIS WITH SULFATED CYCLODEXTRINS

Jozef Šesták, Wolfgang Thormann

P48 DETERMINATION OF BINDING CONSTANTS OF HUMAN INSULIN COMPLEXES WITH SEROTONIN, DOPAMINE, ARGININE, AND PHENOL BY PRESSURE ASSISTED PARTIAL FILLING AFFINITY CAPILLARY ELECTROPHORESIS

Veronika Šolínová, Lenka Žáková, Jiří Jiráček, Václav Kašička

P49 DYNAMICS OF REST-TRF2 INTERACTIONS AND THE FATE OF NEURAL CANCER CELLS

Martin Stojaspal, Tomas Janovic, Pavel Veverka, Ctirad Hofr

P50 A NEW EVALUATION OF COMBINED ANTITUMOR EFFECTS OF NATURAL AND SYNTHETIC NUCLEAR RETINOID RECEPTOR LIGANDS IN HUMAN BREAST CARCINOMA CELLS

Dana Strouhalová, Markéta Laštovičková, Pavel Bobál, Dana Macejová, Barbora Mosná, Julius Brtko, Janette Bobálová

P51 ELECTROMAGNET FOR CAPTURE OF MAGNETIC BEADS FROM LARGE VOLUME INTO MICROFLUIDIC CHAMBER CHIP

Zuzana Svobodova, Rudolf Kupčík, Denisa Smělá, Jakub Roupec, Ondřej Macháček, Lucie Nováková, Zuzana Bilkova

P52 PRECONCENTRATION STRATEGIES FOR APTS LABELED CARBOHYDRATE CE-LIF ANALYSIS

Robert Farsang, Balazs Reider, Mate Szarka, Gabor Jarvas, Andras Guttman

P53 SEPARATION AND DETERMINATION OF ACTIVE PHARMACEUTICAL INGREDIENT AND EXCIPIENTS BY MICROCHIP ELECTROPHORESIS

Peter Troška, Marián Masár

P54 NOVEL ELECTROPHORETIC ACETONITRILE-BASED SAMPLE STACKING FOR SENSITIVE MONITORING OF DIFFERENT KINDS OF PHARMACEUTICALS IN BLOOD PLASMA

Petr Tůma

P55 SURFACE ENHANCED RAMAN SPECTROSCOPY: DETECTION PLATFORMS FOR SAMPLE ANALYSIS WITH AND WITHOUT ELECTROPHORETIC SEPARATION

Anna Tycova, Jan Prikryl, Frantisek Foret, Detlev Belder

P56 PURIFICATION OF HUMAN TELOMERASE TEN DOMAIN AND ITS INTERACTION PARTNER TPP1

Pavel Veverka, Martin Stojaspal, Tomas Janovic, Ctirad Hofr

P57 EPITACHOPHORETIC SEPARATION AND CONCENTRATION OF LARGE VOLUME SAMPLES

Ivona Voráčová, František Foret, Vladimíra Datinská, Jakub Novotný, Pantea Gheibi, Jan Berka, Yann Astier

P58 TEMPERATURE-PROGRAMED MICRO-HPLC ANALYSIS OF FATTY ACID METHYL ESTERS WITH APCI-MS DETECTION

Vladimír Vrkoslav, Barbora Rumlová, Josef Cvačka

P59 GREEN-SYNTHESIZED SILVER NANOPARTICLES AND FOOD PROTECTION

Bozena Hosnedlova, Michaela Docekalova, Branislav Ruttkay-Nedecky, Mojmir Baron, Rene Kizek, Carlos Fernandez, Jiri Sochor

P60 LEAD DETERMINATION IN DRIED BLOOD SPOTS USING DLTV ICP MS

Martin Ďurč, Marek Stiborek, Viktor Kanický, Jan Preisler

P61 DETECTION OF MONOCLONAL FREE LIGHT CHAINS (FLC) BY VARIOUS LABORATORY METHODS

Pavlína Kušnierová, David Zeman, Kamila Revendová, Ondřej Dlouhý

Full Papers - Oral Presentations

BORATE BUFFERS FOR CZE IN BARE CAPILLARIES

Vladislav Dolnik

Alcor BioSeparations LLC, Palo Alto, CA 94303, USA, ladia@dolnik.net

Summary

Borate-containing background electrolytes can suppress, eliminate, and even reverse electroosmotic flow in bare fused silica capillaries. With a fine tuned composition, they allow high-resolution separations in bare fused silica capillaries or glass chips. Boric acid forms complexes with polyol base such as Tris or triethanolamine that interact with silica surfaces and so suppress or even completely eliminate electroosmotic flow. Background electrolytes frequently contain a hydrophilic polymer as a sieving medium to provide size separation of biopolymers. We demonstrate the use of various borate-containing background electrolytes for CZE separations of both proteins and DNA fragments in bare fused silica capillaries.

Introduction

Separation by capillary electrophoresis in bare fused silica capillaries is frequently deteriorated by electroosmotic flow and adsorption of analytes on the capillary wall. A significant number of coatings, both static and dynamic ones, were introduced into capillary electrophoresis [1-7]. The use of the wall coatings was also a subject to several reviews [8-9]. EOF per se can help to perform CE, e.g., by mobilizing low-mobility analytes allowing them to reach the detection cell in a reasonable time [10]. Dynamic coatings frequently suffer from only incomplete suppression of EOF, whereas the use of static coatings may be limited by their relatively short lifetime.

Another option was revealed when high-concentration borate buffers were used as BGE.

Wu and Regnier were the first to use a high-concentration Tris borate buffer for SDS CSE. They believed the increased viscosity of their LPA-containing sieving matrix was the key to suppression of EOF [11]. Later other recipes for SDS CSE were published [12-15].

The ability of boric acid to form complexes with carbohydrates has been known for long time [16]. Formation of mono-chelates, bis-chelates and cage structures was also described between boric acid and triols, specifically Tris, tris(hydroxymethyl)ethane, tris(hydroxymethyl)propane, and triethanolamine [17-21]. The complex anion was modeled as a cage, in which all three oxygen atoms of 1,1,1-tris(hydroxymethyl)ethane are attached to the tetrahedrally-coordinated boron atom [22].

Experimental

DNA markers 50 bp – 10,000 bp HiLo™ were purchased from Minnesota Molecular, (Minneapolis, MN., USA). pBR322 MspI restriction fragments were obtained from New England BioLabs (Ipswich, MA., USA). All other chemicals were purchased from Sigma-Aldrich (Saint Louis, MO., USA).

Bare fused silica capillaries with 50 µm and 75 µm id and 360 µm od were purchased from Polymicro Technologies (Phoenix, AZ., USA).

The CE experiments with UV detection were performed on a 3D CE capillary electrophoresis instrument (Agilent, Waldbronn, Germany) with UV detection at 214 nm. Bare fused silica capillaries having the total capillary length of 335 mm and effective length of 250 mm were used to perform separations.

The CE experiments in capillaries with LIF detection were performed in a prototype instrument for capillary electrophoresis with LIF detection at 488 nm /530 nm as previously described [23].

Electroosmotic mobility was measured by Williams- Vigh method [24].

Results and Discussion

There are several basic polyols that may be useful component of BGE in bare capillaries. We used TEA borate as BGE in CZE of DNA fragments. It turned out that in the presence of HEC as a sieving matrix, the BGE concentration could be lowered without losing resolution. The presence of HEC itself in BGE reduces EOF due to its viscosity. HEC is also polyol and binds borate and that allowed reduction of the BGE concentration to 100 mM TEA and 400 mM borate. Although the mixture of 100 mM TEA, 400 mM boric acid itself does not completely eliminate EOF, in combination with HEC as a sieving matrix, EOF of bare capillaries was sufficiently suppressed to achieve a baseline separation of all 16 DNA fragments (Fig. 1).
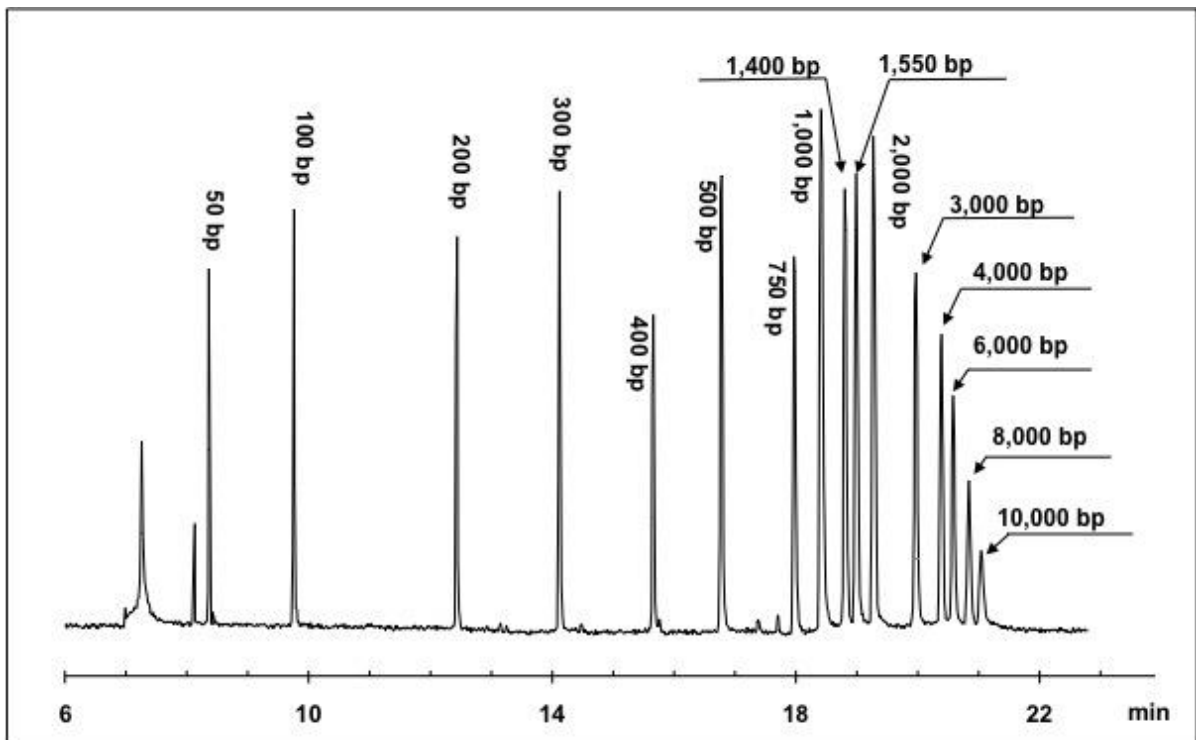
Figure 1. Separation of HiLo™ DNA in TEA borate buffer. Separation medium:12 g/L HEC, 0.8 M DMSO, 100 mM TEA, 400 mM boric acid, 1x SYBR Green II. Bare capillary, total length= 400 mm, effective length= 200 mm, ID= 75 µm, OD= 360 µm. Voltage: -8 kV. LIF detection: 488 nm excitation, 530 nm emission. Electrokinetic injection: 5 s at -8 kV.

We demonstrated separation of DNA with pBR322 MspI restriction fragments as a model DNA mixture in bare fused silica capillaries. background electrolyte containing 100 mM TEA, 400 mM boric acid. All the DNA restriction fragments were fully separated (Fig. 2). Within 10 consecutive runs, the reproducibility of migration times of all restriction fragments ranged 1.29 – 1.54%.
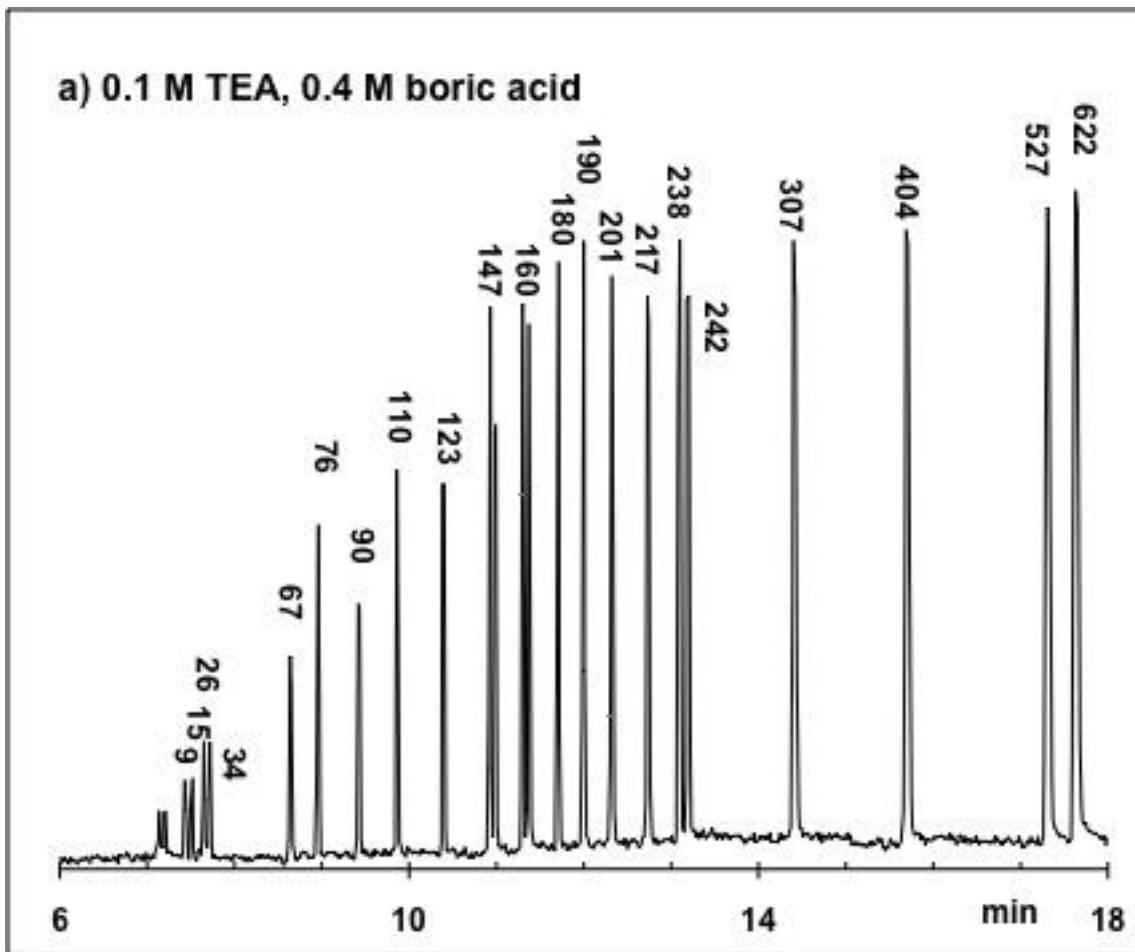
Figure 2. Separation of pBR322 MspI restriction fragments. Separation medium: 12 g/L HEC, 0.8 M DMSO, 1x SYBR Green II, 0.10 mM TEA, 0.4 mM boric acid. Bare capillary, total length= 400 mm, effective length= 200 mm, id= 75 µm, od= 360 µm. Voltage: -8 kV. LIF detection: 488 nm excitation, 530 nm emission. Electrokinetic injection: 1 s at -8 kV. Sample: pBR322 MspI restriction fragments in 10 mM Tris-HCl, pH 8.0, diluted 10x with 0.1 M Tris, HEPES.

Ovalbumin isoforms were separated into 5-7 major peaks by CZE in 200 mM BTP, 400 mM borate (Fig. 3). The repeatability of migration times in 20 runs ranged from 0.3% to 0.43%.
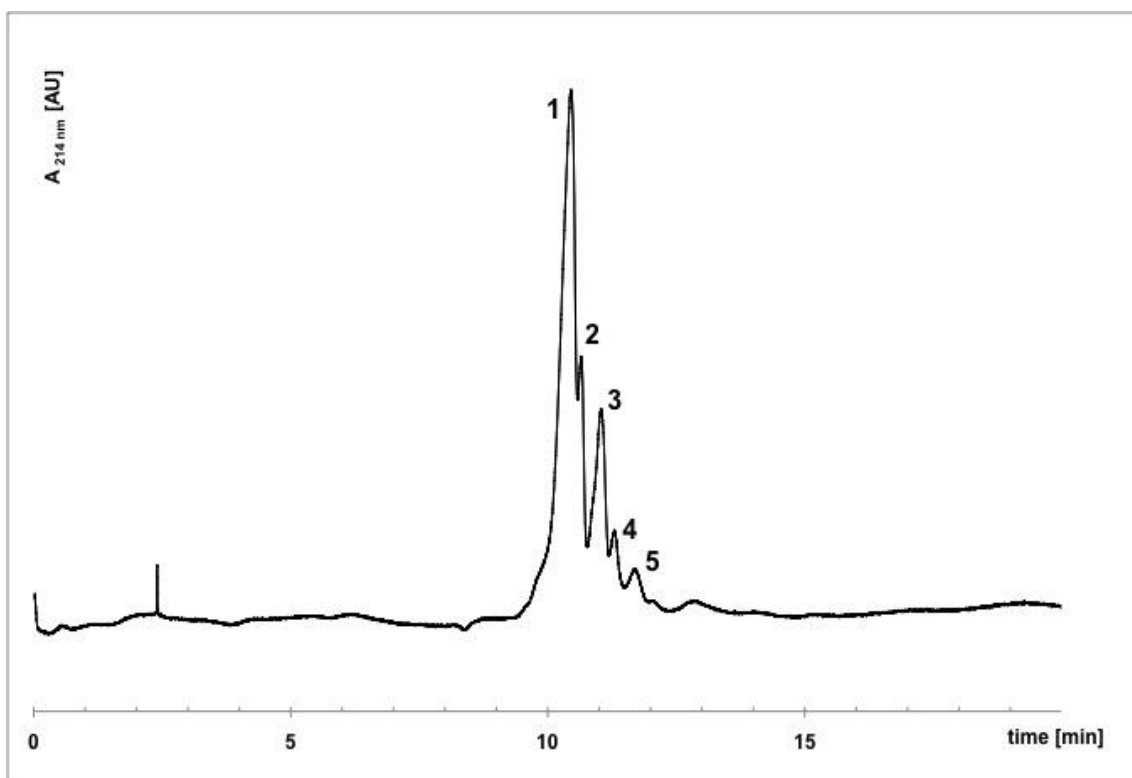
Figure 3. CZE of ovalbumin isoforms in Bis-Tris Propane borate. Separation medium: 0.2 M Bis-Tris Propane, 0. 4M boric acid. Bare capillary, total length= 335 mm, effective length= 250 mm, ID= 50 µm, OD= 360 µm. Separation voltage: -15 kV. UV detection at 214 nm. Pressure injection: 5 s at 50 mbar. Sample: 10 g/L ovalbumin V in water.

Conclusion

Background electrolytes containing high-concentration boric acid preferably mixed with polyol bases suppresses or even eliminates electroosmotic flow in bare fused silica capillaries allowing high-resolution separations by capillary electrophoresis.

Reference

[1] Hjertén, S., *J. Chromatogr. A,* 1985, *347*, 191- 198.

[2] Cobb, K. A., Dolnik, V., Novotny, M. V., *Anal. Chem.* 1990, *62*, 2478-2483.

[3] Chiari, M., Cretich, M., Horvath, J., *Electrophoresis* 2000, *21*, 1521-1526.

[4] Madabhushi R. S., Menchen, S. M., Efcavitch, J. W., Grossman, P. D., U.S. patent 5,567,292.

[5] Dolnik, V., U. S. Patent 7,799,195.

[6] Karger, B. L., Schmalzing, D., Foret, F., U. S. Patent 5,322,608.

[7] Chiari, M., U. S. Patent 6,410,668.

[8] Dolnik, V., Liu, S., Jovanovich, S., *Electrophoresis* 2000, *21*, 41-54.

[9] Horvath, J., Dolnik, V., *Electrophoresis* 2001, *22*, 644-655.

[10] Dolnik V., J. Chromatogr. A 1995, *709*, 99-110.

[11] Wu, D., Regnier, F. E., *J. Chromatogr. A* 1992, *608*, 349-356.

[12] Zhang, Y., Lee, H. K., Li, S. F. Y., *J. Chromatogr. A* 1996, *744*, 249-257.

[13] Harvey, M. D., Bandilla, D., Banks, P. R., *Electrophoresis* 1998, *19*, 2169-2174.

[14] Bean, S. R., Lockhart, G. L., *J. Agric. Food Chem.* 1999, *47*, 4246-4255.

[15] Liu, Y., Reddy, P., Ratnayake, C. K., Koh, E. V., U. S. Patent 7,381.317.

[16] Aronoff, S., Chen, T. C., Cheveldayoff, M., *Carbohydr. Res.* 1975, *40*, 299-309.

[17] van Duin, M., Peters, J. A., Kieboom, A. P. G., van Bekkum, H., *Tetrahedro*n 1984, *40*, 2901-29141.

[18] Taylor, M. J., Grigg, J. A., Rickard, C. E. F., *Polyhedron* 1992, *11*, 889-892.

[19] Michkov, B. M., *Electrophoresis* 1986, *7*, 150-151.

[20] Taylor, M. J., Grigg, J. A., Laban, I. H., *Polyhedron* 1996, *15*, 3261-3270.

[21] Sonoda, A., Takagi, N., Ooi, K., Hirotsu, T., *Bull. Chem. Soc. Jpn* 1998, *71*, 161-166.

[22] Yan, J., Springsteen, G.,Deeter, S., Wang, B., *Tetrahedron* 2004, *60*, 11205-11209.

[23] Bashkin, J., Marsh, M., Barker, D., Johnston, R., *Appl. Theor. Electrophor.* 1996, *6*, 23-28.

[24] Williams, B. A., Vigh, G., *Anal. Chem*. 1996, *68,* 1174-1180.

HOLLOW FIBRE-LIQUID PHASE MICROEXTRACTION OF BASIC DRUGS FROM DRIED BLOOD SPOTS

Miloš Dvořák[1], Blanka Miková[2], Andrea Šlampová[1], Pavel Kubáň[1]

[1]*Institute of Analytical Chemistry of the Czech Academy of Sciences, Veveří 97, 60200 Brno, Czech Republic, dvorak@iach.cz*

[2]*Masaryk University, Faculty of Science, Department of Chemistry, Kamenice 753/5, 625 00 Brno, Czech Republic*

Summary

Hollow fibre-liquid phase microextraction (HF-LPME) was applied for rapid and efficient extraction of basic drugs from dried blood spots (DBS). Basic drugs from DBS were first extracted into 10 mM NaOH solution, which acted as the HF-LPME donor solution, and simultaneously the neutralized drugs were transferred across the HF and preconcentrated in 10 mM HCl acceptor solution inside the HF lumen. Mixture (1:1, v:v) of 1-ethyl-2-nitrobenzene and dihexyl ether was used for impregnation of the porous HF membrane. Analytes in the acceptor solution were injected directly from the HF into capillary electrophoresis instrument for further separation, detection and quantification. Repeatability of the hyphenated analytical system ranged from 9.8 to 13.8 % (RSD) and enrichment factors of 52 – 78 were obtained for model basic drugs spiked to DBS extracts at a concentration level of 0.1 mg/L.

Introduction

Polypropylene hollow fibres (HF) are inexpensive materials, which are often used in sample treatment at industrial scale, but can be also easily applied in a downscaled format, i.e., in liquid-phase microextraction (LPME) technique. The HF-LPME is suitable for sample treatment in environmental and bioanalytical applications [1] and fundamental principles of HF-LPME enable simultaneous clean-up of matrix components of a complex sample (waste water, urine, blood) and selective preconcentration of target analytes in one step. Especially, combination of the efficient sample treatment with sensitive and fast analytical separation technique, which consumes negligible amount of samples, can be very useful. The above requirements offers, for example, capillary electrophoresis (CE) [2]. Moreover, CE enables consecutive injections of extracted samples from microextraction devices without interruption of the extraction process with negligible consumption of the extract.

Dried blood spots (DBS) constitute a convenient method for sampling of blood samples in various fields of clinical analysis [3]. Nevertheless, subsequent processing of DBS samples requires multiple step sample treatment before analytical determination of target analytes and limits the usage of DBS sampling technique. In this contribution, a simple method is described,

which directly couples selective HF-LPME extraction and preconcentration of target analytes from DBS samples to their injection, separation and quantification using a commercial CE instrument. Four basic drugs were selected as model analytes, which usually have low therapeutical concentration level in blood and their determination requires preconcentration step or application of sensitive and expensive analytical instrumentation, such as mass spectrometry.

Experimental

Whatman 903^{TM} collection cards (GE Healthcare Ltd., Cardiff, UK) were used to collect human capillary blood from finger pricks. The first drop of capillary blood was wiped off with a medical wipe and 10 µL of the next blood drop was transferred by a micropipette onto the collection card to form a blood spot. The spots were dried at lab temperature (25°C) for 2 hours and formed the dried blood spots (DBS). Collection cards with DBS were stored in plastic bags with a desiccator and each corresponding spot was cut with a cork borer (9 mm) from the card before analysis. The DBS was transferred to a glass vial (P/N 5182-9697, Agilent Technologies, Waldbronn, Germany) and was topped up with 500 µL of 10 mM NaOH. Four basic drugs, nortriptyline, papaverine, haloperidol and loperamide (Sigma, Steinheim, Germany) were used as model analytes, which were added to the solution in the glass vial at 0.1 mg/L concentration (standard solution) or were not added (blank solution).

One end of 10 mm long segment of a polypropylene HF (Accurel PP 300/1200; Membrana GmbH, Wuppertal, Germany) was firmly pressed with tweezers and thermally sealed. The opposite side of the HF was pulled over the narrow tip of a 1 mL micropipette tip (P/N 961-04, Kartell S.p.A., Noviglio, Italy), which was cut to the total length of 22 mm. To form the SLM, the HF was immersed into a mixture (1:1, v:v) of 1-ethyl-2-nitrobenzene (ENB, ≥ 98%, Fluka) and dihexyl ether (DHE, ≥ 97%, Aldrich) for 10 s. Excess of the solvent at the HF tip was removed by a medical wipe. 5 µL of 10 mM HCl was injected into the HF by a glass syringe (Hamilton, Bonaduz, Switzerland) as an acceptor solution. The micropipette tip with the HF was inserted in the glass vial with DBS/10 mM NaOH solution and the vial was snap-capped by a PE cap (P/N 5181-1507, Agilent). The vial was agitated on a Vibramax 100 (Heidolph Instruments GmbH, Schwabach, Germany) at 800 rpm for 20 min. CE analyses of standard solutions and extracted DBS samples were carried out using a 7100 CE instrument (Agilent). The CE-UV conditions for determination of basic drugs can be found in a former publication [4] and a CE short electrode assembly (P/N G7100-60033, Agilent) was used in this study.

Results and Discussion

In the actual set-up the HF-LPME was coupled to CE for direct determination of model basic drugs in DBS samples. The HF extraction unit was attached to 22 mm long segment of a micropipette tip, which was placed in the glass vial and acted as a guiding tube for CE electrode and separation capillary. The capillary tip extended from the electrode by 8 mm and immersed into the acceptor solution in the HF lumen during CE injection. Blood extraction from the DBS collection card and HF-LPME of the analytes into the HF lumen were carried simultaneously

by placing the cut DBS to the glass vial, adding 500 µL of 10 mM NaOH, immersing the HF into the solution and agitating the vial for 20 min. Efficient HF-LPME of basic drugs from the DBS extract were obtained with enrichment factors of 52, 78, 69 and 53 for nortriptyline, papaverine, haloperidol and loperamide, respectively. The method showed good repeatability of the DBS desorption/extraction and in-line coupled CE-UV analysis with relative standard deviation (RSD) values 9.8 – 13.8% (n=5). The repeatability data correlated well with those of other microextraction techniques directly coupled to CE [2] and complied with requirement on repeatability in bioanalytical method validation [5]. Electropherograms of blank DBS extracts showed no additional peaks originating from the DBS matrix and demonstrated excellent selectivity of the hyphenated analytical method for determination of the model basic drugs.

Conclusion

The actual contribution opens new possibilities for using HF-LPME in combination with CE. A small segment of HF acts as the extraction unit, is directly coupled to CE separation capillary, and enables simultaneous pretreatment of complex samples and injection of the pretreated samples into CE. The method is demonstrated on direct pretreatment and analysis of model basic drugs in DBS samples.

Acknowledgement

Reference

[1] Lee, J., Lee, H.K., Rasmussen, K.E., Pedersen-Bjergaard, S., Anal. Chim. Acta 2008, 624, 253-268.

[2] Kubáň, P., Boček, P., Anal. Chim. Acta 2013, 787, 10-23.

[3] Sharma, A., Jaiswal, S., Shukla, M., Lal, J., Drug Testing and Analysis 2014, 6, 399-414.

[4] Šlampová, A., Kubáň, P., J. Chromatogr. A 2017, 1497, 164-171.

[5] Huang, C.X., Gjelstad, A., Pedersen-Bjergaard, S., J. Membr. Sci. 2017, 526, 18-24.

MALDI-MS IMAGING OF C=C POSITIONAL ISOMERS OF LIPIDS ENABLED BY PATERNÒ-BÜCHI PHOTO-DERIVATIZATION

Antonín Bednařík[1,2], Stefan Bölsker[2], Jens Soltwisch[2,3], Klaus Dreisewerd[2,3]

[1]*Central European Institute of Technology (CEITEC), Masaryk University, Žerotínovo nám. 9, 601 77 Brno, Czech Republic*

[2]*Institute for Hygiene, Biomedical Mass Spectrometry, University of Münster, 48149 Münster, Germany*

[3]*Interdisciplinary Center for Clinical Research (IZKF), University of Münster, 48149 Münster, Germany*

Summary

Recent mass spectrometry imaging (MSI) approaches determine a global picture about the lipid distribution in tissue sections, however, carbon-carbon double bonds (C=C) positional isomers are generally not differentiated. In this study, we introduce matrix-assisted laser desorption/ionization (MALDI) MSI technique based on an "on-tissue" Paternò-Büchi (PB) reaction with benzaldehyde for visualizing the distribution of C=C positional isomers of lipids. The technique revealed highly differential distribution of several C=C positional isomers of phosphatidylcholine and phosphatidylserine species in mouse cerebellum.

Introduction

The field of lipidomics is currently driven by rapid advances in mass spectrometry (MS). Still, analysis of overall lipidome is a difficult task due to the presence of numerous lipids with complex structures present at various levels in highly dynamic system, reflecting the physiological, pathological, environmental state of an organism. One of the unresolved challenges of MS-based lipidomics remains the characterization of physiologically important isomeric species such as C=C positional isomers of phospho- and glycolipids. Powerful techniques that exploit chemical derivatization of C=C bonds followed by specific fragmentation in a CID experiment, such as ozone-induced dissociation (OzID) [1-3] and Paternò-Büchi (PB) photo-derivatization [4-6] have recently emerged. Schematic of PB reaction producing four-membered oxetane ring and the diagnostic ions produced by its fragmentation in the following CID experiment is shown in Fig. 1.
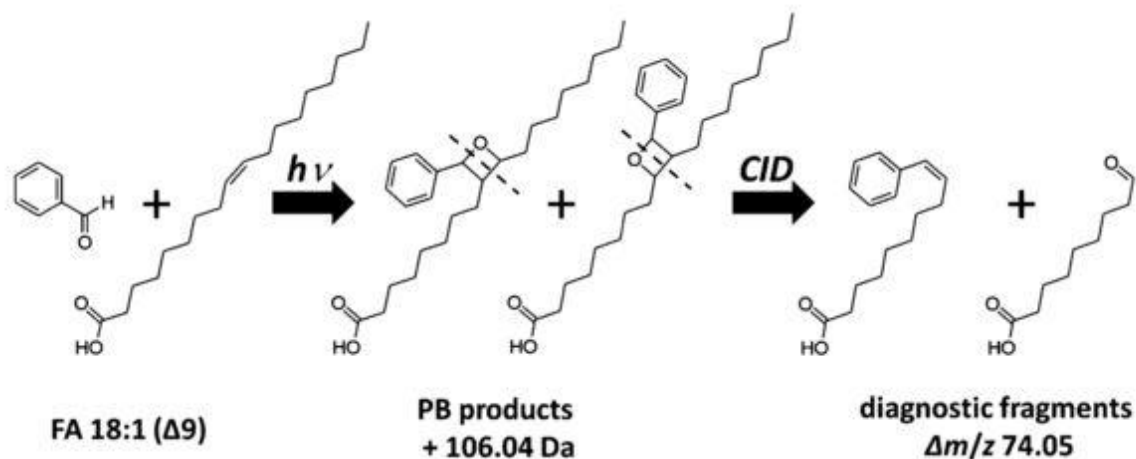
Figure 1: PB reaction of oleic acid with benzaldehyde.

Experimental

PB photo-derivatization was carried out in an enclosed, custom-made reaction chamber with inner dimensions of 6.7 cm × 12.7 cm × 15.0 cm, to which benzaldehyde vapor was introduced on demand. Glass slides with tissue sections were mounted on a copper block, which was cooled down to 6 °C using a Peltier element. Benzaldehyde condensed on the cooled sample producing a thin viscous layer, which evaporated after reheating of the sample to laboratory temperature. PB reaction was triggered by 254-nm UV lamp with power output 5W. Tissue sections were coated with 2,5-dihydroxybenzoic acid (DHB) MALDI matrix in a custom-made sublimation chamber (5 min, 120 °C, 5×10-5 mbar). Recrystallization of the sublimed DHB layer was performed in laboratory drier (75 °C, 2.5 min) in closed Petri dishes holding filter paper wetted by 1 mL of water:ethanol (1000:5, v/v) solution.

MS data were acquired using a Q Exactive Plus Orbitrap mass spectrometer (Thermo Fisher Scientific) equipped with a modified ion funnel MALDI/ESI Injector (Spectroglyph, Kennewick, WA) [7]. A frequency-tripled (349 nm) Nd:YLF laser focused to ~20 µm was used for MALDI and a frequency-quadrupled (266 nm) Nd:YAG laser was employed for laser-induced postionization (PI) of the MALDI generated plume in the MALDI-2 experiments [8, 9].

Results and Discussion

Technique optimization and first experiments were carried out using pig brain homogenate samples. Several PB products of phosphatidylcholines (PC) were readily differentiated in MALDI spectra. Upon subjecting protonated PB products to low-energy CID, diagnostic ion pairs in MS/MS spectra with characteristic mass difference 74.05 Da have emerged. For example reaction product of PC 34:1 yielded two ions pairs at m/z values of 650.44/724.49 and 678.47/752.52, identifying C=C positions as Δ9 and Δ11, respectively. MALDI-2 technique

the analysis of phosphatidylethanolamines (PE), phosphatidylserines (PS) and galactosylceramides (GalCer).

Mouse cerebellum was mapped using MALDI-2 MS/MS imaging at 25 µm lateral resolution. Selected PB products of PC 36:1 and PS 36:2 at mass window m/z 894.6 ± 0.4 were subdued to CID fragmentation and MS images of the detected C=C positional isomers were reconstructed (Fig. 2). Detected isomers were distributed at highly differential levels in the white and gray matter areas of the cerebellum [10].
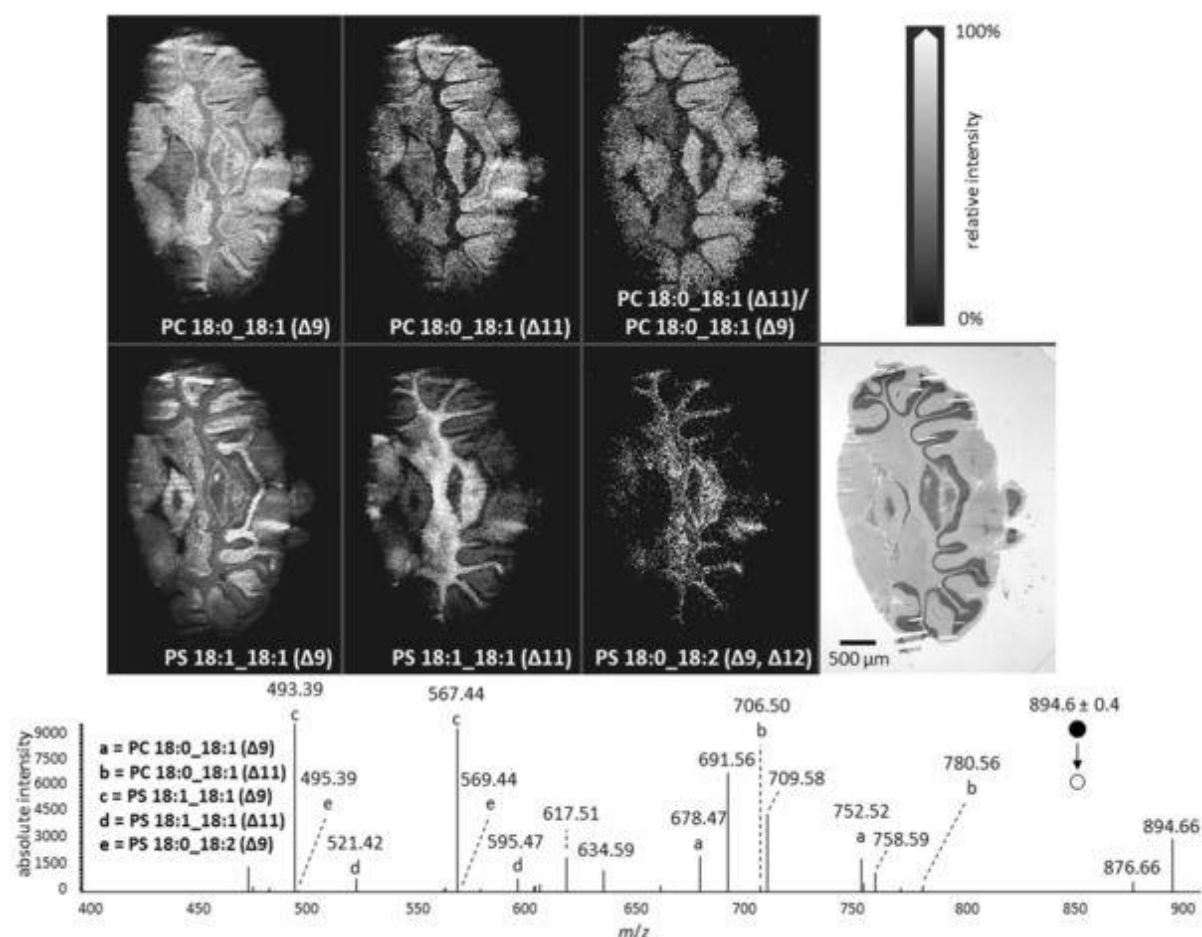

Figure 2: MALDI-2-MS/MS images of PC and PS C=C positional isomers in mouse cerebellum.

Conclusion

Developed PB-MALDI-MS/MS protocol provides a valuable glimpse into the deeper level of phospholipid organization complexity in tissues with a currently unknown biological background. In the future, it could help to better understand the physiological role of these C=C positional isomers as well as to provide novel biomarkers for various pathologies including cancer.

Acknowledgement

Reference

[1] Thomas, M. C, Mitchell, T. W., Harman, D. G., Deeley, J. M., Nealon, J. R., Blanksby, S. J., Anal. Chem, 2008, 80, 303-311.

[2] Pham, H. T., Maccarone, A. T., Thomas, M. C., Campbell, J. L., Mitchell, T. W., Blanksby, S. J., Analyst, 2014, 139, 204-214.

[3] Paine, M. R. L., Poad, B. L. J., Eijkel, G. B., Marshall, D. L., Blanksby, S. J., Heeren, R. M. A., Ellis, S. R., Angew Chem Int Ed Engl., 2018, 57, 10530–10534.

[4] Ma, X. X., Xia, Y., Angew Chem Int Ed Engl., 2014, 53, 2592-2596.

[5] Stinson, C. A., Xia, Y., Analyst, 2016, 141, 3696-3704.

[6] Waldchen, F., Becher, S., Esch, P., Kompauer, M., Heiles, S., Analyst, 2017, 142, 4744-4755.

[7] Belov, M. E., Ellis, S. R., Dilillo, M., Paine, M. R. L., Danielson, W. F., Anderson, G. A., de Graaf, E. L., Eijkel, G. B., Heeren, R. M. A., McDonnell, L. A., Anal. Chem., 2017, 89, 7493-7501.

[8] Soltwisch, J., Kettling, H., Vens-Cappell, S., Wiegelmann, M., Muthing, J., Dreisewerd, K., Science, 2015, 348, 211-215.

[9] Ellis, S. R., Soltwisch, J., Paine, M. R. L., Dreisewerd, K., Heeren, R. M. A., ChemComm, 2017, 53, 7246-7249.

[10] Bednarik, A., Bolsker, S., Soltwisch, J., Dreisewerd, K., Angew Chem Int Ed Engl., 2018, 57, 12092-12096.

HIGH-THROUGHPUT CHARACTERIZATION OF SUBSTRATE SPECIFICITY OF HALOALKANE DEHALOGENASES BY USING CAPILLARY MICROFLUIDICS

Michal Vasina[1], **Tomas Buryska**[1,2], **Pavel Vanacek**[1,2], **Fabrice Gielen**[3,4], **Liisa D. van Vliet** [4], **Zdenek Pilat**[5], **Jan Jezek**[5], **Pavel Zemanek**[5], **Jiri Damborsky**[1,2], **Fabian Hollfelder** [4], **Zbynek Prokop**[1,2]

[1]*Loschmidt Laboratories, Department of Experimental Biology and RECETOX, Faculty of Science, Masaryk University, Brno, Czech Republic, michalvasina@gmail.com*

[2]*International Clinical Research Center, St. Anne's University Hospital, Brno, Czech Republic*

[3]*Living Systems Institute, University of Exeter, Exeter, United Kingdom*

[4]*Department of Biochemistry, University of Cambridge, Cambridge, United Kingdom*

[5]*Institute of Scientific Instruments, Czech Academy of Sciences, Brno, Czech Republic*

Summary

Here, we present a microfluidic platform for characterization of haloalkane dehalogenase substrate specificity in 1000-fold decreased reaction volume and 100-times reduced time requirements as compared to conventional methods. The platform utilizes a novel route for substrate delivery, based on the partitioning of the substrate between the carrier oil and the reaction aqueous phase of the droplet containing the enzyme. We validated the microfluidic system by measuring substrate specificity of model enzyme haloalkane dehalogenase LinB towards 27 halogenated substrates and compared the results with data obtained by conventional and robotic analysis. Subsequently, we utilized the microfluidic system for the high-throughput analysis of substrate specificity profiles for eight HLDs. The obtained results and microfluidic method performance were critically compared with conventional measurements, showing high correlation of $R^2 = 0.89$. The effectivity of this technique makes it highly suitable for high throughput screening of novel biocatalysts.

Introduction

The enormous number of sequence available in public databases currently surpasses our capability of annotation and characterization of the corresponding proteins. There is a need for the development of efficient high-throughput methods for experimental characterization of the increasing sequence diversity [1]. The model enzyme family, haloalkane dehalogenases (HLDs), have recently attracted attention in biotechnology for the ability to convert a broad

range of halogenated substrates including a variety of toxic environmental pollutants or warfare chemicals [2]. In this study, we present a technique, which accelerates the process of substrate specificity screening and analysis of temperature profile in microscale. The method applicability was demonstrated for analysis of HLDs but generally applicable for various enzyme families.

Experimental

The setup of microfluidic platform is described in the Fig. 1. During the experiment, 20 μL of a particular enzyme sample was loaded into the 24-well rack in the Dropix instrument (Dolomite, UK). Oil bath below the rack was prefilled with FC40 oil with 0.5% PicoSurf 1 surfactant. Fine bore polythene tubing (OD 0.4 mm, ID 0.1mm, Smith-Medical, UK) was used for droplet generation and signal observation. Droplets were generated by a syringe pump (Chemyx, USA) running in withdraw mode at a flow rate of 10 μL.min^{-1}. Droplet volume, oil spacing, and sample sequence were controlled using Dropix control software. The tubing was perpendicularly aligned to the excitation/emission optical fiber at in-house build black acetal cube. Excitation was achieved by 450 nm blue laser (12V, 200mW, PRC) focused by a spherical lens into the multimode optical fiber Y-bundle suitable for reflection and backscatter spectroscopy (SQS, Czech Republic). The excitation wavelength was filtered on a dichroic mirror with cut off at 490 nm (ThorLabs, Germany). The analog signal was collected on Si-detector (ThorLabs, Germany), converted to the digital signal by Ni-DAQ 6009 module (National Instruments, USA) and processed by LabView 12 (National Instruments, USA). Raw signal was processed by droplet detection script written in MATLAB 2017b (Mathworks, USA).
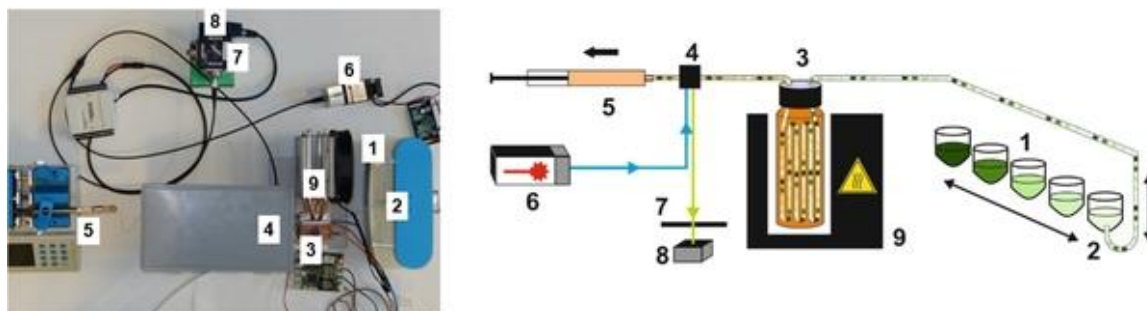

Fig. 1 The microfluidic platform developed in the study. Sampler (1), droplet generator (2), incubation chamber containing substrate (3), detection box (4), syringe pump (5), laser source (6), kinematic cube with filter (7), detector (8), temperature controller (9), substrate (orange) and enzyme variants (green).

The substrate filled in 1.5 mL glass vial with gas-tight screw-capped lid penetrates via the polythene tubing (20 cm, OD 0.4 mm, ID 0.1mm, Smith-Medical, UK) to the oil phase and is finally delivered to the water droplet containing an enzyme sample. The final concentration of the substrate is driven by the partitioning between the carrier oil and the reaction aqueous phase. The vials containing the polythene tubing filled with substrate were stored for a minimum of 12 hours at room temperature to equilibrate prior the experiment. During the experiment, the

vial was placed in a Peltier element that enabled precise control of temperature (Meerstetter, Switzerland).

Results and Discussion

Conventional analysis of the enzyme activity towards multiple substrates is a time demanding process and requires larger amounts of protein sample. A robotic automation combined with the liquid handling system was recently used to increase the throughput and simultaneously reduce the sample requirement [3]. However, the robotic system reduces the reaction volume only 10–fold and the analysis time 3–fold. Incomparable efficiency can be obtained by application of a modern microfluidic systems. These miniaturized integrated devices provide a further increase of analytical throughput and significant reduction of sample requirements. Typical volumes in microfluidic systems that use droplet–on–demand approach are tens of nl [4], in comparison to conventional and robotic methods requiring several mililiters and hundreds of microliters of the sample, respectively. Here we demonstrate the application of droplet-based microfluidics for combinatorial analysis of enzyme substrate specificity. The model enzyme, LinB from Sphingobium japonicum UT26 [5], was used to compare activities towards 27 halogenated substrates. The miniaturized method was validated and compared with the conventional and robotic methods.

A positive enzymatic activity was observed with 23 substrates, while 4 substrates were not converted, which is consistent throughout all three data sets, conventional, robotic and microfluidic (Fig. 2).
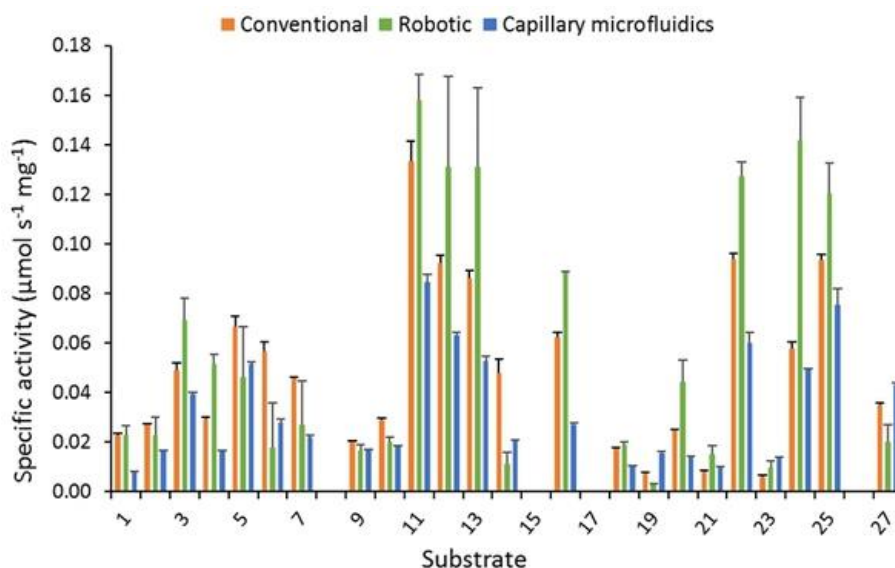

Fig. 2 Comparison of the substrate specificity profiles of the HLDs LinB determined by using conventional method (orange), liquid handling robot (green) and capillary microfluidics (blue), respectively. Error bars represent the standard errors. Specific activities for the conventional measurement were taken from [6].

Robustness and capacity to identify substrates is one of the key properties expected from the screening platforms. The quantitative analysis showed high correlation of conventional measurement with robotic ($R^2 = 0.79$) and microfluidic analysis ($R^2 = 0.89$). The slight shift was observed in absolute values, the robotic data exhibited 23 % increase while microfluidic data showed 37 % decrease in averaged activity values in comparison to the conventionally (manually) measured data set.

Conclusion

The substrate specificity of HLDs was analyzed by the microfluidic system and validated against the conventional and robotic analyses. The use of the conventional method requires about three weeks to measure the substrate specificity profile for a single enzyme. Employment of the robotic liquid handling speeds up the process about 8-fold [1]. However, it still requires relatively large amount of sample. The microfluidic screening of 8 model enzymes with 27 substrates was achieved within seven days which reduces the time demand 24-fold in comparison to the conventional method. The reaction volume was scaled down to 150 nL which represents 65 000-fold reduction of a sample requirement. The presented platform may find use in the future screening campaigns for rapid profiling of substrate specificity and analysis of the temperature optima, which represent the two key characteristics of newly discovered biocatalysts.

Acknowledgement

Reference

[1] Vanacek, P., Sebestova, E., Babkova, P., Bidmanova, S., Daniel, L., Dvorak, P., Stepankova, V., Chaloupkova, R., Brezovsky, J., Prokop, Z., Damborsky, J., ACS Catal. 2018, 8, 2402–2412.

[2] Koudelakova, T., Bidmanova, S., Dvorak, P., Pavelka, A., Chaloupkova, R., Prokop, Z., Damborsky, J., Biotechnol. J. 2013, 8, 32–45.

[3] Buryska, T., Babkova, P., Vavra, O., Damborsky, J., Prokop, Z., Appl. Environ. Microbiol. 2018, 84, e01684-17.

[4] Gielen, F., Vliet, L. Van, Koprowski, B. T., Devenish, S. R. A., Fischlechner, M., Edel, J. B., Niu, X., Demello, A. J., Hollfelder, F., Anal. Chem. 2013, 85, 4761–4769.

[5] Nagata, Y., Hynková, K., Damborský, J., Takagi, M., Protein Expr. Purif. 1999, 17, 299–304.

[6] Koudelakova, T., Chovancova, E., Brezovsky, J., Monincova, M., Fortova, A., Jarkovsky, J., Damborsky, J., Biochem. J. 2011, 435, 345-354.

MICROFLUIDIC DEVICE FOR CELL COUNTING AND ELECTRICAL LYSIS

Tomas Vaclavek[1,2], Jana Krenkova[1], Frantisek Foret[1]

[1]*Institute of Analytical Chemistry of the CAS, v. v. i., Brno, Czech Republic, vaclavek@iach.cz*

[2]*Masaryk University, Brno, Czech Republic*

Summary

This lecture presents two microfluidic devices as essential units for single cell proteomic analysis; firstly a device for cell counting based on resistive pulse sensing as an alternative to optical platforms based on visual control over the sample input, secondly a unit for electrical lysis of cells using direct current voltage pulses to lyse cells one by one with a possibility to analyze the distinct lysate zones by electrospray ionization mass spectrometry.

Introduction

Proteomic analysis of single cells using a mass spectrometer (MS) without antibody labeling still remains a challenging goal in the field of bioanalytical instrumentation. Microfluidic devices show a great potential for such analysis as a single microfluidic chip can be designed to perform multiple operations. In this case, it means to control the number of cells entering the lysis site where the disintegration of cells occurs and intracellular proteins are released for the following detection by electrospray ionization mass spectrometry (ESI-MS). Therefore integration of a cell counting unit represents an important step in development of microfluidic device for cellular analysis.

Cells flowing through the microchannel can be registered visually using camera and sophisticated software image analysis. This approach requires a fast camera with objective and software algorithm to recognize a cell moving through the microchannel, distinguish it from the background and other cells in case of multiple cells moving in a group.

Resistive pulse sensing (RPS) is an alternative approach that is based on monitoring the transient disruptions in electric current. In case of microfluidic systems, a voltage is applied across the microconstriction filled with a conductive liquid. As particles or biological cells are passing through this microconstriction, also called the sensing gate, the resistive pulse is generated by displacing a particular volume of conductive liquid. This volume is proportional to the volume of passing particle and accordingly the height of resistive pulse is proportional to the particle size. Determining the cell size serves in cytometry as the first characterization of cells or as a sorting criterion.

Experimental

Microfabrication procedure

Design of a microfluidic device was created in AutoCAD (AutoDesk, USA). At first a replication mask was created by exposing this design using a high-resolution direct laser-writing system µPG 101 Micro-pattern Generator (Heidelberg Instruments, Germany) on commercially available photomask blank substrates (Nanofilm, USA). This replication mask was then used to transfer the design on borosilicate glass wafers coated with 60 nm of chromium and 70 nm of gold as masking metal layers and S1805 positive photoresist (Dow Electronic Materials, USA). These masking metal layers were sputtered using a Sputter-coater Q300TD (Quorum, England). After development of photoresist and etching of masking metal layers the borosilicate wafer was etched in a diluted mixture of sulfuric and hydrofluoric acid at 45°C for 5 minutes to reach the depth of approximately 12 µm. Then the wafer was washed in deionized water to stop etching, acetone to remove the photoresist and piranha solution (sulfuric acid - hydrogen peroxide, 3:1) to clean the surface for the second metal sputtering process. Only the main channel and the sensing gate were again coated with 60 nm of chromium and 70 nm of gold to protect these areas from further etching. Afterwards the inlet channels were etched to the depth of 250 µm so the platinum electrodes and fused silica capillaries could be smoothly inserted in. Two etched wafers were aligned and thermally bonded in a muffle furnace at 620°C for 10 hours so the resulting microchannel had a circular cross section.

Inlets for platinum wire electrodes and fused silica capillaries were sealed in a plastic frame designed in SketchUp (Google, USA) and printed out using the 3D printer Easy3DMaker (3D Factories, Germany) based on fused deposition modelling technology.

Resistive pulse sensing

The microfluidic device was placed on a SVM 340 synchronized video microscope (LabSmith, USA) to have a visual control over cells running through the sensing gate.

A colibrick A/D converter and Clarity Chromatography Data Station (Data Apex, Czech Republic) were used to monitor resistive pulses by measuring voltage at the output of the conductometric detector (Villa Labeco, Slovakia).

Samples

Initial experiments were performed with monodisperse 10 µm polystyrene (PS) beads (Sigma-Aldrich, Germany), which were chosen as a non-conductive particle size standard, suspended in the phosphate buffered saline (PBS) buffer. In experiments with biological cells was observed excessive clumping of cells especially of Saccharomyces cerevisie cells, therefore it was necessary to add 0.1 mM EDTA into PBS buffer to suppress this cell to cell adhesion. Further were performed experiments with mouse osteoblasts MC3T3-E1 and human prostate cancer PC3 cells. Mouse osteoblasts (MC3T3-E1) and PC3 human prostate cancer cells were

collected and centrifuged at 600 G. Growing medium was removed and the cell pellet was re-suspended in PBS. Samples were then again centrifuged at 600 G and re-suspended in PBS with addition of 0.1 mM EDTA for experiments. Saccharomyces cerevisie cells were purchased as dry pellets and were just re-suspended in PBS buffer containing 0.1 mM EDTA. Sample of RBCs was obtained by suspending 5 µL of whole blood in 1 mL of PBS buffer containing 0.1 mM EDTA and 5 mM glucose (200x dilution) with additional 10x dilution (2000x dilution of whole blood).

Cell lysis

Cell lysis was performed on RBCs, PC3 cells and Saccharomyces cerevisiae using 5 ms high voltage DC pulses ranging from 400 - 4000 V (meaning 800 – 8000 V·cm^{-1} as the distance between platinum electrodes was approximately 5 mm).

Results and Discussion

Microfabrication

The two-step etching process resulted in slightly over-etched edges in microchannels which had been etched in the first step and re-coated with 60 nm of chromium and 70 nm of gold. This re-coating was an insufficient protection from further etching in the second step, especially at the edges of microchannels. Chromium and gold is the best combination of metals for protection in glass etching. In our laboratory it was proven that 60 nm of chromium as a first layer with 70 nm of gold as a second layer was sufficient protection for flat surfaces even in deep etching (reaching depths of approx. 250 µm). However it was insufficient to protect the edges of microchannels etched in the previous step, very likely because the coating process is not equally effective at the edges as at the flat surface even though the sputtering machine had a rotating stage. The resulting diameter of a microchannel was 43 µm according to the scanning electron microscope (SEM) image in Fig. 1 (D2).
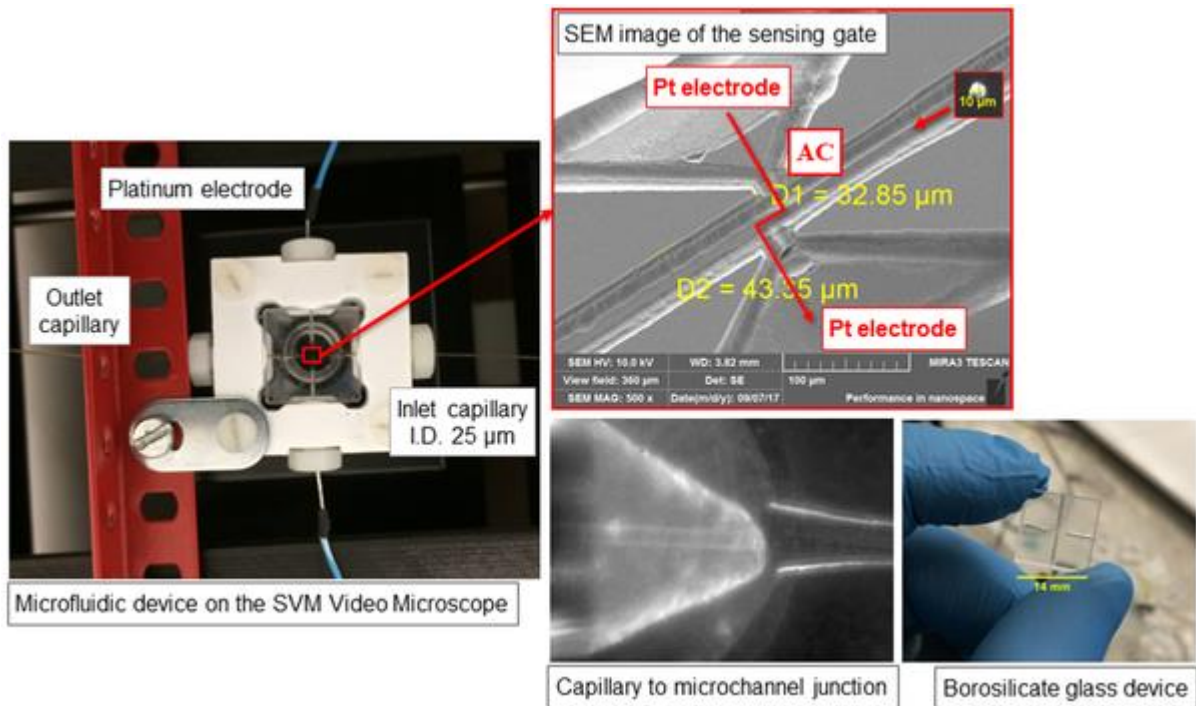
Fig. 1: Design of microfluidic device and representation of sensing circuitry.

Resistive pulse sensing

Particles and especially biological cells may form coagulates it was important to identify single particle peaks by observing particles on a microscope at a reduced flow rate. The digital representation of the voltage output was recorded in a form of a chromatogram (Clarity software was designed for chromatography stations). Clarity chromatograms were exported into MS Excel and as a defining criterion was chosen the peak height, because it refers to particle size. Although in chromatography is commonly used the peak area, in terms of resistive pulses the base of a peak refers to the time of particle passage which differs with the velocity of flow.

An average resistive pulse signals of different particle samples were evaluated by selecting 10 single particle peaks and the height of every peak was calculated by subtracting the averaged value of baseline (averaged value of baseline was calculated by averaging 40 data points surrounding each peak). Resistive pulse signals for PS particles and various types of biological cells are shown in Fig. 2.
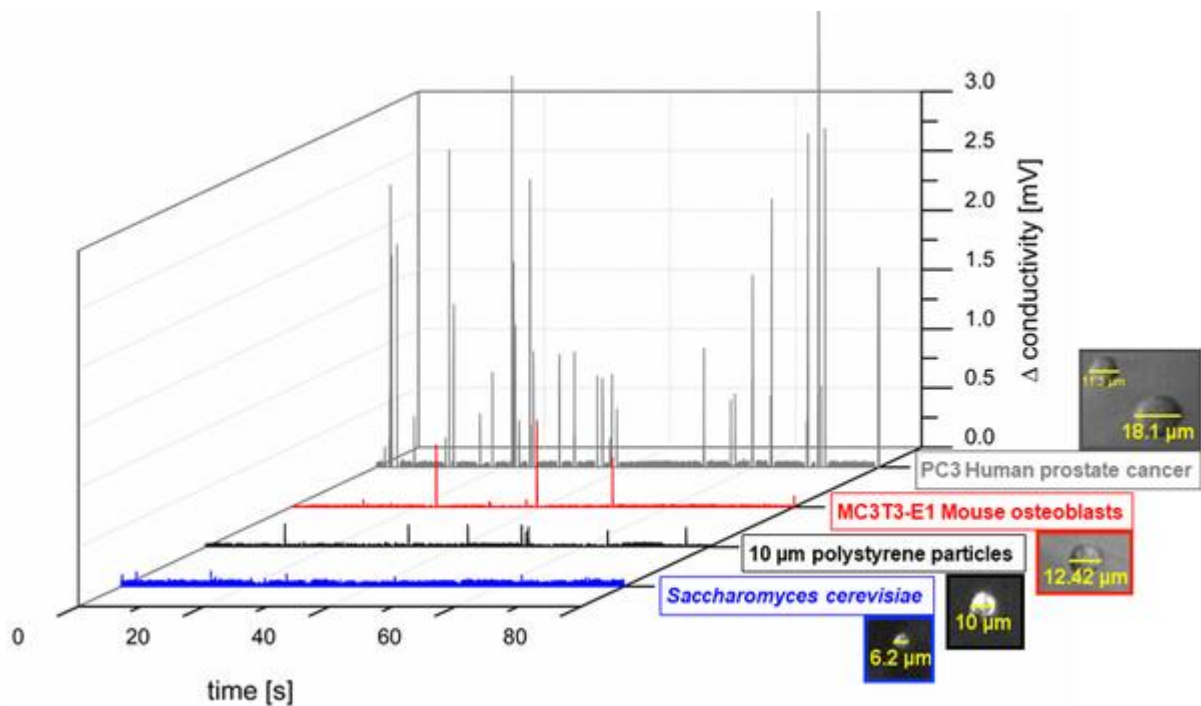
Fig. 2: Resistive pulse signals of PS particles and biological cells.

Cell lysis

RBCs and PC3 cells were effectively lysed by 800 V·cm^{-1} pulses (20–30 pulses), when applying 1200 V·cm^{-1} lysis required 5–10 pulses, at 1600 V·cm^{-1} it was 3–4 pulses, at 2000 V·cm^{-1} only 1–2 pulses.

In contrast with RBCs yeast cells have a sturdy cell wall that maintains its shape. Cell membrane might be permeabilized (maximum 8000 V·cm^{-1}/10 pulses) but it has to be examined by other methods as it is not visible on the video microscope.

Conclusion

Counting of cells using RPS technique and electrical cell lysis, were successfully tested with biological cells. The presented microfluidic device is compatible with fused silica capillaries, therefore it facilitates its combination with electromigration methods in a capillary format. Also as opposed to microfluidic devices based on polydimethylsiloxane, it can be repeatedly disassembled, cleaned using harsh cleaning agents (eq. piranha, chromic acid) and reassembled to achieve full performance after clogging of microchannels.

Future plans include integration of these two steps into single microfluidic device, coupling of this system with MS and automation using Arduino controller platform.

Acknowledgement

THE UREASE BIOSENSOR BASED ON EU(III) TERNARY COMPLEX OF DO3A LIGAND

Filip Smrčka[1], Přemysl Lubal[1,2]

[1]*Department of Chemistry, Faculty of Science, Masaryk University, Kotlářská 2, 611 37 Brno, Czech Republic, filip.smrcka@gmail.com*

[2]*Central European Institute of Technology (CEITEC), Masaryk University, Kamenice 5, 625 00 Brno, Czech Republic*

Summary

This work describes the study of the formation of ternary [Eu(III)DO3A] complexes with "antenna" picolinate-like ligands. The luminescent and electrochemical properties of these ternary Eu(III) complexes can be used for the detection of various organic ions and these properties can be utilized in order to develop a new dual sensor for ion analysis. This was employed for indirect determination of bicarbonate and/or carbonate formed in the course of urea hydrolysis catalyzed by the urease enzyme.

Introduction

Specific spectroscopic, electrochemical and magnetic properties of Ln(III) ions make them perfect candidates for use in many chemical, biological and environmental systems. Ln(III) complexes with macrocyclic ligands (mainly DOTA derivatives) are commonly utilized in medicinal chemistry as radiopharmaceuticals (^{90}Y, [153]Sm, [166]Ho, ^{177}Lu) [1,2] and contrast agents for MRI (Gd) [3]. The 1,4,7,10-tetraazacyclododecane-1,4,7-triacetic acid (H_3DO3A) as heptadentate ligand forms stable binary Ln(III) complexes which can form ternary [Ln(DO3A)L] complexes with some bidentate ligands and this chemical reaction can be employed for their determination.

Experimental

Sodium bicarbonate, picolinic acid (PA), dipicolinic acid (DPA) (all p.a. grade, Sigma-Aldrich, USA) and isoquinoline-3-carboxylic acid (IQCA, Acros Organics, Belgium) were used as received. The macrocyclic ligands, H_3DO3A, were purchased from CheMatech (France). Stock solutions of $EuCl_3$ were prepared by dissolving Eu_2O_3 (p.a. Alfa, Germany) in a small excess of hydrochloric acid and were standardized by chelatometric titration. Luminiscence spectra were recorded on the Quantamaster 300 Plus spectrometer (PTI Canada) with a flash Xe-lamp in the wavelength range 200-800 nm.

Results and Discussion

The 1,4,7,10-tetraazacyclododecane-1,4,7-triacetic acid (H_3DO3A) as heptadentate ligand forms stable complex with europium(III)/terbium(III) aqua ion. The ternary complex exhibits a high luminescence due to antenna effect leading to sensitization of Eu(III)/Tb(III) luminescence by a fluorophore (e.g. picolinic or isoquinolic acid) via efficient energy transfer from ligand to Ln(III) ion. The utilization of those ternary Eu(III) and Tb(III) complexes as selective dual luminescence/electrochemical sensors for determination of carbonate/oxalate using substitution reaction was reported [4, 5]. This was also employed for indirect determination of carbonate formed in the course of urea hydrolysis catalyzed by the urease enzyme.
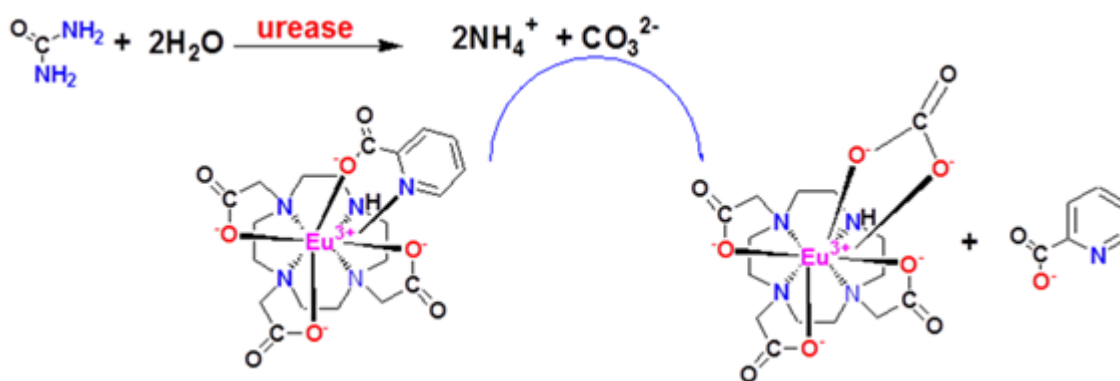
Scheme: The cascade reaction of the ternary [Eu(DO3A)(Pic)]⁻ complex employed for enzymatic determination of urea.

Conclusion

This new analytical procedure was proposed for the determination of both analytes (urea, urease) and the sensitive luminescence-based biosensor can be used in both kinetic time-dependent as well as equilibrium end-point modes [6]. The inhibition effect of some metal ions (e.g. Ag^+, Pb^{2+}, Zn^{2+}, Cd^{2+}) on enzymatic reaction can be employed for their sensitive analytical determination [6]. The proposed analytical procedure is fast, selective and sensitive with metrological parameters comparable for other urea biosensors. As it is known to authors, this new biosensor is the first example of biosensor using the bicarbonate detection as the product of urea hydrolytic reaction catalyzed by urease.

Reference

[1] Wadas TJ, Wong EH, Weisman GR, Anderson CJ (2010) Chem Rev 110:2858.

[2] Försterová M, Jandurová Z, Marques F, Gano L, Lubal P, Vaněk J, Hermann P, Santos I (2008) J Inorg Biochem 102:1531.

[3] Hermann P, Kotek J, Kubíček V, Lukeš I (2008) Dalton Trans 23:3027.

[4] Vaněk J., Lubal P., Hermann P., Anzenbacher P., Jr. (2013) J. Fluorescence 23:57.

[5] Vaněk J., Smrčka F., Lubal P., Třísková I., Trnková L. (2016) Monatsh. Chem. 147:925.

[6] Smrčka F., Lubal P., Šídlo M. (2017) Monatsh. Chem. 148:1945.

MEASURING PHOTON-UPCONVERSION LUMINESCENCE FROM DROPLETS IN MICROFLUIDIC CHIPS

Antonín Hlaváček, **Jana Křivánková, Jan Přikryl**

Institute of Analytical Chemistry of the Czech Academy of Sciences, Veveří 967/97, 602 00 Brno, Czech Republic

Summary

UCNPs are lanthanide-doped nanocrystals that can be excited by near-infrared light and emit light of shorter wavelengths. Advantages of UCNPs include multiple and narrow emission bands, negligible autofluorescence and high photostability, which make UCNPs ideal luminescence label for use in droplet microfluidic. Here, we introduce the instrumentation for reading photon-upconversion luminescence of nanoparticles, which are dispersed in water droplets in a microfluidic chip.

Introduction

Reduced sample volumes, low chemical and energy consumption and effects in the micro-domain make microfluidics attractive and powerful tool in a wide range of applications [1]. From the early times of their introduction, droplet-based microfluidic approaches present a paradigm for high-throughput screening in a broad spectrum of fields from physics to biomedicine. Droplet-based microfluidics uses a two-phase system of aqueous microdroplets (1 pL to 1 µL) embedded in immiscible oil [2]. This system enables to manipulate single droplets at a high-throughput as well as to incubate stable droplets off-chip and reintroduce them into the microfluidic environment for further processing and analysis [2]. UCNPs are lanthanide-doped nanocrystals that can be excited by near-infrared light and emit light of shorter wavelengths. Advantages of UCNPs include multiple and narrow emission bands, negligible autofluorescence and high photostability, which make UCNPs ideal luminescent label for use in droplet microfluidics. Recent technologies allow for preparation of UCNPs sufficiently bright even for single particle detection [3-5]. Here, we introduce the instrumentation for reading photon-upconversion luminescence from water droplets in a microfluidic chip, which was not described previously [6,7].

Experimental

$NaY_{0.80}Yb_{0.18}Er_{0.02}F_4$ nanoparticles coated in carboxylated silica shell were prepared by a method described previously [3-5]. Microfluidic chip was fabricated by a standard method utilizing polydimethylsiloxane bonded to a glass substrate. The cross section of formed microfluidic channels was 100×100 µm. Droplets of UCNP water dispersions were formed in a stream of Fluorinert^{TM} oil. Photon-upconversion luminescence in droplets containing

UCNPs was excited by a focused beam of 5 W 980 nm laser directly in the microfluidic chip. The emitted photon-upconversion luminescence was detected with a CCD spectrometer, which was connected by an optical fiber. The integration time was 100 ms.

Results and Discussion

Synthesis resulted in $NaY_{0.80}Yb_{0.18}Er_{0.02}F_4$ nanoparticles with size of ~90 nm which possessed photon-upconversion emission maxima at 407, 541, 554, 655 nm. The surface of these nanoparticles was coated by the layer of carboxylated silica (thickness ~4 nm, Figure 1A). The dynamic light scattering of UCNP water dispersion was recorded revealing hydrodynamic diameter 119 nm and polydispersity index 0.039. Droplets were created from water dispersions with nanoparticle concentration of 7.5 pmol/L and emission spectrum was recorded with 100 ms integration time.
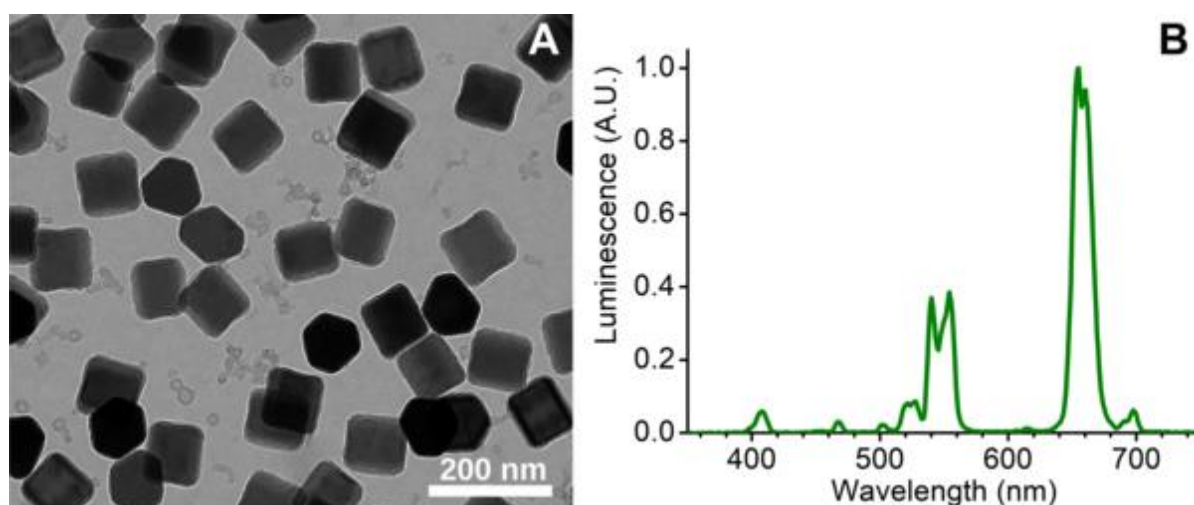

Figure 1. (A) Transmission electron microscopy of investigated UCNPs. (B) Emission spectra of nanoparticles recorded in 300 nL water droplet (nanoparticle concentration 7.5 pmol/L, integration time 100 ms).

Conclusion

Photon-upconversion was successfully measured from droplets in the microfluidic chip containing the water dispersion of $NaY_{0.80}Yb_{0.18}Er_{0.02}F_4$ nanoparticles coated by carboxylated silica shell with diameter ~90 nm. These results confirm the possibility of sensitive detection of photon-upconversion from microdroplets, which allows for developing new techniques for analytical chemistry, biology and material science.

Acknowledgement

Reference

[1] Demello, A. J., Nature 2006, 442, 394–402.

[2] Theberge, A. B., Courtois, F., Schaerli, Y., Fischlechner, M., Abell, C., Hollfelder, F., Huck, W. T. S., Angew. Chem., Int. Ed. 2010, 49, 5846–5868.

[3] Farka, Z., Mickert, M. J., Hlaváček, A., Skládal, P., Gorris, H. H., Anal. Chem. 2017, 89, 11825–11830.

[4] Hlaváček, A., Sedlmeier, A., Skládal, P., Gorris, H. H., ACS Appl. Mater. Interfaces 2014, 6, 6930–6935.

[5] Hlaváček, A., Farka, Z., Hübner, M., Horňáková, V., Němeček, D., Niessner, R., Skládal, P., Knopp, D., Gorris, H. H., Anal. Chem. 2016, 88, 6011–6017.

[6] Sedlmeier, A., Hlaváček, A., Birner, L., Mickert, M. J., Muhr, V., Hirsch, T., Corstjens, P. L. A. M., Tanke, H. J., Soukka, T., Gorris, H. H., Anal. Chem. 2016, 88, 1835–1841.

[7] Prikryl, J., Foret, F., Anal. Chem. 2014, 86, 11951–11956.

CHARACTERIZATION OF ALLIUM TELOMERE REPEAT BINDING PROTEINS

Karolína Kolářová[1], Vratislav Peška[1], Petr Fajkus[1], Jiří Fajkus[1,2]

[1]*Institute of Biophysics, Czech Academy of Sciences, v.v.i., Královopolská 135, CZ-61265, Brno, Czech Republic, karolina.kolarova.k@gmail.com*

[2]*Mendel Centre for Plant Genomics and Proteomics, CEITEC, Masaryk University, Kamenice 5, CZ-62500, Brno, Czech Republic*

Summary

We found several candidates for telomere repeat binding proteins which are orthologous to the TRB proteins from *A. thaliana*. First of all, we analyzed direct protein-protein interactions. We tested formation of homomers and heteromers of AcTRB-like proteins, and interactions between AcTERT and AcTRB-like proteins in *A. cepa*. We found that AcTRB-like3_B, AcTRB-like3_C and AcTRB-like4 form strong homo- and heteromers and they also interact with AcRID1 motif of the AcTERT subunit.

Introduction

Telomeres are nucleoprotein structures which form and protect the ends of eukaryotic linear chromosomes against DNA-damage. Across the plant kingdom, the *Arabidopsis*-type telomeric sequence with the motif $(TTTAGGG)_n$ is dominant. But in some orders such as Solanales or Asparagales, a significant divergence was found in their telomere sequence evolution. Recently, an unusual telomeric sequence $(CTCGGTTATGGG)_n$ was characterized in the genus *Allium* (Asparagales) (Fig. 1.) [1].
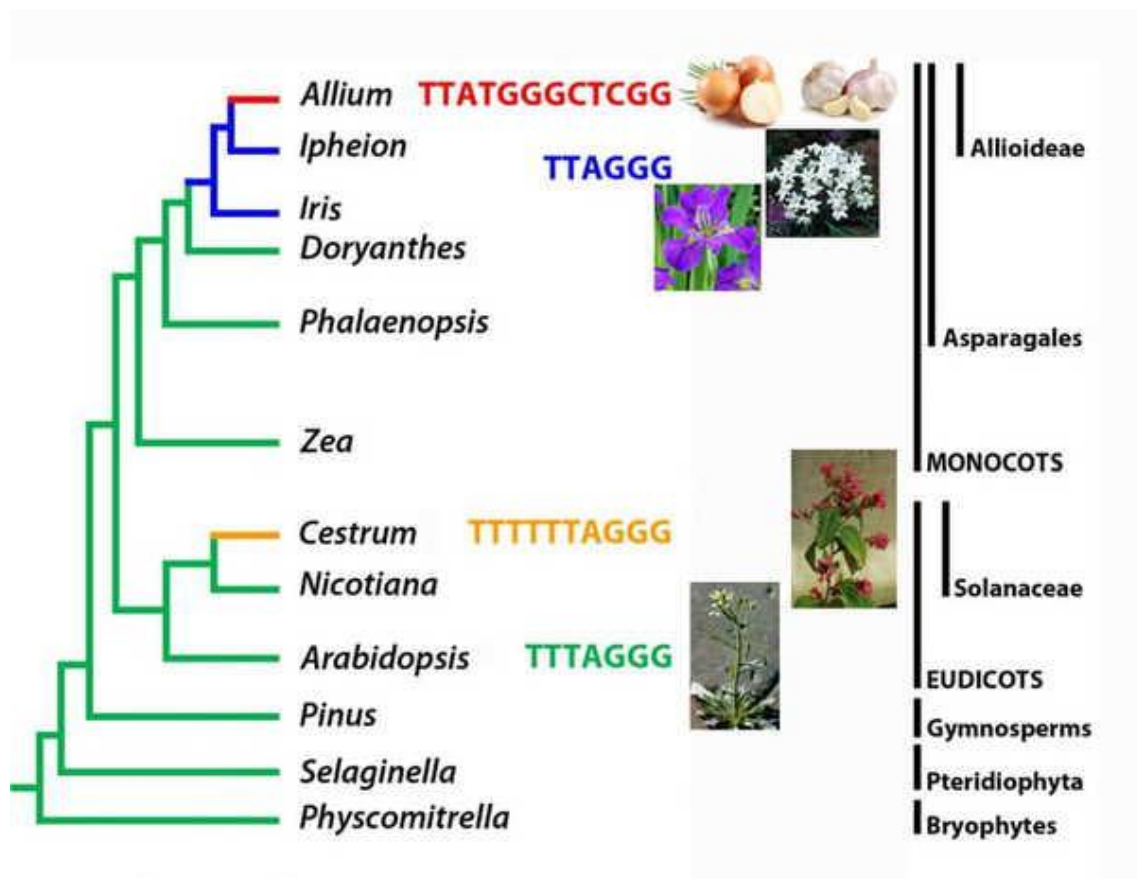
Fig. 1. Summary of knowledge about different telomere types in land plants. The phylogenetic tree indicates the telomeric sequence deviations (red, blue, orange) from the most widespread plant telomeric repeat $TTTAGGG_n$ (green branches). (Modified according to [1])

The elongation of the telomere DNA is usually performed through the action of a ribonucleoprotein enzyme with a reverse-transcriptase activity, the telomerase. And it was also demonstrated that the plant telomere synthesis of both the *Arabidopsis*-like telomere motifs and the unusual repeats (human, Cestrum, and Allium) occurs through the telomerase [1-4]. The telomerase enzyme is composed of two core subunits, a protein - telomerase reverse transcriptasese (TERT) and a templating, telomerase RNA (TR) subunit. The telomerase reverse transcriptase compensates for a replicative telomere shortening caused by the DNA polymerase inability of complete a lagging-strand replication at telomeres. The TERT subunit is consist of four domains: RT (reverse transcriptase) domain, TRBD (telomerase RNA binding domain), C-terminal domain and N-terminal domain (Fig. 2.).
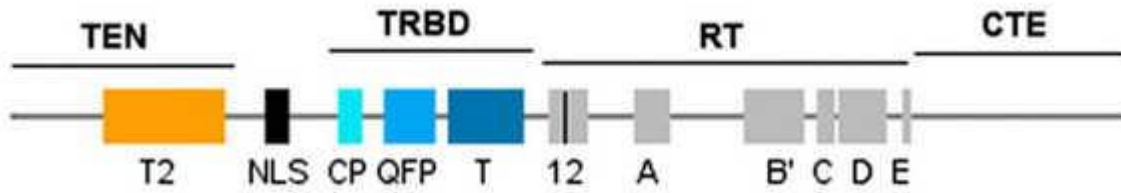
Fig. 2. Schematic view of plant telomerase reverse transcriptase protein subunit and its motifs and domains. TEN- telomerase esential N-terminal domain, TRBD - telomerase RNA binding domain RT – reverse transcriptase domain, CTE – C-terminal domain. (Modified according to [7])

Telomere binding proteins and their complexes play an important role in the maintenance and protection of telomeres. In mammals, the complex of telomere-binding proteins is called shelterin and it consists of proteins which are involved in recognizing of telomeric DNA. In *A. thaliana*, there are five members of telomere repeat binding (TRB) proteins [5,6]. These proteins are plant specific and were recently characterized as components of plant shelterin [7]. TRB proteins show a presence of the N-terminal Myb-like domain which mediates a sequence-specific binding to DNA, a central histone-like domain which mediates protein-protein and non-specific DNA-protein interactions, and the C-terminal coiled-coil domain. TRB proteins form homo- and heteromeric complexes [8]. TRB proteins specifically bind plant telomeric DNA via Myb-like domain and interact with N-terminal part of TERT in *Arabidopsis* [7].

We will present our current results in the identification and characterisation of the candidate telomere proteins in *Allium cepa* (onion), including their interaction with the telomerase and ability to form homo- and heteromeric complexes.

Experimental

RNA isolation and reverse transcription

TRI Reagent® Protocol (Sigma-Aldrich) was used in accordance to manufacturer's protocol for total RNA isolation from seedlings. The cDNA was prepared by reverse transcription of 1 µg RNA using Random nonamers (Sigma) and the M-MuLV reverse transcriptase kit (Finnzymes) according to manufacturer's instructions.

Cloning of cDNA of TRB-like proteins from Allium cepa for yeast two-hybrid assay

The cDNA sequences for proteins AcTRB-like1 (*A. cepa* TRB-like1), AcTRB-like2, AcTRB-like3_B, AcTRB-like3_C, AcTRB-like4, AcTEN (telomerase essential N-terminal domain), AcRID1 (RNA - interacting domain 1) were obtained using PCR with gene-specific primers. The resulting PCR products were precipitated using polyethylene glycol. Then cDNAs were cloned through the pDONR207 entry clones into the destination vectors pGADT7 (prey vector) and pGBKT7 (bait vector) (Clontech) for yeast two hybrid assay. For cloning, the Gateway system (Invitrogen) was used in accordance to manufacturer's protocol.

Yeast two-hybrid (Y2H) system

Protein-protein interactions were examined using Matchmaker Gal4-based yeast two hybrid system (Clontech). PJ69-4α strain of *Saccharomyces cerevisiae* was used for the expression of AcTRB-like1, AcTRB-like2, AcTRB-like3_B, AcTRB-like3_C, AcTRB-like4, AcTEN, AcRID1 genes from the yeast vectors pGADT7 (AD) and pGBKT7 (BD). Tested bait/prey combinations were mixed, co-transformed into PJ69-4α and incubated at the SD agar (Sigma) plates lacking Leu and Trp at 28°C for a few days until colonies had grown. Then co-transformed colonies were inoculated into YPD medium (1% yeast extract, 2% bacteriological peptone, 2% glucose) and cultivated (18h/28°C). Positive interactions were tested on plates with SD agar lacking Leu, Trp and His, and strongest interactions were tested on SD agar lacking Leu, Trp, His and Ade. Ten-times and hundred-times diluted aliquots were dropped onto both -Ade and -His plates. -His plates containing increasing concentrations of 3-aminotriazol (3-AT) which inhibits *His3* activity. The ability of yeast cells grown on higher concentrations of 3-AT correlates with the higher binding affinity of the proteins. For the control of auto-activation, the co-transformations with an empty vector were tested. Each test was carried out in two repeated experiments.

Results and Discussion

Based on the characterization of the *Allium* telomeric sequence and its syntesis by the telomerase, we decided to test the conservation of the previously (in *Arabidopsis*) established direct interactions between the telomere repeat binding proteins (TRB) and the telomerase catalytic subunit (TERT), in our model organism, *Allium cepa*.

Previously, it was shown in Y2H that the AtTRB proteins form homodimeric and heterodimeric complexes. We found four TRB-like proteins in *Allium cepa* which were selected on the basis of similarity with the AtTRB proteins at the level of the amino acid sequence. They were assigned with working names: AcTRB-like1, AcTRB-like2, AcTRB-like3 and AcTRB-like4 where AcTRB-like3 has three possible splicing variants AcTRB-like3_A, AcTRB-like3_B and AcTRB-like3_C. The full length TRB-like coding sequences were cloned into Y2H vectors and tested for forming homo- and heteromeric protein-protein complexes. The variant AcTRB-like3_A could not been tested because cloning of this possible splicing variant has failed. For a verification of the interactions, –His and –Ade plates were used and –His plates with increasing amount of 3-AT up to 3 mM for semi-quantitative test were used. The results show that AcTRB-like3_B, AcTRB-like3_C, and AcTRB-like4 candidates form strong homo- and heteromeric complexes, while the other candidates show only weak or no mutual and self-interactions (Fig. 3.).
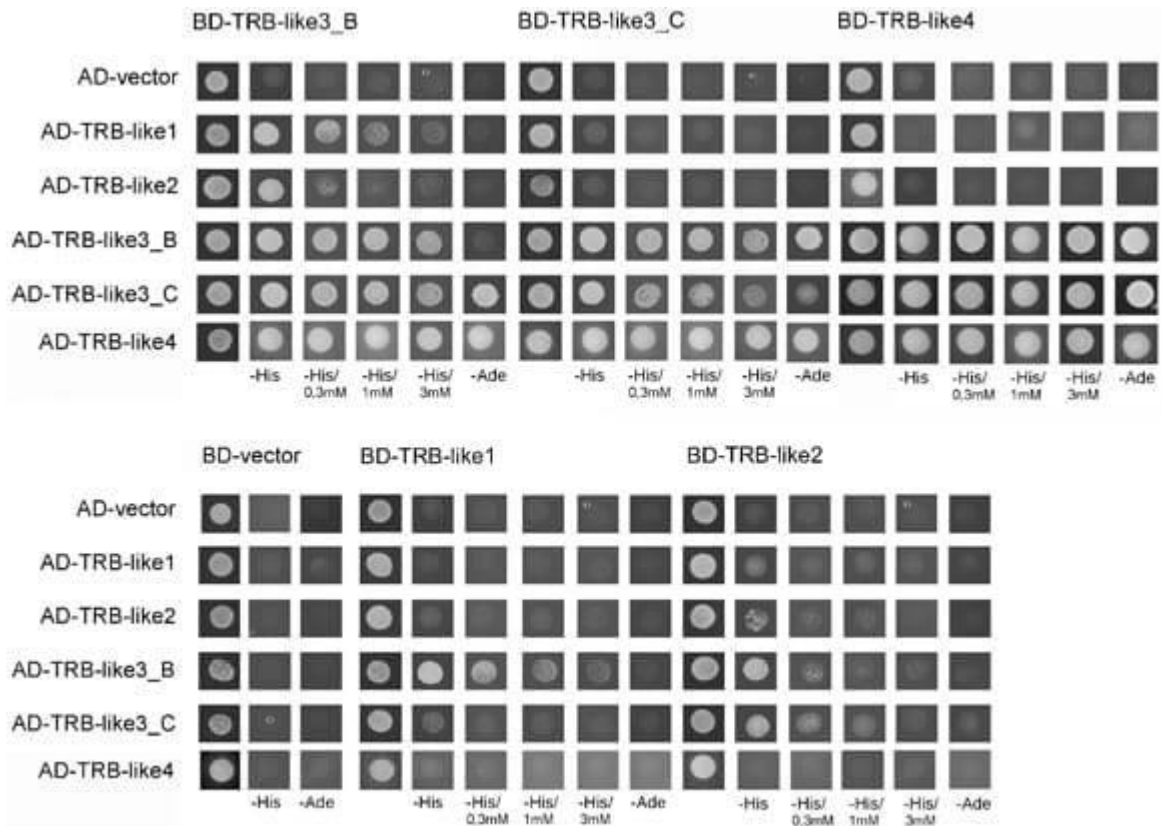
Fig. 3. Yeast-two hybrid system was used to assess interaction of TRB-like candidates in Allium cepa. AcTRB-like3_B, AcTRB-like3_C, AcTRB-like4 proteins form strong homo- and heterodimers. AcTRB-like3_B and AcTRB-like3_C form weak interactions with AcTRB-like2. AcTRB-like1 interacts only weakly with AcTRB-like3_B. Co-transformation with an empty vector (AD/BD vector) was used as negative control.

AtTRB proteins interact directly with the N-terminal fragment of the plant telomerase reverse transcripatese (TERT). TERT fragments with N-terminal domains were used to test direct interactions between TERT and TRB-like proteins in *A. cepa*. The full length cDNA of our AcTRB-like candidates and the two N-terminal fragments of TERT-like protein (Figure 4A) were cloned to Y2H vectors. For a verification of interactions of AcTRB and AcTERT and the same conditions as in the first experiment were used. Our results showed that AcTRB-like4 interacts strongly with the AcTERT fragment called RID1 domain. It was observed under both histidine and adenine selection. And AcTRB-like4 as the only one interacts with the TEN domain of AcTERT. It was observed under histidine selection. Other AcTRB proteins (AcTRB-like3_B, AcTRB-like3_C) interact only with AcRID1 domain and it was observed also only under the histidine selection. Finaly, TRB-like1 and TRB-like2 were negative in all of these interactions (Figure 4B).
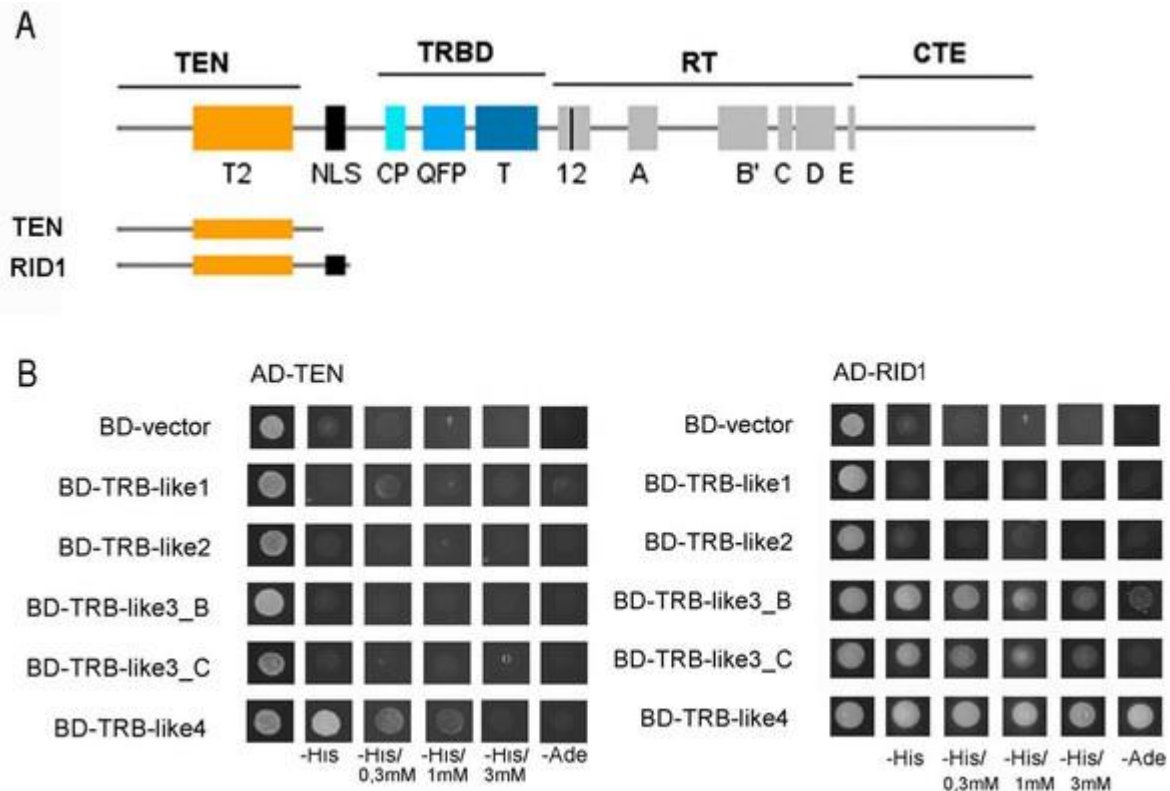
Fig. 4. Interactions of AcTRB-like proteins with AcTERT domains examined using Yeast-two hybrid system. A) Schematic view of plant telomerase reverse transcriptase protein subunit and its motifs and domains. RT – reverse transcriptase domain, CTE – C-terminal domain, TEN-telomerase esential N-terminal domain, NLS -Nuclear localization signal. So called RID1 fragment consists of TEN motif and NLS. (Modified according to [7]) B) AcTRB-like4 forms a strong interaction with AcRID1 and a weak interaction with AcTEN motif. AcRID1 forms complex with AcTRB-like3_B and AcTRB-like3_C. Neither AcTEN nor AcRID1 interacts with AcTRB-like1 and AcTRB-like2. Interactions were performed in both directions (prey x bait), and the results were in an agreement (data not shown). Co-transformation with an empty vector (AD/BD vector) was used as a negative control.

We found that AcTRB-like3_B, AcTRB-like3_C and AcTRB-like4 which form strong homo- and heterodimers interact also with the AcRID1 motif of the AcTERT subunit while AcTRB-like1 and AcTRB-like2 do not show any interaction with the N-terminal part of AcTERT. Interestingly, based on amino acid sequence, AcTRB-like2 and AcTRB-like3 proteins show a clear similarity to each other but AcTRB-like1 is less similar to AcTRB-like2 and AcTRB-like3 proteins. AcTRB-like4 shows a similarity to the others just in the Myb-like domain (not shown).

Future plans

Based on this finding, we are going to prepare fragments of AcTRB-like proteins to characterise a domain involved in interactions between AcTERT and AcTRB-like proteins, as

well as a domain engaged in the formation of homo- and heterodimeric complexes of AcTRB-like proteins. We will verify the interactions identified in Y2H using pull down assay and bimolecular fluorescence complementation (BiFC). Than we would like to test the specificity and affinity of DNA-protein (AcTRB-like) interactions with *Arabidopsis*-type, vertebrate-type and *Allium*-type telomere sequences.

Conclusion

The characterization of *Allium* telomeric sequence provided us with new research aims and questions. One of them adresses the impact of changes in telomeric sequence on the telomere nucleoprotein composition and its capping function. We found several candidates for telomere repeat binding proteins which are orthologous to the TRB proteins from *A. thaliana*. First of all, we analyzed direct protein-protein interactions. We tested formation of homomers and heteromers of AcTRB-like proteins, and interactions between AcTERT and AcTRB-like proteins in *A. cepa*. We found that AcTRB-like3_B, AcTRB-like3_C and AcTRB-like4 form strong homo- and heteromers and they also interact with AcRID1 motif of the AcTERT subunit.

Acknowledgement

Reference

[1] Fajkus, P., Allium telomeres unmasked: the unusual telomeric sequence (CTCGGTTATGGG)n is synthesized by telomerase, Plant J. 2016, 85, 337–347.

[2] Sykorova, E., Telomere variability in the monocotyledonous plant order Asparagales. Proc Biol Sci 2003, 270, 1893–1904.

[3] Sýkorová, E., Asparagales Telomerases which Synthesize the Human Type of Telomeres, Plant Mol. Biol. 2006, 60, 633–646.

[4] Peška, V., Characterisation of an unusual telomere motif (TTTTTTAGGG)n in the plant Cestrum elegans (Solanaceae), a species with a large genome, Plant J. 2015, 82, 644–654.

[5] Marian, C. O., The Maize Single myb histone 1 Gene, Smh1, Belongs to a Novel Gene Family and Encodes a Protein That Binds Telomere DNA Repeats in Vitro. Plant physiol. 2003, 133, 1336–1350.

[6] Schrumpfová, P., Characterization of two Arabidopsis thaliana myb-like proteins showing affinity to telomeric DNA sequence, Genome 2004, 47, 316–324.

[7] Procházková Schrumpfová, P., Telomere repeat binding proteins are functional components of Arabidopsis telomeres and interact with telomerase, Plant J. 2014, 77, 770–781.

[8] Mozgová, I., Functional characterization of domains in AtTRB1, a putative telomere-binding protein in Arabidopsis thaliana. Phytochemistry 2008, 69, 1814–1819.

INTENSITYANALYSER: WEB TOOL FOR ASSESSMENT OF TELOMERE LENGTHS FROM TERMINAL RESTRICTION FRAGMENT ANALYSIS

Martin Lyčka, **Jan Hapala, Petr Fajkus, Miloslava Fojtová, Jiří Fajkus, Vratislav Peška**

Mendel Centre for Plant Genomics and Proteomics, Central European Institute of Technology, Masaryk University, Brno, Czech Republic, 408297@mail.muni.cz

Summary

We have developed a web-based tool IntensityAnalyser that allows the calculation of the weighted median of telomere lengths from TRF intensity profiles taken from a third-party software. The estimation of the weighted median of telomere lengths by IntensityAnalyser was compared to the program TeloTool using TRF data from *Arabidopsis thaliana Rev-7* mutants.

Introduction

Telomeres, nucleoprotein structures that specify chromosome ends, play a crucial role in the maintenance of the eukaryotic genome integrity. Telomere shortening, caused by incomplete replication of chromosome ends by the lagging strand synthesis, is considered as a molecular clock. Due to the importance of telomeres, a determination of telomere lengths represents an often-used research and diagnostic tool [1]. To this day, there are several approaches on how to measure telomere lengths. One set of methods is based on a genomic DNA extraction and its subsequent analysis which includes either terminal restriction fragment (TRF) assessment or PCR-based methods: quantitative (qPCR) and single telomere length analysis (STELA). There are also cytogenetic methods that rely on quantitative fluorescent in situ hybridization (Q-FISH). Principles of these methods are thoroughly summarized in [2]. The most recent tools intended for the telomere length measurement are based on whole genome sequencing (WGS) [3, 4]. However, the TRF analysis remains a "gold standard" that is most commonly used and serves as a validation method for the other techniques [2, 5]. Briefly, the TRF method includes 1) restriction enzyme digestion, 2) ELFO, 3) Southern blot + hybridization with radioactively labelled probe, 4) Signal visualisation using a phosphoimager (intensity of the probe signal corresponding to the length and number of terminal fragments), 5) image analysis, and 6) data analysis. An evaluation of TRF data can be done with several available programs - e.g., TeloTool [6], Telometric 1.2 [7], or using TELORUN, an MS Excel sheet with computational formulas [8]. Nevertheless, all the above-mentioned methods encounter certain limitations, be it with the thought process behind the telomere length computation (reviewed in [5]) or technical difficulties (e.g., incompatibility with the new OS). For these reasons, we have developed a web-based application that is publicly available, user-friendly, and free of charge.

Experimental

IntensityAnalyser was developed in R using Shiny package (http://shiny.rstudio.com/). Below, we describe the workflow for the data analysis of the web app which is also depicted in Figure 1.

The web app IntensityAnalyser does not currently use TRF scan as the input directly but an excel sheet of the intensity profiles in the analysed lanes. Therefore, the image processing is so far reliant on a third-party software like Multi Gauge Ver. 3.0 (FUJI FILM). The exact format of the excel sheet is described in the tab "Upload file" (Fig. 1a). The valid estimation of the average telomere length based on the DNA electrophoretic mobility in agarose gel requires knowledge of the dependence between a respective fragment position and its molecular weight. A model of DNA migration through the gel is based on the intensity profiling in properly defined DNA weight molecular marker. For a regular user it requires to stipulate the marker in the tab "Marker" (Fig. 1b). The first column of the table in this tab contains the molecular weights of the marker fragments (natively set to the values of GeneRuler 1 kb DNA Ladder, Thermo Fisher Scientific). The adjacent column needs to be filled with numbers corresponding to the peaks of respective bands. In the next tab "pixel/MW ratio" (Fig. 1c), a user chooses an order of polynomial function that sufficiently fits the ladder. Based on the ANOVA tests between two adjacent polynomial models in ascending order, the order of polynomial function that met the criterion $p \leq 0.05$ last is recommended. In the tab "Length calc." (Fig. 1d), the user selects the area used for the telomere length calculation for each sample. In the standard cases of a unimodal distribution of the telomere fragments amount, it is recommended to use left and right threshold in the selection process. The intensity values of the left (1) and right (2) threshold line are defined for each sample as

$$OD_{lt} = OD_{lb} + 0.2(OD_{max} - OD_{lb}) \quad (1)$$

$$OD_{rt} = OD_{rb} + 0.2(OD_{max} - OD_{rb}) \quad (2)$$

where OD_{max} is the maximum signal intensity within the sequence $\{OD_n\}$, where n is the vertical number of pixels of the membrane; OD_{lb} is the average intensity of the 1% of the lowest intensity values within the sequence $OD_1, OD_2, ..., OD_m$, where m is the input of OD_{max}; OD_{rb} is the average intensity of 1% of the lowest intensity values within the sequence $OD_m, OD_{m+1}, ..., OD_n$, where n is the vertical number of pixels of the membrane and m is the input of OD_{max}.

To assess weighted median of telomere lengths from the selected area, it is necessary to calculate the sequence of cumulative sum of weighted signal intensities $\{C_n\}$, where each value is defined as

$$C_n = \sum_{k=1}^{n} \left(\frac{OD_k}{L_k}\right) = \frac{OD_1}{L_1} + \cdots + \frac{OD_n}{L_n}$$

where n is the vertical number of pixels of the membrane; OD_i is the signal intensity of pixel i within the sequence $\{OD_n\}$; L_i is the molecular weight of pixel i within the sequence $\{L_n\}$.

Weighted median of telomere lengths is defined as predicted value of L (molecular weight) for a given $C_n/2$ value of C (cumulative sum of weighted signal intensity) from a linear model based on two points $[C_i;L_i]$ and $[C_{i+1};L_{i+1}]$, where C_i and C_{i+1} are the closest values from the sequence $\{C_n\}$ defined as $C_i \leq C_n/2 < C_{i+1}$; $i \in \langle 1;n-1 \rangle$ and L_i and L_{i+1} are values of the same input (i, $i+1$) from the sequence $\{L_n\}$. A user can download a graph of the finished analysis in the tab "Graphic result" (Fig. 1e). Width and height of the graph can be modified.
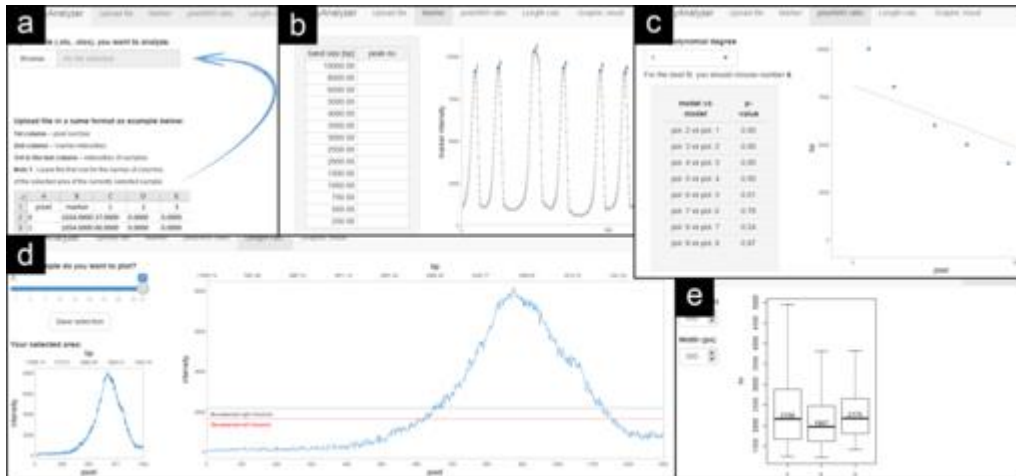

Fig. 1. Workflow of the IntensityAnalyser web app. (a) loading of the excel sheet with specified look; (b) marker setting; (c) determination of the polynomial model; (d) selection of the area of each sample that is used for the telomere length calculation; (e) downloadable graphic result.

Results and Discussion

To compare IntensityAnalyser with TeloTool, we analysed the TRF scan of telomere lengths in *Rev-7* mutants of *Arabidopsis thaliana* (Fig. 2a). It is obvious from the graph comparing both programs (Fig. 2b) that differences between telomere lengths in each sample are more pronounced in the case of Telotool than IntensityAnalyser. This is particularly evident in the case of the sample no. 5 which has estimated mean of telomere lengths of 2 744 bp. That is almost 200 bp from the second highest mean (sample no. 7). In the case of IntensityAnalyser, estimated weighted median of telomere lengths of the sample no. 5 is not much different from neither sample no. 7, nor the rest of the samples. The reason of this divergence is based on different ways how to calculate mean of telomere lengths or median of telomere lengths in both tools. While IntensityAnalyser computes weighted median of telomere lengths from the raw intensity profile values, Telotool fits a Gaussian curve to the intensity profile and models a new curve based on the correction of the higher molecular weight flank [6]. It is possible that IntensityAnalyser currently underestimates the real median of telomere lengths due to the probe intensity correction OD_n/L_n. A possible deviation from a linear dependence between signal intensity and molecular weight needs to be tested. Also, given the fact that the weighted median of telomere lengths calculation by IntensityAnalyser is largely determined by a user's area

selection, it is necessary to involve not only raw data (TRF scan) and resulting weighted median, but also minimal and maximal values of the selected area unless a user has complied with recommended thresholds. This guarantees reproducibility of the calculation.
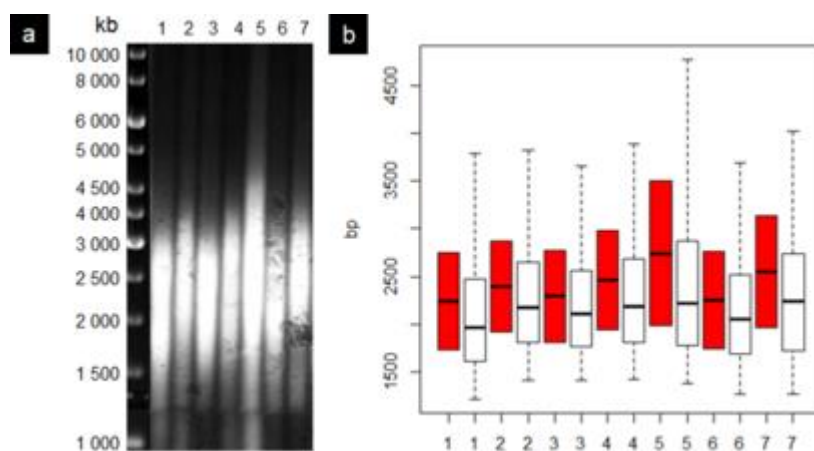

Fig. 2. (a) TRF scan of telomere lengths in *A. thaliana Rev-7* mutants; (b) predicted telomere length of samples from TRF scan (red boxes are corrected measurements from TeloTool v1.3 and white boxplots are measurements from IntensityAnalyser).

Conclusion

We have developed a new user-friendly web application IntensityAnalyser that allows to estimate the weighted median of telomere lengths from TRF intensity profiles taken from third-party software. Further optimization of the signal intensity correction is required as well as development of another web app that would allow to transform TRF scan to intensity profiles.

Acknowledgement

Reference

[1] Fajkus, J., Dvořácková, M., Sýkorová, E., Methods Mol. Biol. 2008, 463, 267-296.

[2] Aubert, G., Hills, M., Lansdorp, P. M., Mutat. Res. 2012, 730(1-2), 59-67.

[3] Ding, Z., Mangino, M., Aviv, A., Spector, T., Durbin, R., UK10K Consortium, Nucleic Acids Res. 2014, 42(9): e75.

[4] Farmery, J. H. R., Smith, M. L., NIHR BioResource - Rare Diseases, Lynch, A. G., Sci. Rep. 2018, 8(1): 1300.

[5] Fojtová, M., Fajkus, P., Polanská, P., Fajkus, J., Bio-protocol 2015, 5(23): e1671.

[6] Göhring, J., Fulcher, N., Jacak, J., Riha, K., Nucleic Acids Res. 2014, 42(3): e21.

[7] Grant, J. D., Broccoli, D., Muquit, M., Manion, F. J., Tisdall, J., Ochs, M. F., BioTechniques 2001, 31(6), 1314-1318.

[8] Baur, J. A., Wright, W. E., Shay, J. W., Methods Mol. Biol. 2004, 287, 121-136.

HOW TO TRAIN OUR CELLS TO BECOME YOUNGER – QUANTITATIVE BIOPHYSICS OF HUMAN TELOMERASE AND ITS GUARD SHELTERIN

Ctirad Hofr[1], Ivona Nečasová[1], Eliška Janoušková[1], Tomáš Janovič[1], Martin Stojaspal[1], Pavel Veverka[1]

[1] *LifeB - Laboratory of interaction and function of essential Biomolecules Chromatin Molecular Complexes, CEITEC and NCBR, Faculty of Science, Masaryk University, Brno, Czech Republic*

Summary

Telomere maintenance is a highly coordinated process that controls cell aging. Misregulation of telomere maintenance is linked to cancer and telomere-shortening syndromes. Recent studies have shown that the TEL-patch is a cluster of amino acids on the surface of the shelterin component TPP1 that is essential for the recruitment of telomerase to the telomere in human cells. The Cech laboratory (Colorado University Boulder) and our laboratory (Masaryk University) optimized an in vitro assay to quantitatively measure binding of the TEL-patch to telomerase and extension of the first telomeric repeat. We quantified how the TEL-patch contributes to the translocation and stabilizes the association between telomerase and telomeric DNA substrates, providing a molecular explanation for its contributions to telomerase recruitment and action. Additionally, we quantitatively described interactions of TRF2 - central shelterin subunit that folds human telomeres into loops to prevent unwanted DNA repair and chromosome end joining. We found that the basic B-domain of TRF2 stabilizes the displacement loop (D-loop) and thus reduces unwinding by RPA and BLM helicase, whereas the formation of the RAP1–TRF2 complex restores DNA unwinding. To understand how the B-domain of TRF2 affects DNA binding and D-loop processing, we analyzed DNA binding of full-length TRF2 and a truncated TRF2 construct lacking the B-domain. We found that the B-domain improves TRF2's binding to DNA via enhanced long-range electrostatic interactions. We determined a structural envelope model revealing that the B-domain is flexible in solution but becomes rigid upon binding to telomeric DNA. We propose a mechanism for how the B-domain stabilizes the D-loop and contributes to improved DNA affinity of TRF2 in general. Additionally, we suggest how human RAP1 regulates TRF2 attraction and specificity to DNA and thus degree of telomere protection by shelterin.

Introduction

Telomeres are specialized nucleoprotein caps at linear chromosomal termini that are essential for genomic integrity. Telomerase is the enzyme responsible for the synthesis of telomeric DNA repeats [1], which are bound by protective telomeric protein complexes [2]. Telomerase

enzymatic action are essential for both germ cells and stem cells to retain proliferative capacity [3]. In dividing somatic cells, in which telomerase is not expressed, telomeres progressively erode as a result of incomplete 3′ end-replication and the cells enter replicative senescence [4]. However, if cells avoid apoptosis by reactivating telomerase, cellular immortalization can occur.

Telomerase activity is molecular marker of 80–95% of cancers [5]. In contrast, telomerase or telomere maintenance deficiencies in proliferative cell populations cause organ failure in a class of telomere-shortening diseases, examples of which include dyskeratosis congenita, idiopathic pulmonary fibrosis, and aplastic anemia [6]. Thus, the proper regulation of telomerase is critical to telomere and genome homeostasis. Telomerase and shelterin work synergistically to promote telomere homeostasis. Human shelterin is the six-protein complex responsible for protecting telomeres and regulating telomerase action [7]. Shelterin proteins are well evolutionary conserved as they regulate telomerase recruitment in mammals and in yeasts as well [2]. TPP1-POT1 sub-complex of shelterin that recruits telomerase [8] and stimulate processivity through (i) decreasing the rate of primer dissociation from the enzyme and (ii) increasing the apparent rate of telomerase translocation and efficiency [9]. Telomeric repeat binding factor 2 (TRF2) plays a central role in the telomeric DNA loop formation and mediates different stages of telomere protection [10].Recently, we showed that the complexation of shelterin proteins TRF2 and RAP1 improves TRF2 binding specificity toward telomeric DNA [11]. Human RAP1 is the closest binding partner of TRF2. RAP1 mediates genome stability as it inhibits non-homologous end-joining at telomeres [12]. Our quantitative biology experiments and available structural data suggest that RAP1 prevents nonspecific DNA binding of TRF2 via its B-domain.

Experimental

Competition telomerase assays: Telomerase reaction was initiated by simultaneous adding of two substrate primers of different length. Previously, primers were incubated in with POT1 and TPP1 (either wild-type or mutant TPP1) for 30 min at room temperature, followed by 20 min at 4 °C. While primers were complexed with TPP1-POT1, reactions containing telomerase, buffer, and dNTPs were assembled and cooled to 4 °C for 20 min. Competition reactions were stopped by removing aliquots of the reaction at various time.

D-loop unwinding assay: The unwinding assay has been performed according to helicase reaction protocols published previously [13]. D-loop substrates fluorescently labeled with fluorescein were incubated with proteins at 25°C for 5 min in the reaction buffer containing an ATP regenerating system.

Results and Discussion

The TEL-patch on TPP1 stimulates the translocation of human telomerase and decrease dissociation rate of telomerase from substrate. Wild-type TPP1-POT1 or TEL-patch mutant TPP1-POT1 with DNA primer were pre-bound to telomerase. The translocation rates of telomerase were measured. Quantitative translocation constants confirmed that the TEL-patch

contributes to the apparent translocation rate and increases the efficiency of translocation. We measured the dissociation rates for primer alone, primer bound by wild-type TPP1-POT1, and primer bound by TEL-patch mutant TPP1-POT1. The results indicate that the TEL-patch stabilizes the interaction between primer-POT1-TPP1 and telomerase during active repeat synthesis and thus increases the efficiency of telomerase translocation.
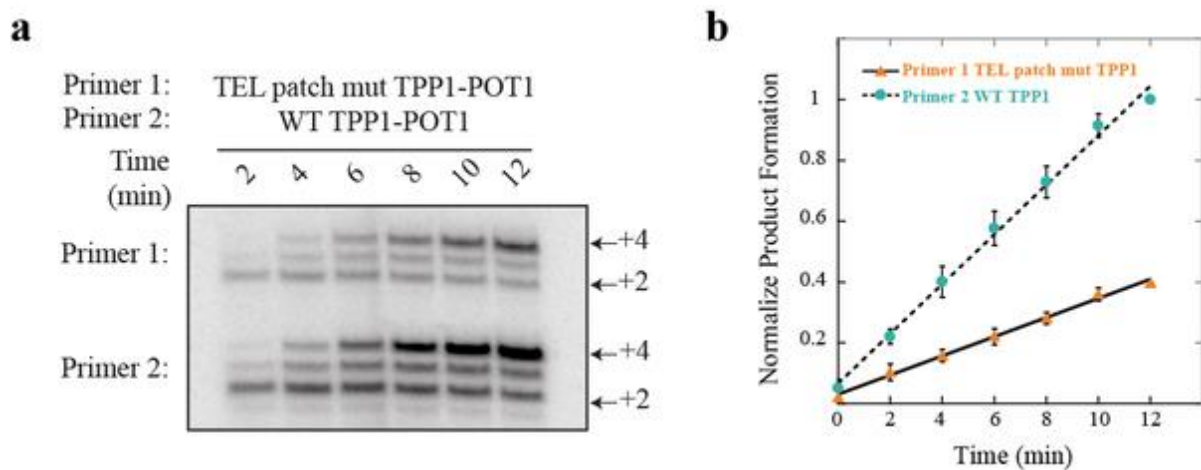

Figure 1. **The TEL-patch of TPP1 contributes to substrate recruitment and extension by telomerase.** (a) *In vitro* telomerase competition assays between two primers: a 38-nt primer 2 bound with wild-type TPP1-POT1 and a 44-nt primer 1 bound by TEL-patch mutant TPP1-POT1. (b) Initial velocity plot for competition assay - circles indicate wild-type TPP1-POT, squares indicate TEL-patch mutant TPP1-POT1 [14].

TRF2 reduces unwinding of D-loops by BLM whereas RAP1 restores DNA unwinding. We observed that TRF2 pre-bound to D-loop R4 reduced significantly DNA unwinding of BLM (Figure 2b). Upon pre-incubation of TRF2 lacking B-domain with D-loops, we observed that the extent of BLM unwinding decreased (Figure 2b). Similarly, upon pre-incubation of RAP1–TRF2 complex with D-loop unwinding levels came back to the level observed for TRF2 lacking B-domain. In other words, the extent of unwinding was restored almost entirely to the original level when the B-domain was removed from TRF2 or RAP1–TRF2 complex occupied the D-loop.
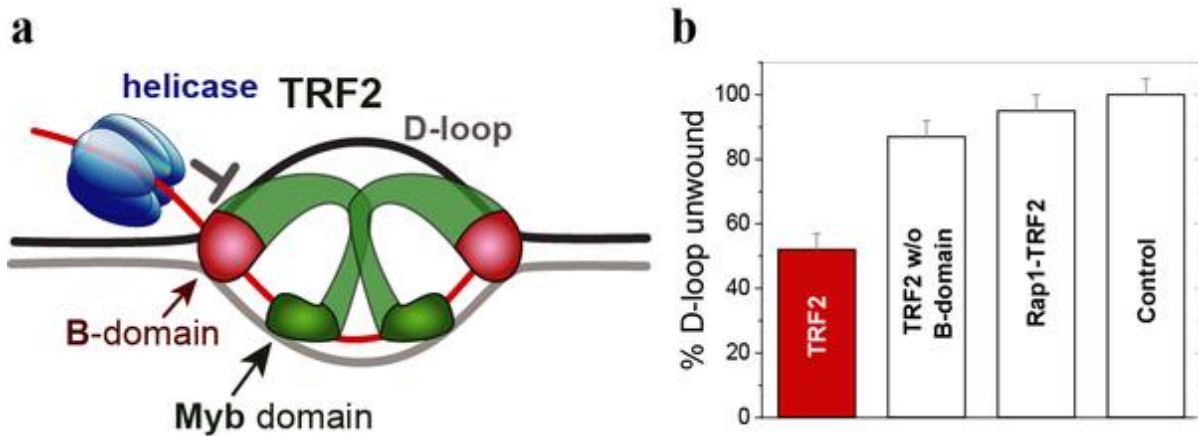
Figure 2. **The B-domain of TRF2 reduces unwinding of D-loops by BLM whereas RAP1 restores DNA unwinding.** (a) Proposed mechanism for how the B-domain of TRF2 inhibits telomeric D-loop unwinding by BLM. (b) A fluorescently labeled D-loop containing four telomeric repeats was unwound by helicase BLM in presence of either full-length TRF2, TRF2 lacking B-domain or RAP1–TRF2 complex [15].

We speculate that TRF2 via its B-domain binds branched parts of D-loops and prevents their resolution. Thus, TRF2 dimer fixes the D-loop structure via simultaneous binding of the Myb domain to double-stranded invading DNA regions and the B-domain to single-double strand junctions in the initial part of the D-loop. When the complex RAP1–TRF2 binds the D-loop, RAP1 prevents the B-domain interaction with DNA. Thus, RAP1 eliminates non-specific DNA binding of TRF2 N-terminus via the B-domain. Hence, RAP1 promotes D-loop unwinding by helicases despite the TRF2 presence.

Conclusion

We have described the contributions of the TEL-patch to telomerase recruitment using in vitro substrate competition assay that showed that the TEL-patch of TPP1 participates in the preferential extension of TPP1-POT1-bound substrates and that mutation of the TEL-patch results in less efficient substrate usage by telomerase. In addition, we showed that TEL-patch mutation decreases the apparent translocation rate along with efficiency of translocation, and increases dissociation extent of primer DNA from telomerase.

Further, we demonstrated that the B-domain of TRF2 reduces unwinding of dsDNA by BLM. We revealed that human shelterin protein RAP1 upon complexation with TRF2 restores D-loop susceptibility to unwinding. Additionally, we demonstrated that the flexible B-domain becomes rigid and structured when bound to DNA, which explains the increased D-loop stability and reduced unwinding in the presence of TRF2. Finally, we propose a model of domain arrangement of the shelterin proteins TRF2 and RAP1 that suggests how the B-domain of TRF2 stabilizes D-loops and similar DNA structures.

Acknowledgement

Reference

[1] Cech, T.R., Cell, 2004. 116, 273-279.

[2] Nandakumar, J. and T.R. Cech, Nat Rev Mol Cell Biol, 2013. 14, 69-8.

[3] Batista, L.F.Z. and S.E. Artandi, Current Opinion in Genetics & Development, 2013. 23,526-53.

[4] Levy, M.Z., et al., Journal of Molecular Biology, 1992. 225, 951-960.

[5] Stewart, S.A. and R.A. Weinberg, Annual Review of Cell and Developmental Biology, 2006. 22, 531-557.

[6] Armanios, M. and E.H. Blackburn, Nature Reviews Genetics, 2012. 13, 693.

[7] de Lange, T., Genes Dev, 2005. 19, 2100-10.

[8] Wang, F., et al., Nature, 2007. 445, 506-510.

[9] Latrick, C.M. and T.R. Cech, The EMBO Journal, 2010. 29, 924-933.

[10] Feuerhahn, S., et al., Trends in Biochemical Sciences, 2015. 40, 275-285.

[11] Janouskova, E., et al., Nucleic Acids Res, 2015. 43, 2691-700.

[12] Sarthy, J., et al., The EMBO Journal, 2009. 28, 3390-3399.

[13] Youds, J.L., et al., Science, 2010. 327, 1254-8.

[14] Dalby, A.B., C. Hofr, and T.R. Cech, J Mol Biol, 2015. 427, 1291-303.

[15] Necasova, I., et al., Nucleic Acids Research, 2017. 45, 12170-12180.

Full Papers - Poster Presentations

P1 INNOVATION OF DIAGNOSTICS ALGORITHM FOR ACUTE KIDNEY INJURY USING A NEW BIOMARKERS – ESTIMATED REFERENCE RANGE FOR HEALTHY CHILDREN

Katerina Andelova[1,2,3], **Zdenek Svagera**[2,3], **Vitezslav Jirik**[1], **Michal Hladik**[4,5]

[1]*Department of Epidemiology and Public Health, Faculty of Medicine, University of Ostrava, Ostrava, Czech Republic*

[2]*Institute of Laboratory diagnostics, University Hospital Ostrava, Ostrava, Czech Republic, katerina.andelova@fno.cz*

[3]*Department of Biomedical Sciences, Faculty of Medicine, University of Ostrava, Ostrava, Czech Republic*

[4]*Department of Pediatrics and Neonatal Care, Faculty of Medicine, University of Ostrava, Ostrava, Czech Republic*

[5]*Pediatrics Clinic, University Hospital Ostrava, Ostrava, Czech Republic*

Summary

A recent epidemiological studies have confirmed that acute kidney injury (AKI) has developed in 30 % of cases in critically ill children and young adults. Serum creatinine is considered as a gold standard in the evaluation of renal dysfunction such as AKI. However, its concentration is influenced by age, muscle mass, hydratation status and other non-renal causes. Several studies have investigated the potential role of urine Neutrophil gelatinase-associated lipocalin (NGAL) and Kidney Injury Molecule 1 (KIM-1) as a new predictive and prognostic biomarkers in AKI. Their levels can be increased in urine in the first 24 hours after acute injury. The early identification of AKI onset and risk stratification of AKI progression or AKI-related complications are essential for early treatment and prevention of the development of chronic kidney disease and end stage renal disease. Therefore, our aim was to assess the urine levels of NGAL and KIM-1 in healthy children and secondly, we estimated reference range of these biomarkers for early diagnostics of AKI.

Introduction

Acute kidney injury (AKI) represents a clinical condition characterized by a rapid decline of renal function with elevated serum creatinine and rapid reduction of a glomerular filtration rate (eGFR) due to ischemia, nephrotoxicity, obstruction of urinary track, sepsis and other causes

[1]. The diagnostic criteria for AKI in children was classified according to pediatric RIFLE criteria (Risk-Injury-Failure-Loss and End stage renal disease - involves stages from initial changes in the eGFR to total organ failure) proposed by clinical practice guidelines by Kidney Disease: Improving Global Outcomes (KDIGO) [2]. In the recent study, Filho and colleagues pinpointed that the urinary NGAL and KIM-1 were expressed and elevated in AKI very early after defined insult and they have been shown to be more sensitive than serum creatinine as the conventional biomarker [1,3].

Neutrophil gelatinase-associated lipocalin (NGAL) is a potential novel biomarker in AKI. NGAL is a low molecular weight protein that is expressed primarily by immune cells (neutrophils) and at very low concentration also in several tissues. NGAL increases massively in the first urine output after early AKI [4, 5]. These characteristics show that NGAL may represent an early, sensitive, non-invasive urinary biomarker for ischemic and nephrotoxic kidney injury.

Kidney Injury Molecule 1 (KIM-1) is a transmembrane protein located and expressed by the proximal tubule epithelial cells at low concentration in the normal function of kidney, but its production can increase 50-fold in urine after acute kidney injury [6]. The extracellular domain of KIM-1 is detected after AKI in urine and the increased urinary KIM-1 has been noted in some form of proximal tubular injury [5].

Therefore, our aim was to assess the urine levels of NGAL and KIM-1 in healthy children and secondly, we estimated reference range for these biomarkers to early diagnostics of AKI.

Experimental

Baseline characteristics of the study group are summarized in Tab. 1. A total of 105 children (60 boys and 45 girls) at the age of 10.9 ± 2.97 years (mean $\pm$ SD) were included. The youngest child was 6 years old and the oldest was 16 years old. The study protocol was approved by the ethical committee University Hospital Ostrava – all participating healthy children and their parents provided written informed consent. The study protocol was in accordance with the principles of the Declaration of Helsinki.

The inclusion criteria of our study group were $0 - 18$ years, without the presence of diseases with non-specific etiology. The exclusion criteria were previous kidney disease and significant proteinuria or microalbuminuria defined as PCR (Protein Creatinine Ratio) ≥ 15.0 mg/mmol and ACR (Albumin Creatinine Ratio) ≥ 3.0 mg/mmol.

Urinary biomarkers determination

Morning urine samples were collected and stored at -80 °C until analysis. Before analysis, the urine samples were centrifuged at 500 g for 10 min at room temperature and supernatant was analyzed. Urine NGAL and KIM-1 was measured by a commercially available ELISA kits: Human NGAL ELISA Kit (BioPorto Diagnostics, Danmark) and Human KIM-1 ELISA Test

Kit (BioAssay Works, USA) with application for human blood and urine samples. All specimens were diluted to obtain the concentration according to ELISA kit instructions. The results of the enzymatic reaction were quantified using an automatic microplate photometer DSX (Dynex Technologies, Germany) using a 450 nm (650 nm) for NGAL and 405 nm (490 nm) for KIM-1 and compared with a standard curve.

In the same urine specimens, the creatinine concentration was determined by the enzymatic assay on AU 5811 analyzer (Beckman Coulter, USA) and albumin concentration using the BN ProSpec analyzer (nephelometric determination, Siemens, Germany).

Tab. 1 Baseline characteristics of the study group

Sex (M/F)	60/45
Age (years – mean ± SD)	10.9 (7.9 – 13.9)
Urinary creatinine (mmol/l)	12.3 (7.1 – 17.5)

Results and Discussion

Statistical analysis was performed using MedCalc statistical software (version 16.1.2, Belgium). Results are expressed as the mean ± standard deviation. The decisive aspect was to exclude probands with renal disease. All results failed the Shapiro–Wilk test for normal distributions ($p < 0.05$). We used a Box-Cox transformation technique to stabilize variance, make the data more normal distribution-like. Partial correlations were performed with adjustment for the various parameters affecting the reference range (age, sex). Outliers were identified and removed according to Tukey's method. The reference range for each biomarker was expressed as the 2.5th and 97.5th quantiles (the 95% reference intervals). 90% confidence interval (CI) for the lower and upper limit of the reference interval was expressed as well (Tab. 2).

Urinary excretion of NGAL and KIM-1 were expressed as NGAL or KIM-1 to creatinine (Crea) ratio (µg/mmol Crea) to standardize and correct the changes in urine (Tab. 3). Our results confirm previous findings for reference range to NGAL in urine, but for the first time we define reference range for KIM-1 in urine in healthy Czech children [7].

Tab. 2 Estimated 95% reference interval for each biomarker by quantile regression

Study group and biomarkers	U_NGAL (µg/l) 2.5th quantile (90% CI)	U_NGAL (µg/l) 97.5th quantile (90% CI)	U_KIM-1 (µg/l) 2.5th quantile (90% CI)	U_KIM-1 (µg/l) 97.5th quantile (90% CI)
Combined (M, F)	9.89 (7.93 – 12.31)	108.4 (88.9 – 131.7)	0.12 (0.07 – 0.19)	2.17 (1.88 – 2.50)

Tab. 3 Estimated reference intervals of NGAL or KIM-1 to creatinine ratio in urine

Study group and biomarkers	U_NGAL/Crea (μg/mmol) 2.5th quantile (90% CI)	U_NGAL/Crea (μg/mmol) 97.5th quantile (90% CI)	U_KIM-1/Crea (μg/mmol) 2.5th quantile (90% CI)	U_KIM-1/Crea (μg/mmol) 97.5th quantile (90% CI)
Combined (M. F)	3.72 (2.46 – 4.98)	12.0 (10.7 – 13.26)	0.08 (0.06– 0.12)	0.27 (0.24 – 0.30)

Conclusion

Renal clinical practice requires highly sensitive and specific diagnostic and prognostic biomarkers for acute kidney injury. The early identification of AKI onset and risk stratification of AKI progression or AKI-related complications are essential for early treatment and prevention of the development of chronic kidney disease and end stage renal disease [8].

Our finding - we investigated a new prognostic and predictive biomarkers for acute kidney injury. Urinary NGAL and KIM-1 are abundantly expressed and elevated in acute kidney injury. In this study we present the range of urinary NGAL and KIM-1 levels determined in a large number of healthy children and secondly we estimated reference range for these biomarkers. In addition, we estimated reference range as the NGAL or KIM-1 to urine creatinine ratio (μg/mmol) to standardize and correct the changes in urine concentration.

Acknowledgement

Reference

[1] Avner, E. D. et al. Pediatric Nephrology. 7th edition, Springer, Berlin 2016.

[2] Kidney Disease: Improving Global Outcomes (KDIGO) Acute Kidney Injury Work Group. KDIGO Clinical Practice Guideline for Acute Kidney Injury. Kidney inter., Suppl. 2012, 2, 1-138.

[3] Filho, L., Grande, A., Colonetti, T., Della E., de Rosa, M. Accuracy of neutrophil gelatinase-associated lipocalin for acute kidney injury diagnosis in children: systematic review and meta-analysis. Pediatr Nephrol 2017, 32, 1979-1988.

[4] Bagshaw, S., Bennett, M., Haase, M., Haase-Fielitz, A., Egi, M., Morimatsu, H., Damico, G., Goldsmith, D., Devarajan, P., Bellomo, R. Plasma and urine neutrophil gelatinase-associated lipocalin in septic versus non-septic acute kidney injury in critical illness 2010, 36, 452-461.

[5] Gearoid, M., Sushrut S. Biomarkers in Nephrology. Am J Kidney Dis 2013, 62(1), 165-178.

[6] OSeaghdha, C., Hwang, S., Larson, M., Meigs, J., Ramachandran, S., Fox, C. Analysis of a Urinary Biomarker Panel for Incident Kidney Disease and Clinical Outcomes. J Am Soc Nephrol 2013, 24, 1880-1888.

[7] Wu, I., Parikh, Ch. Screening for Kidney Diseases: Older Measures versus Novel Biomarkers. Clin J Am Soc Nephrol 2008, 3, 1895-1901.

[8] Tesař, V., Viklický, O. et al. Klinická nefrologie. 2th edition, Grada Publishing, Praha 2015.

P2   BIOANALYTICAL EVALUATION OF A NOVEL DEXRAZOXANE ANALOGUE JAS-2 AND ITS PRODRUG - IN VITRO AND PILOT IN VIVO STUDIES

Hana Bavlovič Piskáčková[1], **Petra Reimerová**[1], **Anna Jirkovská**[2], **Veronika Skalická**[2], **Petra Brázdová**[3], **Martin Štěrba**[3], **Petra Kovaříková-Štěrbová**[1]

[1]*Department of Pharmaceutical Chemistry and Pharmaceutical Analysis, Faculty of Pharmacy in Hradec Králové, Charles University, Akademika Heyrovského 1203, 500 05 Hradec Králové, Czech Republic*

[2]*Department of Biochemical Sciences, Faculty of Pharmacy in Hradec Králové, Charles University, Akademika Heyrovského 1203, 500 05 Hradec Králové, Czech Republic*

[3]*Department of Pharmacology, Faculty of Medicine in Hradec Králové, Charles University, Šimkova 870/13, 500 03 Hradec Králové, Czech Republic*

Summary

The clinical use of one of the most effective anticancer drugs – anthracyclines is limited by the incidence of cardiotoxicity, especially its chronic form, which lead to the development of congestive heart failure. JAS-2 was synthesized as a novel analogue of dexrazoxane, the only approved drug effective in preventing anthracycline induced cardiotoxicity. JAS-2 is more effective in protection of neonatal rat cardiomyocytes from toxic effect of anthracyclines as compared with DEX. The use of JAS-2 is limited by poor solubility. A pro-drug with a code name - GK-667 was prepared to improve the solubility of JAS-2 in water. A modern analytical method is required to investigate the stability of GK-667, its conversion to the active form as well as further metabolism of JAS 2.

Introduction

The limitation of anticancer therapy with anthracyclines (daunorubicine, doxorubicine) is the risk of cardiotoxicity, mainly its chronic form, which may result in heart failure [1]. The pathophysiology of anthracycline induced cardiotoxicity still remains unclear. Apart from other theories, recent investigation suggests, that interaction of anthracyclines with topoisomerase IIβ may be involved in their cardiotoxic effect [1, 2]. This hypothesis is supported by the fact, that dexrazoxane (DEX), the only approved cardioprotective drug against anthracycline-induced toxicity, can interact with topoisomerase IIβ as an inhibitor [3]. JAS-2 was synthetized as a novel analogue of DEX. It was found to be more effective in protection of neonatal rat cardiomyocytes from toxic effect of anthracyclines in vitro as compared to DEX. However, JAS-2 suffers from poor solubility in water which is a certain obstacle for the

examination of its effect in vivo. Therefore, a pro-drug with a code name - GK-667 was prepared to improve the solubility of JAS-2. A modern analytical method is required to investigate the stability of GK-667, its conversion to the active form as well as further metabolism of JAS-2.

The aims of this work were 1) to optimize and validate UHPLC-MS/MS method for determination of GK-667, JAS-2 and its metabolite (JAS-2met) in DMEM medium, plasma and cardiac cells (NVCMs), and 2) to apply the method for analysis of samples from in vitro and in vivo experiments.

Experimental

The analyses were performed using an UHPLC system (Nexera, Shimadzu, Japan) coupled with a triple quadrupole mass spectrometer with ESI ion source (LCMS-8030, Shimadzu, Japan). The optimal separation was achieved on Luna Omega Polar column (100 x 3.0 mm, 2.5 µm, Phenomenex, USA) protected with a guard column. A mixture of ammonium formate and acetonitrile in a gradient mode was used as a mobile phase (Fig. 1). Quantification was done using SRM for higher selectivity.
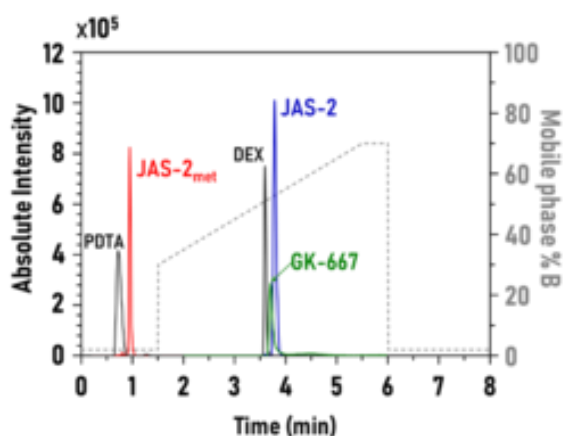
DMEM medium was treated with dilution five times using MeOH 10%. Plasma samples (50µl) were precipitated using 250 µl of MeOH, mixed and then centrifuged (10 min, 10,000 rpm, 4°C). NVCMs were washed twice with PBS (at 4°C) and scraped into a small volume of PBS. The solution was centrifuged (700×g, 10 min, 4°C) and supernatant was removed. The cell pellet was precipitated by MeOH (250 µl), homogenized in ultrasonic bath (2 min, 4°C), mixed on Vortex and then centrifuged (10,000 rpm, 10 min, 4°C). Supernatant from both plasma and NVCMs was filtered (0.22 µm) prior analysis. Each sample was divided into two aliquots. To increase ionization of GK-667 it was necessary to acidify the samples with formic acid (to final concentration of 0.1%) while ionization of JAS-2met was strongly suppressed in acidic pH, therefore they were assayed from separate aliquots. Method was validated according to FDA guideline for determination of JAS-2met, JAS-2 and GK-667 in DMEM medium, plasma and NVCMs with regards to linearity, precision and accuracy.

GK-667 and JAS-2 (100 μmol/l) were incubated in DMEM medium, plasma and with NVCMs at 37°C. NVCMs were collected at 0, 3, 6, 12 and 24 hours and DMEM medty of Medicine in Hradec Kralove, Charles University. Two rabbits received a single dose of GK-667 (5 mg/kg) in 2-minute i.v. infusion into the marginal ear vein, plasma samples were collected at several time intervals to describe the pharmacokinetic profile.

Results and Discussion

The UHPLC-MS/MS method for analysis of GK-667, JAS-2 and JAS-2met was optimized and validated in DMEM, plasma and NVCMs. Linearity of the method was evaluated in both plasma and DMEM medium over the concentration ranges from 1, 0.5 or 0.2 to 100 μmol/l, for GK-667, JAS-2 and JAS-2met, respectively. The following ranges were used for NVCM cells: 10 - 100 pmol/106cells (GK-667), 5 - 100 pmol/106cells (JAS-2) and 2 - 50 pmol/106cells (JAS-2met).

The stability study revealed that GK-667 is rapidly degraded both in the cell culture medium and plasma. Simultaneously, emerging JAS-2 is slowly converted to its open-ringed metabolite, analogically to DEX. In DMEM medium the concentration of JAS-2met determined after 24 hours of incubation is equimolar to the initial concentration of GK-667, in contrast with plasma. While the rate of degradation of JAS-2 in plasma is similar to DEX, the compound JAS-2 is degraded faster in DMEM. Intracellular concentrations of GK-667 were bellow LLOQ which is in line with its fast degradation in DMEM. The concentrations of JAS-2 and JAS-2met measured inside the cells corresponded with data obtained after incubation of NVCMs with DEX. After i.v. administration of GK-667 to rabbit, only JAS-2 was detected. GK-667 and JAS-2met were bellow LLOQ. The method was able to monitor JAS-2 till the end of the experiment (6 hours), which proved its applicability for description of the pharmacokinetic profile of the drug.

Conclusion

The study provides novel data for investigation of the cardioprotective potential of novel DEX analogue, JAS-2. The results of stability study will be further used for correlation of activation/metabolism of GK-667/JAS-2 with cardioprotective effect. Furthermore, it could help understanding the structure-activity relationship in the group of DEX analogues. The developed analytical method will be further used for analysis of samples from ongoing in vivo experiments.

Acknowledgement

Reference

[1] Sterba, M.; Popelova, O.; Vavrova, A.; Jirkovsky, E.; Kovarikova, P.; Gersl, V.; Simunek, T., Oxidative stress, redox signaling, and metal chelation in anthracycline cardiotoxicity and pharmacological cardioprotection. Antioxid Redox Signal 2013, 18 (8), 899-929.

[2] Zhang, S.; Liu, X.; Bawa-Khalfe, T.; Lu, L. S.; Lyu, Y. L.; Liu, L. F.; Yeh, E. T., Identification of the molecular basis of doxorubicin-induced cardiotoxicity. Nat Med 2012, 18 (11), 1639-1642.

[3] Vavrova, A.; Jansova, H.; Mackova, E.; Machacek, M.; Haskova, P.; Tichotova, L.; Sterba, M.; Simunek, T., Catalytic inhibitors of topoisomerase II differently modulate the toxicity of anthracyclines in cardiac and cancer cells. PLoS One 2013, 8 (10), e76676.

[4] Jirkovsky, E.; Jirkovska, A.; Bures J., Chladek, J.; Lencova, O.; Stariat, J.; Pokorna, Z.; Karabanovich, G.; Roh, J.; Brazdova, P.; Simunek, T.; Kovarikova, P; Štěrba, M., Pharmacokinetics of the Cardioprotective Drug Dexrazoxane and Its Active Metabolite ADR-925 with Focus on Cardiomyocytes and the Heart. J Pharmacol Exp Ther. 2018; 364 (3):433-46.

P3 CHARACTERIZATION OF CHOLESTERYL ESTERS USING NANOPARTICLES-ASSISTED DESORPTION MASS SPECTROMETRY

Jakub Bělehrad[1], Vendula Roblová[1], Jan Preisler[1,2]

[1]*Laboratory of Bioanalytical Instrumentation, Department of Chemistry, Masaryk University, Brno, Czech Republic, 423723@mail.muni.cz*

[2]*CEITEC – Central European Institue of Technology, Masaryk University, Brno, Czech Republic*

Summary

This paper deals with the development of a method for the determination of a specific cholesteryl ester by number and position of double bonds of fatty acyl using Surface-Assisted Laser Desorption/Ionization Tandem Mass Spectrometry (SALDI MS/MS). The developed method uses Mesosilver colloid silver suspension for succesfull ionization of these lipids. In SALDI MS analysis, we observed the fragmentation of cholesteryl esters directly in the source. However, we were able to detect only adducts of fatty acyl with silver $[FA+Ag]^+$. Detected $[FA+Ag]^+$ ions served as precursor ions for Post-Source Decay Tandem Mass Spectrometry with Laser-Induced Dissociation (LID PSD MS/MS). The fragmentation of an individual fatty acyl differed by number and position of their double bonds excepting cholesteryl stearate, fatty acyl of which is impossible to fragment by whatever way.

Introduction

Cholesteryl esters

Cholesteryl esters are a group of substances commonly found in blood plasma. These lipids serve as an immediate source of cholesterol for a living organism. However, their high concentrations in the blood can cause atherosclerosis (the disease in which the inside of an artery narrows due to the build-up of plaque), which may result in a many of cardiovascular diseases ending with a heart attack or stroke. Moreover, cholesteryl esters associate with several tumors [1-4] or Alzheimer's disease [5]. The monitoring of these lipids in different biological samples can indicate a possible disease but also help to understand the proportion of individual cholesterol esters in these diseases. This work offers the method that allows fast, simple and definite identification of specific cholesterol esters.

Substrate-Assisted Laser Desorption/Ionization (SALDI)

The Surface-Assisted Laser Desorption/Ionization technique (SALDI) is based on a similar principle to Matrix-Assisted Laser Desorption/Ionization (MALDI). A difference is in the replacement of an organic matrix by a suitable surface which absorbs laser energy and transfers it to the analyte as the matrix in MALDI does. A noninterfering of the surface with analyte signals leading to successful analyzes of low molecules is an advantage of this technique [6]. Nowadays a large surface of nanoparticles and its photo-absorption at the working laser wavelength allows using of nanoparticles of the various elements (Ag, Au, etc.) [7-9] as a matrix.

Experimental

Sample preparation and sample analysis

We selected four cholesteryl esters; cholesteryl stearate, cholesteryl oleate, cholesteryl linoleate, and cholesteryl arachidonate as model standards. Then, we prepared solutions of all standards at a concentration of 1 mg.mL^{-1} by dissolving a weighed amount of the standard in a required amount of hexane or chloroform. In the other step, we applied 0.1 µL of these solutions onto the MALDI plate (MTP Anchor 384), and after solvent evaporation, we overlayed dried droplets by 0.5 µL of colloidal MesoSilver silver suspension with a minimum nanoparticle concentration of 20 ppm. Then the MALDI plate with the analyzed standards was placed into MALDI mass spectrometer (Autoflex Speed, Bruker Daltonics, Germany). Finally, SALDI MS and SALDI MS/MS spectra were measured. The calibration of the mass spectrometer was performed on the observed Ag$^+$ silver ions and Ag^{n+} clusters (n = 2-9).

Results and Discussion

In the SALDI MS analysis, we observed the fragmentation of cholesterol esters directly in the source. The fragmentation led to the formation of the adducts ions of the fatty acyl with silver [FA+Ag]$^+$. Because a bonded silver consists up of two nearly identically abundant isotopes, we easily identified the adduct ions due to their characteristic doublet. We selected these adduct ions as precursor ions for the following SALDI MS/MS due to its high signal intensity. On the other hand, the adduct ions of entire cholesteryl ester molecule with silver (or possibly with another cation) were not observed.

The SALDI MS/MS results show that the degree of post-source fragmentation of cholesteryl fatty acyls increased with the number of double bonds on the fatty acyl. Only the [FA+Ag]$^+$ adduct ions of cholesteryl stearate were not fragmented. Probably due to the absence of a double bond on the carbon chain of the fatty acyl. Cholesteryl oleate [FA+Ag]$^+$ adduct ions gave only one fragment ion, cholesteryl linoleate provided four fragment ions, and for cholesteryl arachidonate twelve fragment ions were observed. Each standard provided different fragment ions depending on the position of the double bonds. In the spectrum of cholesterol linoleate and arachidonate, fragment ions without carboxyl group were found. It is caused by a nonspecifically bond of silver to any double bond of fatty acyl. This finding shows the use of silver for lipids fragmentation differs from other used metals, i.e., barium or lithium which

bond specifically to the carboxyl group of fatty acyls. In conclusion, the use of silver nanoparticles enables new possibilities for the analysis of cholesteryl esters and other lipids.

Conclusion

In this study, the SALDI MS/MS technique was successfully used to characterize various cholesteryl esters according to their different fatty acid. Experiments showed that each cholesteryl ester could be identified on the base of different fragmentation of the bound fatty acid. Unfortunately, a low yield of fragmentation on available instrumentation prevents the use of this method for analyzing of biological samples. But, Collision-Induced Dissociation Tandem Mass spectrometry (CID MS/MS) could be an appropriate alternative of analysis. The use of such instrumentation should increase the yields of detected fragment ions and allow practical application of the developed method.

Acknowledgement

Reference

[1] Krautbauer, S., Weiss, T. S., Wiest, R., Schacherer D., Liebisch, G., Buechler, C., Anticancer Research, 2017, 37, 3527-3535.

[2] Antalis, C. J., Arnold, T., Rasool, T., Lee, B., Buhman, K. K., Siddiqui, R. A., Breast Cancer Research and Treatment, 2010, 122, 661-670.

[3] Lee, H. J., Yue, S. H., Li, J. J., Lee, S. Y., Shao, T., Song, B., Cheng, L., Masterson, T. A., Liu, X. Q., Ratliff, T. L., Cheng, J. X., Molecular Cancer Therapeutics, 2015, 14, 2.

[4] Bemlih, S., Poirier M. D., El Andaloussi, A., Cancer Biology & Therapy, 2010, 9, 1025-1032.

[5] Proitsi, P., Kim, M., Whiley, L., Pritchard, M., Leung, R., Soininen, H., Kloszewska, I., Mecocci, P., Tsolaki, M., Vellas, B., Sham, P., Lovestone, S., Powell, J. F., Dobson, R. J. B., Legido-Quigley, Translational Psychiatry, 2015, 5, 8.

[6] Sunner, J., Dratz E., Chen, Y. C., Analytical Chemistry, 1995, 67, 4335-4342.

[7] Szulc, J., Ruman T., Gutarowska, B., International Biodeterioration & Biodegradation, 2017, 125, 13-23.

[8] Muller, L., Kailas, A., Jackson, S. N., Roux, A., Barbacci, D. C., Schultz, J. A., Balaban, C. D., Woods, A. S., Kidney International, 2015, 88, 186-192.

[9] Vrbková, B., Roblová, V., Yeung, E. S., Preisler, J., Journal of Chromatography A, 2014, 1358, 102-109.

P4 THE EFFECT OF PREANALYTICAL CONDITIONS ON HUMAN N-GLYCOME

Tereza Dědová[1], <u>Karina Biskup</u>[1], Kai Kappert[1,2], Dagmar Flach[3], Rudolf Tauber[1], Véronique Blanchard[1]

[1]*Institute of Laboratory Medicine, Clinical Chemistry and Pathobiochemistry, Charité Medical University Berlin, Germany, karina.biskup@charite.de*

[2]*Center for Cardiovascular Research, German Center for Cardiovascular Research, Charité Medical University Berlin, Germany*

[3]*Sarstedt AG&Co, Nuembrecht, North Rhine-Westphalia, Germany*

Summary

Protein N-glycosylation is an important post-translational modification as glycans participate in many natural cellular processes, such as immune reactions and cell signaling. Several N-glycome-based biomarkers were described for some types of malignancies and infectious diseases, but to the best of our knowledge, the influence of preanalytical conditions on the result of glycan analysis has not yet been comprehensively tested. Our measurements were performed using a combination of MALDI-TOF-MS and CE-LIF to systematically evaluate the influence of preanalytical conditions on different methods. The aim of this work was to investigate if preanalytical variables can influence the results of CE and MALDI analyses and bring to inaccurate conclusions.

Introduction

Protein glycosylation effects various biological roles such as prolongation of protein half-life due to reduced clearance and protection from proteolysis. In recent years, research has shown that N- and O-glycans of serum and plasma glycoproteins are modulated under pathological conditions. This includes genetic diseases, acute and chronic inflammation and malignant diseases such as colon and ovarian cancer. A growing number of studies established that changes in glycome are not only of pathogenic importance, but can also be used as diagnostic biomarkers. Such a glycan-based cancer biomarker, the GLYCOV index score [1], developed in our laboratory, combined qualitative and quantitative changes of serum glycome in patients suffering from epithelial ovarian cancer. It is of great importance to examine the stability of human N-glycome before glycosylation changes could be routinely analyzed in diagnostic laboratories. Intra-individual stability of the glycome in time has been well studied, demonstrating the influence of the lifestyle, medication or environmental factors. However, preanalytical variables may also affect significantly glycome profiles and can lead to inaccurate results. Although there have been about 15,000 entries in PubMed for glycan biomarkers in the past ten years, the preanalytical conditions of MALDI-TOF-MS and CE-LIF glycome analysis

have never been reported in detail. In this work, we evaluate the effect of hemolysis, storage and blood collection, and the influence of various times and temperatures between individual processing steps on the N-glycome using blood samples from healthy volunteers and detection with MALDI-TOF-MS and CE-LIF methods. Additionally, we study the influence of preanalytical conditions not only on single glycan structures but also on GLYCOV, which is built from eleven glycan structures.

Experimental

Venous blood was collected from 10 healthy female donors (age 20-30, mean 25 years) in 11 blood collection tubes with different additives, processed variously to obtain 16 preanalytical variables and N-glycans released from serum or plasma were analyzed by MALDI-TOF-MS and capillary electrophoresis coupled with fluorescence detection (CE-LIF). The relative intensities of 41 MALDI peaks and the relative areas of 23 CE-LIF peaks were collected and the Mann-Whitney U test was performed to assess the statistical significance compared to the reference conditions. Hierarchical clustering performed for CE-LIF results was based on relative areas of peaks with relative areas > 1% to test the variance.

Results and Discussion

Long time storage of deep frozen samples at -20°C or -80°C exerted only a minor influence on the glycome as demonstrated by CE-LIF. The N-glycome was very stable evidenced by MALDI-TOF when stored at 4°C for at least 48 hours and blood collected in tubes devoid of additives. The glycome was stable upon storage after centrifugation and aliquoting, which is an important information considering future diagnostic applications. Hemolysis, however, negatively correlated with an established glycan score for ovarian cancer, when evaluated by MALDI-TOF-MS measurement by affecting relative intensities of certain glycans, which could lead to false negative or false positive results in glycan biomarker studies.

Conclusion

In this work, it could be shown that the glycome is rather stable in serum and plasma as short time delay between centrifugation at various temperatures seemed to have a minor effect on results. In addition, the glycome was stable upon storage at 4°C for at least 48 hours after centrifugation and aliquoting, which is an important information considering future diagnostic applications in clinical laboratories. However, it should be emphasized that hemolysis, a frequently seen clinical phenomenon in routine blood withdrawal procedures affects relative intensities of certain glycans facilitating wrong clinical interpretations.

Acknowledgement

Reference

[1] Biskup, K., Braicu, E. I., Sehouli, J., Fotopoulou, C., Tauber, R., Berger, M., Blanchard, V., Journal of Proteome Research 2013, 12, 4056-4063.

P5   DETERMINATION OF ANIONS IN COFFEE SAMPLES USING CAPILLARY ELECTROPHORESIS

Róbert Bodor, Simona Straňáková, Branislav Žabenský, Marián Masár

Comenius University in Bratislava, Faculty of Natural Sciences, Department of Analytical Chemistry, Bratislava, Slovak Republic, robert.bodor@uniba.sk

Summary

Capillary electrophoresis (CE) performed in an automated separation system and equipped with wide-bore (300 μm i.d.) fluoroplastic capillary and fixed volume sample injection device was used for determination of anions of organic and inorganic acids in brewed coffee samples. The composition of low conductivity BGE was optimized in terms of resolution and sensitivity of conductivity detection. Anions of organic and inorganic acids present in 500-times diluted coffee samples were identified and determined by standard addition method. The proposed CE method is suitable for simultaneous determination of anions at submicromolar concentration levels in 10 minutes.

Introduction

The characteristic aroma, acidity and flavor of brewed coffee are partially attributed to the inorganic anions, organic acids, and chlorogenic acid content [1-4]. Nevertheless, simple aliphatic carboxylic acids and inorganic acids are rarely analyzed in coffee. CE is very convenient for the determination of organic acids and inorganic anions in food samples [5, 6]. Direct spectrophotometry used in CE for detection of carboxylic acids is a sensitive method mainly for aromatic or unsaturated acids. In this mode, the weak absorption band of carboxylic group around 200 nm can be utilized for aliphatic acids. Indirect UV detection as well as conductivity detection (CD) are alternative choices for all types of organic acids to be analyzed by CE. Based on the instrumental setup, CD can be performed either in a contact mode (with a galvanic contact between measuring sensors and background electrolyte (BGE)) or in a contactless mode [5, 6]. CE determination of short-chain organic acids in coffee using UV detection at 200 nm without derivatization was reported by Galli [2]. Some of these acids were determined also by ITP in coffee samples [4, 7].

This work was aimed at the development of sensitive and fast CE method with contact conductivity detection for determination of anions of organic and inorganic acids present in coffee samples.

Experimental

CE separations were performed using a fully automated electrophoretic analyzer EA 202A (Villa Labeco, Spišská Nová Ves, Slovakia) equipped with a 300 μm i.d. capillary tube made of fluorinated ethylene-propylene copolymer, polymethylmethacrylate sample injection block with a sample plug length of 3 mm (500 μm i.d.) and Triathlon autosampler (Spark Holland, Emmen, The Netherlands). CE separations were monitored by AC contact conductivity detector (Villa Labeco) connected to the detection electrodes which was placed at the end of capillary (160 mm effective length).

Results and Discussion

CE separations of anions were carried out in low conductivity BGE under suppressed electroosmotic flow (EOF). Low conductive BGE is beneficial for enhancing the sensitivity of the CD, especially when the CE separation is performed in wide bore capillary. The initial composition of BGE was chosen based on our previous research [8, 9]. The use of less concentrated BGE increased the sensitivity of CD without a lack of peak resolution. In this context, it should be noted that the concentration ratio of single and double charged counter ions (Bis-Tris and Bis-Tris propane) of BGE was modified, but the concentrations of host-guest complexing agents (α- and β-cyclodextrins) were not changed. The CE separations of brewed coffee samples carried out under these conditions showed, that the concentration detectability was more than five times lower (Fig. 1).
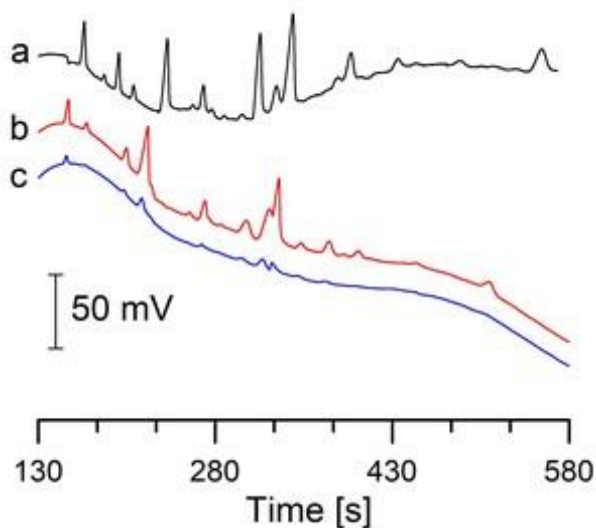

Fig. 1. Electropherograms from the analyses of brewed coffee sample in different BGEs. CE separations were carried out in the BGEs: 10 mmol/L MES, 1.2 mmol/L BisTris, 2.2 mmol/L BisTrisPropane, 0.1% HEC, 20 mmol/L α-CD, 10 mmol/L β-CD, pH=6 (a), 35 mmol/L MES, 3.4 mmol/L BisTris, 6 mmol/L BisTrisPropane, 0.1% HEC, 20 mmol/L α-CD, 10 mmol/L β-CD, pH=6 (b, c). The coffee sample prepared in espresso coffee machine was diluted 500 times (a, c) and 100 times (b). The constant separation current was stabilized at 30 μA (a) and 90 μA (b, c).

Standard addition method was used for peak identification (Fig. 2) as well as for calculation of the concentration of identified analytes. The concentration of standard additions of analytes added to the 500 times diluted coffee sample ranged in 2-50 µmol/L. Concentrations of analytes present in 500 times diluted coffee sample, calculated from peak areas, ranged in 0.2-23.6 µmol/L. The migration time repeatability is an important parameter for correct identification of analytes. RSDs of migration times in six repeated analysis of coffee sample was less than 0.5%.
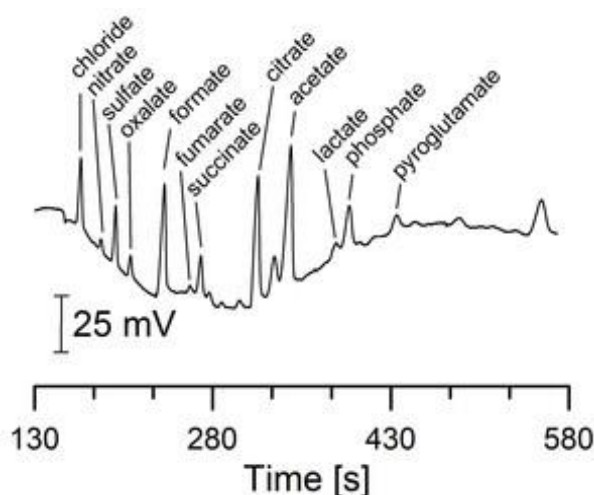

Fig. 2. Electropherogram from the separation of anions identified in coffee sample. Experimental conditions were the same as in Fig. 1a.

Conclusion

The proposed CE method is suitable for fast and sensitive determination of the organic acids (oxalate, formate, fumarate, succinate, citrate, acetate, lactate and pyroglutamate) and inorganic anions (chloride, nitrate, sulfate and phosphate) in coffee without any sample pretreatment, except of dilution step.

Acknowledgement

Reference

[1] Rogers, W. J., Michaux, S., Bastin, M., Bucheli, P., Plant Sci. 1999, 149, 115-123.

[2] Galli, V., Barbas, C., J. Chromatogr. A 2004, 1032, 299-304.

[3] Jeszka-Skowron, M., Zgoła-Grześkowiak, A., Grześkowiak, T., Eur. Food Res. Technol. 2015, 240, 19-31.

[4] Jeszka-Skowron, M., Zgoła-Grześkowiak, A., Food Anal. Methods 2017, 10, 1245-1251.

[5] Klampfl, C. W., Buchberger, W., Haddad, P. R., J. Chromatogr. A 2000, 881, 357-364.

[6] Klampfl, C. W., Electrophoresis 2007, 28, 3362-3378.

[7] Engelhardt, U., Maier, H. G., Z. Anal. Chem. 1985, 320, 169-174.

[8] Lelova, Z., Ivanova-Petropulos, V., Masár, M., Lisjak, K., Bodor, R., Food Anal. Methods 2018, 11, 1457-1466.

[9] Masár, M., Poliaková, K., Danková, M., Kaniansky, D., Stanislawski, B., J. Sep. Sci. 2005, 28, 905-914.

P6 GLYCOSYLATION AS A CRITICAL QUALITY ATTRIBUTE (CQA) OF BIOTHERAPEUTICS

Beata Borza[1,2], Marton Szigeti[1,2], Akos Szekrenyes[1], Laszlo Hajba[2], Andras Guttman[1,2,3]

[1]*Horvath Csaba Laboratory of Bioseparation Sciences, Research Center for Molecular Medicine, Faculty of Medicine, University of Debrecen, Debrecen, Nagyerdei krt. 98., 4032, Hungary, borza.bea1990@gmail.com*

[2]*Research Institute for Biomolecular and Chemical Engineering, University of Pannonia, Veszprem, Hungary*

[3]*SCIEX, Brea, CA 92130, USA*

Summary

Carbohydrate moieties on the polypeptide chains in most glycoprotein such as biotherapeutics and their biosimilars play essential roles in the two major effector functions e.g. antibody-dependent cell mediated cytotoxicity (ADCC), complement-dependent cytotoxicity (CDC), anti-inflammatory functions and serum clearance [1]. Thus, N-glycosylation should be rigorously monitored during all stages of the manufacturing process in biopharmaceutical industry. Glycosylation is considered as one of the most important critical quality attributes (CQA) of protein therapeutics, and obviously for their biosimilar alternatives [2]. Capillary electrophoresis is an electric field driven high performance separation technique, featuring high separation power and excellent detection limits for oligosaccharides [3]. In this study we introduce a rapid, capillary gel electrophoresis based process to quantitatively assess the glycosylation aspect of biosimilarity, based on their N-linked carbohydrate profiles. Differences in sialylated, core fucosylated, galactosylated and high mannose glycans were all quantified. As the mechanism of action of the measured biotherapeutics is TNFα binding, only mannosylation was deemed as CQA for glycosimilarity assessment due to its influence on serum half-life [4].

Introduction

Patent expiration on several biotherapeutics has facilitated for the pharmaceutical industry to develop biosimilars, as the counterparts of the innovative biomolecules, which are similar but not identical to the innovator product. Even minor changes in their carbohydrate structures can cause significant changes in their safety, efficacy, serum half-life and immunogenicity. Thus, comprehensive analysis of all critical quality attributes (CQA) including their glycosylation is required to prove biosimilarity during the development and release of biosimilars [1]. Proper glycosylation pattern is essential in the mechanism of action of protein therapeutics. Therefore,

accurate quantitative N-glycosylation analysis provides crucial information as a critical quality attribute (CQA) of biologics development [1].

Mannosylation at the Fc fragment of monoclonal antibody therapeutics and IgG fusion proteins enhance clearance, so should be closely scrutinized during manufacturing and release. Etanercept (Enbrel®) is a highly glycosylated IgG Fc fusion protein that binds tumor necrosis factor alpha (TNFα) involved systemic inflammation [2]. Adalimumab (Humira®) is a recombinant human IgG1 type anti-tumor necrosis factor-alpha (TNFα) binding monoclonal antibody. All of the above mentioned proteins were developed to treat rheumatoid arthritis. Since TNFα binding represents the mechanism of action at both etanercept and adalimumab, Fc function associated glycan residues like sialylation, core fucosylation or terminal galactosylation are not high significance from glycosimilarity point of view [4].

Capillary gel electrophoresis with laser induced fluorescent detection (CGE-LIF) is a high sensitivity glycoanalytical technique to analyze fluorophore (e.g., aminopyrenetrisulfonate - APTS) labeled oligosaccharides [3]. In addition, CGE-LIF with the recently introduced triple internal standard based automated GU calculation method is capable of instant structural assignment for the separated glycans [5].

Experimental

Etanercept (Enbrel® - innovator, Benepali® - biosimilar) and adalimumab (Humira®) were kindly provided by the Medical School of University of Debrecen (Debrecen, Hungary). The Fast Glycan Sample Preparation and Analysis kit was from SCIEX (Brea, CA), the PNGase F enzyme from New England Biolabs (Ipswich, MA). The labeled glycan pools were analyzed with CGE-LIF system. All other chemicals were purchased from Sigma-Aldrich (St Louis, MO). The separations were implemented in 50 cm effective length (50 μm I.D.) bare fused silica capillary columns filled with HR-NCHO gel buffer (SCIEX). For analysis and data acquisition 32Karat, version 10.1 software package (SCIEX) was used. Furthermore, relative peak areas were employed for quantitative comparison of the N-glycan profiles of Enbrel and its Benepali. PA800 Plus Pharmaceutical Analysis System (SCIEX) with laser induced fluorescent detection was applied to precisely measure the presence and concentration of the mannose-5 structure in the adalimumab (Humira®) glycan pool with the goal to establish a method that fulfills the quantitative CQA analysis requirement.

Results and Discussion

Adequate determination of glycosimilarity requires proper evaluation of all important carbohydrate associated features. In the case of etanercept since anti-inflammatory characteristics of di- and mono-sialo structures have no mode of action importance, even with the average of ~33% difference in their abundance did not represent a CQA issue, similarly to afucosylated neutral glycans since ADCC was not a mechanism of action requirement of etanercept. Huge difference was also in a core fucosylated biantennary glycan (FA2), however, CDC was not the part of mechanism of action either. Since mannosylation on the Fc fragment

influences the rate of serum clearance in humans, the presence of high mannose glycans were deemed as a critical quality attribute of glycosimilarity in the near future. Besides of the above mentioned fusion proteins TNFα binding glycoprotein was investigated as well, controversially this time a monoclonal antibody (mAb), adalimumab was chosen. PNGase F released adalimumab N-glycan pool was spiked with different amounts of mannose-5 (Man5) standard before the APTS labeling step. The spiked traces of Humira® glycans were aligned using the three internal standards and the profiles are shown as the function of GU units. Finally, results showed that independence of the N-glycan subtypes of high mannose (Man5), core fucoslyated complex (FA2) and afucosylated complex (A2G2), the actual concentration of the oligosaccharide of interest was accurately calculated in a wide concentration range establshing the required quantitative CQA assessment.

Conclusion

Significant quantitative differences were found in sialylated, core-fucosylated and galactosylated structures between Enbrel® and Benepali®, because ADCC and CDC functions were not critical to the mechanisms of action of these products. Differently, mannosylation has an essential role in serum clearance, so quantification based similarity evaluation of the high mannose structures represented an important CQA. Our results showed that biosimilar version of etanercept (Benepali®) complied the criteria of similarity assessment in the level of glycans as well, in particular high mannose structures. Accurate quantitation was possible with the use of electrokinetic injection allowing establishing very precise prediction to describe the relationship between peak area and the N-glycan concentration in the sample. To prove the adequacy of the method another TNFα-binding biotherapeutics, adalimumab with the same mode of action was observed. It was spiked with accurate amount of mannose. The Man 5 spiked traces of adalimumab glycan pool were aligned using the three internal standards of DP2, DP3 and DP15. The RFU values were normalized to the highest peak in the electropherograms, which was the FA2.

Our results showed that independent of the N-glycan subtypes of high mannose (Man5), core fucoslyated complex (FA2) and afucosylated complex (A2G2), the actual concentration of the carbohydrate of interest was accurately calculated in a wide concentration range. The normalization steps on both axes resulted in easy run-to-run comparability that enabled accurate peak area calculation from the electropherograms, supporting quantitative CQA assessment.

With this work was proved that study of the N-glycosylation of biotherapeutics is a promising method to compare the similarity between the innovator and biocimilar counterpart from CQA point of view. Furthermore, glycan mode of action does not depend on the type of production (i.e. fusion protein or monoclonal antibody). Thus, analysis of N-glycosylation helps the comparison of innovator vs biosimilar glycoprotein and the better understanding of individual carbohydrate's role in protein based biotherapeutics as well.

Acknowledgement

Reference

[1] Hajba, L., Szekrenyes, A., Borza, B., Guttman, A., Drug discovery today 2018, 23, 616-625.

[2] Borza, B., Szigeti, M., Szekrenyes, A., Hajba, L., Guttman, A., Journal of pharmaceutical and biomedical analysis 2018, 153, 182-185.

[3] Guttman, A., Nature 1996, 380, 461-462.

[4] Szigeti, M., Chapman, J., Borza, B., Guttman, A., Electrophoresis 2018, 39, 2340-2343.

[5] Jarvas, G., Szigeti, M., Chapman, J., Guttman, A., Anal Chem 2016, 88, 11364-11367.

P7 IMPACT OF POST-HARVEST PROCESSING, GEOGRAPHICAL LOCALITY AND PRODUCTION YEAR ON QUALITY OF SELECTED MEDICINAL PLANTS

Lenka Burdejova[1], Martin Polovka[2], Jaromir Porizka[3]

[1]*Institute of Analytical Chemistry of the Czech Academy of Sciences, Brno, Czech Republic, burdejova@iach.cz*

[2]*National Agricultural and Food Centre, Food Research Institute, Bratislava, Slovak Republic*

[3]*Department of Food Chemistry and Biotechnology, Faculty of Chemistry, Brno University of Technology, Brno, Czech Republic*

Summary

This study deals with the assessment of the impact of post-harvest treatment, geographical location and production years on 32 selected characteristics of medicinal plants grown in the Czech Republic. Dimethyl sulfoxide herbal extracts characteristics were evaluated by spectroscopic and chromatographic techniques. The results were processed by analysis of variance and multivariate statistical tools. Obtained results clearly proved the successful differentiation of herbal samples by means of canonical discrimination analysis according to post-harvest treatment (100%), geographical origin (82.9%) and production year (96.1%) confirming that studied factors may have significant effect on quality of medicinal plants.

Introduction

Medicinal plants are considered as valuable available source of antioxidants, vitamins, minerals and other beneficial phytochemicals. Their chemical composition may vary with genus, families, varieties, species and is substantially influenced by environmental, geographical and post-harvest processing factors [1, 2]. Limited data are available to assess the impact of different factors, e.g. geographical origin, comprising post-harvest treatment, or production year on the quality respectively chemical composition of medicinal plants originating from the Czech Republic.

Thus, the objectives of the present study were to investigate the impact of the above-mentioned conditions on properties of ten selected medicinal plants, commonly growing in the Czech Republic.

Experimental

Examined samples and preparation of herbal extracts

Ten selected medicinal plants: *Lavandula angustifolia, Calendula officinalis, Hypericum perforatum, Salvia sclarea, Melissa officinalis, Galega officinalis, Hyssopus officinalis, Mentha piperita, Salvia officinalis and Silybum marianum* were analysed. Herbs were harvested in their full ripeness in The Medicinal Herbs Centre Brno, Czech Republic and Faculty of Horticulture Mendel University Lednice, Czech Republic during summer 2015 and 2016. After harvest, each herbal sample was divided into two parts and processed by two different ways. The first part was immediately frozen and stored at -18 °C in polyethylene bags and the second part was air-dried on trays at 30 °C and stored in paper bags until analysis. Extraction procedure was performed on the basis of optimized extraction procedure [3]. Dimethyl sulfoxide (DMSO) at room temperature was used for dynamic solvent extraction.

Monitored parameters of herbal extracts

Total phenolic content (TPC) was determined applying Folin-Ciocalteu modified method [3]. Total flavonoid content (TFC) was determined by modified method using 2-aminoethyl-diphenylborate reagent [3]. Color coordinates L*, a*, b*, C*, h° and browning index (BI) of extracts were investigated according to this method [3] using UV-VIS-NIR spectrophotometer Shimadzu 3600 with accessories. 2,2′-azino-bis(3-ethyl-benzothiazoline-6-sulphonic acid) cation radical (ABTS$^{•+}$) scavenging assay respectively $^{•}$OH radicals scavenging assay were performed in the same manners as previously described [3] using X-band EPR spectrometer e-scan (Bruker, Germany) with accessories.

High-performance liquid chromatography (HPLC) Agilent 1260 Infinity apparatus equipped with diode array detector (DAD) was used for determination of individual phenolic compounds. Instrumental conditions and monitored phenolic compounds were identical to these previously described [3]. The mobile phase consisted of acetonitrile (solvent A) and 2.5% solution of formic acid (v/v) (solvent B). The gradient conditions were as follows: 92% B, 0–25 min; 85% B, 25–30 min; 88% B, 30–45 min; 85% B, 45–53 min; 80% B, 53–56 min; 92% B, 56–65 min. Additional parameters were similar as mentioned in study [3].

10 elements (Al, Ca, Cu, Fe, K, Mg, Mn, Na, P and Zn) were analyzed in herbal extracts by inductively coupled plasma optical emission spectrometry (ICP-OES) Horiba Ultima 2 instrument (Horiba Scientific, France). Instrumental settings were as follows: RF power: 1350 W; gas: argon; flow rates: plasma gas: 12.5 l/min; auxiliary gas: 0.1 l/min; nebulizer gas: 0.85 l/min; heath gas: 0.5 l/min; plasma view: radial; nebulizer: Meinhard, nebulizer pressure: 3 bar.

Statistical analysis

Statistical analysis was performed using the Unistat v. 6.0 statistical package (Unistat, London, United Kingdom). Analysis of variance (ANOVA) using Tukey's HSD test and multivariate statistical analysis, involving principal component analysis (PCA) and canonical discriminant analysis (CDA).

Results and Discussion

The results of ANOVA analysis confirmed that freezing is more suitable post-harvest treatment for preservation of functional components. Statistically higher values were recorded for TPC, gallic, caffeic, ferulic acid, Cu, Fe, K, Mg, Na, P and Zn contents for frozen samples with comparison to the dried ones. Obtained results are in good agreement with previous studies [4, 5] pointing that temperature during the heat treatment has considerable effect on the stability of some herbal components.

In case of localities, insignificant differences were found for most parameters (for 30 of 32), suggesting similarities of localities in most characteristics except the contents of Na and Cu. The localities were 50 km far from each other so similar climatic and environmental conditions were expected. As regards the comparison of production years, significant differences in caffeic acid, Cu, Na and Al contents and RS% values, higher values were determined for medicinal plants produced in the year 2015 were found.

Due to the high number of the monitored samples and evaluated parameters, the measured characteristics were statistically processed using multivariate analysis. PCA was used for graphical expression of differences between DMSO herbal extracts regardless to any factor; and CDA was used in order to quantify these differences.

By means of PCA, the first four principal components cumulatively explain 60.2% of the variability of the entire system. TPC, TFC, $TEAC_{ABTS\bullet+}$, contents of Al, Cu, rutin, chlorogenic and ferulic acid are the most important parameters in the first four components. Results of PCA analysis of DMSO extracts separate herbal samples into two clustering areas according to post-harvest treatment. It is apparent, that this factor has the dominant effect on sample properties.

Further, CDA was used in order to quantify the differences between the samples following from respective factors. The results confirmed that medicinal plants can be well distinguished according to post-harvest treatment (classification score 100%) and the production years (classification score 96.1%). Even the discrimination based on geographical origin is possible (82.9% samples correctly classified), although this criterion resulted in the lowest discrimination score, in accord with the discussion above.

Conclusion

The combination of UV-VIS-NIR, EPR, HPLC-DAD and ICP-OES followed by multivariate statistical analysis represents an effective tool to characterize the properties of medicinal plants

extracts in a complex way. The obtained results confirmed unambiguously that the properties of medicinal plants are significantly influenced by the post-harvest production, geographical aspects and can vary within production years. Of these factors, postharvest treatment affects the properties of samples most significantly.

Acknowledgement

Reference

[1] Pandey, A. K., Savita, Pharma Innovation 2017, 6, 229–235.

[2] Ghorbanpour, M., Varma, A., Medicinal Plants and Environmental Challenges, Springer, Berlin 2017.

[3] Butorová, L., Polovka, M., Pořízka, J., Vítova, E., Chem. Pap. 2017, 71, 1605–1621.

[4] Rubinskienė, M., Viškelis, P., Dambrauskienė, E., Viškelis, J., Karklelienė, R., Zemdirbyste 2015, 102, 223–228.

[5] Volf, I., Ignat, I., Neamtu, M., Popa, V., Chem. Pap. 2014, 68, 121–129.

P8 SYNTHETIC APPROACHES FOR NEW LABELING TAGS FACILITATING GLYCAN ANALYSIS

Richard Čmelík, Jana Křenková, František Foret

Institute of Analytical Chemistry of the CAS, v. v. i., Brno, Czech Republic, cmelik@iach.cz

Summary

This study is focused on the synthesis of labels based on the pyrene core bearing several ionizable quaternary amines and the efficient carbonyl-reactive group, such as primary amine or hydrazine. A set of different synthetic ways were proposed, experimentally implemented, and evaluated.

Introduction

Glycosylation is the most common modification of proteins, which has a profound effect on both the structure and function of proteins affecting stability, immunogenicity, and biological activity of proteins. Therefore, an important part of the detailed characterization of glycoprotein represents determination of the glycan structure. Due to inherent complexity, low concentration levels, poor ionization efficiency, and the lack of chromophores and fluorophores the identification of glycans is challenging and requires their selective derivatization. The particular label used in glycan analysis depends on the nature of the analyte as well as the mode of subsequent analysis. Labeling reactions are based on the structure specific reaction with carboxylate, amino, hydroxy, and especially carbonyl group [1]. The most common means of glycan labeling is through reductive amination imparting a fluorescent moiety to the labeled molecule [2]. A promising alternative is the use of hydrazine/hydrazide labeling [3].

Experimental

Reaction pathways started with commercially available compounds (1-aminopyrene, 1-hydroxypyrene, trisodium 8-hydroxypyrene-1,3,6-trisulfonate), all reagents were applied without purification. To prevent side reactions and intermediate decomposition, synthetic experiments were done under inert (argon) atmosphere and dry conditions. Degrees of conversion were monitored using thin layer chromatography (TLC Silica Gel 60 F254, Merck) and electrospray mass spectrometry (ESI-MS). Structures of prepared compounds were supported by spectra of nuclear magnetic resonance (Bruker Avance III 300 MHz) and MS (Bruker amaZon).

Results and Discussion

As a part of our strategy, a label suitable for glycan analysis was defined as providing speed, efficiency, and improved sensitivity of detection. We focused on the synthesis of new tags which are reactive towards glycans, fluorescent, and having ionizable/ionized (introducing a positive charge) moieties in order to increase the electrophoretic mobility as well as the response in MS. The attention was paid to promising compounds based on the pyrene core bearing several ionizable quaternary amines and carbonyl-reactive functionality.

We have considered four synthetic routes starting with 1-aminopyrene, 1-hydroxypyrene or its trisulfonates depicted in Figure 1. They included two crucial steps: 1/ chlorosulfonylation on the aromatic ring with subsequent substitution of chlorine with secondary amine and 2/ modification of aromatic amino or hydroxy group to the more reactive functionality (aliphatic primary amino or hydrazino groups).
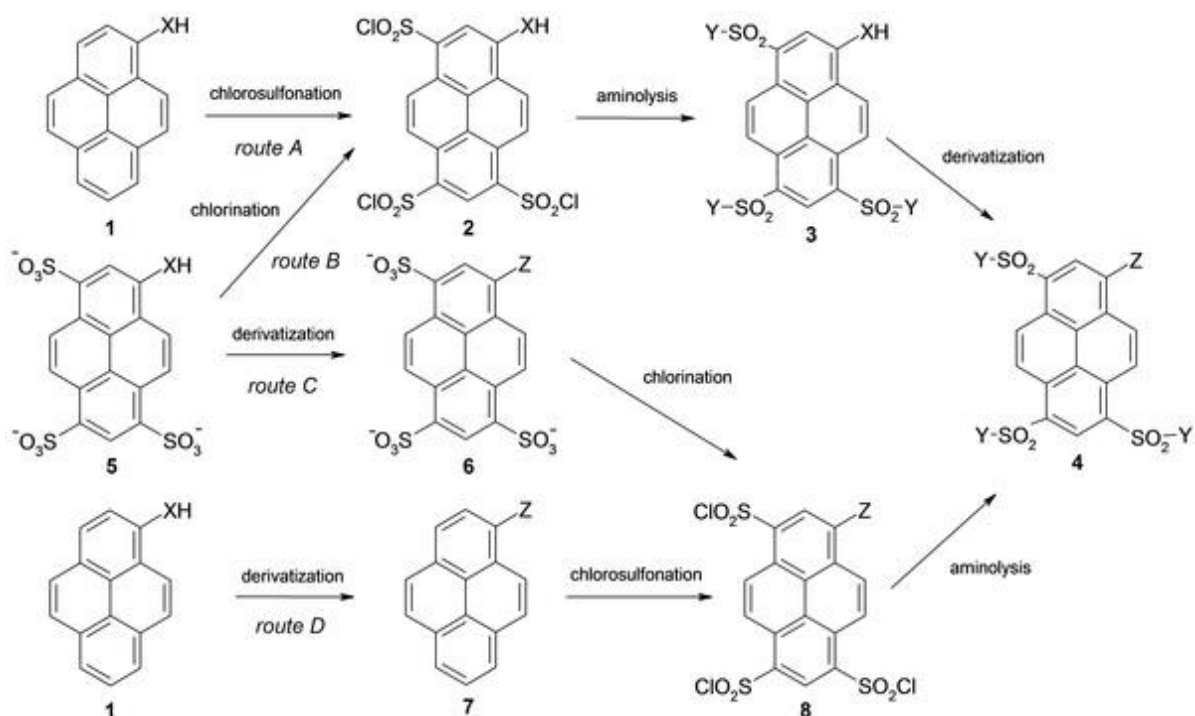

Figure 1: Synthetic scheme (X = NH, O; Y = R_2N; Z = linker-(NH)NH_2).

Particular steps were experimentally tested on selected precursors. In the case of *route A* (here and bellow see Figure 1) reaction of **1** (X = NH) with chlorosulfonic acid provided a trisubstituted derivative **2**, that by aminolysis with *N*-methylpiperazine led to the formation of corresponding trisulfonamide **3**. This compound were treated with chloroacetyl chloride and then with sodium azide. A terminal azide group is susceptible to conversion to the desired amine **4** (Z = $NHCOCH_2NH_2$) by Staudinger reduction. Chlorine can be alternatively substituted with hydrazine to produce a hydrazinyl derivative **4** (Z = $NHCOCH_2NHNH_2$).

Route B was represented by chlorination (with thionyl chloride) of acetylated (protected) trisulfonate **5** (XH = $OCOCH_3$) to a tris(chlorosulfonated) derivative **2**, which was

subsequently treated with secondary amine to trisulfonamide **3** with simultaneous deprotection of hydroxy group. There were compared two secondary amines differing in reactivity in subsequent reaction: dimethylamine and *N*-methylpiperazine.

In both *routes C* and *D* we started with hydroxy derivatives (**1**, **5**; X = O) treated with ethyl bromoacetate providing corresponding alkylated derivatives (**6**, **7**; Z = OCH$_2$COOCH$_2$CH$_3$). Chlorosulfonylated compounds **8** were obtained after chlorosulfonylation or chlorination of corresponding precursors **6**, respectively **7**. Final conversion on compound **8** includes several steps with careful selection of reaction conditions due to the presence of two competitive reactive centers: chlorosulfonyl and ester groups.

Conclusion

During this study the concept of a new reactive, fluorescent and CE/MS active tag for glycans was constituted. The synthetic strategy based on available starting compounds were proposed and particularly experimentally evaluated. A suitable method seems to be that of described as *route A* which promised synthesis up to five steps. Synthesized products will be tested in the following model labeling reactions.

Acknowledgement

Reference

[1] Harvey, D. J., J. Chromatogr. B, Anal. Technol. Biomed. Life Sci. 2011, 879, 1196–1225.
[2] Ruhaak, L. R., Zauner, G., Huhn, C., Bruggink, C., Deelder, A. M., Wuhrer, M., Anal. Bioanal. Chem. 2010, 397, 3457–3481.
[3] Lattova, E., Perreault, H., Mass Spectrom. Rev. 2013, 32, 366–385.

P9   EFFECT OF CAPILLARY LENGTH IN CE-LIF ANALYSIS OF N-GLYCANS: A WALL INTERACTION STUDY

Apolka Domokos[1], Márton Szigeti[1], Máté Szarka[1,2], András Guttman[1,2]

[1]*Horváth Csaba Memorial Institute for Bioanalytical Research, Research Center for Molecular Medicine, Faculty of Medicine, University of Debrecen, Debrecen, 98 Nagyerdei Krt, Debrecen, 4032, Hungary*

[2]*MTA-PE Translational Glycomics Research Group, Research Institute of Biomolecular and Chemical Engineering, University of Pannonia, 10 Egyetem Street, Veszprém, 8200, Hungary*

Summary

Capillary length is a key parameter in separation optimization for CE analysis.

The capillary length effect on the separation of N-gylcans was carried out using three types of glycoproteins, owning different characteristics in their carbohydrate profile. The injection parameters were varied to maintain a constant electric field during the injection. Migration times, area, %area distribution and resolution values were calculated and compared to each other in case of all used capillary lengths (total, 30-100cm).

Linear correlation was found between the migration times and capillary length. Increasing the capillary length also increase the overall deviation of the measurements. The integrated area valued and the %area distribution of the glycan pools in all three instances did not change by altering the length of the capillary. Thus, by correcting the applied electric field with the length of the capillary, results can be quantitatively used independent of the actual separation length.

Introduction

Capillary electrophoresis with laser induced fluorescence detection (CE-LIF) is considered as one of the most significant tools in the bioseparation of N-glycans due to the high performance and rapid analysis of glycan isomers [1, 2]. Most of the critical physical parameters of the analysis of carbohydrates already have been examined. However, some of the aspects are important to re-explore experimentally when using a different separation media [3]. It was found that capillary length is an important physical factor. Separation efficiency is dependent by the possible interactions of the analyte molecules and the inner surface of the bare fused silica capillary column. Shifts in the migration velocity of a given molecule can be caused by several circumstances (electroosmotic flow, solute-wall interaction, pH, ionic strength, air bubbles, siphoning effect, current, temperature, etc.) [4, 5]. Thus, the effect of capillary length does not follow the conventional chromatographic conventions. Furthermore, both sample injection method in CE – pressure and electrokinetic – are affected by the parameters of the

capillary altering the sample introduced into the capillary. Therefore, capillary length is a key – CQA – parameter in separation optimization for CE analysis.

In this work, the effect of capillary length was examined for high-resolution N-glycan analysis using electrokinetic injection. Field strengths during injection and separation were altered to be able to examine the overall linearity of the parameter change [5, 6].

Experimental

The Fast Glycan Sample Preparation and Analysis kit (Sciex, Brea, CA) was used for sample preparation and fluorophore labeling. Briefly, 100 µgs of human immunoglobulin G1, Fetuin and RNase B (Sigma Aldrich, Saint Louis, US) were prepared using the Fast Glycan method supplemented with 1.0 µL of PNGase F enzyme (1.5 IUB/µL; Asparia Glycomics, San Seabstián, Spain). The released glycans were labeled via APTS flourophore dye (8-Aminopyrene-1,3,6-Trisulfonic Acid) and were purified by magnetic microparticles. Capillary electrophoresis measurements of the labeled glycans were carried out using a P/ACE MDQ (Beckman Coulter, Brea CA, US). Bare fused silica capillaries (50 µm ID, 30 cm – 100 cm total length) with HR-NCHO separation gel buffer were used at 25°C. The applied electric field of the electrokinetic injection and separation were altered between 1.0 kV to 3.0 kV (for 3.0 sec) and 9.0 kV to 30 kV, respectively. The 32Karat (version 8.0) software package (Sciex) was used for data acquisition and processing.

Results and Discussion

The capillary length effect on the separation of N-gylcans was carried out using three types of glycoproteins, owning different characteristics in their carbohydrate profile. These commercially available standard glycoproteins were: IgG (neutral biantennary glycan containing), fetuin (highly sialylated) and RNaseB (high mannose type) [1, 7]. The labeled N-glycans from all three glycoproteins were introduced into the capillary via elektrokientic injection considering the length of the capillary. Thus, the injection parameters were varied to maintain a constant electric field during the injection. The separations were carried out in the same manner, where the electric field strength kept on a constant value to be able to compare the results. From each analysis, migration times, area, %area distribution and resolution values were calculated and compared to each other in case of all used capillary lengths. By the corresponding parameters were established for the series of experiments, linear correlation was found between the migration times and capillary length. It was also noted, that increasing the capillary length also increase the overall deviation of the measurements. Furthermore, the integrated area valued and the %area distribution of the glycan pools in all three instances did not change by altering the length of the capillary. Thus, by correcting the applied electric field with the length of the capillary, results can be quantitatively used independent of the actual separation length.

Conclusion

In this work, the effect of capillary length was examined on the separation of PNGase F released N-glycans of the three major glycosylaion types, highly sialilated, high mannose and neutral (mixed). The applied electric fields during the injection and separation resulted linear correlation between separation time and capillary length and length parameter independent behavior regarding integrated area values and %are distribution. Thus, quantitative analysis can be performed using different capillary lengths for N-glycan separation.

Acknowledgement

Reference

[1] Szigeti, M., et al., J Chromatogr B Analyt Technol Biomed Life Sci, 2016, 1032, 139-143.
[2] Guttman, A., Nature, 1996, 380, 461-2.
[3] K. D. Lukacs, J.W.J., Journal of High Resolution Chromatography 1985, 8, 407 - 411.
[4] Mayer, B.X., J Chromatogr A, 2001, 907, 21-37.
[5] Weinberger, R., Practical Capillary Electrophoresis. 2000. Second Edition. (462).
[6] K. D. Lukacs, J.W.J., Journal of High Resolution Chromatography 1985, 8, 407 - 411.
[7] Varki, A. et al., Essentials of Glycobiology, rd, et al., Editors. 2009: Cold Spring Harbor NY.

P10 A VALIDATION OF NON-INVASIVE METHOD FOR DIAGNOSIS OF CYSTIC FIBROSIS BASED ON ION RATIOS DETERMINED BY CE-C4D

Pavol Ďurč[1,2], Júlia Lačná[1,2], Věra Dosedělová[1], František Foret[1,3], Lukáš Homola[4], Eva Pokojová[5], Miriam Malá[4], Jana Skřičková[5], Milan Dastych[6], Hana Vinohradská[6], Pavel Dřevínek[7], Veronika Skalická[7], Petr Kubáň[1,2,3]

[1]*Department of Bioanalytical Instrumentation, CEITEC Masaryk University, Veveří 97, 602 00 Brno, Czech Republic, durc@mail.muni.cz*

[2]*Department of Chemistry, Masaryk University, Kotlářská 2, 611 37 Brno, Czech Republic*

[3]*Department of Bioanalytical Instrumentation, Institute of Analytical Chemistry of the Czech Academy of Sciences, v.v.i., Veveří 97, 602 00 Brno, Czech Republic*

[4]*Cystic Fibrosis Centre and Clinic of Pediatric Infectious Diseases, University Hospital Brno, Jihlavská 20, 625 00 Brno, Czech Republic*

[5]*Department of Respiratory Diseases and TB, University Hospital Brno, Jihlavská 20, 625 00 Brno, Czech Republic*

[6]*Department of Clinical Biochemistry, University Hospital Brno, Jihlavská 20, 625 00 Brno, Czech Republic*

[7]*Cystic Fibrosis Centre, Motol University Hospital, V Úvalu 84, 150 06 Praha 5, Czech Republic*

Summary

A validation of novel approach for diagnosis of cystic fibrosis (CF) is presented. The method is very simple and fast, since for collection of samples, only wiping of the skin of forearm is needed. The collected sample is analyzed by capillary electrophoresis with contactless conductometric detection (CE-C^{4}D). Ion ratios are determined as ratios of peak area of chloride anion and peak areas of selected cations. It is possible to distinguish between cystic fibrosis patients and healthy individuals when ion ratio is applied as diagnostic factor. In here, we present analytical parameters of developed method (limits of detection, limits of quantification, repeatability of migration times, repeatability of peak areas) and ROC curve, which reveals high sensitivity and specificity of the developed method.

Introduction

Cystic fibrosis is a genetic disease that is caused by a mutation in transmembrane conductance regulator gene (CFTR), which results in defective ion transfer through the epithelial cellular membranes [1]. This defective ion transfer further causes formation of sticky mucus in the lungs, pancreas and other organs leading to chronic lung infections and inflammation [2]. The current CF new born screening plan consists of immunoreactive trypsinogen (IRT) analysis, DNA genetic analysis and sweat test. This screening plan has significantly improved the detection rate and lead to improved survival rate due to the early treatment initiation.

Currently, the sweat test is considered a golden standard for confirmatory CF diagnosis. The sweat test is based on measuring elevated chloride concentration in sweat of CF patients (above 60 mmol/L) in comparison to healthy individuals (typically less than 30 mmol/L). However, the sweat test is time-consuming and may be uncomfortable, plus may lead to inconclusive diagnosis, when the chloride value falls between 30 and 60 mmol/L (so called "grey area").

Here, we present a validation of fast sampling technique and capillary electrophoresis method for analysis of ionic content in sweat and skin wipe samples, developed by us earlier [3].

Experimental

Electrophoretic system

Ion analyses were performed using Agilent CE system (Model G7100) at -15kV for anions and +15kV for cations. A fused silica capillary (50 μm ID/375 μm OD, 40/31.5 cm total/effective length, Microquartz GmbH, Germany) was used for the separations. The cassette for housing the separation capillary was equipped with a custom made contactless conductivity detector (C^4D), ADMET (Ver. 5.06, ADMET, Prague, Czech Republic). Samples were injected hydrodynamically (50mbar 5s).

The optimized background electrolyte consisted of 20 mM 2-(N-morpholino)ethanesulfonic acid (MES), 20 mM L-histidine (HIS), 2 mM 18-Crown-6 and 30 μM cetyltrimethylammonium bromide (CTAB), pH 6.

Chemicals

All chemicals were of reagent grade and DI water (Purite, Neptune, Watrex, Prague, Czech Republic) was used for stock solution preparation and dilutions. 10 mM stock solutions of inorganic anions were prepared from their sodium salts (chloride, nitrate, nitrite, sulfate all from Pliva-Lachema, Brno, Czech Republic). 10 mM stock solutions of inorganic cations were prepared from their chloride salts (potassium, sodium, calcium, magnesium) except for ammonium that was prepared from ammonium fluoride (all from Pliva-Lachema, Brno, Czech Republic). The standard sample solutions used in the analysis were prepared separately for anions and cations by diluting the respective standard solutions to the required concentrations with DI water. BGE for CE measurements was prepared daily by diluting 100 mM stock

solutions of L-histidine (HIS, Sigma-Aldrich) and 2-(N-morpholino)ethanesulfonic acid (MES, Sigma-Aldrich) to the final concentration of 20 mM for both of them. 18-crown-6 was prepared as 100 mM stock solution and was added to the BGE to yield the final concentration of 2 mM. Cetyltrimethylammonium bromide (CTAB) was prepared from 10 mM stock solution and was added to the BGE to yield the final concentration of 30 µM.

Sweat samples

Sweat samples were obtained by the Macroduct® Sweat Collection System [4]. The procedure consisted of the application of pilocarpine on the forearm skin followed by application of an electric current for 10 minutes to induce sweating. The induced sweat was then collected by Macroduct Sweat Collector device (spiral shape collection tube) for 30 minutes. The analysis of chloride content in sweat was performed by coulometry using chloride analyzer (926A chloride analyzer, Sherwood Scientific, UK) and by CE (described earlier). All samples were stored at -20°C.

Skin wipe samples

Skin wipe samples were obtained as follows: a cotton swab was thoroughly rinsed with DI water to remove residual ion contamination and dried with nitrogen prior to sampling. Just before the sampling, the cotton swab was wetted with 100 µl of DI water and defined area of skin (1 x 5 cm) was repeatedly (10x) wiped. The cotton swab was then immersed in 400 µl of DI water, let stand for 3 min to extract the analytes and discarded. The extract was then analyzed by CE. All samples were stored at -20°C when not analyzed immediately.

Results and Discussion

All skin wipe samples and sweat samples were analyzed by CE in the optimized separation electrolyte system (described in Experimental section). Typical electropherograms of cations and anions of skin-wipe samples of healthy individual (blue lines) and cystic fibrosis patient (red lines) are shown on Figure 1. All analytes present in the samples were separated from each other and the separations of both, cations and anions were performed under 2 minutes.
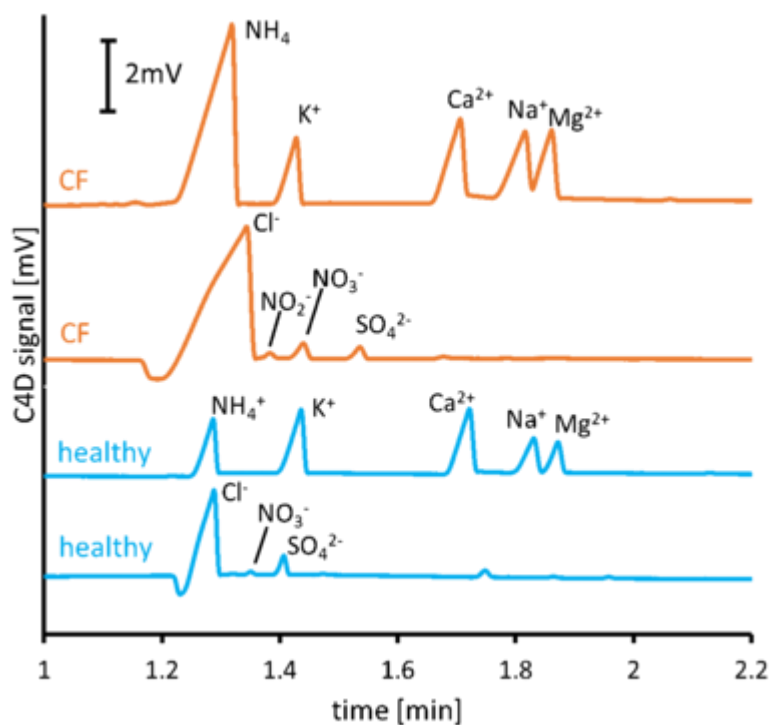
Figure 1. The electropherograms of skin wipe samples, where anions and cations of healthy individual (blue lines) and CF patient (red lines) were analyzed. CE conditions are described in Experimental section.

The limits of detection (LOD) for all selected ions possessing diagnostic value were under 4.5 µmol/L and the limits of quantification (LOQ) were under 14.9 µmol/L. These concentrations are well below the concentrations commonly found in real skin-wipe and sweat samples. The repeatabilities of migration times of all analytes were below 1.1% and the repeatabilities of peak areas were below 4.1%.

Moreover, the developed method was validated by calculating the correlation of chloride concentrations in sweat samples measured by coulometry (clinically approved method) and by our CE-C^{4}D method. The measured data showed very good correlation as the calculated Pearson correlation coefficient was 0.9972 (data not shown).

For assessment of the method´s diagnostic performance and to describe the sensitivity and specificity of the presented method a receiver operating characteristic (ROC) curve was constructed. The ROC is shown in Figure 2. The ROC curve is composed from calculated ion ratios in samples of skin wipe extracts of 70 CF patients and 26 healthy individuals.
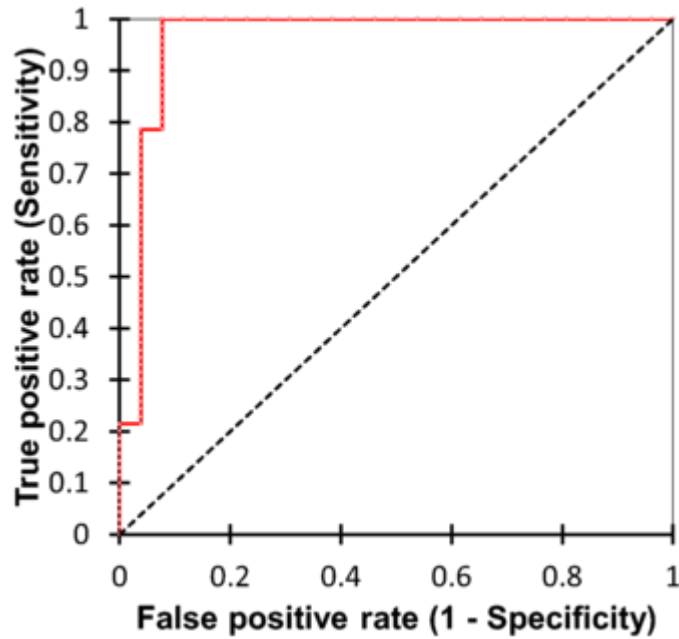
Figure 2. The ROC curve composed of ion ratio values measured in skin-wipe samples of 70 CF patients and 26 healthy individuals.

To receive the highest sensitivity and specificity of the method, a proper ion ratio borderline value needs to be selected. For this purpose, the dependence of sensitivity and specificity of the developed method on different ion ratio values was constructed and is shown in Figure 3. The highest sensitivity (0.97) and specificity (0.92) of the method was obtained, when the ion ratio borderline value of 4.4 was selected.
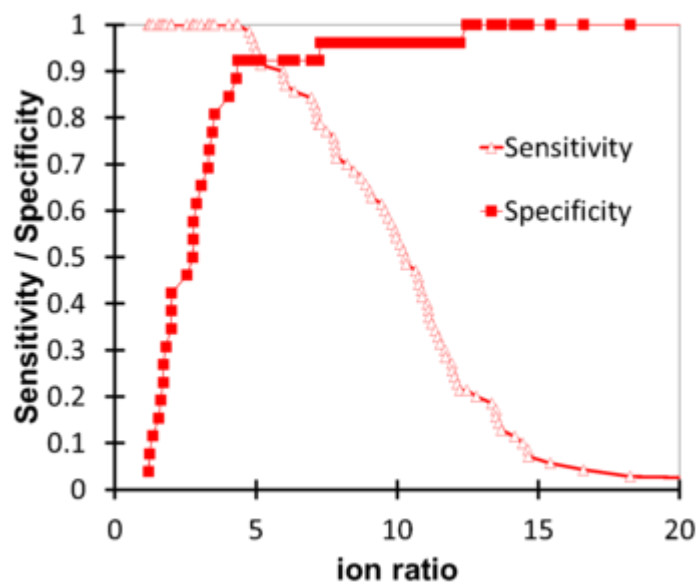

Figure 3. The dependence of sensitivity and specificity of the method on the ion ratio values.

Conclusion

CE-C^{4}D analysis of ionic content in skin-wipe samples is fast as all analyzed cations and anions migrate under 2 minutes. By the selection of ion ratio of selected ions and respective cut-off value of this ratio, high sensitivity and the specificity of the method was obtained. Our developed sampling technique and CE-C^{4}D method for multi-ion analysis can be a suitable surrogate to standard sweat test in CF diagnostics. Our developed method is simpler, cheaper and completely non-invasive.

Acknowledgement

Reference

[1] Kerem, B., Rommens, J.M., Buchanan, J.A., Markiewicz, D., Cox, T.K., Chakravarti, A., Buchwald, M., Tsui, L.C., Science 1989, 245, 1073–1080.
[2] Davies, J.C., Alton, E.W.F.W., Bush, A., Br. Med. J. 2007, 335, 1255–1259.
[3] Durc, P., Foret, F., Pokojova, E., Homola, L., Skrickova, J., Herout, V., Dastych, M., Vinohradska, H., Kuban, P., Anal. Bioanal. Chem., 2017, 409, 3507-3514.
[4] Hammond, K.B., Turcios, N.L., Gibson, L.E., J. Pediatr., 1994, 124, 255–260.

P11 EVALUATION OF THE 33 SYNTHESIZED NITROPHENOL-BASED MARKERS OF ISOELECTRIC POINT

Filip Duša, **Dana Moravcová, Karel Šlais**

Czech Academy of Sciences, Institute of Analytical Chemistry, Brno, Czech Republic

Summary

33 nitrophenol-based compounds, which absorb at ultraviolet as well as visible wavelengths, were selected as candidates for marking isoelectric points (pI) over the pH range from 3 to 10. The evaluation and selection of the candidate structures included structure-based calculations of acid-base properties. The selected compounds were further tested experimentally using capillary isoelectric focusing. The experimental analysis excluded two compounds due to producing double peaks during the analysis. Overall, 31 novel compounds were identified as suitable pI markers.

Introduction

In this abstract we present preliminary data from the analysis of 33 in-lab synthesized markers of isoelectric point (pI). The unifying feature of those pI markers is a phenolic core structure with nitro group attached either in position 2, 4, or 6 on the phenol. Apart from absorption at 280 nm, this structure gives absorption peaks with maximum around 430 nm depending on the rest of the attached groups. In turn all the markers are detectable in both UV and VIS region. This considerably increases the range of applicability of such pI markers compared to the regularly used reference peptides and proteins absorbing only in UV range.

First, the acid-base properties of the structures were analyzed with computer calculation and compared with the data obtained by titration using 11 well established nitrophenol-based markers (see table 1 - dark yellow rows). The computer data proved to be relevant to the experimentally obtained values with the first set of the established pI markers and, therefore, further 33 nitrophenol-based candidate structures were selected based on the calculations and their suitability for pI marker utilization was evaluated experimentally.

Experimental

The nitrophenol-based compounds were prepared as described earlier [1, 2] with the Mannich reaction. All chemicals were supplied by (Sigma-Aldrich, St. Louis, MO, U.S.A.) and were of the analytical grade standard. The acid-base calculations were performed using Chemaxon software suite (ChemAxon, Chemaxon Ltd., Hungary). The structures were first drawn using the Marvin sketch application and, after adjusting the structures in the planar mode, the pK_A (macro mode), pI (pH step of 0.1), and slope of the molecule net charge change versus the pH

at the pI - $(dz/dpH)_{pI}$ (using the ten points closest to the zero charge from the pI calculation curve) was calculated. Capillary isoelectric focusing was done on the P/ACE™ MDQ plus capillary electrophoresis instrument (AB Sciex LLC, Framingham, MA, U.S.A.) using the capillary isoelectric focusing protocol from the manufacturer.

Results and Discussion

The computer calculated values generally followed the trend of the experimentally determined pIs of the nitrophenol-based markers. The higher difference in the computer calculated values and obtained titration could be observed within the basic side of the investigated pH range 3-1 (see table 1 - red colour intesity designates the higher relative difference). The highest difference in the values reached up to almost two units of pH (1.77) while the calculation was as precise as 0.01 unit of pH in a few cases (see table 1). Further, the difference between the pK_As was determined and the corresponding values of all the investigated compounds were below 3 pH units, easily fitting within the recommended limit of 4 pH units pK_As difference for a well focusing ampholyte. The $(dz/dpH)_{pI}$ values, determining how fast will the particular ampholyte focus into its isoelectric zone, ranged from -0.15 to -1.0 . While the $(dz/dpH)_{pI}$ values range almost over one order of magnitude, due to the very low molecular weights of the markers (a few hundreds g·mol^{-1}) the compounds where focusing fast and no retardation or need for prolonged focusing times was observed. The focusing abilities of the presented pI markers were also evaluated with capillary isoelectric focusing were they focused into a well-defined peaks. Two pI markers from the set (nr. 21 and 31) manifested double peaks most probably due to an impurity from the synthesis and purification process. Based on the findings two pI markers were excluded from the set.

Table 1 - Summary of the analysis results of the nitrophenol-based pI markers

pI marker designation number	pI estimated by titration	pI calculated	pI difference	calculated pK_A	$|pK_{A1}-pK_{A2}|_{pI}$	$(dz/dpH)_{pI}$
1	10.0	9.42	0,58	8.80; 10.02	1.22	-0,744
2	10.1	9.05	1,05	8.21; 8.90	0.69	-0,950
3	10.4	8.83	1,57	8.05; 8.98	0.93	-0,850
4	9.6	8.65	0,95	8.16; 9.20	1.04	-0,829
5	10.0	8.45	1,55	7.76; 9.20	1.44	-0,642
6	9.0	8.42	0,58	6.95; 9.97	3.02	-0,152
7	10.1	8.33	1,77	7.63; 9.07	1.44	-0,643
8	8.9	7.95	0,95	7.47; 8.14	0.67	-0,942
9	8.6	7.85	0,75	7.40; 8.05	0.65	-0,961
10	8.5	7.76	0,74	7.38; 8.00	0.62	-0,982
11	8.4	7.62	0,78	7.23; 7.86	0.63	-0,971
12	7.8	7.30	0,50	6.54; 7.47	0.93	-0,857
13	7.9	7.01	0,89	6.17; 7.86	1.69	-0,390
14	7.7	6.94	0,76	6.15; 7.74	1.59	-0,425
15	8.3	6.75	1,55	6.12; 7.04	0.92	-0,928
16	7.9	6.68	1,22	5.96; 6.86	0.9	-0,862
17	7.2	6.47	0,73	5.87; 6.89	1.02	-0,746
18	6.4	6.43	0,03	5.30; 7.58	2.28	-0,311
19	7.4	6.41	0,99	5.37; 7.57	2.2	-0,335
20	7.0	6.36	0,64	5.85; 6.92	1.07	-0,613
21	7.5	6.36	1,14	5.98; 6.83	0.85	-0,301
22	6.2	6.35	0,15	5.30; 7.40	2.1	-0,371
23	7.0	6.32	0,68	5.36; 7.42	2.06	-0,391
24	6.3	6.31	0,01	5.81; 6.92	1.11	-0,828
25	6.6	6.24	0,36	5.72; 6.76	1.04	-0,815
26	7.5	6.17	1,33	4.91; 6.68	1.77	-0,628
27	5.9	6.12	0,22	5.37; 6.93	1.56	-0,585
28	6.9	6.08	0,77	5.94; 6.44	0.5	-0,933
29	6.6	6.08	0,52	4.69; 7.56	2.87	-0,185
30	6.5	5.48	1,02	5.01; 6.04	1.03	-0,659
31	5.0	5.21	0,21	3.69; 6.73	3.04	-0,144
32	4.5	5.06	0,56	4.03; 6.09	2.06	-0,215
33	5.3	5.01	0,29	5.48; 4.56	0.92	-0,933
34	4.9	4.75	0,15	3.60; 5.91	2.31	-0,321
35	4.9	4.53	0,37	3.04; 5.73	2.69	-0,276
36	4.5	4.47	0,03	5.90; 3.05	2.85	-0,325
37	4.5	4.39	0,11	3.25; 5.56	2.31	-0,305
38	4.9	4.38	0,47	2.81; 5.80	2.99	-0,185
39	5.3	4.19	1,11	3.22; 4.89	1.67	-0,703
40	3.9	4.13	0,23	3.00; 4.97	1.97	-0,534
41	4.2	4.08	0,12	2.96; 4.90	1.94	-0,541
42	4.0	4.06	0,06	3.13; 4.71	1.58	-0,700
43	3.7	3.92	0,22	2.59; 4.96	2.37	-0,378
44	4.0	3.70	0,30	2.93; 4.49	1.56	-0,822

Conclusion

Based on the applied approach we were able to identify and evaluate 31 novel UV-VIS absorbing pI markers suitable for isoelectric focusing. Thorough analysis with reference compounds is planned in near future to precisely define the nitrophenol-based marker pIs.

Acknowledgement

Reference

[1] Slais, K., Friedl, Z., J. Chromatogr. A 1994, 661, 249–256.
[2] Slais, K., Friedl, Z., J. Chromatogr. A 1995, 695, 113–122.

P12   IN SITU OPTICAL MONITORING OF SINGLE PARTICLE INTERACTION USING SPR-TIRE

Jan Dvořák[1], Dušan Hemzal[1,2], Tomasz Kabzinski[3], Karel Kubíček[1,3], Josef Humlíček[1,2]

[1]Department of condensed matter physics, Masaryk University, Kotlářská 2, 611 37 Brno, Czech Republic, jdvorak@physics.muni.cz

[2]CEITEC, Masaryk University, Kotlářská 2, 611 37 Brno, Czech Republic

[3]CEITEC, Masaryk University, Kamenice 5, 625 00 Brno, Czech Republic

Summary

In this contribution we present our running-work results on using the high sensitivity of SPR-enhanced optical measurements to develop a two-step methodology to control the interaction of biomolecules on the single molecule level. Namely, we use the SPR-enhanced ellipsometry (TIRE) in connection with microfluidic setup to deposit Rtt103 protein in a controlled way over gold and silver nanoparticles immobilized atop the selected area of an SPR chip. To reach the desired accuracy of identification, we first build a PEI-PSS-PAH polyelectrolyte multilayer over a FIB masked region on the SPR chip using the microfluidic setup. Setting the concentration of the subsequent injection, we determine the density of nanoparticles immobilized over this region. Finally, having chosen properly the surface charge of the nanoparticles capping, the protein is selectively adsorbed on the nanoparticles.

Introduction

SPR measurements provide, among few others, the valuable information on binding kinetics of the weak (Kd of the order 10-3 M) protein-protein interactions [1]. Accompanying the classical reflectivity measurement with spectroscopic ellipsometry, the SPR-enhanced total internal reflection ellipsometry (TIRE, for short) shows about an order of magnitude improvement in the sensitivity thanks to using also the phase information (ellipsometric angle D) during reflection.

In classical setting the surface of the SPR chip is covered with uniform layer of gold with approximately 50 nm thickness. The measurement area is then defined by dimension of the spot created by focusation probes (about 100-200 mm in diameter) on the surface of the chip. All the information is, consequently, averaged over this region. As a first step in our treatment we modify locally the gold layer such that a ring of material is removed around a selected position. Choosing the inner and outer diameter of the ring, we take over the control over an area which will contribute to SPR signal.

To immobilize biomolecules over the SPR chip, the self-assembled monolayers (SAMs) are used. We prefer the polyelectrolyte multilayer [2], since it gives control over the the surface charge through alternation of the positive and negative polymer. After creating the multilayer, we provide one additional step, consisting in immobilization of the nanoparticles. Of course, the final layer of the polyelectrolyte SAM must be chosen to have the charge inverse to that of the nanoparticles, to facilitate the binding and the charge of the nanopaticles themselves must be chosen to be opposite to that of the protein to be binded.

Having modified the surface with polyelectrolyte multilayer and the nanoparticles, binding of the selected protein can take place.
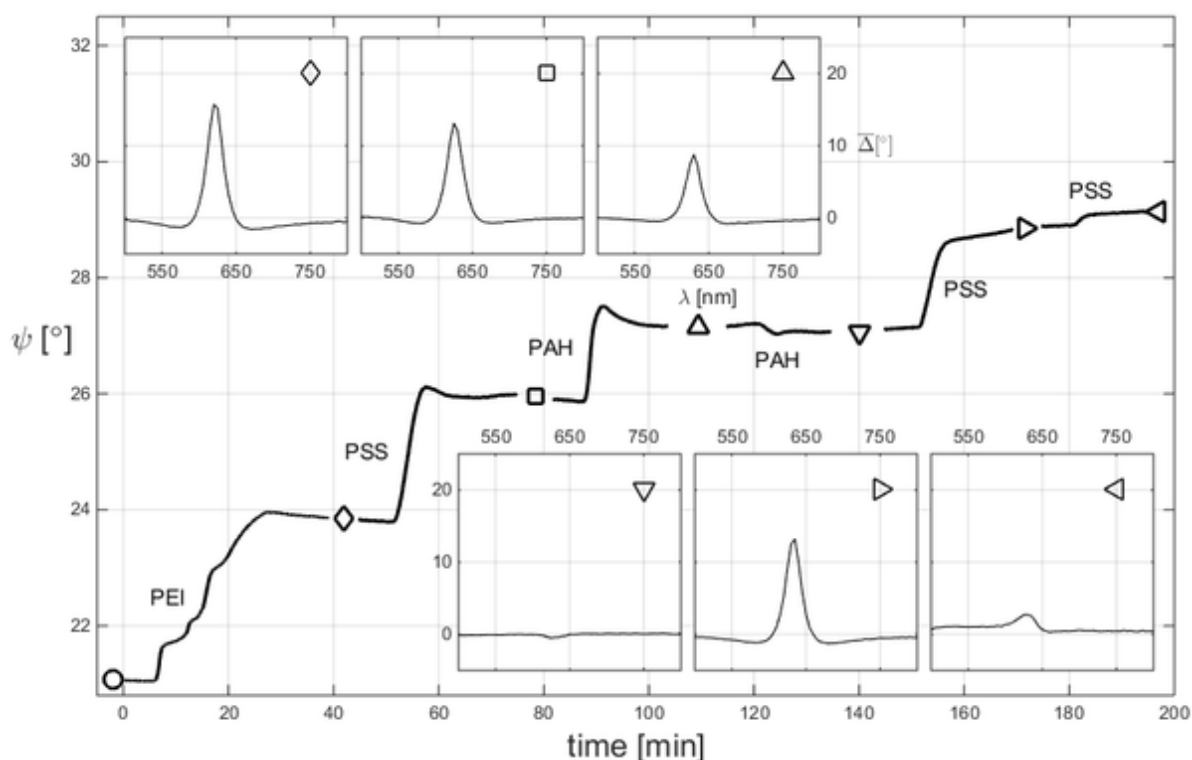

Fig 1. TIRE monitoring of the PEI-PSS-PAH polyelectrolyte multilayer formation. The insets show steady-state difference spectra in D.

Experimental

Each SPR chip was freshly prepared by PVD sputtering of 50 nm gold over cleaned BK7 slide. Subsequently, gold was removed in a ring of varying diameters using FIB (TESCAN LYRA3). The chip was loaded in the home-made microfluidic setup connected to an ellipsometer (Woollam VASE) to allow for the TIRE monitoring. After thorough rinsing the PEI-(PSS-PAH)n multilayer was created on the surface ending with desired charge (PSS for negative, PAH for positive). Subsequently, the nanoparticles were injected through the microfluidic setup. We use classical Turkevich type gold nanoparticles (~16 nm diameter, [3]) and halide shaped silver nanoparticles (~10 nm spheres to ~60 nm prisms of ~10 nm thickness, [4]). After synthesis, both types of the nanoparticles used are citrate stabilized. Finally, we use the CTD-

interaction domain (CID) of the Rtt103 protein [5] to bind over the nanoparticles. The final samples were examined using AFM and STM (NT-MDT Solar II).

Results and Discussion

The main benefit of using FIB to modify the SPR chip surface comes from determination of the area, which contributes to the SPR signal. When FIB is set to erase most of the gold in the ring area, there is no SPR signal there, so the selected position can be found easily using navigation across the chip. Given the high sensitivity of TIRE, the selected area (diameter of the inner circle) can be even smaller than the spot size - one can profit from active area restricting for as long as the resonance remains detectable.

Having prepared the multilayer over the active area one can immobilize the nanoparticles. The density of the nanoparticles on the surface of the chip is controlled through concentration of their injection and the flow-speed. The final layer of the polyelectrolyte multilayer must be chosen to have the same charge as the protein to be binded and the nanoparticles must have the opposite charge. In this way, the protein will not bind to the free polyelectrolyte surface, but only to the nanoparticles. In this way, further restriction of the active area has been reached.

Conclusion

We have used TIRE as a sensitive tool to monitor protein immobilization to the SPR chip. Using a sequence of FIB, polyelectrolyte multilayer deposition and nanoparticles immobilization, we have succeeded in restricting the area with active SPR signal used for the protein binding. In this way, we facilitate the collocalization of the subsequent characterization of the samples using SPM.

Acknowledgement

Reference

[1] D. Hemzal, Y.R. Kang, J. Dvorak et al: Treatment of SPR background in Total internal reflection ellipsometry. Characterization of RNA polymerase II films formation, under review in Applied Spectroscopy.

[2] S.T. Dubas, J.B. Schlenoff: Factors Controlling the Growth of Polyelectrolyte Multilayers, Macromolecules 32, 8153-8160 (1999).

[3] G. Frens: Controlled Nucleation for the Regulation of the Particle Size in Monodisperse Gold Supsensions, Nat. Phys. Sci. 242, 20-22 (1973).

[4] N. Cathcart, A.J. Frank and V. Kitaev: Silver nanoparticles with planar twinned defects: effect of halides for precise tuning of plasmon resonance maxima from 400 to 4900 nm, ChemComm 46, 7170-7172 (2009).

[5] O. Jasnovidova, T. Klumpler, K. Kubicek et al: Structure and dynamics of the RNAPII CTDsome with Rtt103, PNAS 114 (42), 11133-11138 (2017).

P13   N-GLYCOMIC ANALYSIS OF SEVERAL ACUTE PHASE GLYCOPROTEINS OF INFLAMMATORY AND MALIGNANT LUNG DISEASE IMPORTANCE

Anna Farkas[1], Brigitta Mészáros[1], Zsuzsanna Kovács[1], Renáta Kun[1,2], Eszter Csánky[2], Miklós Szabó[2], András Guttman[1]

[1]*Horváth Csaba Laboratory of Bioseparation Sciences, Molecular Medicine Research Center, Faculty of Medicin, University of Debrecen, Hungary*

[2]*Semmelweis Hospital, Miskolc, Hungary*

Summary

Protein N-glycosylation is one of the most frequent co-and post-translational modification in eukaryotic cells, which can influence several biological properties of the host proteins including stability [1, 2], signal transduction, motility, enzyme activity [3], half-life.

We have investigated the glycosylation profiles of five high abundant human serum glycoproteins (haptoglobin, transferrin, alpha-1 antitrypsin, IgA and IgG) in serum samples from patients with COPD, lung cancer and their comorbidities (COPD and lung cancer) compared to healthy controls using capillary electrophoresis with laser-induced fluorescent detection (CE-LIF). In this study, we have demonstrated that the total serum N-glycosylation profile could be modelled by mixing these high abundant proteins in their respective concentration, resulting in a less time-consuming, more economical process compared to their individual immunodepletion before analysis, which can be also easier in medical diagnostic laboratories.

During the study of the healthy serum N-glycome were identified multisialo, monosialo and neutral glycan structures. 40 N-glycan structures were detected in the samples of healthy controls using exoglycosidase enzymes. In the next phase of the project we have investigated the serum samples obtained from patient suffering COPD, lung cancer, their comorbidity and the healthy controls. As one can observe differences were in the neutral structures (FA2[6]G1+M7, FA2[3]G1 and FA2B[56]G1+M8 using comparative analyses.

Introduction

Protein N-glycosylation is one of the most frequent co-and post-translational modification in eukaryotic cells, which can influence several biological properties of the host proteins including stability [1, 2], signal transduction, motility, enzyme activity [3], half-life. Linkage of N-glycans via the asparagine residue of the proteins at the consensus sequence of Asn-X-Thr/Ser (X= Pro) motif [4, 5] is a result of numerous cell and tissue specific

glycosyltransferases and glycosydases [6], which can create gender and age related glycan structures. Typical changes in glycan biosynthesis were confirmed by several scientific papers resulting in a variety of modifications in the co- and post-translational modification of cell surface and circulating glycoproteins including acute phase proteins [7-9], which can be indicative of the emergence or progress of the diseases.

Patients with Chronic Obstructive Pulmonary Disease (COPD), which characterized by irreversible airflow destruction and limitation [10] as well as acute inflammation, have a high risk for developing lung cancer [11]. Thus, one of the major causes of death of patients diagnosed with mild-to-moderate chronic obstructive pulmonary disease is lung cancer [12], which could be explained by the asymptomatic feature of the early stage diseases, and the lack of the appropriate diagnostic tools.

We have investigated the glycosylation profiles of five high abundant human serum glycoproteins (haptoglobin, transferrin, alpha-1 antitrypsin, IgA and IgG) in serum samples from patients with COPD, lung cancer and their comorbidities (COPD and lung cancer) compared to healthy controls using capillary electrophoresis with laser-induced fluorescent detection (CE-LIF). In this study, we have demonstrated that the total serum N-glycosylation profile could be modelled by mixing these high abundant proteins in their respective concentration, resulting in a less time-consuming, more economical process compared to their individual immunodepletion before analysis, which can be also easier in medical diagnostic laboratories.

Experimental

N-glyosidic linkages between the carbohydrates and proteins were cleaved by applying 1.0 µL of PNGase F enzyme (200 mU). The digestion was performed at 50°C 60 minutes. After digestion, the samples were cooled down in ice for 1 minute, diluted with the addition of 120 µL of ice-cold MeCN and dried at 60°C for 1 hour (SpeedVac). The dried samples were labelled with 4.0 µl of 40 mM 8-aminopyrene-1,3,6-trisulfonic acid (APTS) in 20% acetic acid and 2.0 µl of NaBH3CN (1 M in THF) and 4 µl 20% acetic acid incubated with closed cap at 50°C for 60 min and with open cap at 55°C for 80 minutes. The excess dye was removed by using CleanSeq magnetic beads. In the purification step the magnetic beads with samples were washed with the mixture of MeCN and water. The purified N-glycans were analyzed by capillary electrophoresis with laser-induced fluorescent detection (CE-LIF). In order to identify the glycosylation alterations in the samples, they were also digested with various exoglycosidases: sialidase, galactosidase and hexosaminidase.

Results and Discussion

By mixing these glycoproteins we successfully modelled the total human serum N-glycan profile establishing the option to analyze the glycosylation of these proteins without the complicated, time-consuming and expensive depletion from human serum. During the study of the healthy serum N-glycome were identified multisialo, monosialo and neutral glycan

structures. 40 N-glycan structures were detected in the samples of healthy controls using exoglycosidase enzymes. In the next phase of the project we have investigated the serum samples obtained from patient suffering COPD, lung cancer, their comorbidity and the healthy controls. As one can observe differences were in the neutral structures (FA2[6]G1+M7, FA2[3]G1 and FA2B[56]G1+M8 using comparative analyses.

Conclusion

As in other areas of health care, in pulmonary diseases the personalized medicine will become more pronounced, in which biomarkers play a prominent role. The modification of N-glycosylation was reported in several diseases so the alterations of glycosylation in some proteins could be invaluable biomarkers for pathologic conditions.

We studied glycosylation alterations of the five most abundant glycoproteins in human serum samples from patients with chronic and malignant lung diseases. Based on our results using commercially available standard glycoproteins, it was concluded that introduction of immunoprecipitation methods was not necessary to gain information of their N-glycosylation modifications in serum of patients. This approach provided a cost- and time-effective process to investigation of the serum samples obtained from patients.

Acknowledgement

Reference

[1] Mitra, N., Sinha, S., Ramya, T. N., Surolia, A., Trends in biochemical sciences 2006, 31, 156-163.
[2] Hanson, S. R., Culyba, E. K., Hsu, T. L., Wong, C. H., Kelly, J. W., Powers, E. T., Proceedings of the National Academy of Sciences of the United States of America 2009, 106, 3131-3136.
[3] Skropeta, D., Bioorganic & medicinal chemistry 2009, 17, 2645-2653.
[4] Weerapana, E., Imperiali, B., Glycobiology 2006, 16, 91R-101R.
[5] in: rd, Varki, A., Cummings, R. D., Esko, J. D., Stanley, P., Hart, G. W., Aebi, M., Darvill, A. G., Kinoshita, T., Packer, N. H., Prestegard, J. H., Schnaar, R. L., Seeberger, P. H. (Eds.), Essentials of Glycobiology, Cold Spring Harbor (NY) 2015.
[6] Kornfeld, R., Kornfeld, S., Annual review of biochemistry 1985, 54, 631-664.

[7] Saldova, R., Royle, L., Radcliffe, C. M., Abd Hamid, U. M., Evans, R., Arnold, J. N., Banks, R. E., Hutson, R., Harvey, D. J., Antrobus, R., Petrescu, S. M., Dwek, R. A., Rudd, P. M., Glycobiology 2007, 17, 1344-1356.

[8] Arnold, J. N., Saldova, R., Galligan, M. C., Murphy, T. B., Mimura-Kimura, Y., Telford, J. E., Godwin, A. K., Rudd, P. M., Journal of proteome research 2011, 10, 1755-1764.

[9] Varadi, C., Mittermayr, S., Szekrenyes, A., Kadas, J., Takacs, L., Kurucz, I., Guttman, A., Electrophoresis 2013, 34, 2287-2294.

[10] Vestbo, J., Hurd, S. S., Agusti, A. G., Jones, P. W., Vogelmeier, C., Anzueto, A., Barnes, P. J., Fabbri, L. M., Martinez, F. J., Nishimura, M., Stockley, R. A., Sin, D. D., Rodriguez-Roisin, R., American journal of respiratory and critical care medicine 2013, 187, 347-365.

[11] Skillrud, D. M., Offord, K. P., Miller, R. D., Annals of internal medicine 1986, 105, 503-507.

[12] Sin, D. D., Anthonisen, N. R., Soriano, J. B., Agusti, A. G., The European respiratory journal 2006, 28, 1245-1257.

P14   HIGH EFFICIENCY EVAPORATIVE FLUOROPHORE LABELING OF GLYCANS

Balázs Reider[1], Márton Szigeti[2], Csenge Filep[2], András Guttman[1,2]

[1]*MTA-PE Translational Glycomics Research Group, University of Pannonia, Hungary*

[2]*Horvath Csaba Laboratory of Bioseparation Sciences, Research Center for Molecular Medicine, Faculty of Medicine, University of Debrecen, Hungary*

Summary

Newer and more efficient sample preparation methods are being developed in analytical glycomics. Albeit, numerous reductive amination based carbohydrate labeling protocols have been reported, the preferred way to conduct the reaction is in closed vials. We implemented a novel evaporative labeling protocol with the great advantage of continuously concentrating the reagents during the tagging reaction, therefore accommodating to reach the optimal reagent concentrations for a wide range of glycan structures in a complex mixture. The optimized conditions of the evaporative labeling process minimized sialylation loss, otherwise representing a major issue in reductive amination based carbohydrate tagging. Complete and uniform dispersion of dry samples was obtained by supplementing the low volume labeling mixtures (several microliters) with the addition of extra solvent (e.g., THF). It is important to note that evaporative labeling is automation-friendly, i.e., suitable for standard open 96 well plate format operation with the use of liquid handling robots.

Introduction

As glycomics research is getting more and more important in systems biology and for the biopharmaceutical industry, new glycoanalytical tools and the associated sample preparation protocols are continuously developed. Procedures reported in the literature apply comparable but not unified reaction conditions and reagent volumes for fluorescent labeling [1], most of them suggesting overnight labeling at 37ºC [2,3] or several hours of reaction times at higher temperatures (50ºC) [4]. Recently introduced rapid labeling approaches required only 20 minutes reaction time, but at 60ºC [5]. Here we introduce a novel, evaporative process based glycan labeling protocol utilizing an open vial format during the tagging reaction [6].

Experimental

Sample preparation started with the denaturation step (60ºC, 8 minutes) with the addition of denaturation solution from the Fast Glycan Labeling and Analysis Kit. The denaturation followed by the digestion: PNGase F addition to the mixture and incubation at 60ºC for 20 minutes. The released N-linked carbohydrate samples were aliquoted and dried under reduced pressure and mixed with labeling solution (SCIEX). The reaction mixtures were incubated in a heating block at 40ºC, 50ºC and 60ºC with closed (no evaporation) or open lid (evaporative

labeling) vials with additional 20% acetic acid and THF as specified later. After the labeling step, the samples were magnetic bead purified according to the Fast Glycan protocol (SCIEX). Analysis: with PA 800 Plus Pharmaceutical Analysis System (SCIEX, Brea, CA). Data processing: with 32Karat, version 10.1 software package (SCIEX).

Results and Discussion

This method took advantage of the continuous evaporation of the reaction mixture components, with the assumption that the optimal reagent concentration is reached at some point of the process for a great diversity of carbohydrate structures, thus increasing derivatization yield as manifested in greater peak areas. The optimized conditions of the evaporative labeling process minimized sialylation loss.

Conclusion

An optimized, reductive amination based carbohydrate labeling method is presented for capillary electrophoresis analysis utilizing a novel, open vial based fluorophore tagging approach. We can conclude that the evaporative labeling approach resulted in higher derivatization yield and greater sialylated peak area % values compared to the closed lid methods. The reagent volume was increased by the addition of tetrahydrofuran, which allowed the use of simple vortexing based uniform sample reconstitution without increasing the reaction times or altering any other conditions. The optimized labeling protocol for 100 µg glycoprotein (hIgG1 and eternecept, in our case) was as follows: 60 minutes in closed vial followed by 60 minutes evaporative labeling (combined method) at 50°C with the standard labeling reagents of 3.0 µl of 40 mM APTS (in 20% acetic acid) and 2.0 µl of NaBH3CN (1M in THF) using additional 4.0 µl of extra 20% acetic acid and 6.0 µl of THF (total reaction volume: 15 µl).

Acknowledgement

Reference

[1] L.R. Ruhaak, G. Zauner, C. Huhn, C. Bruggink, A.M. Deelder, M. Wuhrer, Glycan labeling strategies and their use in identification and quantification, Anal Bioanal Chem 2010, 397(8), 3457-81.

[2] R.A. Evangelista, A. Guttman, F.T. Chen, Acid-catalyzed reductive amination of aldoses with 8-aminopyrene-1,3,6-trisulfonate, Electrophoresis 1996, 17(2), 347-51.

[3] F.-T.A. Chen, R.A. Evangelista, Profiling glycoprotein N-linked oligosaccharide by capillary electrophoresis, Electrophoresis 1998, 19(15), 2639-2644.

[4] C. Váradi, C. Lew, A. Guttman, Rapid Magnetic Bead Based Sample Preparation for Automated and High Throughput N-Glycan Analysis of Therapeutic Antibodies, Anal Chem 2014, 86(12), 5682-5687.

[5] M. Szigeti, C. Lew, K. Roby, A. Guttman, Fully Automated Sample Preparation for Ultrafast N-Glycosylation Analysis of Antibody Therapeutics, J Lab Autom 2016, 21(2), 281-6.

[6] B.Reider, M.Szigeti, A.Guttman, Evaporative fluorophore labeling of carbohydrates via reductive amination, Talanta 2018, 185, 365–369.

P15 VITAMIN D STATUS AND ITS ASSOCIATION WITH CARDIOMETABOLIC RISK FACTORS IN HEALTHY MEDICATION - FREE SLOVAK POPULATION

Zuzana Gogalova[1], Maria Konecna[1], Janka Poracova[1], Janka Porubska[2], Marta Mydlarova Blascakova[1]

[1]*University of Presov, Faculty of Humanities and Natural Sciences, Department of Biology, 17th November Street 1, 081 16 Presov, Slovak Republic, zuzana.gogalova@smail.unipo.sk*

[2]*University of Presov, Faculty of Humanities and Natural Sciences, Department of Ecology, 17th November Street 1, 081 16 Presov, Slovak Republic*

Summary

The population of the Slovak Republic belongs to the European population with a low concentration of vitamin D in blood serum. Our work focused on electrochemiluminescence detection of 25-hydroxyvitamin D_3 - $25(OH)D_3$ in blood serum of 105 medication - free probands from Presov region in the Slovak Republic. We found statistically significant correlation between cardiometabolic risk factors and content of $25(OH)D_3$. The results revealed statistically significant correlation between content of $25(OH)D_3$ and lipid profile in total cholesterol ($p<0.05$) for women and in triglycerides ($p<0.05$) for men. An effect of outdoor and indoor character of work was confirmed both for women and for men ($p<0.05$) with a positive influence of the exterior for vitamin D concentrations. Statistically significant higher vitamin D content was found in non-smoking women, while no such observation was observed in tested men.

Introduction

In recent years, cases of high prevalence of low doses or insufficient vitamin D status have been reported in Europe. Vitamin D status in various European countries shows great differences due to different latitudes, skin pigmentation and different eating habits. Most people living in Central and Western Europe have a concentration of 25-hydroxyvitamin D - $25(OH)D$ in the range of 30-50 ng/ml in the blood serum. Vitamin D production is virtually impossible beyond 40 degrees north of latitude from October to March due to reduced sunlight [1-5].

Vitamin D belongs to the fat-soluble vitamins. It is present in two forms in human body. Vitamin D_2 (ergocalciferol) is taken through the diet into our body and it represents 10 % of the serum vitamin D_2 concentration. On the other hand, vitamin D_3 (cholecalciferol) is produced through the sunlight in the skin and it forms 90 % of the serum vitamin D

concentration [6, 7]. Metabolic processes that convert biologically inactive structures of vitamin D to active forms include two hydroxylations [7-9]. The first hydroxylation is in liver. Enzymatic hydroxylation at 25th carbon from cholecalciferol (D_3) and ergocalciferol (D_2) gives 25(OH)D. The second hydroxylation occurs in kidney, especially in the proximal tubule. Hydroxylation is catalysed by an enzyme of the cytochrome P450, the mitochondrial enzyme CYP27B1 (D-1α-hydroxylase). The effect of this enzyme is metabolized by 25(OH)D on the 1st carbon. In this way biologically and hormonally active form of 1,25-dihydroxyvitamin D - $1,25(OH)_2D$ - is formed. It also binds intracellularly to the vitamin D receptor (VDR), which is responsible for the most of its biological effects [6, 10].

Many studies showed that vitamin D affects not only bone metabolism, but can also affect the risk of many chronic diseases, including type I diabetes, multiple sclerosis, rheumatoid arthritis, cancer, heart and infectious diseases [11, 12].

The Slovak Republic is ranked among 10 % of the European countries with a low concentration of 25(OH)D. Vitamin D status in Slovakia is scarcely reviewed. There is a lack of appropriate data on the status of vitamin D in blood serum among men and women of all age groups [13, 14].

The aim of our study was the determination of $25(OH)D_3$ in blood serum and seeking a potential relation between vitamin D and the lipid profile in healthy working population of Slovakia. Cardiometabolic risk factors such as smoking and low physical activity were also recorded in probands. The vitamin D status was also evaluated in relation to work in the exterior and interior.

Experimental

Probands

The vitamin D status was evaluated based on the serum concentration of $25(OH)D_3$. The study included healthy men and women from the majority population of the Presov region in the Slovak Republic. The probands were aged 18-63 years and without medical treatment and nutritional supplements.

Methods

Blood pressure was monitored for each proband. As the risk systolic blood pressure (SBP) limits were defined values of pressure ≥ 130 mm Hg and for diastolic blood pressure (DBP) values of pressure ≥ 85 mm Hg [15]. From the height and weight, body mass index (BMI) was calculated for each proband. Furthermore, the lipid profile of each proband – triglycerides (TG), total cholesterol (TCH), high-density lipoprotein (HDL) and low-density lipoprotein (LDL) - were considered. The concentration scale of $25(OH)D_3$ was considered as deficient for values ≤ 20 ng/ml, an optimal level of $25(OH)D_3$ in the range of 20-30 ng/ml and a satisfactory concentration of ≥ 30 ng/ml [16]. Based on the questionnaire, each proband responded "yes"

and "no" to the question of smoking, physical activity and the work done in the exterior and interior. Physical activity presented sport activity or other physical activity (e.g. garden work, walking) - activity performed at least three times a week for more than half an hour. Any outdoor character of work (e.g. farmer) was considered as the exterior work and work in office or in lab was taken as an interior kind of work in the length of eight hours or more.

Measurements

Blood was sampled in tubes (Sarstedt S-Monovette, Germany) with a volume of 5 ml after overnight fasting in the morning. It was processed by centrifugation (Hettich Universal 320R, Switzerland) at 9000 rpm in 10 minutes at laboratory of The Centre of Excellence of the Animal and Human Ecology at the University of Presov in Presov. Blood serum was stored at -21 °C. $25(OH)D_3$ was determined in blood serum using a fully automated immunochemical analyser with electrochemiluminescence detection Cobas e411 (Roche Diagnostics, Germany).

Statistical analysis

The obtained data were processed and evaluated by software Statistica, ver. 13.1. For a better orientation in the results, the mean ± standard deviation (x ± SD) was included. Data were evaluated using non-parametric tests – Mann-Whitney U test and Spearman correlation test. Significance levels for all statistical analysis as well as correlation coefficients are given in the Table 1.

Tab. 1. Cohort characteristics and 25(OH)D$_3$ levels with regard to lipid profile, blood pressure, body mass index, smoking status, physical activity and outdoor/indoor work in whole cohort, males and females.

	All	Males	Females	p
N (%)	105	68 (65%)	37 (35%)	-
Age (years)	40.41±12.39	41.72±12.62	28.02±11.73	0.12
BMI (kg/m^2)	29.42±4.42	30.53±4.39	27.39±3.73	**< 0.001**
SBP (mm Hg)	122±8.55	124±7.90	117±7.38	**< 0.001**
DBP (mm Hg)	76±4.39	77±4.65	75±3.58	**< 0.05**
Vitamin D concentration (ng/ml)				
25(OH)D3	28.50±4.02	28.11±3.98	29.22±4.03	0.15
Lipid profile (ng/ml)				
TCH	5.20±1.01	5.06±0.97	5.46±1.06	-
p	0.10	0.80	**0.02**	-
TG	1.29±0.70	1.43±0.78	1.04±0.43	-
p	**0.01**	**0.01**	0.08	-
HDL	1.46±0.39	1.36±0.34	1.66±0.41	-
p	0.73	0.62	0.41	-
LDL	3.44±0.84	3.37±0.83	3.56±0.87	-
p	0.05	0.60	0.05	-
Blood pressure (mm Hg)				
Normotension	28.84±4.15	28.47±4.26	29.37±3.99	0.46
Hypertension	26.87±2.86	27.04±2.85	24.00±0.00	1.00
p	0.06	0.41	0.68	-
BMI (kg/m^2)				
Obesity	28.25±3.82	28.24±3.95	28.28±3.33	0.83
Normal	28.71±4.19	27.95±4.09	29.49±4.22	0.15
p	0.69	0.71	0.53	-
Smoking status				
Smokers	27.78±3.92	27.68±4.03	27.96±3.81	0.69
Non-smokers	29.56±3.98	28.71±3.93	31.32±3.61	**0.03**
p	**0.02**	0.20	**0.01**	-
Physical activity				
Physical active	28.46±3.90	27.99±4.04	29.1±3.72	0.24
Sedentary	28.55±4.16	28.20±4.01	29.45±4.53	0.45
p	0.95	0.58	0.59	-
Outdoor/Indoor work				
Outdoor work	33.71±2.21	33.81±2.38	33.57±2.05	0.79
Indoor work	26.22±1.08	26.06±1.88	26.58±2.20	0.37
p	**< 0.05**	**< 0.05**	**< 0.05**	

Results and Discussion

The research was attended by 105 healthy probands aged 18-63 years without medical treatment and without using dietary supplements.

Effect of lipid profile

We have found statistically significant correlation between content of 25(OH)D$_3$ and total cholesterol in blood serum for women (r = 0.378; p = 0.02). Such association was not confirmed for men (r = 0.030; p = 0.80). The results show that there is an apparent positive correlation

between TG values and 25(OH)D$_3$ content in the blood serum for men ($r = 0.303$, $p = 0.01$), but this correlation was not observed for women ($r = 0.285$; $p = 0.08$). No statistically significant correlation was found for 25(OH)D$_3$ content and LDL and HDL concentrations, respectively.

Effect of blood pressure

Values of 25(OH)D$_3$ in relation to blood pressure was not evaluated, because of insufficient probands suffering from high blood pressure in the cohort.

BMI and vitamin D status

No differences were observed for obese and non-obese probands at all ($p = 0.69$) and significant differences were not identified in obese and non-obese women and men ($p = 0.83$; $p = 0.15$), respectively.

Smoking status and vitamin D

For non-smoking women statistically significant higher 25(OH)D$_3$ content (31.32 ± 3.61 ng/ml) was found than in smoking women (27.96 ± 3.81 ng/ml) at $p = 0.01$. However, non-smoking women in general revealed higher concentration of 25(OH)D$_3$ than non-smoking men (31.32 ± 6.61 and 28.71 ± 3.93), respectively ($p = 0.005$).

Effect of physical activity

We have found no differences for physical active and sedentary probands at all ($p = 0.95$) and significant differences were not identified even between active and non-active women and men ($p = 0.59$; $p = 0.58$), respectively.

Effect of outdoor and indoor work

As we assumed there were observed considerable differences in 25(OH)D$_3$ concentrations between probands working in exterior and interior in general. It was confirmed both for women and for men ($p<0.05$; $p<0.05$).

Conclusion

Based on the result we assume, that whole well-being (health condition, physical activity, exposure to sun, BMI, etc.) as well as blood biochemical parameters (lipid profile) affect somehow vitamin D concentration in blood serum, however further research is needed, in which other techniques would focus on all forms of vitamin D and its metabolization in blood. The aspect of varying rate and form of metabolization of vitamin D in individuals should be considered. Thus, in the next stage of our research we plan to apply chromatographic techniques for vitamin D analysis in blood serum.

Acknowledgement

Reference

[1] Hilger, J., Friedel, A., Herr, R., Rausch, T., Roos, F., Wahl, D.A., Pierozz, D. D., Weber, P., Hoffmann, K., British J. of Nutrition 2014, 111, 23-45.

[2] Pludowski, P., Grant, B.W., Bhattoa, P.H., Bayer, M., Povoroznyuk, V., Rudenka, E., Ramanau, H., Varbiro, S., Rudenka, A., Karczmarewicz, E., Lorenc, R., Czech-Kowalska, J., Konstantynowicz, J., J. of Endocrin. 2014, 2014, 1-12.

[3] Van Schoor, N. M., Lips, P., J Clin Endocrinol Metab. 2011, 25, 671-680.

[4] Lips, P., J Steroid Biochem Mol Biol. 2010, 121, 297-300.

[5] Mithal A., Wahl, D.A., Bonjour, J.P., Burckhardt, P., Dawson-Hughes, B., Eisman, J.A., El-Hajj Fuleihan, G., Josse, R.G., Lips, P., Morales-Torres, J., IOF Committee of Scientific Advisors (CSA) Nutrition Working Group, Osteoporos Int. 2009, 20, 1807-1820.

[6] Topolcan, O., Kinkorova, J., Vondra, K., Med. Praxi. 2012, 9, 174-178.

[7] Lehmann, B., Meurer, M., Dermatologic Therapy. 2010, 23, 2-12.

[8] Laaksi, I., Acta Electronic. Universitatis Tamperensis. 2012, 20.

[9] Mangin, M., Sinha, R., Fincher, K., Inflamm Res. 63, 803-819.

[10] Christakos, S., Ajibade, V. D., Dhawan, P., Fechner, J.A., Mady, J.L., Endocrinol Metab Clin North Am. 2010, 39, 243-253.

[11] Holick, M.F., Mol Aspects Med. 2008, 29, 361-368.

[12] Norman, P.E., Powell, J.T., Circulaton Research. 2014, 114, 379-393.

[13] Lips, P., Duong, T., Oleksik, A., Black, D., Cummings, S., Cox, D., Nickelsen, T. J Clin Endocrinol Metab. 2001, 86, 1212-1221.

[14] Sebekova, K., Krivosikova, Z., Gajdos, M., Podracka, M., Bratisl Med J. 2016, 117, 702-709.

[15] Alberti, K., Eckel, R.H., Grundy, S.M., Zimmet, P.Z., Cleeman, J.I., Donato, K.A., Fruchart, J.C., James, W.P., Loria, C.M., Smith, S.C. Jr; International Diabetes Federation Task Force on Epidemiology and Prevention; Hational Heart, Lung, and Blood Institute; American Heart Association; World Heart Federation; International Atherosclerosis Society; International Association for the Study of Obesity. Circulation 2009. 120, 1640-1645.

[16] Holick, M.F., N Engl J Med. 2007,357, 266-281.

P16 COMBINATION OF RP-HPLC AND SEC USING MICROBORE SIZE COLUMN FOR CHARACTERIZATION OF HUMIC SUBSTANCES ISOLATED FROM SOIL AND PEAT

Róbert Góra, **Milan Hutta, Erik Beňo**

Department of Analytical Chemistry, Faculty of Natural Sciences, Comenius University in Bratislava, Ilkovičova 6, 842 15 Bratislava, Slovakia, robert.gora@uniba.sk

Summary

The aims of the presented work was fractionation, analysis and characterization of humic substances (HS) isolated from soil and peat using off-line combinations of two chromatographic methods, RP-HPLC – SEC with consideration of the possibilities of their on-line combination. Among the chromatography methods size–exclusion chromatography (SEC) occupies the largest application area in the field of HS relative molar mass determination and is extensively used also for purpose of macromolecule size based fractionation. Widely used inner diameter of SEC columns is 7.8 mm, but in recent years, narrow-bore columns (3.0 – 4.6 mm, i.d.) and microbore columns (1.0 – 3.0 mm, i.d.) have been developed. Reversed-phase high performance liquid chromatography (RP-HPLC) as prevailing chromatographic method has achieved in the field of analysis and characterization of HS only limited application. With respect to the non-common approach we focused to evaluation of its potential to create orthogonal, two dimensional separation methods.

Introduction

Humic substances (HS) are created by a complex mixture of amorphous, yellow to black colored, hydrophilic, polyelectrolyte poly-disperse macromolecules and maybe no two molecules are identical [1]. From the point-of-view of chemical analysis, characteristic feature of these analytes is diffuse non-distinct analytical signal produced by many detection principles. Therefore, we could call them loosely defined or fuzzy chemical systems. This signal does not usually result in an exact numerical physical-chemical data, but is described also by their distribution function or range of validity.

Separation methods play an important role in universal approach outlined below mainly during the isolation of environmental macromolecules and during their separation and/or fractionation into relatively well defined sub-fractions. Among the chromatography methods [2] size–exclusion chromatography (SEC) occupies the largest application area in the field of HSs relative molar mass determination and is extensively used also for purpose of macromolecule

size based fractionation [3,4]. Widely used inner diameter of SEC columns is 7.8 mm, but in recent years, narrow-bore columns (3.0 – 4.6 mm, i.d.) and microbore columns (1.0 – 3.0 mm, i.d.) have been developed [5]. With optional flow rates between 0.1 to 0.5 mL min^{-1}, narrow-bore columns reduce the consumption of mobile phase up to 80% and increase the sensitivity of measurement [6]. Reversed-phase high performance liquid chromatography (RP-HPLC) as prevailing chromatographic method has achieved in the field of analysis and characterization of HS only limited application [7,8].

Complexity of HSs invokes need for more comprehensive solutions of their separation. This dictates the necessity of development of automated complex separation procedures with minimal sample pretreatment, and the use of on-line multidimensional chromatographic techniques is a logical solution to these requirements. Multidimensional chromatography has proven to be useful for the analysis of complex samples such as humic substances [9,10].

The aim of this work is an introductory study of off-line combination RP-HPLC and SEC. With respect to the non-common approach we focused to evaluation of its potential to create orthogonal, i.e. on different separation principles working two dimensional comprehensive separation methods.

Experimental

All chromatographic experiments involving RP-HPLC fractionation and SEC characterization of the selected groups of humic substances were carried out by the HPLC system LaChrom (Merck-Hitachi, Darmstadt, Germany) using a LiChroCART column 250x4mm filled by wide pore octadecylsilica LiChrospher WP 300 RP-18, 5mm spherical particles. Measured dwell volume of the RP-HPLC system including column was 3.80 ml and should be considered when gradient mixing profile and chromatogram appearance is to be compared [7,11].

SEC separation was carried out using a stainless-steel column 250x2.2 mm filled by Spheron HEMA 100 (copolymer of hydroxyethylmetacrylate with ethylenedimetacrylate) hydrophilic gel, spherical particles diameter was below 25 µm. Pump operated at flowrate 0.2 ml.min^{-1}. Volumes 20 µl of sample from selected HSs fractions were injected to SEC system. Void volume (V_0; 0.35 ml) and total permeation volume (V_i; 0.95 ml) of the column were determined using Blue Dextran 2000 (Pharmacia Fine Chemicals AB, Uppsala, Sweden) and toluen, or nitrobenzene (Lachema, Brno, Czech Republic), respectively. The column system was calibrated using polystyrene standards (Polymer Laboratories, Amherst, USA) with different nominal molar mass for estimating the averaged molar mass of injected fraction of HSs. Target group of humic substances was obtained by the procedures published by [10,12]. Solutions of humic substances were prepared daily fresh by dissolution of weighed HS at cca. 3 mg.ml^{-1} concentration level in initial composition of mobile phase for RP-HPLC slightly adjusted by 0.05 M NaOH.

Results and Discussion

The devised stepwise gradient chromatographic [7,10,11] method with tandem photometric (DAD) and fluorimetric detection was used for characterization and fractionation of HS by their chromatographic profiles. Each fraction was collected in time range which was obtained according to the FLD response. Volume of these fractions was 400 µl collected around their peak maximum. Selected major fractions were analyzed by the second chromatographic method (SEC). Relative molar mass exclusion limits of polymers in Spheron HEMA 100 range from 70 000 to 250 000 according to the manufacturer data. During development of SEC method for the reliable characterization of HS and their fractions, several mobile phases were tested (1% DMF / 99% phosphate buffer, pH = 3.00 (v/v); 50% DMF / 50% phosphate buffer (v/v); 99% DMF / 1% phosphate buffer (v/v). Finally, mixture of 99% DMF / 1% phosphate buffer, pH = 3,00 (v/v) was chosen.
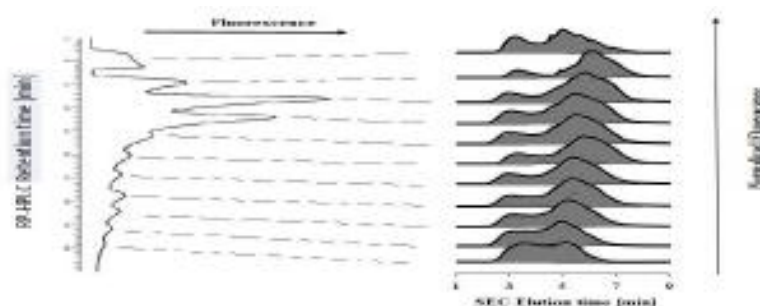

Fig.1. Multi-chromatogram of HA I obtained by application of combination of chromatographic methods RP-HPLC and SEC. Vertically located record is background corrected RP-HPLC profile obtained using FLD at Ex 470 nm/Em 530 nm, flow-rate 1 ml/min, after injection of 100 µl sample volume. Horizontally located records are SEC profiles of major HA I fractions (FLD at Ex 470 nm/Em 530 nm) using flow-rate 0.2 ml/min. Injection volume was 50 µl.

Horizontally located chromatograms (RP-HPLC profiles) in the following figure (Fig.1.) show typical examples of the profiles as resulted from analysis of humic acid (HA isolated from soil). From the drawing it is evident that the combination of chromatographic methods is capable to distinguish among the fractions of humic acids. The records show that in each of collected fractions from RP-HPLC we can find different peaks by SEC that code distribution of HA fractions with the highest signal in the region below relative molar mass value 5000. It means that regardless the hydrophobicity and/or interaction HA-DMF ability of humic acids – their SEC profiles are similar but not identical under the FLD detection conditions.

To prove the non-existence of retention times (RP-HPLC/ SEC) correlation (its existence is defined as H0 hypothesis) we did statistical test by Spearman rank correlation and Pearson product-moment correlation coefficient. It means that retention and elution data are not correlating, what means also that both methods separation mechanisms are not correlating or redundant. It creates basic condition for effective evaluation of 2 dimensional separation space for unique positioning of individual constituent molecules of humic acids within larger

separation space than is offered by the two combined methods. This gives us potential for further study of humic acids under investigation.

Conclusion

The results suggest that the devised off-line 2D RP-HPLC and SEC method is highly reliable for characterization and fractionation of soil HAs in a wide concentration range and also at trace concentration levels. Analysis of individual fractions obtained by the described RP-HPLC method by the method working on independent separation principles – described SEC method - provided data of even higher dimensionality needed for HSs investigation. Obtained results indicate, that such methods could be combined in a compact, automatic, orthogonal separation systems for characterization of such complicated natural substances as are examined humic acids and obtain so more information about their character.

Acknowledgement

Reference

[1] Choudhry, G., G., Humic Substances. Structural aspects, and photophysical, photochemical and free radical characteristics, in Hutzinger O. Ed., The Handbook of Environmental Chemistry Vol. 1., Part C., The Natural environment and the biogeochemical cycles, Springer Verlag, Heidelberg, 1989, 1.

[2] Jánoš, P., J. Chromatogr. A 2003, 983, 1-18.

[3] Peuravuori, J., Pihlaja, K., Anal. Chim. Acta 1997, 337, 133-149.

[4] Janoš, P., Zatřepálková, I., J. Chromatogr. A 2007, 1160, 160-165.

[5] Wu, C., S., Handbook of size exclusion chromatography and related techniques, Marcel Dekker, New York, USA,

[6] Beňo, E., Góra, R., Hutta, M., J. Sep. Sci. 2018, 41, 3171-3346.

[7] Hutta, M., Góra, R., J. Chromatogr. A 2003, 1012, 67-79.

[8] Hutta, M., Góra, R., Halko, R., Chalányová, M., J. Chromatogr. A 2011, 1218, 8946-8957.

[9] Whelan, T.-J., Shalliker, R., A., McIntyre, C., Wilson, M., A., Ind. Eng. Chem. Res. 2005, 44, 3229-3237.

[10] Góra, R., Hutta, M., Rohárik, P., J. Chromatogr. A 2012, 1220, 44-49.

[11] Góra, R., Hutta, M., J. Chromatogr. A 2005, 1084, 39-45.

[12] Procháčková, T, Góra, R., Kandráč, J., Hutta, M., J. Radioanal. Nucl. Chem. 1998, 229, 61-65.

P17   PNGASE F PERFORMANCE STUDY FOR IMPROVED GLYCOSYLATION ANALYSIS FROM HUMAN SERUM SAMPLES

Eszter Jóna[1], Márton Szigeti[1], <u>András Guttman</u>[1,2]

[1]*Translational Glycomics Research Group, Research Institute of Biomolecular and Chemical Engineering, University of Pannonia, 10 Egyetem Street, Veszprem, 8200, Hungary, guttman@mik.uni-pannon.hu*

[2]*Horvath Csaba Memorial Institute for Bioanalytical Research, AOK, MMKK, University of Debrecen, 98 Nagyerdei Krt, Debrecen, 4032, Hungary*

Summary

Analysis of the circulating human serum glycome becomes more and more important in the fields of life sciences. Disease related changes in glycan expression and structures could be valuable indicators in early recognition and in distinction between illnesses with similar symptoms – such as lung cancer and COPD. For this purpose, a reliable and robust sample preparation method is required to be able to provide statistically valuable results for data evaluation. One of the key steps is the enzymatic release of glycans using the endoglycosidase PNGase F. In this work, the denaturation parameters of the glycoprotein and the PNGase F digestion parameters were optimized for human serum N-glycome profiling of lung cancer and COPD patients. The released N-glycans were labeled with APTS (8-aminopyrene-1,3,6-triwsulfonate, APTS) followed by magnetic bead based purification and capillary electrophoresis analysis with laser-induced fluorescence (CE-LIF) detection.

Introduction

N-linked glycosylation, a co- and post-translational protein modification is present in all domains of life and characterized by high structural diversity among different species and in homeostatic and disease states. Glycosylation analysis, thus, could play a major role in the field of biomarker discovery [1]. The rapid disease related changes in the N-glycosylation patterns of important serum glycoproteins hold a promise for early recognition – such as lung cancer [2, 3]. Furthermore, the analysis can be done using a simple blood test, unlike commonly used methods involving invasive organ biopsies. In general, sample preparation of N-glycan analysis includes four major steps: 1) glycoprotein denaturation, 2) enzymatic N-glycan release, 3) fluorophore labeling and 4) cleanup – excess dye removal [4]. While processing of these steps seem straight forward, the effects of the various parameters within each step cumulatively build up may result in false result, therefore, incorrect conclusions. In addition, human serum represents a very complex biological matrix from which various components may alter the performance of the sample preparation and analysis mostly manifested by high

variability in the distribution of the separated glycan peaks. Besides, PNGase has unique and intriguing properties, one of the most important one is the inhibition of its action by the presence of the released oligosaccharides piling up during the reaction. By focusing on the denaturation and enzymatic N-glycan release steps and using the evaporative labeling technique of our recently published work [5], the parameters of the sample preparation were optimized for high yield glycan release and increased labeling efficiency.

Experimental

The Fast Glycan Sample Preparation and Analysis kit (Sciex, Brea, CA) was used for sample preparation and fluorophore labeling. Briefly, optimized amount of human serum samples (2.0 µL) were denatured by glycerol supplemented denaturing mixture at different temperatures for 10 minutes. The glycans were released by the addition of 1.0 µL of PNGase F enzyme (Asparia Glycomics, San Seabstián, Spain; 1.5 IUB/µL) to the reaction mixture and incubated at 50°C for 60 minutes. Then, threefold amount of acetonitrile was added to precipitate the high amount of protein present in the serum and the supernatant was removed for further processing as that contained the released glycans. After drying the supernatant under reduced pressure at 60°C for 45 minutes, the released glycans were fluorophore labeled with APTS (8-aminopyrene-1,3,6-trisulfonate), incubated in a heating block at 50°C with the lid closed for one hour and at 55°C with lid open for one hour (evaporative labeling technique [5]). The excess dye was removed by the use of magnetic microparticles as we reported earlier [6]. The fluorescently labeled glycans were then analyzed by a PA800 Plus Pharmaceutical Analysis System (Sciex) with laser induced fluorescence detection (λex=488 nm / λem=520 nm). A bare fused silica capillary was used (40 cm effective length, 50 µm ID) with HR-NCHO separation matrix at 25°C. The applied electric voltage was 30 kV in reversed polarity mode (cathode at the injection side, anode at the detection side). A two-step electrokinetic sample injection was applied: 1) 3.0 psi for 5.0 sec water pre-injection and 2) 1.0 kV for 1.0 sec sample injection. The 32Karat (version 10.1) software package (Sciex) was used for data acquisition and processing.

Results and Discussion

In this study, the parameters of glycoprotein denaturation for PNgase F digestion were optimized for high performance N-glycan analysis of human serum samples. First, denaturation parameters were optimized to ensure the accessibility of the glycosylation moieties of the glycoproteins for the endoglycosidase. The denaturation solution of the Fast Glycan Kit was supplemented with glycerol to avoid protein precipitation during the incubation and the reaction temperature was varied between 30°C and 80°C during the denaturation step. The amount of serum used was also optimized to 2.0 µL also limiting the probability of protein precipitation.

Next, the parameters of the enzymatic release of the glycans were scrutinized. Although, PNGase F works in a wide pH range with the reaction speed still considered to be optimal, different buffers are usually employed to set the pH value. The problem was, however, that the

suggested concentrations of the buffers were not sufficient to set the pH to the desired level and did not have the sufficient buffer capacity to maintain it during the reaction. Furthermore, some buffer components tend to decompose over time – such as HCO3-, COOH- – that alters the yield of the enzymatic reaction. Also, salt addition has a negative effect in glycan separation with capillary electrophoresis when electrokinetic sample injection is used as the much higher mobility salts ions are preferentially transferred into the capillary instead of the glycans. In spite of all these, buffering the reaction has increased yield compared to its non-buffered counterpart in a given time frame. More interestingly, our results suggested that even ammonium ion containing buffers showed significant (> 20%) yield increase, despite of the fact that it was previously suggested not to use for PNGase F digestion [7]. However, if temperature and reaction time parameters are sufficiently optimized, buffering related yield increase was apparently negligible compared to digestion performed in HPLC grade water. The salts of the storage solution of the enzyme properly facilitated the enzymatic reaction in water without having any negative effect from use of additional buffers that resulted a robust and reproducible sample preparation protocol. The digestion temperature and the reaction time were also varied, 40°C to 60°C and 5.0 min to 16 hour (overnight), respectively. In addition, the PNgase F enzyme concentration and amount was also varied considering the batch-to-batch differences in enzyme activity. It was found that 1.0 µL of 1.5 IUB/µL PNGase F enzyme was optimal for the deglycosylation of serum glycoproteins.

It was apparent that protein precipitation was crucial during the sample preparation process due to the high amount of proteins are in the sample. Precipitation was accomplished by adding 3x amount of acetonitrile to the sample (by volume). The precipitated proteins were then partitioned with centrifugation and the glycan containing supernatant was dried under reduced pressure. The released glycans were then labeled by our evaporative labeling technique and the excess dye was removed by magnetic beads. Due to these changes in the protocol, a robust and reproducible sample preparation method was established for N-glycan analysis in human serum samples.

Conclusion

Denaturation and PNGase F digestion parameters were optimized for circulating human serum N-glycome analysis with capillary electrophoresis – laser induced fluorescent detection. By establishing the proper sample amount (max 2.0 uL), glycerol supplemented denaturation solution and optimized PNGase F digestion parameters, a robust and reproducible sample preparation was achieved. The released and fluorophore labeled N-glycans were analyzed by CE-LIF with high reproducibility (RSD < 2%) including the entire sample preparation and analysis process providing reliable data for glycol-biomarker discovery.

Acknowledgement

Reference

[1] Varki, A., Cummings, R., Esko, J., Freeze, H., Stanley, P., Bertozzi, C., Hart, G.W., Etzler, M. Essentials of Glycobiology, nd, et al., Editors. 2009: Cold Spring Harbor NY.

[2] Schwedler, C., et al., Anal Bioanal Chem, 2014. 406(28) 7185-93.

[3] Kovacs, Z., et al., Electrophoresis, 2017. 38(17) 2115-2123.

[4] Varadi, C., C. Lew, and A. Guttman, Anal Chem, 2014. 86 (12) 5682-7.

[5] Reider, B., M. Szigeti, and A. Guttman, Talanta, 2018. 185, 365-369.

[6] Szigeti, M., et al., J Lab Autom, 2016. 21 (2) 281-6.

[7] Kuster, B. and D.J. Harvey, Glycobiology, 1997. 7 (2) vii-ix.

P18   HIGH THROUGHPUT GLYCAN ANALYSIS: THE C100HT MULTICAPILLARY ELECTROPHORESIS SYSTEM

Laszlo Hajba[1], Balázs Reider[1], Beáta Borza[1,2], András Guttman[1,2]

[1]*Translational Glycomics Research Group, Research Institute of Biomolecular and Chemical Engineering, University of Pannonia, Veszprem, Hungary, hajba@mukki.richem.hu*

[2]*Horváth Csaba Memorial Institute for Bioanalytical Research, University of Debrecen, Debrecen, Hungary*

Summary

N-glycosylation analysis of human biological samples (e.g. serum, tissue) and biotherapeutics are important both from diagnostic and therapeutic points of view. We utilized a multicapillary electrophoresis system with laser induced fluorescence detection for high throughput N-glycosylation analysis of IgG samples. Because of the large number of samples, automation of the sample preparation was also applied to reduce the total analysis time.

Introduction

Recombinant protein biologics and their biosimilars (e.g., monoclonal antibodies, fusion proteins, antibody-drug conjugates, etc.) are typically glycosylated and their glycosylation has a significant impact on biological activity, effector functions, serum half-life and immunogenicity in case of drug products. Glycosylation profiles of biologics and their biosimilars are critical quality attributes (CQA), which need to be tightly monitored and controlled during every stage of the manufacturing process [1]. Glycans can also be used in clinical diagnostics as disease markers due to the glycosylation alteration, e.g., fucosylation and sialylation during malignant transformation and cancer progression [2]. The large number of samples collected during clone selection or biomarker discovery processes need high a throughput glycoanalytical platform [3,4]. We applied a multicapillary electrophoresis system for high throughput N-glycan analysis of IgG samples.

Experimental

Sample preparation of the different IgG samples were performed with the C100HT Glycan Labeling and Analysis kit (Sciex, Brea, CA), based on the fast glycan sample preparation protocol [5]. Briefly, the samples were denatured, digested with PNGase F enzyme, labeled with 8-aminopyrene-1,3,6-trisulfonic acid (APTS) fluorescent dye and purified by magnetic bead based technology. Capillary electrophoresis measurements were performed on a 12 capillary electrophoresis system (C100HT Biologics Analyzer), equipped with a LED-induced

fluorescent detector. The samples were injected electrokinetically: 3 kV for 3 s and the separation voltage was 10 kV.

Results and Discussion

First, standard human and mouse IgG samples in 10 mg/ml concentration (both from Sigma-Aldrich, St. Louis, MO) were run on the C100HT Biologics analyzer, 12 from each, respectively. The C100HT software identified the main IgG glycans based on their glycose unit (GU) values. The RSD% values of corrected area % of the glycan peaks were adequate (e.g. FA2G1 glycan peak, RSD%=3.224 for 12 parallel runs). Next the N-glycan analysis of 25 IgG samples extracted from biological samples (IgG samples from human serum) were performed on the multicapillary electrophoresis system. Adequately evaluable electropherograms were obtained even from low concentration samples (0.126 mg/ml).

Conclusion

The glycosylation pattern of different glycoproteins are of great interest from biopharmaceutical and biomedical point of view. Concerning the large sample numbers generated e.g. during the manufacturing process of monoclonal antibodies a whole 96 sample plate can be processed in <3 hours (excluding sample preparation) to get adequately evaluable electropherograms for N-glycan identification. We can also automate the sample preparation process with a liquid handling robot to reduce the total analysis time and the random errors may occur during manual sample preparation.

Acknowledgement

Reference

[1] Hajba, L., Szekrényes, Á., Borza, B., Guttman, A. Drug Discov. Today 2018, 23 616-625.

[2] Varki, A., Cummings, R., Esko, J., Freeze, H., Stanley, P., Bertozzi, C., Hart, G.W., Etzler, M. Essentials of Glycobiology. 2nd ed. Cold Spring Harbor Laboratory Press: Plainview, NY, 2009.

[3] Szekrényes, Á, Roth, U., Kerékgyártó, M., Székely, A., Kurucz, I., Kowalewski, K., Guttman, A. Anal. Bioanal. Chem. 2012, 404, 1485-1494.

[4] Reusch, D., Haberger, M., Kailich, T., Heidenreich, A-K., Kampe, M., Bulau, P., Wuhrer, M. mAbs 2013, 6, 185–196.

[5] Guttman, A., Szigeti, M., Lou, A., Gutierrez, M.. Fast Glycan Labeling and Analysis: High-Resolution Separation and Identification in Minutes. Sciex Application Note. 2017.

P19   HUMAN TRF1 EXCHANGES TRF2 BOUND TO TIN2 BUT TOLERATES TRF2 IN TPP1 PRESENCE

Tomáš Janovič, **Martin Stojaspal, Pavel Veverka, Ctirad Hofr**

LifeB, Chromatin Molecular Complexes, CEITEC and Functional Genomics and Proteomics, National Centre for Biomolecular Research, Faculty of Science, Masaryk University, 62500 Brno, Czech Republic

Summary

Telomeric repeat binding factors TRF1, TRF2 along with TIN2 form a shelterin-core responsible for selective double-strand DNA binding to telomeres. The dynamics of TRF1-TIN2-TRF2 interactions is important for regulating the assembly of the whole six-protein shelterin complex. We applied a single molecule approach called Fluorescence Cross-Correlation Spectroscopy (FCCS) to study TRF1-TIN2-TRF2 complex assembly.

When we employed FCCS to describe quantitatively the interchange of TRF1 and TRF2 in complex with TIN2 in solution at physiological conditions, we found that TRF1 effectively substituted TRF2 in TIN2-TRF2 complex. Additionally, we extended our FCCS studies to TPP1. TPP1 is critical for telomerase regulation as TPP1 recruits telomerase to telomeres. We tested if TPP1 presence alters TIN2 interactions.

Our data demonstrate that TPP1, upon binding to TIN2, induces allosteric changes that expand TIN2 binding capacity, so TIN2 can accommodate both TRF1 and TRF2 simultaneously. Finally, we verified, at the single-molecule level, that TPP1 is essential for the stable formation of TRF1-TIN2-TRF2 complex.

Introduction

Human telomeres are maintained by telomerase (1,2) and protected by telomeric proteins (3,4). Shelterin as a six-protein telomeric complex comprising of TRF1, TRF2, TIN2, TPP1, POT1 and RAP1 is responsible for recruiting telomerase to telomeric DNA (5). Shelterin interacts with telomeric DNA and protects it from DNA damage response machinery (4). TRF1 and TRF2 bind the double-stranded telomeric DNA (6,7). RAP1 interacts with TRF2 and regulates TRF2's binding specificity to telomeric DNA (8). TIN2 binds both TRF1 and TRF2 and interconnects it with TPP1 which creates heterodimer with POT1 (9). TIN2 therefore plays role as a central hub of shelterin complex, see Figure (1).

The dynamics of TRF1-TIN2-TRF2 interactions is important for regulating the assembly of the whole shelterin complex. We applied a single molecule approach called Fluorescence Cross-Correlation Spectroscopy (FCCS) to assess what are the requirements for stable TRF1-

TIN2-TRF2 complex formation. We were curious whether both TRF1 and TRF2 bind TIN2 simultaneously or if there is an order preference. Next, we wanted to know if TPP1 binding to TIN2 can affect interaction of TIN2-TRF2 so that TIN2 can accommodate both TRF1 and TRF2 simultaneously.

Figure 1: Shelterin complex and how it protects telomeric DNA.

Experimental

Fluorescence Cross-Correlation Spectroscopy (FCCS) monitors simultaneously fluorescence signals of two differently labelled proteins and determines how the two proteins coincident fluctuations correlate to each other if the proteins are bound and moving together. FCCS describes binding of measured proteins independently of diffusion rate. The cross-correlation fit with an appropriate model provides us with the degree of complexation of two fluorescently labeled molecules. Under ideal conditions (absence of FRET – Fluorescence Resonance Energy Transfer and spectral crosstalk of used fluorophores) the cross-correlation amplitude is directly proportional to the concentration of bound species (10,11).

Results and Discussion

We wanted to know whether TIN2 can accommodate both TRF1 and TRF2 simultaneously. We mixed and incubate together fluorescently labeled TRF2 and TIN2 with Alexa Fluor 594 and 488, respectively. After measuring their initial relative cross-correlation we started to titrate it with unlabeled TRF1. We observed significant decrease of TRF2-TIN2 relative cross-correlation, which suggested that TRF1 replaced TRF2 in complex with TIN2 (Figure 2A). On the other hand when we used Alexa Fluor 594 labeled TRF1 and mixed it with Alexa Fluor 488 labeled TIN2 their relative cross-correlation stayed intact even after addition of unlabeled TRF2, so the TRF2 has no influence on TRF1-TIN2 complex (Figure 2B). If we repeated the

first experiment and add also TPP1 protein we found out that the TRF2-TIN2 relative cross-correlation remained at high level so that the TIN2 can accommodate both TRF1 and TRF2 simultaneously (Figure 2C). To confirm it we prepared complementary experiment where TRF1 and TRF2 were labeled by Alexa Fluor 488 and 594, respectively. First the unlabeled TIN2 was added to the mixture of labeled TRF1 and TRF2. After TIN2 addition we observed no significant change in amplitude of relative cross-correlation. On the contrary when we added preformed complex TIN2-TPP1 into TRF1 and TRF2 mixture, we detected substantial increase of relative cross-correlation between TRF1 and TRF2 (Figure 2D).
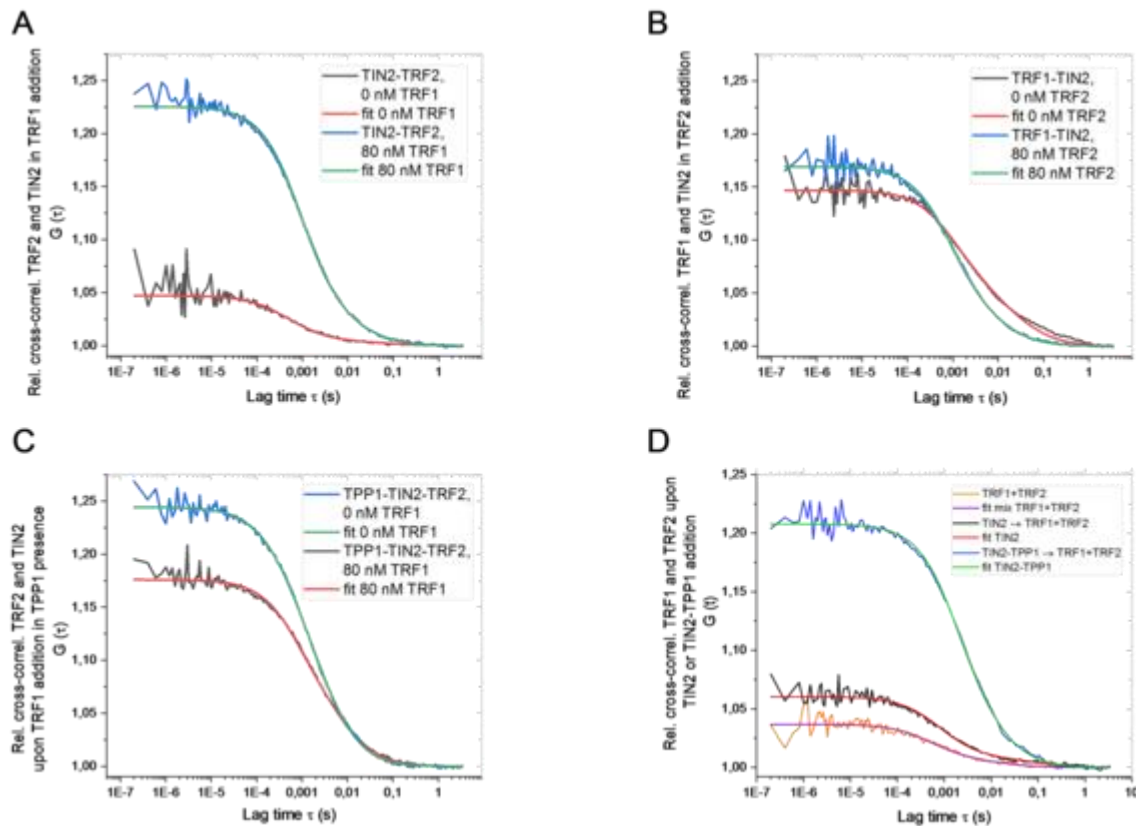
Figure 2: (A) TRF2-TIN2 Relative cross-correlation decrease indicates that TRF1 releases TRF2 from TIN2. (B) Upon TRF2 addition, the relative TRF1-TIN2 cross-correlation stays intact. (C) In TPP1 presence the relative TRF2-TIN2 cross-correlation remains at high level upon addition of TRF1. (D) TPP1 is essential for proper TRF1-TIN2-TPP1-TRF2 complex assembly.

Based on the results we can propose a model of shelterin core assembly where TRF1 occupies TIN2 and TRF2 binding to TIN2 is compromised. When TPP1 binds TIN2 it can allosterically activate TIN2 binding site for TRF2, hence the TRF2 can bind TIN2 also in TRF1 presence so that TIN2 can accommodate both TRF1 and TRF2 simultaneously. TPP1 plays a key role in this scenario.
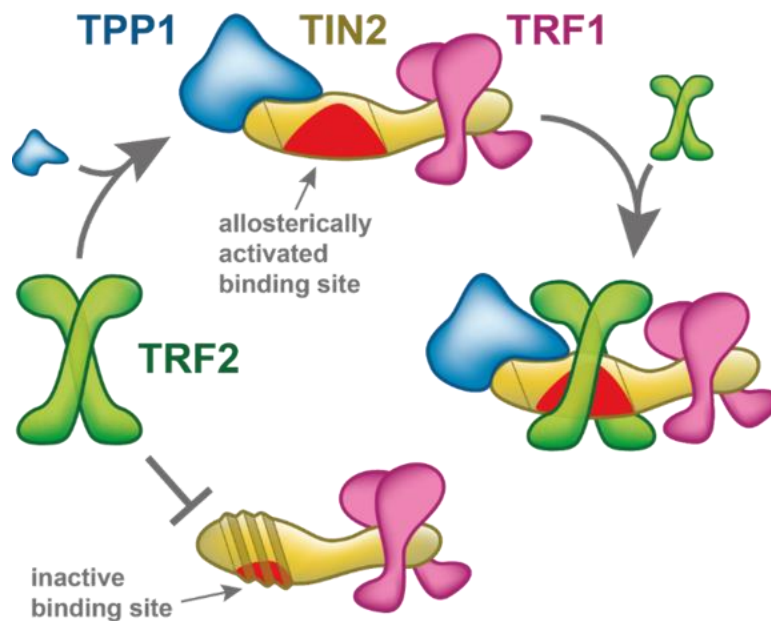
Figure 3: Model for sequential assembly of shelterin core complex. TRF1 prevents TRF2 from binding to TIN2 if TPP1 is absent, as TRF1 occupies the preferential binding site on TIN2 (lower part of the scheme). On the contrary, when TPP1 binds TIN2, TPP1 induced allosteric structural changes that open the second binding site on TIN2 and the binding site for TRF2 becomes active (upper part of the scheme). TRF2 binds TIN2-TPP1 along with TRF1 (middle part of the scheme). A stable shelterin core complex TRF1-TIN2-TPP1-TRF2 is formed.

Conclusion

Our FCCS studies shows how particular shelterin core components are formed and assembled to create one functional complex. We found out that the key factor is TPP1 protein which can allosterically affect TIN2 in a way that it can accommodate both TRF1 and TRF2 simultaneously. Without TPP1 there is an order preference where TRF1 has higher affinity to bind TIN2 so it can outcompete TRF2.

Our results with the core shelterin complex TRF1-TIN2-TRF2 extend the knowledge, so far limited to previous structural interaction studies that have been carried out only with isolated protein domains and oligopeptides. The next challenging tasks will be to describe the effects of the DNA scaffold on shelterin assembly and monitor the dynamics of telomeric proteins associations in living cells.

Acknowledgement

Reference

[1] Blackburn, E.H. Switching and Signaling at the Telomere, 2005, Cell, 106, 661-673.

[2] Greider, C.W. and Blackburn, E.H. Identification of a specific telomere terminal transferase activity in Tetrahymena extracts, 1985, Cell, 43, 405-413.

[3] Schmutz, I. and de Lange, T. Shelterin, 2016, Current Biology, 26, R397-R399.

[4] de Lange, T. Shelterin: the protein complex that shapes and safeguards human telomeres. Genes & development, 2005, 19, 2100-2110.

[5] Nandakumar, J. and Cech, T.R. Finding the end: recruitment of telomerase to telomeres, 2013, Nat Rev Mol Cell Biol, 14, 69-82.

[6] Bilaud, T., Koering, C.E., BinetBrasselet, E., Ancelin, K., Pollice, A., Gasser, S.M. and Gilson, E. The telobox, a Myb-related telomeric DNA binding motif found in proteins from yeast, plants and human, 1996, Nucleic acids research, 24, 1294-1303.

[7] Zhong, Z., Shiue, L., Kaplan, S. and de Lange, T. A mammalian factor that binds telomeric TTAGGG repeats in vitro, 1992, Molecular and cellular biology, 12, 4834-4843.

[8] Necasova, I., Janouskova, E., Klumpler, T. and Hofr, C. Basic domain of telomere guardian TRF2 reduces D-loop unwinding whereas Rap1 restores it, 2017, Nucleic acids research, 45, 12170-12180.

[9] Baumann, P. and Cech, T.R. Pot1, the Putative Telomere End-Binding Protein in Fission Yeast and Humans, 2001, Science, 292, 1171-1175.

[10] Bacia, K. and Schwille, P. Practical guidelines for dual-color fluorescence cross-correlation spectroscopy, 2007, Nat Protoc, 2, 2842.

[11] Kim, S.A., Heinze, K.G., Waxham, M.N. and Schwille, P. Intracellular calmodulin availability accessed with two-photon cross-correlation, 2004, Proceedings of the National Academy of Sciences of the United States of America, 101, 105-110.

P20 THE METHOD TO DECREASE IBUPROFEN CONCETRATION LIMIT IN ELECTROPHORESIS

Lenka Janštová, Jan Pospíchal

Mendel University in Brno, Brno, Czech Republic, xjanstov@mendelu.cz

Summary

An online method consisting of transient electrokinetic dosing on-line coupled to ITP was performed for the pre-concentration, pre-separation and analytical determination of a model substance ibuprofen in aqueous samples containing very low concentration of the analyte. Various parameters were investigated in the framework of an optimisation study; the aim was to reach maximal cLOD decreasing in minimum time.

The method consists of 2 phases. In the first one, an ibuprofen with addition of dosing electrolyte is electrokinetically dosed to the ITP column where it was stacked on the leading electrolyte. The accumulated zone of ibuprofen is slowly moving through the column. After 800 second of the dosing, the dosing electrolyte has been replaced with the terminating one.

The cLOD concentration was dosed to the column on various times. The dosing time was thoroughly optimized and 10fold accumulation in 13 minutes was reached.

Introduction

Due to various human activities, many pollutants are released back into the environment, large part of them directly into the water. Although wastewater treatment plants are able to decompose some of them, many of pollutants which stay in the water system. From there, they can get into plants, to the organisms of the animals or people. [1]

Ibuprofen (2-(4-isobutylphenyl) propionic acid) is a pharmaceutical drug widely used by the large part of population. It falls into the group of nonsteroidal drugs which are the most commonly used medication because of their ability to blocking cyclooxygenase (COX)-2.[2] Ibuprofen is an acidic substance; we can found it in the enviromnent as a pollutant.

It has been found in aquatic ecosystem in a many countries. In the Czech Republic, the degradation of ibuprofen by constructed wetlands was studied. Only 55% of ibuprofen content was removed this way.[1]

Experimental

The investigated method is primary used as an on-capillary preconcentration technique. It is useful for the separation of diverse analytes of varying character and size. The principle of this

method is based on a continual electrokinetic dosing of ionised ampholyte into a stationary neutralisation boundary. The analyte of interest is de-protonised and stacked on this boundary. The accumulated analyte can be further mobilised and detected in the analytical column. [3,4]

Several parameters can be optimised, like the pH range of the neutralisation boundary and composition or nature of the electrolyte, i.e. dissociation degree of the ampholyte in both electrolytes, dosing time and current and the electric current.

Commercial isotachophoretic apparaturs (CS Isotachophoretic Analyzer, Labeco, Slovak Republic) was used for individual analyses. The analytical column was coupled to a conductivity meter as a detector. The analyses were performed with constant current during the whole time of analysis. The Clarity program was used to record the analyses and process data.

Histidine base was obtained from Ner., s.r.o., Neratovice, Czech Republic. Histidine hydrochloride was purchased from Serva Feinbiochemica, Heidelberg, Germany. 2-(N-Morpholino) ethanesulfonic acid hydrate, 4-Morpholineethanesulfonic acid (MES) were all obtained from Sigma-Aldrich, SPADNS Lachema N.P. Brno, Czech Republic and ibuprofen was obtained from sanofi-aventis, s.r.o., Praha, Czech Republic. The operating electrolytes in various concentrations (see Fig.1) were used for individual analyses.

Parameter	Basic primary LE	Acid primary DE	Terminating TE
Solvent	water	water	water
Anion	HCl^-	MES	MES
Concentration	0.02 M	0.01M	0.02M
Cation	Histidine	Histidine	H^+
Concentration	0.008 M	0.006 M	

Fig.1. The operating electrolytes used for individual analyses. Abbreviations: LE – leading electrolyte; DE – dosing electrolyte; TE – terminating electrolyte

Results and Discussion

In the framework of metod validation a continuous dosing of ibuprofen was performed. As a dosing electrolyte, zwitterionic histidine buffer was used because of several advantages; excellent buffering abilities and low conductivity that enables quicker dosing, as well as the increased stability of stationary asymmetric neutralization boundary. After the dosing, the migration mode was changed to the ITP mode; the dosing electrolyte was substituted by the terminating electrolyte. This way, the neutralization balance was disturbed and the deprotonated sample, which up to now slowly migrated in the leading electrolyte, created the isotachophoretic zones that migrated together in the steady state right into the detector. Conductivity detection was performed at 250 µA in the first 800 seconds and after that the value was degreased to 150 µA.

The classical ITP analysis (see Fig.2) was used for the cLOD determination. Thanks to the electrolytes used, the cLOD of 1.10-6 mol.l-1 was reached. For the dosing experiment the 0.006 M histidine pI 7.4 was selected and used as DE buffer and 0.01 M MES was used as the terminating electrolyte (see Fig. 3). As shown on Fig.3 the dependence of accumulated substance on the dosing time is fairly linear. Selected dosing electrolyte is alkaline enough to dissolve atmospheric carbon dioxide which is focused on the boundary and creates its own zone and decreases the sensitivity. Thus, it was necessary to remove hydrogen carbonates from both electrolytes.
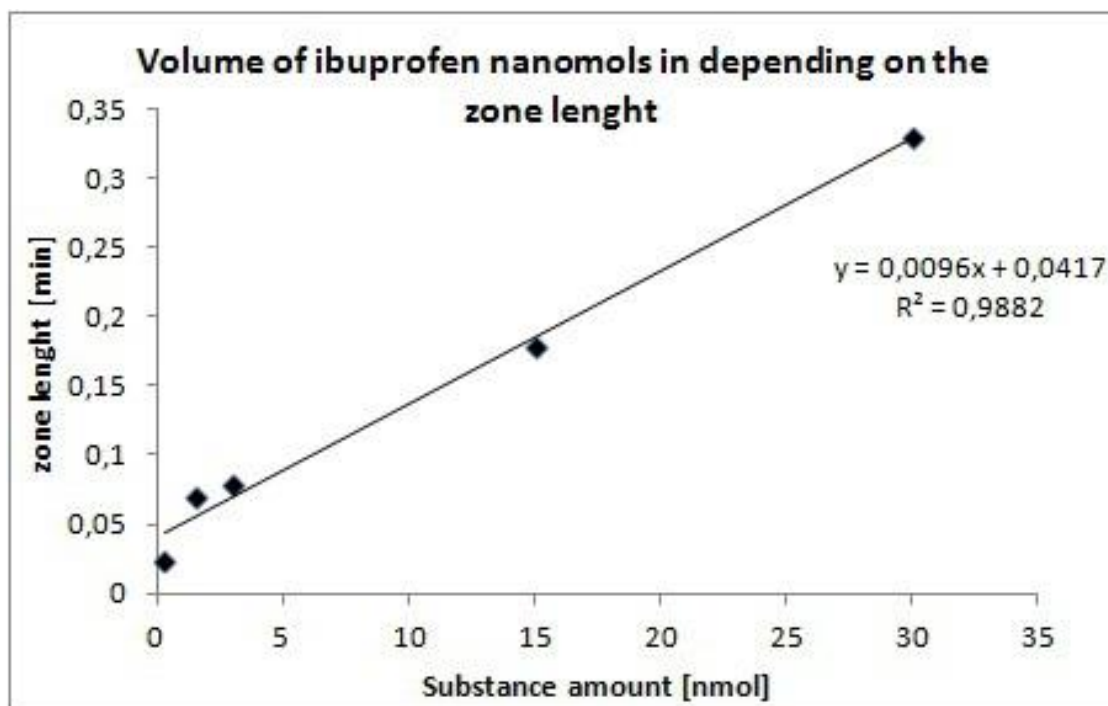
Fig.2. The calibration curve: The dependence of the zone length of ibuprofen on the amount of injected sample (300 µL)
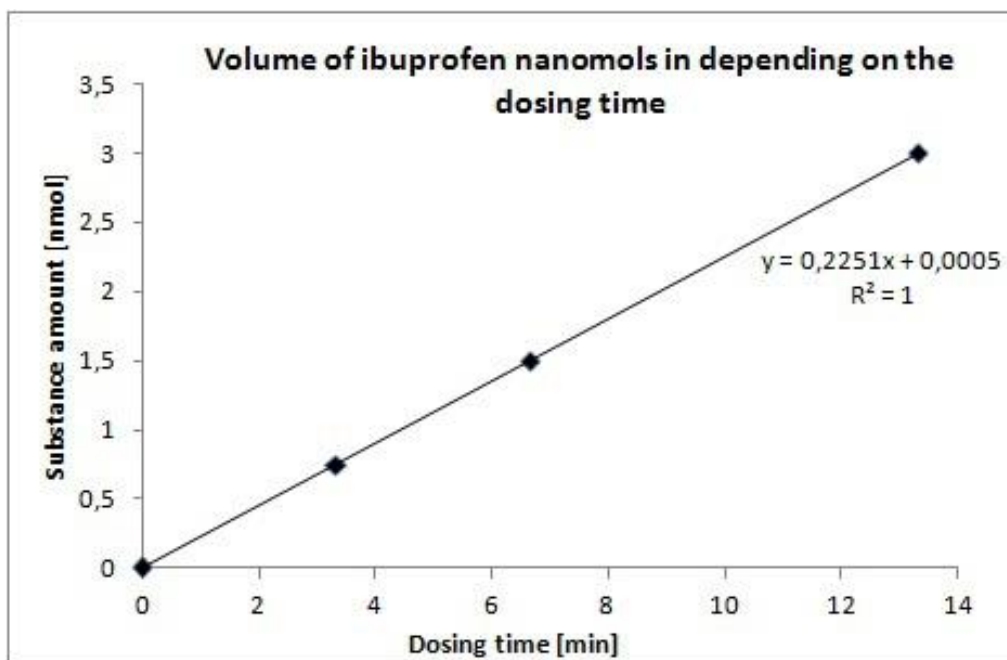
Fig.3.The calibration curve: dependence of the accumulated nanomols of ibuprofen on the dosing time. TE: 0,02M MES, LE: 0,0008M HIST + 0,006 M DE: 0,006 M HIST +0,01M MES + 0,000001 M SPADNS + ibuprofen

The concentration of ibuprofen 10times higher than determined cLOD was dosed to the column on various times. The dosing time was thoroughly optimized and 10fold accumulation was reached in 13 minutes.

After the dosing to the column, the dosing electrolyte was changed for the terminating one and the ITP analysis with conductivity detector was performed.

Conclusion

The new method of ibuprofen determination is performed by dosing of the sample with addition of convenient buffer (dosing electrolyte) to the ITP column with proper leading electrolyte. The electrolyte composition and the dosing time were thoroughly optimized and 10 fold accumulation in comparison to classical ITP analysis was reached in 13 minutes.

Reference

[1] Vymazal, J., Dvořáková Březinová T., Koželuh M., Kule L., E. Engineering 2017, 98, 354-364.
[2] Ahmetaj-Shala, B.,et al. BBRC. 2017, 484, 762-766.
[3] Pospíchal, J., Glovinová, E., J. Chromatogr. A. 2001, 918, 195-203.
[4] Landers, J., Handbook of capillary and microchip electrophoresis and associated microtechniques. 3rd ed., CRC Press, Boca Raton 2008.

P21 DESIGN OF AN ADJUSTABLE CE-MS INTERFACE: ANALYSIS OF APTS-LABELED N-GLYCANS OF BIOPHARMACEUTICAL INTEREST

Gábor Járvás[1,2], Márton Szigeti[1,2], András Guttman[1,2]

[1]*MTA-PE Translational Glycomics Research Group, Research Institute of Biomolecular and Chemical Engineering, University of Pannonia, 10 Egyetem Street, Veszprem, 8200, Hungary*

[2]*Horvath Csaba Memorial Institute for Bioanalytical Research, Faculty of Medicine, Research Center for Molecular Medicine, University of Debrecen, 98 Nagyerdei Krt, Debrecen, 4032, Hungary*

Summary

Glycosylation plays an important role in cellular interactions, protein folding, and monoclonal antibody (mAb) stability. For characterization, N-linked glycosylation on mAbs is routinely analyzed by CE-LIF after endoglycosidase based glycan release and fluorophore labeling. CE separation provides structural resolution and migration time-based identification of glycans, but coupling with MS detection offers additional structural information. The integration of CE and ESI into a single dynamic process (CESI) provides the capability of performing CE separation and MS ionization with ultra-low flow rate, resulting in reduced ion suppression and improved sensitivity. CESI-MS has been optimized and evaluated for released, APTS-labeled mAb and formalin-fixed parafin-embedded glycan analysis.

Introduction

Since introduced as a biological tissue sample fixative by F. Blum in 1893, formalin fixation has been still an almost exclusively used method for tissue preservation. Fixation using this reagent makes clinically relevant samples stable that can be stored at ambient condition for decades in depositories. Combined with paraffin embedment, formalin fixed tissues become FFPE specimens (formalin fixed paraffin embedded) that are amenable for long-term storage and can be universally used in histopathological laboratories. The clinicopathological significance of formalin-fixed paraffin-embedded (FFPE) archival specimens has led many researchers to utilize and annotate these "unmasked treasures" beyond their main histopathological utilization even at the molecular level. Several clinico-molecular assays for oncological prognosis and treatment decision have been developed based on FFPE tissue analysis. Recently capillary electrophoresis has been introduced as a method to probe the N-glycosylation pattern of these precious samples.

Experimental

Sample Preparation: A maltooligosaccharide ladder, released IgG1 glycans, and released formalin-fixed paraffin-embedded (FFPE) glycans were labeled with APTS and cleaned-up. For deparaffinization, the FFPE samples were washed twice by xylene for 20 min and centrifuged at $5000 \times$ g for 10 min. This was followed by ethanol wash, two times for 20 min and centrifugation at $5000 \times$ g for 10 min. For protein extraction, all samples were first homogenized in a 1 mL Tapered Tissue Grinder (VWR, Budapest, Hungary) and solubilized with 100 µL of RIPA buffer (25 mM Tris-HCl, pH 7.6, 150 mM NaCl, 1% NP-40, 1% sodium deoxycholate, 0.1% SDS) containing 10 µL of 50 mM DTT. The solubilization mixture was first incubated at 100°C for 20 min, then 65°C for 60 min. After the solubilization step, 10 µl of 50 mM iodoacetamide was added and incubated at 37°C for 30 min in dark. For buffer exchange, 10 kDa spin filters were used at $5000 \times$ g for 10 min. To release the N-glycans, 49 µL of 20 mM $NaHCO_3$ buffer (pH 7.0) and 1 µL PNGase F Ultra enzyme (2.5 mU, Prozyme, Hayward, CA) were added to the sample on the filters and incubated for 1 h at 50°C. The released N-glycans were centrifuged though the spin filters at $5000 \times$ g for 10 min and dried in a centrifugal vacuum evaporator. 6 µL of 20 mM APTS and 2 µL of 1 M NaCNBH3 (in THF) was added to the dry pellet and incubated at 37°C overnight. The labeled samples were magnetic bead purified (CleanSeq, Beckman Coulter, Indianapolis, IN) and immediately used or stored at –20°C for later analysis.

CESI 8000 Plus Stand-Alone CE Mode Conditions: The separations were monitored by laser induced fluorescence (LIF) detection using a 488 nm solid state laser with a 520 nm emission filter. 50 cm effective (60 cm total) length with 50 µm id NCHO capillaries were used filled with NCHO gel buffer system (both from SCIEX) in reversed polarity mode (cathode at the injection side). The samples were injected by 1 psi pressure for 5 s.

CESI 8000 Plus MS Mode Conditions: CESI experiments were carried out with a SCIEX CESI 8000 Plus system equipped with a temperature controlled autosampler and a power supply with the ability to deliver up to 30 kV. CESI-MS analyses were performed using a SCIEX CESI 8000 Plus system. CESI-MS experiments also employed a TripleTOF® 6600 system. CESI-MS separations were achieved using an OptiMS bare fused-silica capillary cartridge by application of -30 kV and low pressures (2 for 7.5 min and 5 psi for 10 min). Ammonium acetate (7.5 mM, pH 4.5) with 10% isopropanol (IPA) was used as the background electrolyte (BGE). Samples were dissolved in 10% BGE to 10 mL and loaded into nanoVials (P/N 5043467) for ~15 nL pressure injections.

MS/MS Conditions: A SCIEX TripleTOF® 6600 system with a NanoSpray® III source and CESI adapter were used. Negative ESI was performed at -1750 V scanning from 250 - 2000 m/z with 250 ms (MS).

Data Analysis: High resolution MS and MS/MS spectra were analyzed using SCIEX PeakView®. Glucose unit (GU) values were calculated by the GUcal software (http://www.gucal.hu) and preliminary assignment of the glycan structures of interest were aided by the Glycobase ver 3.0 from NIBRT (Dublin, Ireland).

Results and Discussion

The transition from current CE-LIF APTS-glycan analysis methods to CESI-MS requires the use of MS-compatible buffers. Separations of an APTS-labeled carbohydrate ladder and mAb glycan standards were analyzed to evaluate the general capabilities of CESI-MS for the analysis of APTS-labeled released glycans from proteins of interest. Separation and detection of the carbohydrate ladder and mAb glycan standards illustrated efficient separations (~6 sec peak widths) and sensitive detection in negative ESI mode.

Separations of mAb glycan standards using a MS-compatible ammonium acetate buffer (pH 4.5) were also compared to the industry-accepted CE-LIF analyses using the stand-alone CE functionality of the CESI 8000 Plus instrument. Very similar separation profiles were observed, indicating ease of method transfer and correlation.

The CESI-MS method was evaluated using real samples with additional sample preparation. Prior to CESI-MS experiments, the released glycan samples were first characterized with industry-accepted CE-LIF analyses using the stand-alone CE functionality of the CESI 8000 Plus instrument. FFPE glycans from different mouse tissues were analyzed and compared. Glycan sequencing was performed with a combination of glycolytic enzymes to determine the carbohydrate content of each glycan.

Conclusion

The combined CESI-MS and stand-alone CE functionality of the CESI 8000 Plus system provides powerful methods to characterize and quantify released glycans from biologics and FFPE samples. Both analyses deliver high resolution separations, structural characterization, and relative quantitation. When coupled with the TripleTOF® 6600 system, the high sensitivity CESI-MS analyses are achieved from small sample amounts (~10 ng) and volumes (1 – 5 mL) using the nanoVial. Further analyses by MS/MS would facilitate confirmation of glycan structures and correlation to CE-LIF sequencing results.

Acknowledgement

P22 HEADSPACE IN-TUBE MICROEXTRACTION OF CHLOROPHENOLS FOR CAPILLARY ELECTROPHORESIS-MASS SPECTROMETRY

Sunkyung Jeong, Doo Soo Chung

Department of Chemistry, Seoul National University, Seoul, Korea

Summary

HS-ITME was in-line coupled with CE/MS. Dichlorophenols and trichlorophenols in an acidified aqueous solution were enriched into a basic acceptor plug at the entrance of the capillary. The chlorophenols were enriched about 20-300 times with a 20-min HS-ITME at 25°C, and successfully analyzed by CE/MS.

Introduction

Capillary electrophoresis/mass spectrometry (CE/MS) is a powerful analytical tool combining high performance separation of CE and information-rich MS. Single drop microextraction (SDME) was in-line coupled with CE-MS [1]. The small surface-to-volume ratio of the drop enables to be obtained high enrichment factors (EFs) in a short time. But SDME has a difficulty of keeping the drop attached to the inlet part of a capillary stably.

Headspace in-tube microextraction (HS-ITME) uses same principle but has no drop. It is the simplest possible scheme of liquid phase microextraction, providing sample cleanup and enrichment for volatile compounds [2, 3]. As a means of improving the power of CE/MS further, HS-ITME was in-line coupled with CE/MS. Here, dichlorophenols and trichlorophenols are tested as examples of volatile organic compounds.

Experimental

Without any physical modification of the CE/MS setup, HS-ITME was in-line coupled with CE/MS. when HS-ITME was coupled with CE/electrospray (ESI)-MS, the capillary outlet is exposed to the open air and there was a problem of air plug formation due to evaporation of the run buffer in the capillary. By running a small amount of the sheath liquid during the extraction, the evaporation problem was solved.

Dichlorophenols and trichlorophenols in an acidified aqueous solution were enriched into a basic acceptor plug at the entrance of the capillary and many parameters for HS-ITME-CE/MS were optimized.

Results and Discussion

With a 40 mM ammonium acetate buffer, all DCPs and TCPs could be separated. Although a migration time is similar in CE, the overlapping parts could be distinguished with different m/z values. Many parameters (acceptor, pre-injection volume, waiting time and extraction time) for HS-ITME-CE/MS were optimized. Basic acceptor is tested with NaOH or sodium phosphate and NaOH with pH 13 was more effective. After that, pre-injection amount was optimized. HS phase was pre-injected into the capillary before separation so as not to lose the enriched analytes. The optimum pre-injection amount was at 0.3 psi for 6 s (0.3% of the total length of the capillary). HS-ITME was performed for 5–25 min to observe the improvement in the extraction and 20 min was selected to maximize the effectiveness. Therefore, chlorophenols were enriched about 20-300 times with a 20-min HS-ITME at 25°C, and successfully analyzed by CE/MS.

Conclusion

HS-ITME can be combined as a simple sample clean up process for CE/MS. So, this application will help to increase abilities of CE/MS without any modifications of commercial instruments.

Reference

[1] J. Kim, K. Choi and D. S. Chung, Anal Bioanal Chem (2015) 8745.
[2] H. R. Lee, S. M. Cho, J. Kim, and D. S. Chung, J. Chromatogr. A (2014) 117.
[3] S. M. Cho, B. S. Park, W. S. Jung, S. W. Lee, Y. Jung, and D. S. Chung, Talanta (2016) 729.

P23　ADSORPTIVE REMOVAL OF COPPER AND CADMIUM IONS USING FLY ASH RESULTING FROM CFBC TECHNOLOGY

Tomasz Kalak, **Ryszard Cierpiszewski**

Department of Commodity Science and Ecology of Industrial Products, Faculty of Commodity Science, Poznań University of Economics and Business, Poznań, Poland

Summary

Fly ash was examined for the removal efficiency of Cu(II) an Cd(II) ions from water in batch experiments. This is industrial waste generated from the combustion of sewage sludge using the circulating fluidized bed combustion (CFBC) technology. The material was characterized using several methods, such as fraction analysis, particle size distribution, bulk density, composition, morphology, thermal analysis, the SEM-EDS, BET, BJH and FT-IR method. The influence of initial concentration, pH and contact time was conducted. The experiments demonstrated that this material had binding properties with respect to both these heavy metals. However, greater process efficiency was observed for cadmium than for copper. To conclude, the fly ash obtained in the combustion of sewage sludge is a promising low cost adsorbent for the effective recovery of copper and cadmium from industrial effluents.

Introduction

In recent years, interest in the development of bioenergy technologies around the world has increased due to environmental risks associated with the use of fossil fuels, the search for new energy sources and alternative technologies. The goal of many countries is to increase the amount of biomass fuels, which, using properly adapted technologies, will reduce the emission of greenhouse gases [1, 2]. One of the promising solutions used, inter alia, in the reduction of sewage sludge is the circulating fluidized bed combustion (CFBC) technology recommended by the European Union. The main advantages are minimizing odors, low air pollution, high combustion and energy efficiency or significant reduction of waste mass. The combustion products are fly ash and slag, which are characterized by significant physical and chemical properties, such as irregular shape with a porous surface, high mineral content, high specific surface area. As a result, the materials exhibit very good binding properties in relation to heavy metal ions. It is worth noting that, like biomass waste from food industry, they are also industrial waste, which makes them low cost adsorbents. Thus, the development of potential applications of cheap fly ash and slag generated in CFBC technology can be very important for the separation of metal ions from wastewater in the future [3, 4].

The aim of the research was to examine the adsorption capacity of fly ash obtained in the combustion process of sewage sludge for the removal of copper and cadmium ions from

aqueous solutions under the influence of different conditions, such as initial metal ions concentration, pH and contact time. In addition, the purpose was to characterize the adsorbent fly ash by analysis of fraction, particle size distribution by laser diffraction, bulk density, elemental analysis, morphology of the adsorbent by SEM images, SEM–EDS spectrometry mapping and analysis, qualitative analysis by X-ray diffraction, thermal analysis, the texture by the BET adsorption isotherms analysis, specific surface area, pore volume distribution by BJH method and FT-IR analysis.

Experimental

The fly ash used in this study was generated in a sewage treatment plant located in Poland in the combustion process in the new sludge thermal transformation installation based on the circulating fluidized bed combustion (CFBC) technology. Fly ash samples were taken from a fluidized bed ash reservoir and dried at temperature of 105°C. Fractions of less than 0.212 mm in diameter, analytically pure chemicals, distilled water were used. The measurements were performed three times.

Batch experiments were carried out at room temperature (23 ± 1°C) to examine the possibility of removal of copper ($CuSO_4$) and cadmium ($CdCl_2$) using fly ash from aqueous solutions. After adsorption processes solutions with the remaining content of metal ions were measured by atomic absorption spectrophotometry (F-AAS) using SpectrAA 800 (Varian, Palo Alto, USA) apparatus at a wavelength $\lambda = 324.8$ nm for copper and $\lambda = 228.8$ nm for cadmium.

Results and Discussion

The analysis of grain composition of fly ash revealed that particles of less than 0.212 mm in diameter were the dominant grain fraction of fly ash (87.6%) and then were used in this studies. Determination of particle size distribution showed only one peak in the plot, which refers to particle size of 1205 nm. Bulk density performed by loosely filling fly ash into a cylinder and by the thickening process indicated the results as follows: 0.7 ± 0.01 g/cm3 and 1.45 ± 0.02 g/cm3, respectively. The SEM-EDS analysis pointed out the predominant presence of oxides CaO, SiO_2, P_2O_5, Al_2O_3, Fe_2O_3, CO_2. Thermogravimetric measurements showed characteristic tendencies of the weight loss of fly ash with increasing temperature. The BET adsorption analysis determined the specific surface area (11.9 m2/g), volume of the pores (0.11 cm3/g) and average pore diameter (4.73 nm). Pore volume distribution analysis by BJH method demonstrated fly ash particles as mesopores (2.0 - 50 nm). The presence of bonds of silicon oxides and other oxides was shown based on the FT-IR analysis. SEM images showed the particles as heterogeneous, small, small, acicular, elongated, irregular in shape with presence of pores.

The impact of the initial concentration of Cu(II) and Cd(II) ions on the adsorption efficiency was shown in Figure 1. As it is seen adsorption capacity increased with an increase in metal ions concentration. In case of Cd(II) maximum adsorption capacity was reached at 11.8 mg/g and was slightly higher than compared to the result of Cu(II) adsorption (9 mg/g). This can be

explained in the way that the adsorption capacity increased, because there were still sufficient active sites to fill. The number of active sites affects the process of removing ions.
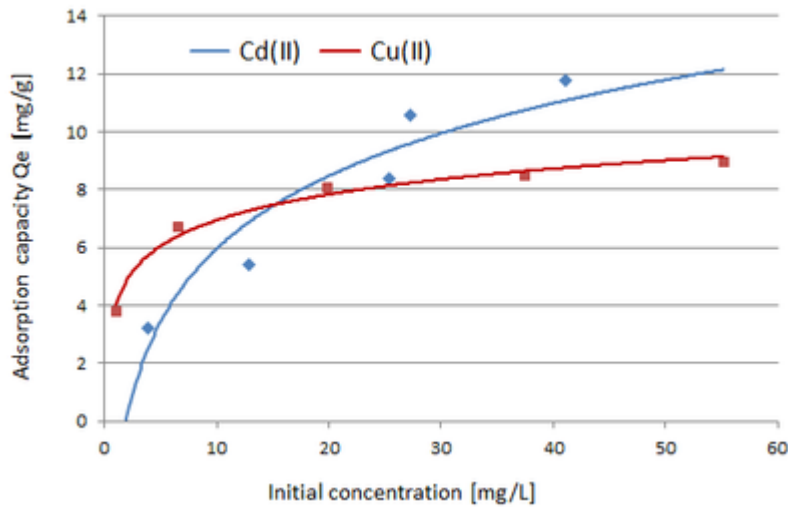

Figure 1. The effect of initial concentration on Cu(II) and Cd(II) adsorption (initial pH 2; contact time 30 min.; mass of adsorbent 100 mg).

The influence of initial pH on the adsorption was shown in Figure 2. Low process efficiency at initial pH 2-3 was observed due to the competition between H+ and Cu2+ and Cd2+ ions for the active sites in fly ash. The adsorption strongly depends on the interfacial tension at the solid-liquid interface [5]. At higher pH 4.5 - 6 the concentration of H+ ions rapidly decreased and the adsorption of the metal ions increased up to about 12 mg/g because of the greater affinity for the active sites. The charge of oxides SiO2, Al2O3 and others (included in the ash composition) is related to the pH of solution, thus it may be the cause of the ions behavior.
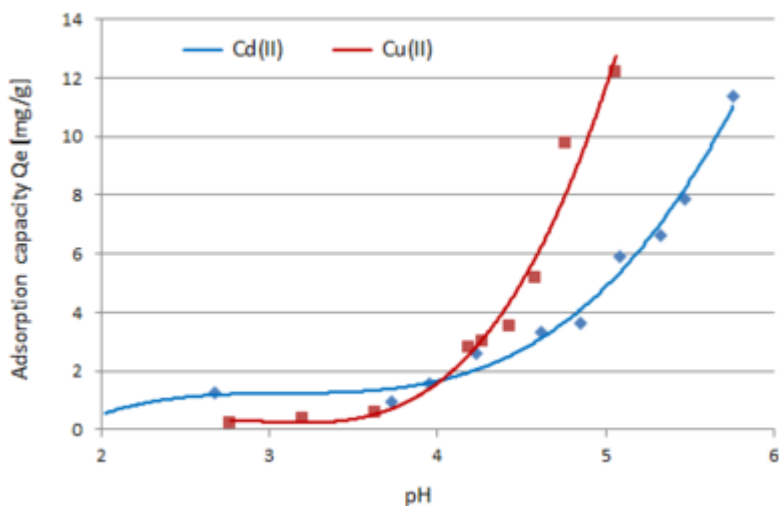
Figure 2. The effect of pH on Cu(II) and Cd(II) adsorption (initial concentration 100 mg/L; contact time 30 min.; mass of adsorbent 100 mg).

The effect of contact time on the adsorption presented in Figure 3. During the first 10 min. a rapid increase in the efficiency of the process is observed and after that an equilibrium was achieved at 15 min. in both cases. This may result from the presence of free sites on the fly ash surface and the high Cu(II) and Cd(II) concentration at the interface between the adsorbent and the solution. Thus, the adsorption was gradually decreasing as a consequence of the occupancy of active sites.
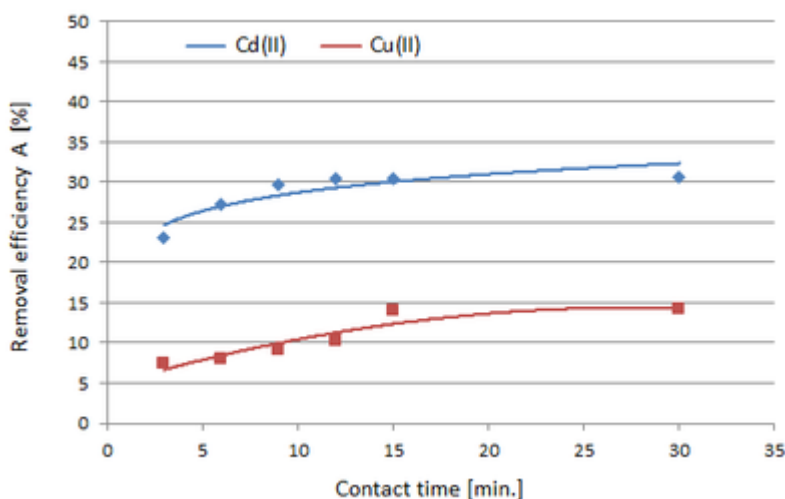

Figure 3. The effect of contact time on Cu(II) and Cd(II) adsorption (initial concentration 100 mg/L; initial pH 2; mass of adsorbent 100 mg).

Conclusion

Fly ash, generated in the process of circulating fluidized bed combustion (CFBC) technology in Poland, was used in this studies on the adsorption of Cu(II) and Cd(II) ions from aqueous solutions. The material was characterized by several analytical methods, such as fraction analysis, particle size distribution by laser diffraction, bulk density, thermal analysis, SEM–EDS, BET, BJH and FT-IR analysis. The influence of initial concentration, pH and contact time on adsorption efficiency was examined. It was revealed that adsorptive removal of Cd(II) was slightly greater than in case of Cu(II). The maximum adsorption capacity reached 11.8 mg/g (pH 2; 41.1 mg/L) and 9 mg/g (pH 2; 55.2 mg/L). Summing up, fly ash resulting from the sewage sludge combustion in the CFBC technology may be successfully used as a low-cost material for the removal of copper and cadmium ions from wastewater.

Acknowledgement

Reference

[1] Vamvuka, D., Kakaras, E. Fuel Process. Technol. 2011, 92, 570–581.
[2] Kalak, T., Strus, B. Energy&Fuels 2014, 28, 1926−1939.

[3] Kalak, T., Cierpiszewski, R., Dudczak, J., CECE 2015 12th International Interdisciplinary Meeting on Bioanalysis, 119-122.

[4] Fytili, D. Zabaniotou, A. Ren. Sustainable Energy Rev. 2008, 12 116-140.

[5] Kalak, T., Cierpiszewski, R., Text. Res. J. 2015, 85, 1884-1906.

P24 TRIMETHYLSILYL ACETATE-BASED COATINGS FOR BIOAPPLICATIONS

Štěpánka Kelarová, **Vojtěch Homola, Michal Kuchařík, Vilma Buršíková**

Department of Physical Electronics of Masaryk University, Brno, Czech Republic,
bittstep@gmail.com

Summary

The aim of the present work was to prepare organosilicon thin films with carbonyl functionalities based on trimethylsilyl acetate (TMSA) monomer using plasma of RF glow discharge. This study deals with properties of TMSA thin films that are prospective for bioapplications. Properties crucial for these applications such as chemical composition, stability in aquaeous environment and hydrophobic/hydrophilic character of the surface were investigated.

Introduction

Plasma polymerized organosilicon coatings have been attracting interest of many researches mainly due to the possibility to vary their properties in a very wide range. These materials have a great potential to succeed in large field of industrial applications such as anti-scratch coatings, corrosion protection films, barrier films etc. [1]. These materials are very perspective for several medical applications as well [2,3]. This study deals with preparation of organosilicon coatings based on gaseous admixture of trimethylsilyl acetate (TMSA) monomer and oxygen in plasma of RF glow discharge. The aim of this work is to create water-resistant organosilicon plasma polymers with content of carbonyl functionalities. Apart from water stability for 48 h, chemical structure and degree of hydrophobicity of these unique materials was investigated in dependence on the ratio of flow rates of carrier gas and TMSA during PECVD process. Sufficient stability of TMSA plasma polymers in aquaeous environment was achieved by appropriate choice of discharge parameters.

Experimental

Organosilicon thin films were prepared in RF glow capacitively-coupled discharges from mixture of TMSA ($CH_3CO_2Si(CH_3)_3$) and O_2 in a parallel plate reactor. The bottom electrode served as the substrate holder and it was coupled to RF generator (13.56 MHz) via a blocking capacitor. The supplied power was kept at 50 W for all depositions. The flow rates of used gases were varied. The flow rate variations are represented by O_2 to TMSA flow rate ratio *R*. The prepared thin films were studied by several diagnostic methods. Chemical composition was determined using non-destructive FTIR spectroscopy (spectrometer Bruker Vertex 80v). The degree of hydrophobicity of TMSA coatings deposited on glass substrate was determined by water contact angle (WCA) measurements (See System, Advex Instruments). The resistance

of thin films to water environment for 48 h at temperature of 37 °C was investigated by confocal microscope LEXT OLS4000. 3D images of films were acquired and the structural changes caused by delamination were studied. Changes in the film thickness were studied by ellipsometry in spectral range of 1-5.5 eV at the angle of incidence 65° using Jobin Yvon UVISEL device and PJDOS model integrated in newAD program [4]. Analyzed plasma polymers were immersed in liquid within 14 days after deposition.

Results and Discussion

The chemical structure of plasma-polymerized TMSA was strongly dependent on deposition parameter R (range of values 0-3) according to acquired IR spectra. The amount of hydrocarbon chains and Si−CH$_3$ groups decreased with increasing R (increasing O$_2$ content in original gaseous mixture during deposition). Reaching high values of $R > 1$ caused significant increase of OH bond content in deposited films. Simultaneously, Si−CH$_3$ groups became negligible contrary to Si−O−C/Si−O−Si bonds. All spectra of studied plasma polymers exhibited presence of C=O functionalities, however most of intergrated carbon was bonded in CH$_x$ and Si−C/Si−O−C network.
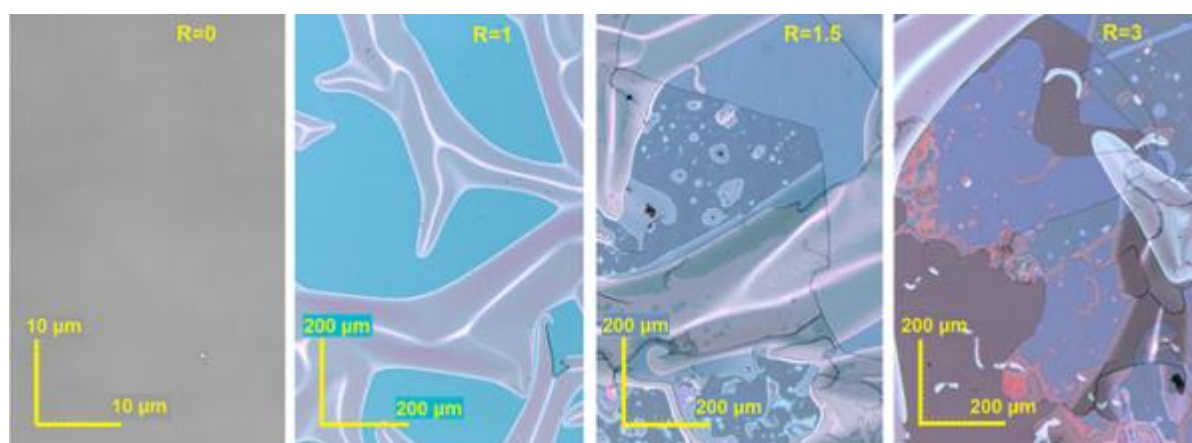
Fig. 1. Surface structure of chosen TMSA coatings after immersion in water.

The variation in amount of TMSA monomer in gaseous mixture used for preparation of plasma polymerized thin fims had significant influence on stability of analyzed samples in water. Thin films prepared using $R \geq 1$ were delamined after 48 h in water (**Fig. 1.**). Plasma polymers prepared using higher amounts of TMSA during PECVD process were considered to be stable. No signs of delamination were observed (**Fig. 1.**) and thickness losses determined by ellipsometric measurements were around ~3 %. TMSA coatings with good stability in liquid had hydrophobic character: WCA reached values from 87.5° to 95.3° (**Fig. 2.**).
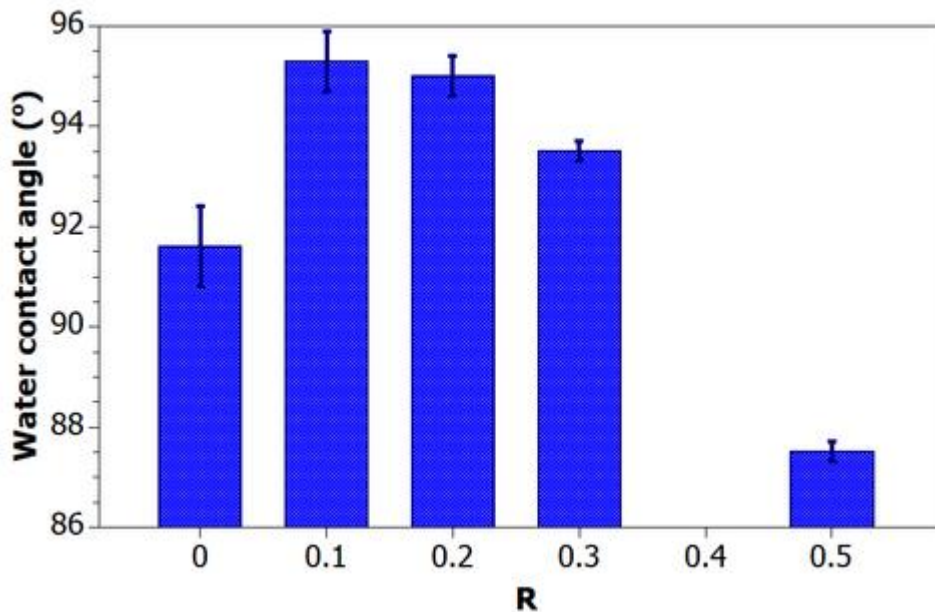
Fig.2. Dependence of WCA on deposition parameter R.

Conclusion

Properties of TMSA-based plasma polymers prepared in RF glow discharge were investigated by several characterization methods. Chemical structure of deposited coatings is directly linked to settings of flow rates of TMSA monomer and oxygen during PECVD process. Results included in present work proved that it is possible to prepare organosilicon thin films with good stability in water for 48 h using suitable ratio of O_2 and TMSA flow rates. These types of materials have a great potential to be applied in medicine e.g. as coatings for dental implants [5], therefore their next research based on reported results will be oriented in this direction.

Acknowledgement

Reference

[1] Zajíčková, L., Buršíková, V., Kučerová, Z., Franclová, J., Sťahel, P., Peřina, V., Macková, A., J. Phys. Chem. Solids 2007, 68, 1255–1259.

[2] Vogel, K., Westphal, N., Salz, D., Thiel, K., Wittig, L., Ciacchi, L.C., Grunwald, I., Surf. Innov. 2015, 3, 27-38

[3] Batory, D., Jedrzejczak, A., Kaczorowski, W., Kolodziejczyk, L., Burnat, B. Diam. Relat. Mater. 2016, 67, 1–7

[4] Franta, D., Nečas, D., Zajíčková, L. Optics Express 2007, 15, 16230–16244

[5] Hyawaka, T., Yoshinari, M., Nemoto, K. Biomaterials 2004, 25, 119-127

P25 ELECTROPHORETIC QUANTIFICATION OF RAPAMYCIN IN SERUM SAMPLES WITH USING OFF-LINE AND ON-LINE PRECONCENTRATION TECHNIQUES

Piotr Kowalski[1], Ilona Olędzka[1], Alina Plenis[1], Natalia Miękus[1,2], Tomasz Bączek[1]

[1]*Department of Pharmaceutical Chemistry, Medical University of Gdańsk, Hallera 107, 80-416 Gdańsk, Poland, piotr.kowalski@gumed.edu.pl*

[2]*Department of Animal and Human Physiology, Faculty of Biology, University of Gdańsk, Wita Stwosza 59, 80-308 Gdańsk, Poland*

Summary

The combination of two preconcentration techniques: off-line (solid phase microextraction) and on-line (field amplifield sample injection - sweeping) for the determination of rapamycin in blood serum samples has been developed. This allowed to obtain more than 30 times of the enhancement the signal using the spectrophotometric detection. The elaborated method could be useful tool in biomedical and clinical practice.

Introduction

Relative interest of rapamycin has increased since it has been shown to inhibit successful restenosis of veins after being used as an antiproliferative drug to stents placed within the blood vessels of the patients. The creation of stents that enable the secretion of drugs is a huge advance in cardiology and is a hope for patients with coronary artery disease. Therefore, to determine rapamycin in blood serum different attempts have been made, which is an important analytical approach to monitor the level of this macrolide in patients serum samples. Due to the lack of specific chromophores of the lactone ring, its low solubility in water, the ability to decompose under the influence of storage (even in the refrigerator at 4 °C), lability due to the number of physico- and chemical factors (including light and pH values and extremely trace amounts in biological samples, the determination of rapamycin is a great challenge for the analyst.

Experimental

Several techniques for the isolation of this macrolide drug from biological samples have been tested (SPE, DLLME, SPME), however the most effective was the SPME technique. After simple deproteinization of the serum sample (0.5 mL) with ACN (1 mL) and 100 µL of 40 % zinc sulfate, the sample was centrifuged for 5 min at 10 000 rpm, evaporated to dryness and

subjected to the SPME procedure. The residue was suspended in water (1 mL) using an ultrasonic bath. Subsequently, the SPME C18-sorbent was preconditioned with 1 mL of the mixture of MeOH/water (50:50, *v/v*) for 60 min and next analyte was extracted from the SPME C18 blades (60 min). Next, SPME sorbents were washed with deionized water for 10 s and then desorption step with 1 mL of the mixture of ACN/MeOH (50:50, *v/v)* for 60 min was carried out. All steps of SPME protocol (preconditioning, extraction, desorption and washing) were conducted at the temperature of 40˚C with agitation at 850 rpm. Next, desorption phase was transferred to clean Eppendorf tubes and evaporated to dryness in a thermoblock at 45˚C. Finally, the residue was dissolved with 50 μL of 2 mM borax diluent, centrifuged at 10 000 rpm (5 min) and injected into the capillary electrophoresis system. Rapamycin-contained samples were determined by micellar electrokinetic capillary chromatography (MEKC) using a 10 mM borax and 40 mM SDS as a separation buffer. Our tests were based on the SPME methodology described in the literature [1]. The few double bonds present in the macrolide structure allowed the use of DAD-based spectrophotometric detection at 284 nm.

Results and Discussion

To enrich trace amounts of rapamycin in serum samples we adopted an *off-line* sample preconcentration procedure based on the SPME and a unique procedure of combined sweeping and field amplifield sample injection (FASI) technique called as sequential stacking featuring sweeping (*on-line* method). Moreover, the electrokinetic injection with pressure filling (a simultaneous electrokinetic and hydrodynamic injection, SEHI) was used to obtain a signal amplification effect. As the optimal parameters of the pressurized electrokinetic method were selected: dosing at –5 kV (reversed polarity) with simultaneous applying pressure of 0.5 psi for 1.5 min. It allowed to obtain a signal amplification for rapamycin at the level 6.6 and to an electrokinetic injection of over 30 times - in relation to the traditional hydrodynamic injection. The signal amplification effect was calculated based on the height ratios obtained by hydrodynamic, electrokinetic and electrokinetic with pressure filling (SEHI) injection methods.

Conclusion

1. As a result of the above series of experiments, a method for the determination of rapamycin in serum samples by means of MEKC technique was developed.

2. Due to the application of the signal amplification method for rapamycin samples, subjected to the SPME procedure, a detection limit of 33 ng/mL was obtained in the developed method, while the limit of quantification of 100 ng/mL was estimated.

3. The developed MEKC method supported by elaborated techniques based on the SPME, FASI-sweeping method for the determination of rapamycin in serum samples could be useful tool in biomedical and clinical practice.

Acknowledgement

Reference

[1] Olędzka, I., Kowalski, P., Plenis, A, Miękus, N., Grabow, N., Eickner, T., Bączek, T., Electrophoresis, 2018, (DOI) - 10.1002/elps.201800081.

P26 SYNOVIAL FLUID, THE FORGOTTEN BIOLOGICAL MATERIAL?

Iveta Kozarova[1,2], **Pavlina Kusnierova**[1,2], **Pavel Walder**[3]

[1]*Department of Biomedical Sciences, Faculty of Medicine, University of Ostrava, Ostrava, Czech Republic, iveta.kozarova@fno.cz*

[2]*Institute of Laboratory Diagnostics, University Hospital Ostrava, Ostrava, Czech Republic*

[3]*Department of Orthopaedics, University Hospital Ostrava, Ostrava, Czech Republic*

Summary

Background. The analysis of synovial fluid is important in the diagnosis of joint disease. Synovial fluid analysis can provide a lot of information about joint biology, and useful clinical treatment algorithms are introduced based on these findings. Our aim was to evaluate the current state of synovial fluid analysis and, through this information, to unify biochemical, hematological and microbiological parameters in the future. Synovial fluid is the site of primary infection, so its diagnosis should theoretically be more sensitive than that of serum. Rapid detection of bacteria or new biomarkers in joint infections would allow for the development of target treatment regimens and prevention of the chronic complications.

Methods. 176 synovial fluid samples between 2014 and 2018 were included in this retrospective study. Biochemical parameters (glucose (GLU), lactate (LAC), uric acid (UA), total protein (TP), C-reactive protein (CRP)) in synovial fluid were determined using an AU 5800 analyzer and hematological parameters (relative and absolute counts of high-fluorescence cells (HF-BF, HF-BFA), white blood cell (WBC-BF) counts, red blood cell (RBC-BF) counts, relative and absolute counts of mononuclear cells (MNP, MNA), relative and absolute counts of polymorphonuclear cells (PMN, PMNA) were examined by the analyzer Sysmex XN-9000 in special Body Fluid mode.

Results. With regard to the non-normal distribution of measured data, the results of analysis were evaluated by Spearman's correlation coefficient. A statistically significant correlations were found between the coefficient of energy balance (KEB) and LAC (r_s = -0.961; P<0.0001), HF-BF and MNP (r_s = 0.803; P<0.0001), HF-BF and PMN (r_s = 0.803; P<0.0001), MNP and PMN (r_s = -1.000; P<0.0001). The knee joint is the most frequent source of synovial fluid. The most common diagnosis among the 176 patients were: presence of orthopedic joint implants, juvenile rheumatoid arthritis, pain in the joint and primary gonarthrosis.

Conclusion. This retrospective study was performed to show the current state of the laboratory methods used for synovial fluid examination in our hospital and to study the basic relationships between biochemical and hematological parameters. The results proved the

adequate ability of lactate, glucose, CRP concentration, and the coefficient of energy balance, MNP, PMN and HF-BF to assess the inflammatory response. These data show the need to create a standard panel of methods that would allow the improve diagnostics in inflammatory joint disease in our hospital and the resolution between the viral and bacterial etiology of inflammation.

Introduction

Synovial fluid is viscous, mucinous substance, an ultrafiltrate or dialysate of plasma and contains levels of glucose and uric acid that are equivalent to plasma. Synovial fluid protein, however, is at about one third lower level than plasma. The analysis of synovial fluid is important in the diagnosis of joint disease [1]. The normal range for synovial fluid protein is 10–30 $g \cdot L^{-1}$, synovial fluid glucose levels are less than 0.56 $mmol \cdot L^{-1}$ lower than serum levels, normal range for synovial fluid uric acid is 357-476 $\mu mol \cdot L^{-1}$, synovial fluid lactate is less than 2.78 $mmol \cdot L^{-1}$, but it can be as high as 111 $mmol \cdot L^{-1}$ in septic arthritis [2, 3]. The WBC count on normal synovial fluid ranges from 0 to 150 cells per microliter. The mean distribution of these nucleated cells is neutrophils 7 %, lymphocytes 24 %, monocytes 48 %, macrophages 10 %, and synovial lining cells 4 %. Neutrophils may be vacuolated or contain bacteria or crystals [1].

Joint infections that occur under the patient's overall condition and typical joint fluid are usually not a diagnostic problem. However, joint infections occurring under non-specific imaging are difficult to diagnose, mainly due to the absence of specific clinical signs and symptoms, a relative lack of accurate laboratory tests, low virulence due to previous treatments, and biofilm pathogenicity. This is especially true for patients who have been treated with non-target ATBs, including patients with implanted joint replacements. Current diagnostics focus on the measurement of inflammatory factors such as WBC, serum CRP, microbiological synovial fluid analysis and imaging methods, such as CT or CAT scan, magnetic resonance imaging and positron emission tomography, possibly the most modern combination of methods such as SPECT/CT and PET/CT. Nevertheless, most of these tests do not show 100% sensitivity and specificity, therefore a combination with clinical history and symptoms is essential [4-12].

Some patients may suspect infection at the time of the postoperative period. In this situation, a quick decision is made as to whether irrigation and debridement should be done to preserve the implanted prosthesis, which is an important issue as it is a time-honored procedure and should be done prior to introducing an implantable drug-resistant biofilm or earlier than an osteomyelitis anchored in periprosthetic bones [13]. However, when CRP hits a peak on days 2 or 3 after surgery and decreases normal values in postoperative week 2, erythrocyte sedimentation rate shows a slower natural progress than CRP. Therefore, we can miss the chance to save the implant early intervention if we rely solely on these tests. Kim et al. [14] evaluated the causes of elevated CRP levels in the early postoperative period after primary TKA (total knee arthroplasty). It was found that 24% caused by postoperative infection, 20% idiopathic, 16% urological, 14% gastrointestinal, 13% vascular and 13% respiratory.

Methods

We examined a group of 176 synovial fluid samples from patients with different diagnosis from the Department of Orthopaedics, University Hospital Ostrava. Synovial fluid samples for biochemical analysis were centrifuged at 2500 g for 6 minutes at 4°C. Synovial fluid glucose, lactate, C- reactive protein, uric acid and total protein concentrations were measured on the AU 5800 analyzer (Glucose, ref. OSR6221, Lactate, ref. OSR6193, CRP Latex, ref. OSR6299, Uric Acid, ref. OSR6298, Total Protein, ref. OSR6232, Beckman Coulter, Inc., Brea, CA, USA). The value of KEB was calculated [15, 16]. KEB values >28.0 in extravascular fluid indicate normal condition, but cannot exclude a possible slight serous inflammation in particular organ. The cell elements were measured on the hematology analyzer Sysmex XN-9000 (Sysmex Co., Kobe, Japan) in special Body Fluid mode (WBC-body fluid, RBC-body fluid, Mononuclears-body fluid (MNP) as % and absolute number, Polymorphonuclears-body fluid (PMN) as % and absolute number, Fluorescent Cells-body fluid (HF) as % and absolute number). Four special reagents were used (Cellclean – ref. 83401621, Fluorocell WDF – ref. CV377552, Fluorocell WPC – ref. BU306227, Lysercell WPC – ref. CS412800). Statistical evaluation of results was performed using MedCalc software version 11.4 (Frank Schoonjans, Belgium).

Results

The basic statistics of the variables and the D'Agostino-Pearson normality test are presented in Table 1, which shows that the synovial fluid glucose and hematological parameters in special Body Fluid mode are the most frequently examined. With regard to the non-normal distribution of measured data, the results of analysis were evaluated by Spearman's correlation coefficient. A statistically significant correlations were found between the coefficient of energy balance (KEB) and LAC ($r_s = -0.961$; $P<0.0001$), HF-BF and MNP ($r_s = 0.803$; $P<0.0001$), HF-BF and PMN ($r_s = 0.803$; $P<0.0001$), MNP and PMN ($r_s = -1.000$; $P<0.0001$), Figure 1-2. Other biochemical parameters were not included in statistical evaluation due to the small number of samples in the test group. The knee joint is the most frequent source of synovial fluid. The most common diagnosis among 176 patients were: presence of orthopedic joint implants, juvenile rheumatoid arthritis, pain in the joint and primary gonarthrosis.

Table 1: Basic statistics of the variables and the D'Agostino-Pearson normality test.

Parameters	Units	N	Mean	SD	Median	Minimum	Maximum
CRP[*]	mg·L⁻¹	48	28.54	39.11	9.550	0.200	185.0
LAC[*]	mmol·L⁻¹	20	4.076	2.381	4.075	1.460	11.52
GLU[*]	mmol·L⁻¹	76	4.008	2.711	4.125	0.010	12.47
UA[*]	μmol·L⁻¹	26	342.5	120.2	336.0	134.0	625.0
TP[*]	g·L⁻¹	22	42.82	7.986	42.50	26.10	53.90
KEB[*]	-	20	-320.0	1543	27.13	-6874	33.98
HF-BF[*]	%	74	4.224	8.870	0.900	0.000	48.50
HF-BFA[*]	×10⁹·L⁻¹	74	1.023	7.597	0.040	0.000	65.00
MNA[*]	×10⁹·L⁻¹	74	3.253	3.596	2.494	0.024	19.40
MNP[*]	%	74	44.63	31.436	39.65	3.100	99.00
PMN[*]	%	74	55.37	31.436	60.35	1.000	96.90
PMNA[*]	×10⁹·L⁻¹	74	11.02	20.852	2.562	0.005	154.8
RBC-BF[*]	×10¹²·L⁻¹	74	0.010	0.0195	0.003	0.000	0.103
WBC-BF*	×10⁹·L⁻¹	74	14.27	22.537	8.064	0.033	170.6

[*]P-value <0.0001
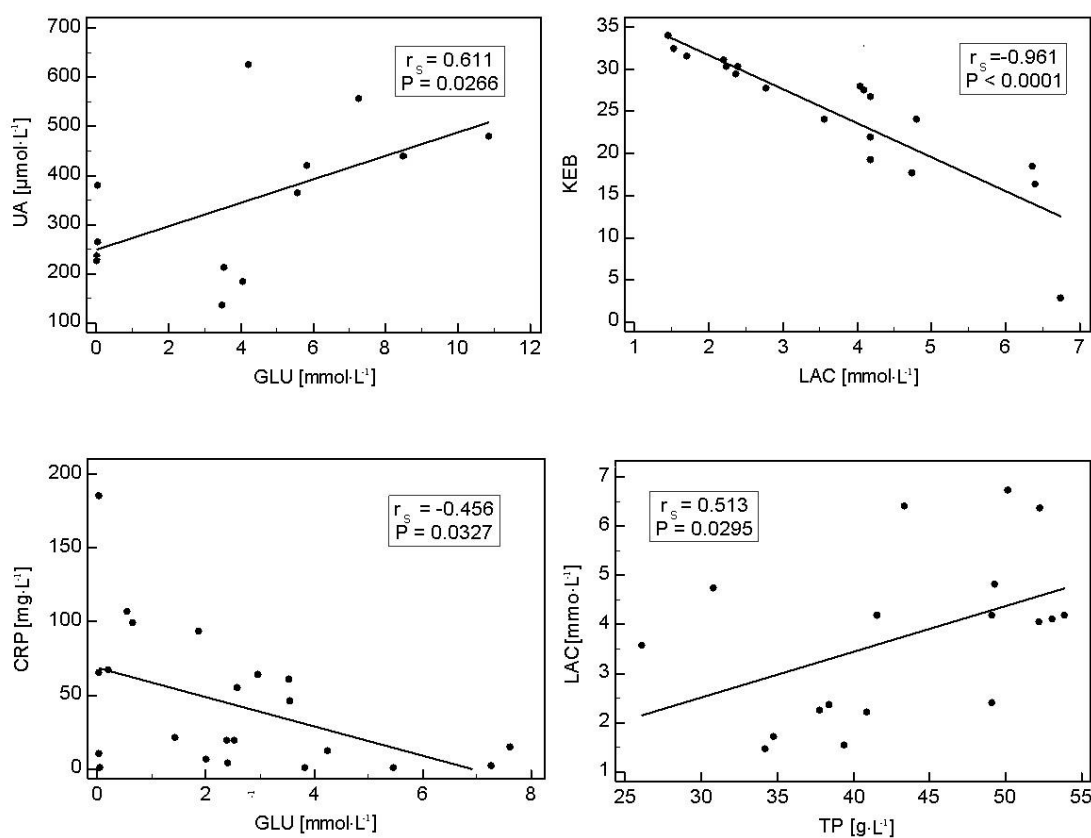
Figure 1. Correlation analysis between individual biochemical markers. $r_{s...}$ Spearman's correlation coefficient
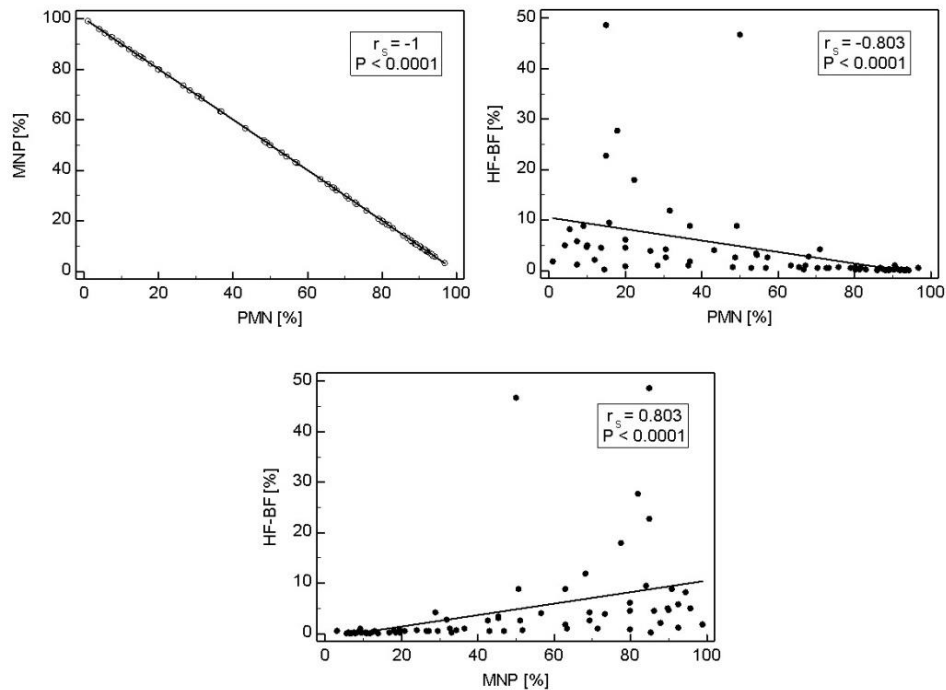
Figure 2. Correlation analysis between individual hematological parameters. $r_{s...}$ Spearman's correlation coefficient

Conclusion

This retrospective study was performed to show the current state of the laboratory methods used for synovial fluid examination in our hospital and to study the basic relationships between biochemical and hematological parameters. The results proved the adequate ability of lactate, glucose, CRP concentration, and the coefficient of energy balance, MNP, PMN and HF-BF to assess the inflammatory response. These data show the need to create a standard panel of methods that would allow the improve diagnostics in inflammatory joint disease in our hospital and the resolution between the viral and bacterial etiology of inflammation.

Acknowledgement

Reference

[1] Gatter R.A., Schymacher H.R. A Practical Handbook of Joint Fluid Analysis. 2nd Ed. Philadelphia: Lea & Febiger, 1991.
[2] McBride L.J. Textbook of Urinalysis and Body Fluids: A Clinical Approach. Philadelphia: Lippincott, 1998.
[3] Ross D.L., Neeley A.E. Textbook of Urinalysis and Body Fluids. New York: Appleton-Century-Crofts, 1983.
[4] Lorenzo P., Aspberg A., Saxne T., Onnerfjord P. Quantification of cartilage oligomeric matrix protein (COMP) and a COMP neoepitope in synovial fluid of patients with different joint disorders by novel automated assay. Osteoarthritis and Cartilage. 2017; 25: 1436-1442.

[5] Keisuke M., Sayuki K., Shiho H., Tsutomu Y., Kei-ichiro N. and Tohru N. Identification of Specific Protein Markers of Rheumatoid Arthritis in Synovial Fluid and Serum. Journal of Hard Tissue Biology. 2018; 27(1): 55-58.

[6] Guomin Ren, Ian Lutz, Pamela Railton, J. Preston Wiley, Jenelle McAllister, James Powell and Roman J. Krawetz. Serum and synovial fluid cytokine profilig in hip osteoarthritis: distinct from knee osteoarthritis and correlated with pain. BMC Musculoskeletal Disorders 2018; 19: 39.

[7] Renjun Yang, Dianying Zhang, Kai Yu, Luping Sun, Jie Yang, Chunmei Zhao, Xiang Li, Yuhong Chen. Detection of miR-22, miR-140 and Bone Morphogenetic Proteins (BMP)-2. Expression Levels in Synovial Fluid of Osteoarthritis Patients Before and After Arthroscopic Debridement. Med Sci Monit. 2018; 24: 863-868.

[8] Silvia Díaz-Prado, Claudia Cicione, Emma Muiños-López, Tamara Hermida-Gómez, Natividad Oreiro, Carlos Fernández-López and Francisco J Blanco. Characterization of microRNA expression profiles in normal and osteoarthritic human chondrocytes. BMC Musculoskeletal Disorders 2012; 13: 144.

[9] Bauer T. W. CORR Insights1: How Reliable Is the Alpha-Defensin Immunoassay Test for Diagnosing Periprosthetic Joint Infection? A Prospective Study. Clin Orthop Relat Res. 2017; 475: 416–418.

[10] Tausche A.K., Gehrisch S., Panzner I., Winzer M., Range U., Bornstein S.R., Siegert G., Wunderlich C., Aringer M. A 3-day delay in synovial fluid crystal identification did not hinder the reliable detection of monosodium urate and calcium pyrophosphate crystals. J Clin Rheumatol. 2013; 19(5): 241-245.

[11] Yin C.M., Suen W.C., Lin S., Wu X.M., Li G., Pan X.H. Dysregulation of both miR-140-3p and miR-140-5p in synovial fluid correlate with osteoarthritis severity. Bone Joint Res. 2017; 6(11): 612-618.

[12] Zhang Y., Lee S.Y., Zhang Y., Furst D., Fitzgerald J., Ozcan A. Wide-field imaging of birefringent synovial fluid crystals using lensfree polarized microscopy for gout diagnosis. Sci Rep. 2016; 30; 6: 28793.

[13] Fehring T.K., Odum S.M., Berend K.R. et al. Failure of irrigation and debridement for early postoperative periprosthetic infection. Clin Orthop Relat Res. 2013;471(1):250.

[14] Kim T.W., Kim D.H., Oh W.S. et al. Analysis of the causes of elevated C-reactive protein level in the early postoperative period after primary total knee arthroplasty. J Arthroplast. 2016;31(9):1990.

[15] Kelbich P., Hejčl A., Selke-Krulichová I., Procházka J., Hanuljaková E. et al. (2014) Coefficient of energy balance, a new parameter for basic investigation of the cerebrospinal fluid. Clin Chem Lab Med. 52: 1009-1017.

[16] Kelbich P., Hejčl A., Procházka J., Hanuljaková E., Staněk I. et al. (2016) Cytological-energetic examination of the extra-vascular body fluids, including the cerebrospinal fluid. Biochem Anal Biochem 5:4.

P27   UTILIZATION OF WASTE MATERIAL FROM THE WINE PRODUCTION FOR REMOVING COPPER IONS FROM WASTEWATER

Jakub Krikala, **Pavel Diviš**

Department of Food Chemistry and Biotechnology, Institute of Chemistry, Brno University of Technology, Brno, Czech Republic

Summary

The primary objective of this work was to characterize the grape waste by IR analysis, optimization of adsorption conditions, isotherms construction and determination of maximum adsorption capacity of grape waste for Cu(II). From the parameters influencing adsorption efficiency, the adsorbent load was optimized (m/V ratio = 0,02); optimal pH was found at 5 and the contact time to reach the equilibrium was 30 minutes. Maximum adsorption capacity for copper ions was calculated from adsorption isotherms by applying the Langmuir model and found to be 4,445 0 mg.g^{-1} and 4,678 4 mg.g^{-1} on grape waste from white wine and red wine production, respectively. The results of the work confirm a good adsorption potential of copper ions on grape waste.

Introduction

Heavy metals pollution in the aquatic ecosystem si a current global problem, especially due to their toxic effects. In addition, some metallic elements (especially CdII, CrVI, HgII and PbII) have high sedimentation and accumulation coefficients and also they are not biodegradable. Therefore heavy metals can be easily incorporated and accumulated in living tissues, causing various diseases and disorders [1].

Today, metal removal from wastewater is a subject of great interest, especially in the environmental field. Several methods such as chemical precipitation, ion exchange, electrolysis, coagulation and others have been used for removal heavy metals from wastewater. However, the high capital cost of these conventional treatment processes limits their large-scale use, so the development of new, cheap and also environmentally friendly processes is necessary. Within these necessities, adsorption processes appear to be a suitable technique because of its high efficiency and variability in physicochemical properties of different types of adsorbents. Consequently, more effective adsorbents are being developed intensively, especially in the area of a low-cost natural and waste materials [1].

In the present work, the usefullnes of grape waste generated in the wine production process has been investigated for the removal copper ions from aqueous solution. The grape harvest is

about 60 millions tones per year. About 80 % of the harvest is utilized in the wine industry, so about 10 tones of grape waste is generated per year worldwide. Waste material from the wine production is commonly used for composting or biofuel production, but recent years more studies is focused on the secondary use of grape waste as a low-cost adsorbent, especially due to high content of polyphenolic compounds. Thus, the main aim of this work was to evaluated the potentialities of grape waste as an adsorbent material through its chemical characterization and optimization of adsorption conditions, and to establish the maximum adsorption capacity for Cu(II) ions applying the Langmuir isotherm model [2].

Experimental

Adsorbent material

Grape waste, obtained from a production of white and red wines (Rakvice, South Moravia region, Czech Republic), was stored at -70° C before adsorption experiments. After thawing at room temperature, grape waste was rinsed with drinking and distilled water to remove residual sugar and soluble impurities, dry in an oven at 80° C until constant weight, cut and sieved for a particle size of 0,8 – 2,0 mm. Afterwards, the material was stored in polypropylene bags and used without any physical or chemical treatment.

Reagents

Aqueous solutions of Cu(II) was prepared by dissolving appropriate amounts of $CuSO_4 \cdot 5H_2O$ (PENTA, Prague, Czech Republic) in distilled water. The pH of the Cu(II) solution was adjusted with prepared 1M NaOH and 1M HCl solutions. Cu(II) reference solution of 1 000 mgL-1 (ČMI, Brno, Czech Republic) was used for ICP-OES calibration.

Effect studies

Metal uptake experiments including optimization of adsorption conditions were carried out in the batch mode at room temperature. All adsorption experiments were performed in 50ml Erlemeyer flasks by shaking the mixture of adsorbent and adsorbate solution in given ratio at 150 rpm. Doses effect were performed with 25 ml of copper solution and with a mass of adsorbent in the range of ratios from 1:5 to 1:200. The effect of pH on the sorption was studied by adjusting the initial solution pH within the range 2 – 6. In adsorption contact time optimization, the samples were drawn at intervals from 0 to 120 minutes. In optimization experiments initial metal concentration was 100 mgL-1.

Adsorption studies

After the optimization, adsorption isotherm were carried out by shaking the mass of adsorbent with metal solutions having concentrations from 10 to 500 mgL-1 in the given ratio. After adsorption the solid was removed by filtration through a cellulose filter paper (Munktell) and the copper contretation in the diluted filtrates as well as in the initial solutions was determined

by ICP-OES spectrometer (Ultima 2, Horiba Scientific) at wavelenght of 327,396 nm. The amount of metal adsorbed (Qad) was calculated using the equation follows:

$$Q_{ad} = ((c_1 - c_e)*V)/m \, ,$$

where c_1 (mgL^{-1}), c_e (mgL^{-1}), m (g) and V (L) denote the initial metal concentration, equilibrium metal concentration, dry weight of adsorbent and the volume of solution, respectively.

Results and Discussion

Characterization of the adsorbent

Grape waste was previously characterized using a FT-IR spectrometer to qualitatively analyze surface functional groups and aromatic rings, that are largely responsible for the adsorption potential. The infrared spectrum (Fig. 1) displays many of adsorption peaks indicating the complex nature of the material examinated and also the different structure between grape wastes from red and white wine production. The broad adsorption peaks around 3 300 cm^{-1} are indicative of the existence of bonded hydroxyl groups containings in alcohols, phenols and carboxylic acids. At 2 920 cm^{-1}, a peak assigned to the stretching C–H bond was founded. The peak observed at 1 730 cm^{-1} can be assigned to the C=O group and the peaks aroud 1 590 cm^{-1} correspond to the C=C stretching that may be attributed to the aromatic rings presented in the lignin structure. The strong C–O band at 1 110 cm^{-1} also confirms the lignin structure of the grape waste [3, 4].
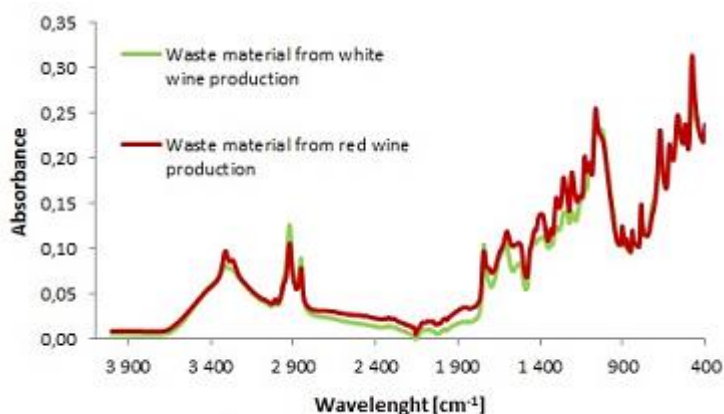
Fig. 1. FT/IR spectra of the grape waste

Effect of doses

Effect of grape waste doses on copper adsorption is shown in Fig. 2. The results indicated, that the percent removal of copper rapidly increased with increasing doses, because more active sites on the surface were available. The decrease of maximum adsorption capacity is then an implication of incomplete saturation of the adsorbent at the same contact time. Due to these results the ratio 1:50 of adsorbent mass to volume of metal solution was chosen.
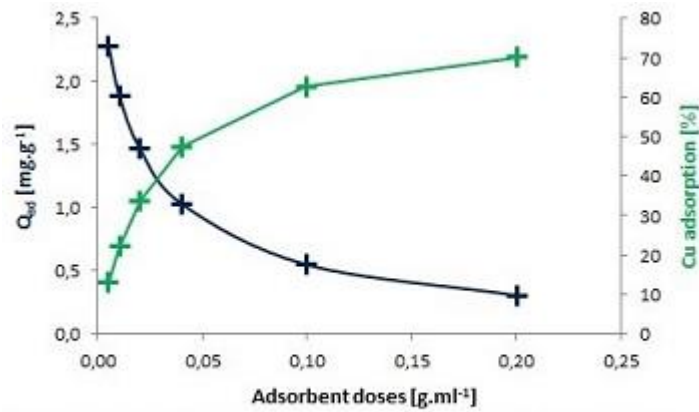
Fig. 2. Effect of adsorbent doses on the copper removal onto grape waste.
Initial metal concentration: 100 mg/l at pH 4; contact time: 30 minutes

Effect of pH

The pH is one of the most important parametres affecting adsorption processes. The pH dependence of metal uptake is closely related to the acid-base properties of various functional groups on the surface of the adsorbent. In Fig. 3 the percentage of Cu(II) adsorbed onto grape waste against equilibrium solution pH has been plotted. As shown, metal removal increased with increasing pH until the maximum was reached about pH 4. The worse sorption at low pH values is due to a higher concentration of H+ ions, which can compete with metal cations for active sites on the adsorbent surface. A decrease in metal removal at high pH values is a consequence of the reaction between copper cations and hydroxyl anions to formed an electro-neutral compound. Due to these results further experiments were carried out at pH 4.
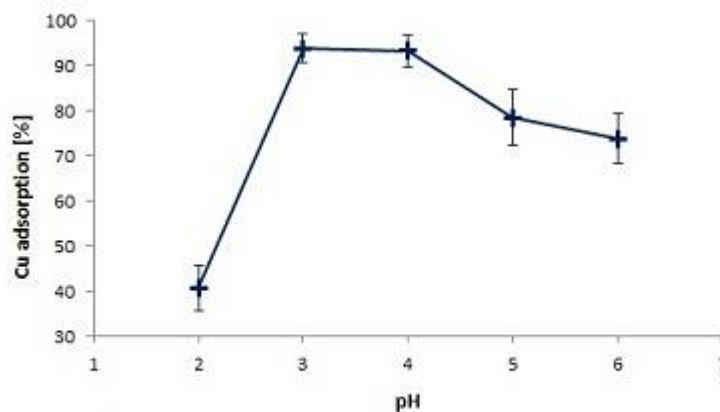
Fig. 3. Effect of pH on the copper adsorption onto grape waste.
Initial metal concentration: 100 mg/l; contact time: 30 minutes

Effect of contact time

Fig. 4 shows the effect of contact time on the amount of copper adsorbed onto grape waste. It can be seen that within first minutes of experiment major amount of metal was adsorbed and then the reaction curve started to be flattened. So the equlibrium time 30 minutes was determinated.
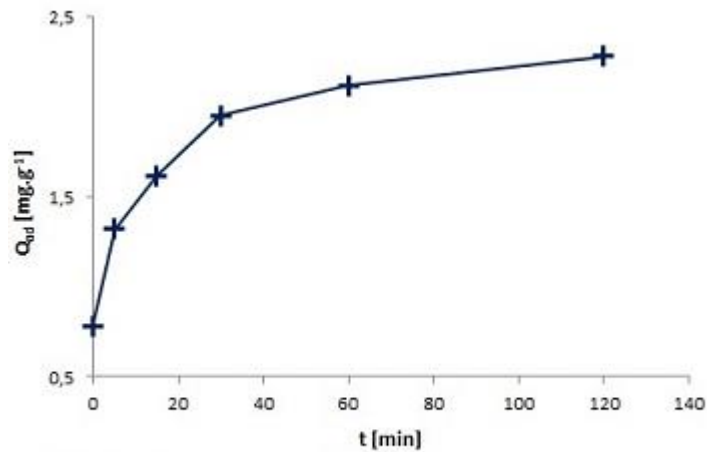
Fig. 4. Effect of contact time on the copper adsorption onto grape waste. Initial metal concentration: 100 mg/l at pH 4

Adsorption isotherms

To describe adsorption processes two parametres isotherm models are usually used. Freudlich isotherm model is widely applied in heterogenous systems especially for adsorption of organic compounds or higly interactive species onto activated carbon or molecular sieves. The mathematical expression of Freudlich isotherm is described below:

$$q_e = K_F * c_e^{1/n},$$

where q_e is the amount of substance adsorbed in equilibrium [mg.g^{-1}], c_e is the equilibrium concentration of adsorbate in solution [mgL^{-1}], K_F and n are empirical constant indicative of sorption capacity [mg$^{1-1/n}$.l$^{1/n}$.g^{-1}] and intensity, respectively [5, 6].
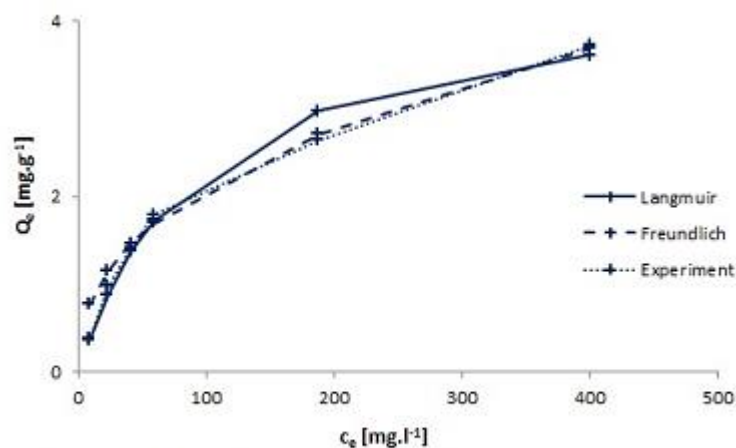
Fig. 5. Sorption isotherms of Cu(II) using grape waste. pH value: 4; contact time: 30 minutes

Langmuir isotherm assumes monolayer adsorption at finite number of definite localized active sites, that are identical and equivalent, with no lateral interaction or steric hindrance between

the adsorbed molecules. The mathematical expression of Langmuir isotherm is described by followed equation:

$$q_e = (Q_m*b*c_e)/(1+b*c_e)$$

where q_e is the amount of substance adsorbed in equilibrium [mg.g^{-1}], c_e is the equilibrium concentration of adsorbate in solution [mgL^{-1}], Q_m [mg.g^{-1}] is the value for maximum adsorption capacity and b [l.mg^{-1}]is the Langmuir constant related to the affinity of substance to the adsorbent [5, 6].

Table 1. Freundlich and Langmuir parametres for copper adsorption onto grape waste

Grape waste	Freundlich isotherm			Langmuir isotherm		
	k_F [mg$^{1-1/n}$.l$^{1/n}$.g^{-1}]	n	R^2	Q_{max} [mg.g^{-1}]	b [l.mg^{-1}]	R^2
White grapes	0,324 9	2,464 3	0,989 8	4,445 0	0,010 9	0,983 3
Red grapes	0,160 5	2,119 1	0,980 5	4,678 4	0,003 5	0,999 1

Conclusion

Grape waste is an easily accessible low-cost material with many possibilities of secundary utilization. Various functional groups were detected by FT/IR analysis indicating high content of biologically active compounds in grape waste. This specific structures also effectively act as adsorption sites for the metal ions. In view of experimental data obtained in this work it can be seen, that the efficiency of adsorption processes strongly depends on the optimization of experimental conditions such as dose of adsorbent, pH value, contact time and the others. The efficiency for copper removal was explained through its maximum adsorption capacity, which was determined by applying Langmuir isotherm model.

Finally, the results of this work confirm that grape waste can be considered as an alternative natural adsorbent for heavy metals. However, further optimization of adsorption coditions and additional experiments are necessary. Another studies may also focus on determining more adsorption parameters such as kinetics or thermodynamics, or experiments with chemical treated adsorbent would be interesting.

Acknowledgement

Reference

[1] Villaescusa, I., N. Fiol, M. Martínez, N. Miralles, J. Poch, J. Serarols, Removal of copper and nickel ions from aqueous solutions by grape stalks waste, Water Res., 38 (2004), 992–1002.

[2] Chand, R., K. Narimura, H. Kawakita, K. Ohto, T. Watari, K. Inoue, Grape waste as a biosorbent for removing Cr(VI) from aqueous solution, J. Hazard. Mater. 163 (2009), 245–250.

[3] Farinella, N.V., G.D. Matos, E.L.Lehmann, M.A.Z. Arruda, Grape bagasse as an alternative natural adsorbent of cadmium and lead for effluent treatment, J. Hazard. Mater. 154 (2008), 1007–1012.

[4] Hossain, M.A., H.H. Ngo, W.S. Guo, T. Setiadi, Adsorption and desorption of copper(II) ions onto garden grass, Biores. Tech., 121 (2012), 386–395

[5] Foo, K.Y., B.H. Hameed, Insights into the modeling of adsorption isotherm systems, Chem. Eng. J., 156 (2010), 2–10.

[6] Martínez, M., N. Miralles, S. Hidalgo, N. Fiol, I. Villaescusa, J. Poch, Removal of lead(II) and cadmium(II) from aqueous solutions using grape stalk waste, J. Hazard. Mater. 133 (2006), 203–211.

P28 DROPLET-BASED MICROFLUIDIC CHIP WITH PASSIVE MIXER FOR ANALYSIS WITH PHOTON-UPCONVERSION NANOPARTICLES

Jana Křivánková, Jan Přikryl, Antonín Hlaváček

Institute of Analytical Chemistry of the Czech Academy of Sciences, v. v. i.,
jana.krivankova@iach.cz

Summary

Mixing of the fluids in microfluidic chips is important especially in applications, where droplet contents need to be rapidly homogenized. Here, a passive method for mixing in polydimethylsiloxane (PDMS) microchannels is presented. Droplet homogenization was firstly tested with organic stains and subsequently applied for mixing water dispersions of photon-upconversion nanoparticles (UCNPs).

Introduction

Mixing in microfluidic systems driven by diffusion is time-consuming and inefficient for nanoparticles, which possess low diffusion coefficients. In order to speed up the mixing, several active methods (ultrasonic, magnetic stirring, etc.) have been applied [1]. These methods revealed excellent mixing efficiency, however, their integration into the microfluidic chip is cumbersome. Compare to them, passive mixers represented by channel design refinements and in-plane microstructures have the advantages of low cost and ease of fabrication [2]. Photon-upconversion is currently a highly active field of research and further progress in the development of upconversion nanomaterial properties is expected.

Nowadays, UCNPs have been proved valuable as convenient luminescent labels for chemical and biological sensing [3, 4]. We report droplet-based microfluidic device including in-plane passive mixer for effective mixing of several streams of organic stains and UCNPs dispersed in a water.

Experimental

PDMS microfluidic chip with 6-inputs, cross-junction and serpentine mixing parts was designed and fabricated using a conventional lithography (Heidelberg μPG 101 Laser Writer) on negative photoresist SU-8 3050 (MicroChem Corp.) (**Fig. 1**).
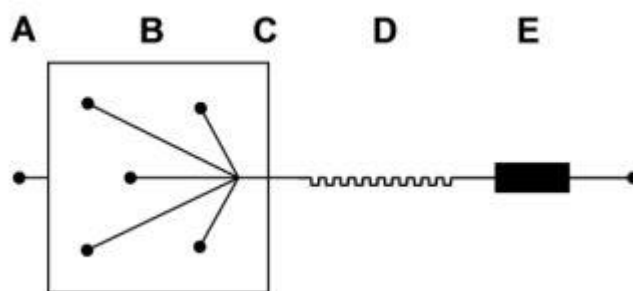
Fig. 1 Design of the chip: A) oil inlet; B) inlets for water phases with confluence; C) chip cross-junction; D) mixer; E) reservoir. The width and the depth of channels were 100 μm.

Microfluidic chip in PDMS kit (Dow Corning, Midland, MI, USA) was prepared by a common procedure [5]. As an oil phase, 3M FluorinertTM FC-40 (Sigma Aldrich) with 1% (w/w) of Pico-Surf I (Dolomite Microfluidics) were used (Fig. 1A) and blue-(Methyl Green) and yellow-dyed (Rhodamine) water phases (dispersions) were injected via one of the 5 inlets (Fig. 1B). Different types of UCNPs were synthesized according to a previously reported method [6]. The flow rates of oil phase (FluorinertTM FC-40) and water dispersions were precisely controlled by pressure driven pumps. Images were taken on an inverted microscope (Intraco Micro spol. s r.o.) equipped with digital camera XIMEA (ELCOM, a. s.).

Results and Discussion

To monitor synchronization of flows and to characterize mixing efficiency, water phases containing blue and yellow dye were used. Because of low Reynolds numbers, laminar flows in the inlet channels were observed. Up to five water streams were merged together in the chip confluence (**Fig. 1B**), where diffusion at low flow rates dominated (**Fig. 2A**). Contrary, the integration of passive mixer was necessary for homogenization of a droplet content at high flow rates (**Fig. 2B**).
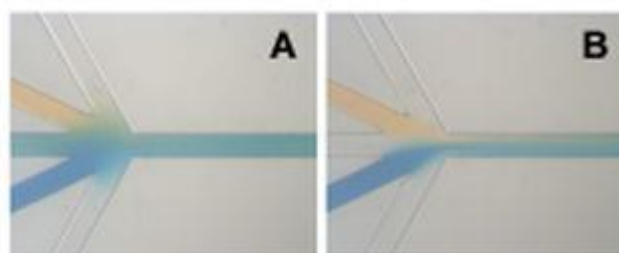
**Fig. 2** Chip confluence: A) at low flow rate and B) at high flow rate.

For droplet homogenization, we used a serpentine mixer based on Wang et al. [7] with the stretching and folding parts. Taking into account channel geometry, the optimal aspect ratio (length/width) of droplets was set by changing the ratio of water to oil (w/o, Figure 3). At low

w/o, long droplets were observed (**Fig. 3A**). With decreasing w/o, droplets became smaller and rounded (**Fig. 3C**). Optimal aspect ratio was reached when w/o was set to 1/15 (**Fig. 3B**).
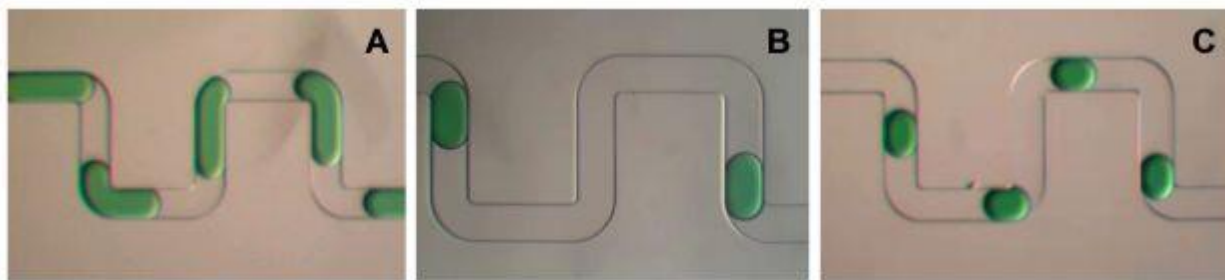
Fig. 3 Droplets in the chip mixer under different w/o ratios: A) w/o = 1/3; B) w/o = 1/15; C) w/o = 1/45.

Due to quick pressure pump response, it was possible to visualize and record the mixing performance. Generated droplets of different color intensity were collected in the chip reservoir (**Fig. 4A**). Finally, the mixer was used for preparing homogeneous droplets of UCNPs dispersed in water (**Fig. 4B**).
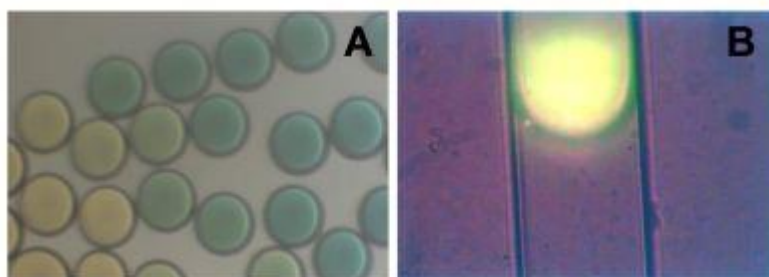
Fig. 4 Droplets in the chip reservoir: A) containing different amounts of organic dyes and B) dispersion of UCNPs.

Conclusion

PDMS microfluidic chip with in-plane mixer have reached sufficient mixing performance, where both convection and diffusion mixing concepts participated on the fluid stream lines formation. Proposed device equipped with pressure-driven flow controller proved its ability to produce homogeneous droplets over a wide range of flow conditions. Combination of a new class of optical material represented by UCNPs with droplet-based microfluidic opens new possibilities for use in analytical chemistry, biology and material science.

Acknowledgement

Reference

[1] Cai, G. Z.; Xue, L.; Zhang, H. L.; Lin, J. H. Micromachines 2017, 8, 274 − 301.

[2] Chen, C. M.; Zhao, Y. J.; Wang, J. M.; Zhu, P. A.; Tian, Y.; Xu, M.; Wang, L. Q.; Huang, X. W. Micromachines 2018, 9, 160 − 176.

[3] Haase, M; Schafer, H. Angew. Chem.-Int. Edit. 2011, 50, 5808 − 5829.

[4] Farka, Z.; Mickert, M. J.; Hlaváček, A.; Skládal, P.; Gorris, H. H. Anal. Chem. 2017, 89, 11825 − 11830.

[5] Friend, J., Yeo, L., Biomicrofluidics 2010, 4, 026502.

[6] Hlaváček, A.; Farka, Z.; Hübner, M.; Horňáková, V.; Němeček, D.; Niessner, R.; Skládal, P.; Knopp, D.; Gorris, H. H. Anal. Chem. 2016, 88, 6011 − 6017.

[7] Wang, J. J.; Wang, J. A.; Feng, L. F.; Lin, T. RSC Adv. 2015, 5, 104138 − 104144.

P29   ACETONITRILE-ASSISTED ENZYMATIC DIGESTION USED FOR ANALYSIS OF PROTEINS OF CANCER ORIGIN

Markéta Laštovičková[1], Pavel Bobál[2], Dana Strouhalová[1], Janette Bobálová[1]

[1]*Institute of Analytical Chemistry of the Czech Academy of Sciences, Brno, Czech Republic,*
lastovickova@iach.cz

[2]*Department of Chemical Drugs, Faculty of Pharmacy, University of Veterinary and Pharmaceutical Sciences Brno, Brno, Czech Republic*

Summary

In this study, in-gel trypsin digestion protocol using aqueous-acetonitrile solvent system was developed to facilitate bottom-up proteomic identification of proteins isolated from human breast cancer cells.

Introduction

Some of the proteins suffer from limited solubility, which can result in their reduced accessibility to the proteolytic enzymes. Since digestion of proteins is a crucial step of analytical proteomics, it is necessary to search alternative digestion methods for such proteins to enhance the digestion efficiency and following MS analysis. One of the possibilities of improvement is the digestion in presence of various reagents that can be divided in several classes including organic solvents, chaotropic agents or surfactants [e.g., 1-7].

This work was aimed at the investigation of a positive influence of acetonitrile (ACN), added to the reaction mixture during enzymatic digestion of proteins, on efficiency of the proteomic identification especially on the impact on sequence coverage and number of detected peptides. This alternative digestion protocol was used to identify target proteins from samples of cancer origin.

Experimental

As standard protein samples bovine serum albumin (BSA), carbonic anhydrase (CA) and ovalbumin (OVA) were utilized. The estrogen receptor negative breast carcinoma cell line MDA-MB-231 was used as an example of real complex sample.

The separation of standard as well as real protein mixtures was carried out using 12 % gels under denaturing conditions. The protein visualization was carried out using Coomassie Brilliant Blue G-250 dye.

Selected protein bands were excised and enzymatically digested in-gel by trypsin according to protocol that is based on Jensen´s one [8]. Briefly, the protocol comprises these steps: (1) excision of gel bands; (2) washing of gel pieces (3) reduction and alkylation; (4) rehydration of gel particles by a tryptic digestion buffer (12.5 ng/mL in 2 mol/L NH4HCO3/0-80% ACN (v/v); 45 min; 4 °C) and (5) overnight digestion of gel pieces (2 mol/L NH4HCO3/0-80% ACN (v/v); 16 h; 37 °C).

Peptides obtained after digestion were analyzed by MALDI-TOF/TOF mass spectrometry and identified by using SwissProt databases (Mascot, ProFound).

The evaluation of digestion approaches was based on the comparison of MASCOT score, sequence coverage and the number of matched peptides of positively identified proteins (random match probability <0.05). Experiments were statistically evaluated by ANOVA tests. Values in figures are expressed as means ± standard deviations. The significance level thresholds for statistically significant influence of ACN addition were assessed as p-value < 0.05.

Results and Discussion

Acetonitrile (ACN), as representative of water-miscible organic solvents, may changes the conformation of substrate and enzyme and thus it can increase the solubility of insoluble proteins without significant impact on activity of enzyme. In this way, it could make enzymatic cleavage more efficient and improve consequential MS identification of proteins. This assumption led us to focus our attention on optimization of alternative digestion protocol using ACN with respect to improvement of the in-gel analyses and identification of proteins from complex samples.

For the initial experiments, three protein standards with different proteolytic susceptibilities (BSA, CA and OVA) were used for the optimization of experimental conditions (concentration of ACN; the addition of ACN during different stages of digestion procedure). Standard proteins were separated on SDS gels, excised from the gels and enzymatically in-gel digested by trypsin. Digestion approaches were evaluated based on the comparison of sequence coverage (%), the number of matched peptides and MASCOT score of the identified proteins. The most noticeable enhancement of evaluated criteria was obtained with the protocol where 80 % of ACN was present during the rehydration of gel particles with trypsin digestion buffer.

Based on these preliminary results the developed digestion protocol has been applied to proteins isolated from the human breast carcinoma cell line. Protein extracts were purified and separated by using GE (Fig. 1A). As an example, a band with average intensity and mass of approximately 50 kDa was selected for subsequent investigations. Studied protein band was subjected to conventional as well as modified in-gel digestion procedures. Four proteins were identified in selected GE band. Both procedures revealed the presence of two major proteins – beta tubulin TBB 5 and tubulin TBB 4B. The column graphs (Fig. 1B-D) show that all of the evaluated parameters (especially identification scores) were improved after ACN addition.

Moreover, modified protocol allowed the identification of two more proteins – VIME and tubulin TBB 2B. One possible explanation for such enhancement is ACN support during cleavage of poorly digested proteins, e.g. those post-translationally modified (such as VIME).
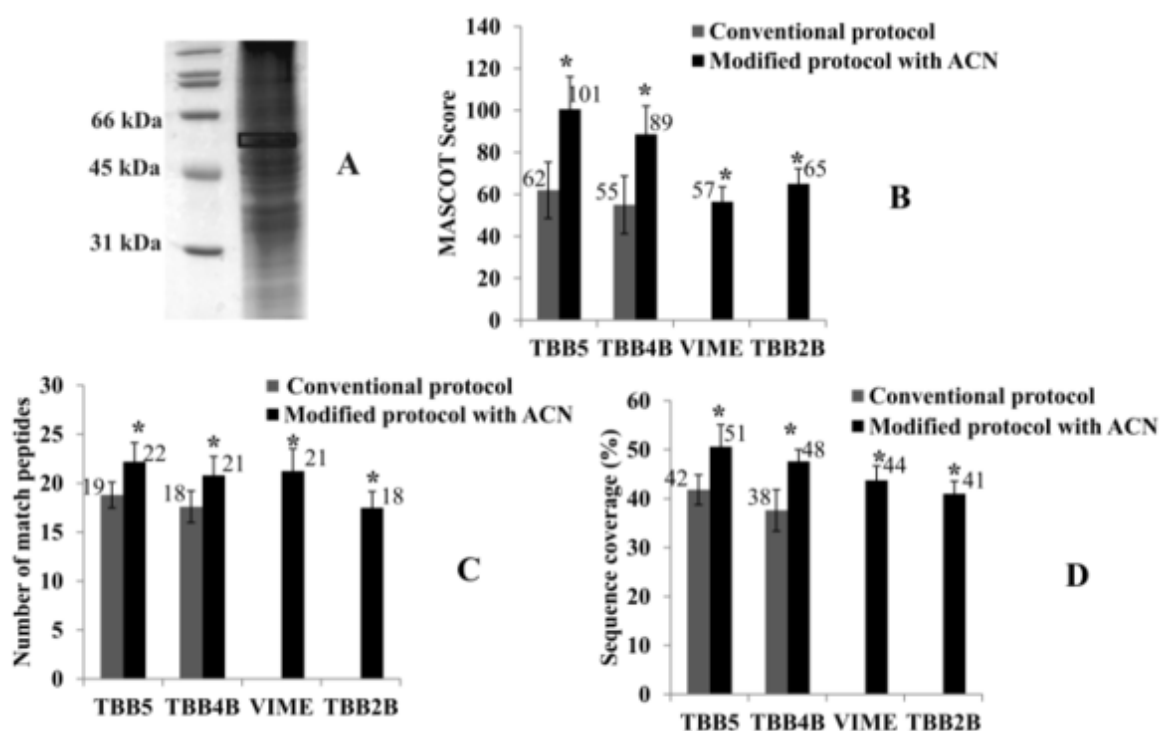

Fig. 1 Comparative study of digestion of proteins isolated from breast cancer cells. (A) SDS-gel with marked protein band used for this study; (B-C) column graphs with the results obtained after conventional and modified tryptic digestion protocols. The evaluation of database searching was based on (A) MASCOT score, (B) a number of matched peptides, and (C) sequence coverage of matched proteins. Vertical error bars represent the average standard deviation of means from triple replicated digests. * denote significant differences ($p < 0.05$) compared to samples digested by using the conventional method.

Conclusion

The results of MS analyzes, along with the database searches, have confirmed that using of ACN-assisted digestion contributes to a more successful identification of the studied proteins compared with the conventional digestion method. Obtained data indicate that procedure applied here has the potential for facilitation of proteomic investigation of human samples that are characterized by a broad concentration dynamic range of proteins and by the presence of modified proteins.

Acknowledgement

Reference

[1] Waas, M., Bhattacharya, S., Chuppa, S. et al., Anal. Chem. 2014, 86, 1551-1559.

[2] Slysz, G.W., Schriemer. D.C., Rapid Commun. Mass Spectrom. 2003, 17, 1044-1050.

[3] Hustoft, H.K., Reubsaet, L., Greibrokk, T., et al., J. Pharm. Biom.Anal. 2011, 56, 1069-1078.

[4] Wall, M.J., Crowell, A.M.J., Simms, G.A., et al., Anal. Chim.Acta 2011, 703 194–203.

[5] Proc, J.L., Kuzyk, M.A., Hardie, D.B., et al. J. Proteom. Res. 2010, 9, 5422-5437.

[6] Wu, S., Zhang, H., Yang, K., et al. Sci. China Chem. 2015, 58, 526–531.

[7] Russell, W.K., Park, Z-Y., Russel, D.H. Anal. Chem. 2001, 73, 2682-2685.

[8] Jensen, O.N., Wilm, M., Shevchenko, A., Mann, M. in: A.L. Link, (Ed.), Methods in Molecular Biology (vol. 112), Humana Press, Totowa 1999.

P30   A MICROFLUIDIC DEVICE FOR MONITORING CELL MIGRATION

Vojtěch Ledvina[1,2], Karel Klepárník[1], Soňa Legartová[3], Eva Bártová[3]

[1]*Institute of Analytical Chemistry of the Czech Academy of Sciences, Brno, Czech Republic, ledvina@iach.cz*

[2]*Faculty of Science, Masaryk University, Brno, Czech Republic*

[3]*Institute of the Biophysics of the Czech Academy of Sciences, Brno, Czech Republic*

Summary

A polydimethylsiloxane microfluidic device for monitoring directed cell migration was developed. The device comprises a main channel barred by pillar arrays with decreasing spacing and utilizes chemotactic movement of cells in the direction of increasing gradient of fetal bovine serum. HeLa cell line transfected with Premo FUCCI Cell Cycle Sensor was used as a model organism. The cells were imaged for several days using a scanning confocal microscope and the rate of migration in different cell cycle phases was evaluated.

Introduction

Chemotaxis describes a directed movement of cells in response to an extracellular chemical stimulus and it is commonly the result of three separate steps: chemosensing, polarization and locomotion. Chemoreceptors are distributed on the surface of the cell and enable detection of a chemical gradient. When the receptor is activated, it triggers a series of signaling events that leads to cytoskeletal reconstruction and migration in the direction of the increasing chemical gradient. Chemotaxis has huge importance in many physiological processes, such as migration of inflammatory cells to a site of infection, organ development during embryogenesis, tissue growth or wound healing. In cancerous cells, the chemotactic pathways are often reprogrammed in favor of tumor cell dissemination [1]. During metastasizing, the cancer cells firstly detach from the primary tumor, intravasate into the blood stream, extravasate to new tissue and form a secondary tumor at a distant site that can significantly reduce the patient's chance of survival. The various types of cancer may vastly differ in their invasivity and the related rate of migration. It is therefore important to study and compare the migration potential of different cancer cells because it may provide a valuable information on the potential malignancy during diagnosis.

To study the rate of migration and deformability of different cell populations, we have developed a simple flow-free microfluidic device made of polydimethylsiloxane (PDMS) that exploits the chemotactic movement of cells in the direction of increasing gradient of nutrient through a set of barriers. The device comprises a main channel barred by pillar arrays with

decreasing spacing that simulate pores within tissues and all the liquid handling is done only by pipetting and does not require any sophisticated instrumentation.

Experimental

As a model organism for the experiments, HeLa cell line transfected with Premo FUCCI Cell Cycle Sensor was used. The cells were cultured in DMEM medium supplemented with 10 % of fetal bovine serum (FBS). Before the experiment, cells were gathered by trypsinization and suspended in a serum-free medium. The sensor utilizes the red and green fluorescent protein sequence fused to the gene for antagonist proteins Cdt1 and geminin that are expressed in different phases of the cell cycle. Cdt1 peaks in G1 phase, geminin in S, G2 and M phase. The cells therefore exhibit change of the fluorescence emission based on the actual cell cycle phase.

The chip was fabricated by standard soft lithography techniques using the SU-8 3025 negative photoresist and PDMS casting. The master mold was created by spin-coating and exposing 25 µm thick layer of the SU-8 photoresist on a glass wafer to form a negative replica of the chip. The PDMS was then casted on the master mold and the polymerized block was bonded to a thin glass bottom Petri dish after air plasma treatment. The device comprises two 5 µL reservoirs connected by a central channel that contains pillar arrays with 10, 7 a 5 µm spacing (Fig. 1). The cells are seeded into the left reservoir in the serum-free medium and a medium with 10 % FBS is pipetted into the right reservoir. The live cells were imaged at 37°C and 5 % CO2 using a Leica TSC SP5 X laser scanning confocal microscope equipped with incubator chamber. The acquired time lapse sequences were processed by ImageJ software and the migration rates were calculated using the Manual Tracking plugin.

Fig. 1. Left - chromium mask for the fabrication of PDMS device. Right – assembled device used for confocal microscopy time lapse imaging.

Results and Discussion

To induce the directed cancer cell migration, a chemotactic gradient of FBS was generated by pipetting different concentrations of FBS into individual reservoirs and diffusion. Other effects like accumulation of waste metabolites and cell proliferation may also influence the migration. The whole PDMS chip was bonded to a thin glass bottom Petri dish which allows using objectives with short working distance and immersion. The dish can also be filled with water or PBS buffer which prevents evaporation of the media and maintains high humidity. The cells

were imaged using the scanning confocal microscope for a total of 83 hours and the red and green fluorescent protein emission was monitored (Fig. 2). First cells started adhering to the glass surface 2 hours after seeding into the chip. After 9 hours, almost all of the cells were already adherent and started migrating and proliferating. In each experiment, 10 cells were randomly picked for manual tracking and the average rate of migration was calculated to be 4.91 $\mu m \cdot h^{-1}$. The migration rate decreased slightly when the cells started penetrating through the 7 μm pillar array and then increased in the free channel. The effect of cell cycle phase on the migration rate was also observed. No significant changes were observed between the G1, S and G2 phases. The only exception was the mitosis phase, during which cells completely stopped moving and detached from the glass surface. After the mitotic division was complete, the daughter cells again adhered to the surface and started migrating.
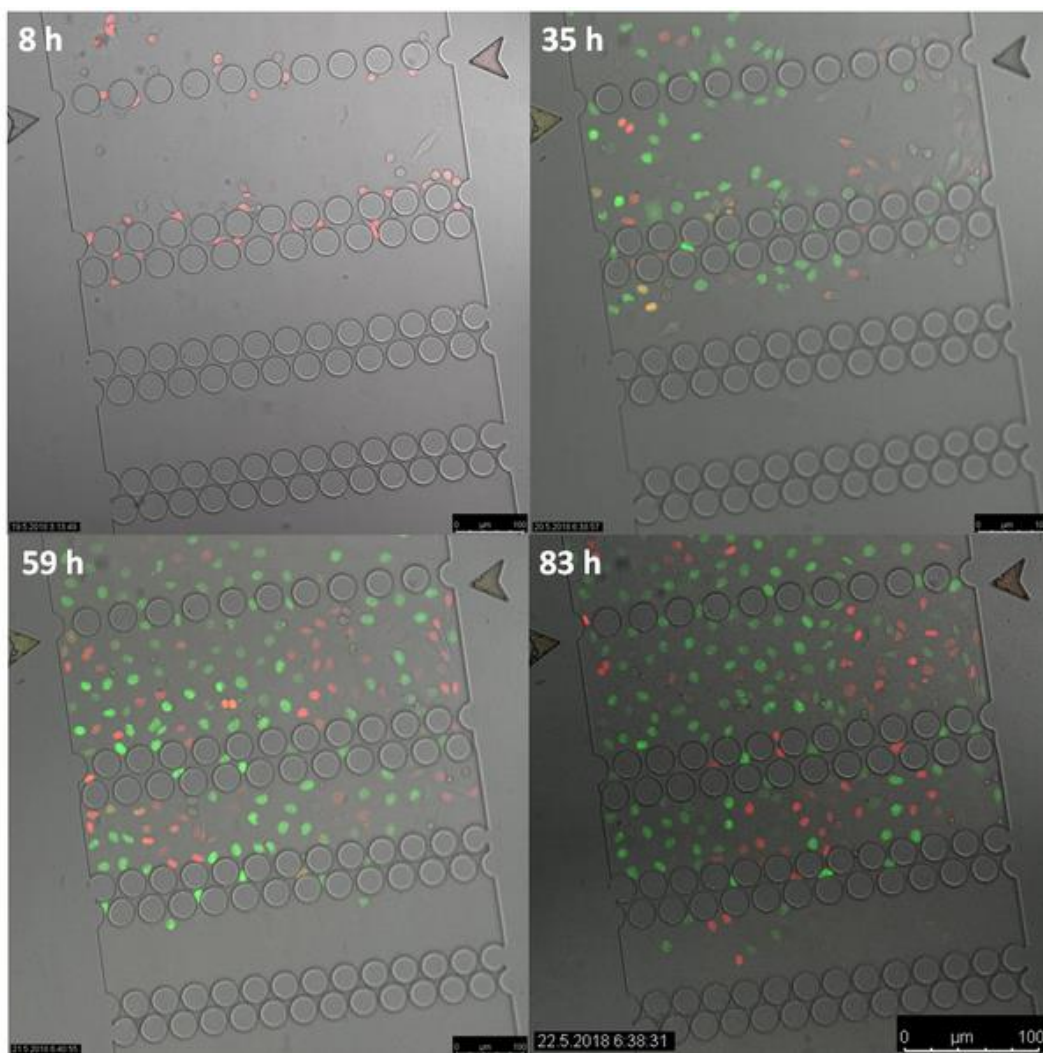
Fig. 2. Time lapse sequence of the HeLa cell line transfected with Premo FUCCI Cell Cycle Sensor. Individual images were taken after 8, 35, 59 and 83 hours of cultivation in the chip respectively. Red fluorescence correspond to the G1 phase of the cell cycle, yellow to the transition from G1 to S phase and green to the S, G2 and M phase. Shortly after mitosis the cells remain colorless before new Cdt1-RFP is expressed.

Conclusion

We have developed a flow-free microfluidic device for monitoring cell migration through narrow spaces in 2D environment. The device is fully compatible with confocal laser scanning microscopes and thanks to the fact that the PDMS is bonded to a thin glass bottom Petri dish, the experiments might run for several days and various objectives with or without immersion can be used for observation. Apart from the incubator unit, no sophisticated pumping system is needed for the operation. Combined with the relatively low price per unit the device could potentially find its use in personalized medicine for evaluation of cancer cell malignancy.

Acknowledgement

Reference

[1] Roussos, E. A., Condeelis, J. S., Patsialou, A., Nat Rev Cancer 2011, 11(8), 573-587.

P31 PLASMA PROTEIN BOUND HYDROPHOBIC METABOLITE RELEASE WITH PROTEINASE K AS A NEW APPROACH TO ENRICH METABOLOME COVERAGE IN UNTARGETED METABOLOMICS

Renata Wawrzyniak[1], Anna Kosnowska[1], Szymon Macioszek[1], Rafał Bartoszewski[2], Michał J. Markuszewski[1]

[1]*Department of Biopharmaceutics and Pharmacodynamics, Medical University of Gdańsk, Hallera 107, 80-416 Gdańsk, Poland, markusz@gumed.edu.pl*

[2]*Department of Biology and Pharmaceutical Botany, Medical University of Gdańsk, Hallera 107, 80-416 Gdańsk, Poland*

Summary

In the present study, a commonly applied plasma preparation procedure was modified with an additional step including incubation with PK. Additionally, various organic solvents for PP in LC-MS-based plasma non-targeted metabolomics were used and evaluated. The developed and optimized approach was tested for plasma samples derived from urogenital tract cancer patients. The proposed new and optimized procedure increased the number as well as the signal intensity of putatively identified endogenous metabolites. Furthermore, the proteinase K procedure allows detection of individual metabolites in plasma samples, significantly enriching plasma metabolome coverage. To the best of the authors' knowledge, this is the first study to apply this new plasma preparation procedure for LC-MS-based untargeted metabolomics. The proposed methodology may provide an enrichment of plasma metabolome coverage, mainly in terms of metabolite groups such as phospholipids, sphingolipids, fatty, and bile acids, acylcarnitines and amino acids. Finally, enriching the procedure with the PK digestion step allows clear detection of hydrophobic metabolites including, among others, hydrophobic amino acids, fatty acids, and phospholipids. Given the potential involvement of hydrophobic metabolites in human cardiovascular and cancer diseases, the method proposed here may constitute a novel approach in related metabolomics analysis.

Introduction

The untargeted metabolomic approach constitutes one of the most frequently applied methods in metabolomics studies. It aims to measure the comprehensive metabolomic profiles of various biological samples. Plasma untargeted metabolomics is a common method for evaluation of the mechanisms underlying human pathologies and identification of novel biomarkers. The plasma proteins provide the environment for the transport of hydrophobic metabolites. The

current sample preparation protocol relies on the immediate precipitation of proteins and thus leads to co-precipitation of a significant fraction of hydrophobic metabolites.

Experimental

A new simple procedure that overcomes the co-precipitation problem and improves metabolome coverage has been presented. Introducing an additional step preceding the protein precipitation, namely limited digestion with proteinase K, allows the release of associated metabolites through the relaxation of the native proteins tertiary structure.

Results and Discussion

The parameters, such as recovery, coverage, repeatability, matrix effects, selectivity as well as the orthogonality of all methods tested, were evaluated and compared. The results obtained in the study showed a high degree of overlap, which resulted in metabolite coverage increases of 34–80% depending on the LC-MS method used as compared to the single extraction procedure (methanol/ethanol precipitation). The modified protocol allows clear detection of hydrophobic metabolites including fatty acids and phospholipids.

Conclusion

Considering the potential involvement of the hydrophobic metabolites in human cardiovascular and cancer diseases, the method may constitute a novel approach in plasma untargeted metabolomics. To the best of the authors' knowledge, this is the first study to apply new sample preparation including the addition of PK, which is the focus of the issue of metabolite co-precipitation, for LC-MS-based untargeted metabolomics.

Reference

[1] Wawrzyniak R., Koskowska A., Macioszek S., Bartoszewski R., Markuszewski M.J., Scientific Reports, 2017, 8, 9541-9551.

P32 DEVELOPMENT OF SEPARATION GEL FOR SDS-CGE-MS

Brigitta Meszaros[1,2], Marton Szigeti[1,2], Andras Guttman[1,2]

[1]*Horvath Csaba Laboratory of Bioseparation Sciences, Research Center for Molecular Medicine, Faculty of Medicine, University of Debrecen, Debrecen, Hungary.*
brigi.meszi@gmail.com

[2]*MTA-PE Translational Glycomics Research Group, Research Institute of Biomolecular and Chemical Engineering, University of Pannonia, Veszprem, Hungary*

Summary

Host cell protein (HCP) analysis in biopharmaceutical manufacturing is crucial to ensure purity of the marketed products. [1] These proteins are the potential residues originated from the cell lines used for production and because of the low concentration; their analysis is usually limited and challenging. Due to its versatility, easy to use methodology, separation capability and rapid analysis time, the optimal analysis method for host cell proteins would be SDS-CGE separation hyphenated with mass spectrometry [2]. However, currently used materials in capillary gel electrophoresis are not compatible with the mass spectrometer, therefore, challenging to establish the hyphenation. Thus, the aim of this work was to develop an MS compatible separating buffer enabling hyphenated separation of proteins via capillary electrophoresis – mass spectrometer.

Introduction

During antibody production, the target drug proteins are harvested from clones derived from a single parent cell. Despite of the high quality protein purification processes, potential host cell proteins maybe present in the product and can be important to be identified. The quantitative and qualitative analyses of these host cell proteins are challenging due to their limited concentration in the final product after protein purification, therefore highly sensitive and informative analytical methods such as capillary electrophoresis hyphenated with mass spectrometry is needed. However, coupling CE-with MS has its limitations like non-MS compatible capillary electrophoresis separation gel buffers [3]. In this study, development of an MS compatible separation gel system was initiated. In general, protein separation media consists the following: polymers, buffers and detergents [4]. The main aim was to replace each component of the protein separating gel to MS compatible materials. Thus, host cell protein analysis would be possible in an automated fashion enabling deep investigation of the proteins via the utilization of mass spectrometry.

Experimental

Mass spectrometry compatible separation buffer development was carried out using a capillary electrophoresis system (P/ACE MDQ, Sciex) equipped with high sensitivity laser induced fluorescent detector. The separations were performed by fluorescent-labeled standard protein ladder (BenchMark Fluorescent Protein Standard, Invitrogen Thermo Fischer). In order to maintain the high resolution separation of the proteins as well perform it in an MS compatible manner, different polymers were investigated that can solidify into the capillary. Besides, separating media should contain MS compatible or degradable detergent as well. Taking all of the above into account, different separation matrix compositions were examined for MS compatible separation media for capillary electrophoresis.

Results and Discussion

Aiming MS compatible CE separation, several compositions were tested during this development stage of the work. The two major approaches were to 1) change currently applied components to MS compatible materials and 2) if it is not beneficially feasible, prevent the non-compatible components getting into the mass spectrometer. Thus, several sol-gel polymers were evaluated as separation gel in combination with linear polymers such as polyacrylamide and polyethylene oxide. The polymers were buffered in lithium-acetate, ammonium-acetate, amino-caproic acid and acetic acid. One of the critical step during the developing process was the replacement of sodium dodecyl sulfate (SDS) to other compatible surfactants. Therefore, the following MS compatible detergents were tested: N-Lauroylsarcosine sodium salt and ammonium perfluorooctanoate. At this stage of the development process, it was achieved that the MS compatible separation matrix was capable to separate the proteins. But, further development is necessary to replace the currently used background electrolyte to an MS compatible one maintaining the achieved separation resolution.

Conclusion

In this work, the development of MS compatible separating gel matrix was carried out aiming CE-MS hyphenation for size separation of proteins and their analysis by MS. A sol-gel based separation media was established where the components were prevented to reach the mass spectrometer contained MS compatible components and detergents that could be reduced before getting into the MS.

Acknowledgement

Reference

[1] Obrstar, D., Kröner, F., Japelj, B., Bojic, L., Anderka, O., Anal. Chem. 2018, 90, 11240-11247.

[2] Gahoual, R., Leize-Wagner, E., Houze, P., Francois, Y. N., Rapid Commun Mass Spectrom 2018.

[3] Klampfl, C. W., Electrophoresis 2009, 30, S83-S91.

[4] Guttman, A., Nolan, J., Anal. Biochem. 1994, 221, 285-289.

P33 EFFICIENT SAMPLE MIXING IN CAPILLARY ELECTROPHORESIS

Lenka Michalcová, Hana Nevídalová, Zdeněk Glatz

Department of Biochemistry, Masaryk University, Kamenice 5, 625 00 Brno, Czech Republic,
lenna@mail.muni.cz

Summary

The capillary electrophoresis-frontal analysis (CE-FA) is commonly used method for determination of drug-protein binding parameters in their native states without immobilization or labelling. Classical CE-FA sample preparation process uses off-line mixing reagents outside the capillary. On the other hand, as in the case of enzymatic or derivatization reaction, CE can prepares samples directly in the capillary using by electrophoretically mediated microanalysis (EMMA) or transversal diffusion laminar flow profile (TDLFP). Both approaches lead to the other advantages such as smaller sample consumption besides full automation. The main objective of this study was to test the TDLFP methodological approach of sample preparation for CE-FA application.

Introduction

The capillary electrophoresis (CE) is commonly use methods for separation and determination of different types of analytes. Another its less common application is the study of interactions between binding partners such as protein-proteins, protein-saccharides, protein-nucleic acids, nucleic acid-nucleic acids and protein-small molecules. These binding do not only give fundamental insights into the biological processes but also prepare the way to modify them by therapeutic molecules – drugs. Besides the main benefits of CE like less consumption of the reagents and sample, high efficiency and rapid analyses, CE based affinity interaction studies take advantages of native state of interacting partners without immobilization or labelling [1-3].

One of the most using of CE method for binding studies is capillary electrophoresis-frontal analysis (CE-FA). Long-injection plug is a typical for CE-FA. For comparison, the typical injection volumes in CE analyses are less than 1% of total volume of capillary while for CE-FA approaches, these volumes are more than 10%, in particular cases even more than 20%. Classical CE-FA samples are prepared manually and mixing of reagents takes place outside the capillary, so called off-line approach [1, 2]. In special CE applications, such as enzymatic or derivatization reactions, the sample are mixed directly in the capillary – on-line approach. These mixing approaches use either electric field in electrophoretically mediated microanalysis (EMMA), or diffusion in transversal diffusion laminar flow profile (TDLFP). The mixing procedure based on diffusion is robust and universal because diffusion represents an inherent property of all molecules. Therefore TDLFP can be used for mixing reaction mixtures with

changeable compositions. The combination of CE and one of these on-line approaches leads to the smaller consumption of reagents and full automation of the assays [4, 5].

The aim of this study was to test coupling of TDLFP and CE-FA.

Experimental

Chemicals

All reagents were obtained in analytical grade. Sodium hydroxide, sodium phosphate, were obtained from Sigma-Aldrich (Steinheim, German), hydrochloric acid was obtained from Fluka (Buchs, Switzerland).

The BGE in all experiments was the 20 mM phosphate buffer, pH 7.4. All samples were prepared by dissolution in this buffer. All solutions were prepared using water from a Millipore system (Merck, Milford, MA, USA).

Instrumentation

All experiments were performed in an Agilent 3DCapillary Electrophoresis System (Agilent Technologies, Waldbronn, Germany) equipped with a diode-array UV-Vis detection system. The analyses were carried out in a 75 μm I.D., 375 μm O.D. uncoated fused silica capillary with length 32.5/24 cm (Ltot/Leff) from Polymicro Technologies (Phoenix, AZ, USA) thermostated at 25 °C. The injection and separation parameters were optimized, the relationship between the individual parameters was sought. The samples were injected into the capillary with a pressure and operational voltage was applied in positive polarity and the detection wavelength was set to 214 nm.

Results and Discussion

In this study, we considered and optimized several factor important for injection and mixing procedure. Four parameters such as width of zone, time of incubation, number of zones and incubation plug, had a more significant effect and were optimized.

Formation of typical plateau in CE-FA using TDLFP was successful. The comparing of results of classical CE-FA and CE-FA coupling with TDLFP shown usability of this coupling.

Conclusion

The coupling of TDLFP with affinity method based on CE seem to be available. For other application will be necessary other testing.

Acknowledgement

Reference

[1] Vuignier, K., Schappler, J., Veuthey, J. L., Carrupt, P. A., Martel, S., Anal Bioanal Chem 2010, 398, 53-66.

[2] Michalcová, L, Glatz, Z., Chemické Listy 2016, 110, 4, 249-257.

[3] Nevídalová, H., Michalcová, L., Glatz, Z., Electrophoresis, 2018, 39, 581-589.

[4] Okhonin, V., Liu, X., Krylov, S. N., Anal. Chem., 2005, 77, 5925-5929.

[5] Pelcová, M., Řemínek, R., Sandbaumhuter, F. A., Mosher, R. A., Glatz, Z., Thormann, W., J.Chromatogr. A, 2016, 1471, 192-200.

P34   NOVEL IONIC LIQUID-BASED EXTRACTION APPROACH FOR THE ISOLATION OF SELECTED NEUROTRANSMITTERS (NTS) FROM RAT BRAIN SAMPLES

Natalia Miękus[1,2], Ilona Olędzka[2], Darya Harshkova[3], Ivan Liakh[4], Alina Plenis[2], Piotr Kowalski[2], Michał Jaskulski[1], Tomasz Bączek[2]

[1]*Department of Animal and Human Physiology, Faculty of Biology, University of Gdansk, Wita Stwosza 59, 80-308 Gdansk, Poland, miekusn@gmail.com*

[2]*Department of Pharmaceutical Chemistry, Medical University of Gdańsk, al. Gen. J. Hallera 107, 80-416 Gdańsk, Poland*

[3]*Department of Plant Physiology and Biotechnology, University of Gdańsk, Wita Stwosza 59, 80-308 Gdańsk, Poland*

[4]*S. I. Gelberg Department of Microbiology, Virology and Immunology, Grodno State Medical University, Vilenskaja str., 19, 230023 Grodno, Belarus*

Summary

Performance of several extraction protocols has been checked. The most efficient experimental protocol has been chosen and used for the extraction of several neurotransmitters from rat brain samples. The solid-phase microextraction as well as capillary electrophoresis has been applied in this study.

Introduction

The new discoveries in the neuroscience are driven by the adequate determination of analytes from the brain tissues obtained from animals, among others. The capillary electrophoresis (CE) is known for its flexibility and versatility when it comes to biomedical researches and could be applied for the neuroscience researches. Nevertheless, the low concentration sensitivity is one of its most significant limitation, especially while the analysis of trace amounts of compounds in the complex biological sample is required. Therefore, the preparation of the brain sample prior to CE remains the concentration sensitivity-limiting step and needs to be carefully planned before experimental procedure.

Experimental

We evaluated the performance of several experiments for the isolation, preconcentration and determination of NTs in rat brains enriched with L-tyrosine, L-tryptophan, dopamine (DA),

adrenaline (A) and noradrenaline (NA). The studied group consisted of brain slices which were supplemented with the standard solution of NTs (each analyte at the concentration of 10 g/g) (n = 6). The control samples were supplemented with an equal volume amount of MeOH (n = 6).

Results and Discussion

We developed a methodology for the isolation of selected NTs from brain tissue using an ionic liquid (IL) in order to increase the efficiency of solid-phase microextraction (SPME). The quantitative analysis of analytes was conducted with the capillary electrophoretic system (P/ACE MDQ Capillary Electrophoresis System, Beckman Instruments, Fullerton, CA, USA). Also, the amount of brain tissue used for homogenization was reduced to fulfill the requirements for the miniaturization of sample and solvents usage [1,2].

Conclusion

The relatively simple procedures (based on IL-SPME) for the preparation of brain cortex slices, along with the short electromigration separation time, may offer a significant advantage over many other published methods, especially when long stages of sample preparation or derivatization procedures are involved. In here, the first successful attempt to realize the off-line preconcentration SPME procedure with ionic liquid (1-ethyl-3-methyl imidazolium tetrafluoroborate) to improve the extraction efficiency of six NTs (DA, A, NA, L-Trp, L-Tyr, 5-HT) from brain samples was presented. The proposed procedures can be successfully applied for the determination of this group of compounds, possessing great potential as a significant tool for clinical and neurological studies [1,2].

Acknowledgement

Reference

[1] N. Miękus, I. Olędzka, D. Harshkova, I. Liakh, A. Plenis, P. Kowalski, T. Bączek. Comparison of three extraction approaches for the isolation of neurotransmitters from rat brain samples, International Journal of Molecular Sciences, 2018, 19, 1-11.
[2] N. Miękus, I. Olędzka, N. Kossakowska, A. Plenis, P. Kowalski, A. Prahl, T. Bączek. Ionic liquids as signal amplifiers for the simultaneous extraction of several neurotransmitters determined by micellar electrokinetic chromatography, Talanta, 2018, 186, 119-123.

P35 CHROMATOGRAPHIC SEPARATION OF AFLATOXIN ANALOGUES

<u>Dana Moravcová</u>[1], Josef Planeta[1], Kamila Lunerová[2], Filip Duša[1], Jozef Šesták[1], Oldřich Kubíček[2], Marie Horká[1]

*[1]Czech Academy of Sciences, Institute of Analytical Chemistry, Brno, Czech Republic,
moravcova@iach.cz*

[2]National Institute for NBC Protection, Brno, Czech Republic

Summary

Three short particle-packed columns (50 x 2.1 mm) were compared for the rapid and efficient chromatographic separation of aflatoxin G1, G2, B1 and B2 analogues.

Introduction

Aflatoxins G1, G2 and B1, B2 are highly toxic secondary metabolites produced by variety of species belonging to genus *Aspergillus*. These substances show carcinogenic, mutagenic and teratogenic effects and they can be found in different food sources such as grains, nuts, dried fruits, and milk products [1]. These days, ELISA is routinely performed for screening of total aflatoxins while the high performance liquid chromatography with UV or fluorescence detection is widely used to identify and quantify aflatoxins in foods and feeds. The reversed-phase chromatography separation mode prevails over other modes to analyse aflatoxins. The separation can be run under gradient or isocratic conditions. From practical point of view, avoiding the gradient elution is of significant benefit, when the sample throughput is increased and the solvent consumption reduced.

Presented study is focused on the characterization of short particle-packed chromatographic columns suitable for the rapid and efficient isocratic separation of aflatoxins.

Experimental

Analyses were performed using the Agilent 1200 Series LC system with UV detector (2 µm cell) (CA, USA). Evaluated columns were 2.6 µm SpeedCore RP18-Amide (50x2.1mm), 2.6 µm SpeedCore C18/PFP (50x2.1mm), and 3 µm Fortis H_2O (50x2.1mm) (Fortis Technologies Ltd., Great Britain). Methanol (gradient grade) and acetic acid were obtained from Sigma Aldrich (Austria). Water purified with a Milli-Q A10 Gradient (Millipore, MA, USA) was used in experiments. Standard containing 2 µg/mL of Aflatoxin B1 and Aflatoxin G1 and 0.5 µg/mL of Aflatoxin B2 and Aflatoxin G2 in acetonitrile was purchased from Romer Labs Diagnostic GmbH (Austria). The standard mixture was diluted with water in ratio 1:2 and used for all measurements.

Results and Discussion

Three C18 stationary phases SpeedCore RP18-Amide, SpeedCore C18/PFP and Fortis H_2O were evaluated for separation of aflatoxin analogues G1, G2 and B1, B2. The SpeedCore RP18-Amide is C18 stationary phase with embedded polar functionality, the SpeedCore C18/PFP stationary phase combines C18 and pentafluorophenyl ligands on its surface and the Fortis H_2O is C18 stationary phase with polar endcapping. **Fig. 1A** shows the selectivity of characterized stationary phases to aflatoxins G1, G2 and B1, B2 with an isocratic mobile phase composed of 50% methanol and 50% water containing 0.5% of acetic acid. The selectivity for aflatoxin analogues is similar between SpeedCore C18/PFP and Fortis H_2O stationary phase where the baseline separation of aflatoxins was obtained in 6.7 min and 7.2 min, respectively. The stationary phase SpeedCore RP18-Amide shows the lower selectivity and retention for aflatoxins. Aflatoxin analogues G1 and B2 are not baseline resolved on this stationary phase under used separation conditions. However, further optimization of the mobile phase composition could result in a baseline separation. Fortis H_2O stationary phase was utilized in the next experiments because it exhibited the highest retention and selectivity to aflatoxins.
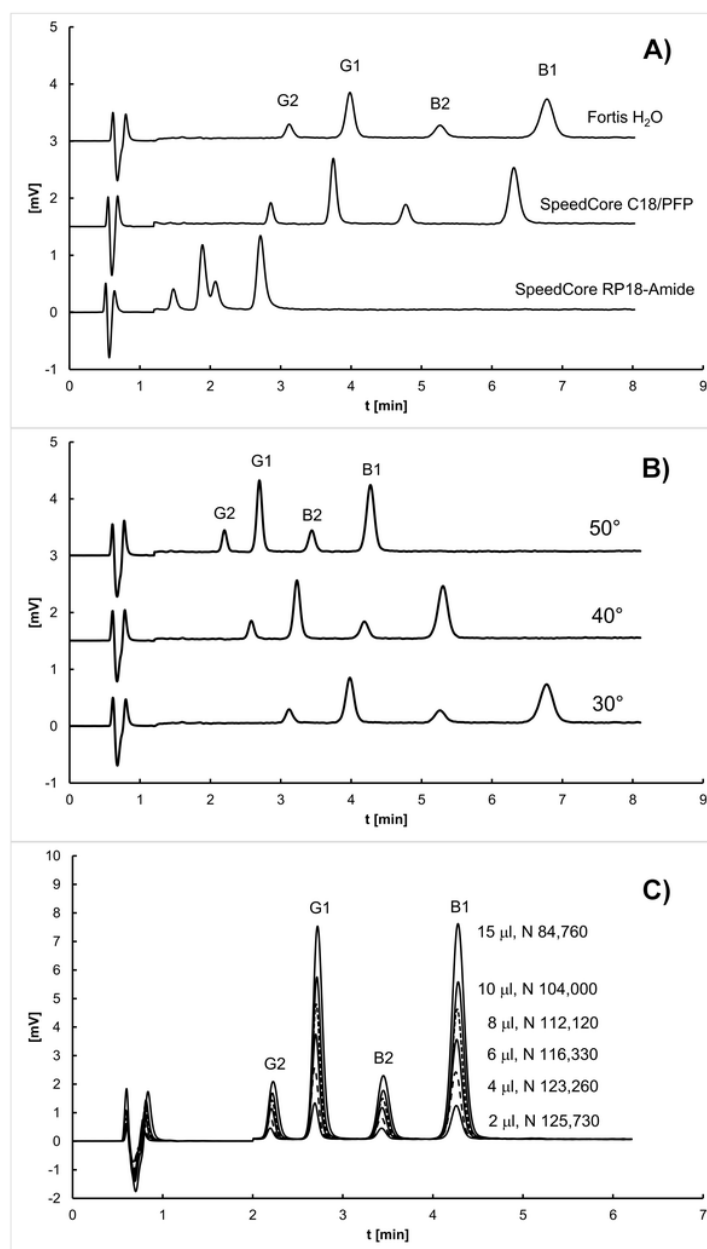
Fig. 1. Retention characteristics of aflatoxin analogues on short particle-packed columns. (A) the selectivity of the selected stationary phases to aflatoxins G1, G2 and B1, B2; (B) an effect of the increasing column temperature on the retention characteristics of the Fortis H2O stationary phase; (C) an effect of the increasing injected sample volume on the efficiency of the Fortis H2O stationary phase. Operating conditions: mobile phase: 50% methanol and 50% water containing 0.5% of acetic acid; flow rate 0.2 mL/min; UV detection at 362 nm; injected volume (A) and (B) 2 µL, (C) stated in figure; column temperature (A) 30°C, (B) stated in figure, (C) 50°C; N – the number of theoretical plates per meter.

Fig. 1B shows an impact of the increasing column temperature on the retention characteristics of the Fortis H$_2$O stationary phase. The total time of analysis was decreased from 7.2 min to 4.5 min when temperature was elevated from 30°C to 50°C. The sample loading capacity was evaluated for Fortis H$_2$O column in the next step. **Fig. 1C** shows dependency between column

efficiency and injected sample volume. The difference in column efficiency for the injected volume 2 µL and 4 µL was less than 2%. However, the injected volume of 15 µL of the sample caused a loss in column efficiency of 32.6% comparing to 2-µL injection.

Conclusion

Short particle packed columns SpeedCore C18/PFP and Fortis H_2O (50 x 2.1 mm) are good alternative for rapid and efficient isocratic chromatographic analysis of aflatoxin analogues. The total analysis time on Fortis H_2O column (50 x 2.1 mm) did not exceed 4.5 min if column temperature 50°C and mobile phase 50% methanol and 50% water containing 0.5% of acetic acid at flow rate of 0.2 mL/min were applied to the analysis.

Acknowledgement

Reference

[1] Shanakhat, H., Sorrentino, A., Raiola, A., Romano, A., Masi, P., Cavella, S., J. Sci. Food Agric. 2018, 98, 4003-4013.

P36   AFFINITY MICROFLUIDIC CHIP BASED ON PACKED MICROBEADS

Jakub Novotny[1,2], Veronika Ostatna[3], Frantisek Foret[1]

[1]*Institute of Analytical Chemistry of the Czech Academy of Sciences, Brno, Czech Republic, email: novotnyj@iach.cz*

[2]*Department of Biological and Biochemical Sciences, Faculty of Chemical Technology, University of Pardubice, Pardubice, Czech Republic*

[3]*Institute of Biophysics of the Czech Academy of Sciences, Brno, Czech Republic*

Summary

In this project, a plastic device was fabricated using CNC milling in polycarbonate. Chip contains integrated pneumatic valves for flow control and allows for injection and stacking of beaded supports. Intended use of these supports is formation of packed affinity columns suitable for glycoprotein assays.

Introduction

Affinity microfluidic chips generally utilize surface modification of the channel or formation of monoliths to create target-specific zones. In this case, the surface treatment was not a liable choice because of the requirements on chip functions. These demands were resolved by the decision to make a plastic chip manufactured by machining. Polycarbonate is not the optimal material for surface modification, which is why it was decided to create chip design which could be loaded with commercial affinity beaded support pre-treated with the desired affinity molecule.

As a method of fabrication of the microfluidic devices, micro-machining is a technique popular usually for creating masters for casting elastomer devices or inject-molded thermoplastics. Microfluidic channels can also be milled directly into the final device as in the case of this chip. Due to the limitation of the CN control, the method can be reproducibly used to manufacture mostly devices with larger channels. Advantage of the method is that it can also be used for construction of other auxiliary components of the system in addition to the core microfluidic component.

Experimental

While the subsequent experiments count with the use of lectins as the stationary phase and the glycoprotein as the mobile phase sample, out of practical reasons a reversed system was chosen in this initial setting. Store-bought ready-to-use bisacrylamide/azlactone biosupport was coupled with the RNase b glycoprotein and stacked inside the microchannel. Fluorescent-

labeled concanavalin A was employed as lectin sample to assess specific interactions with the stationary phase. Non-specific interactions were tested using fluorescein-labeled bovine serum albumin (BSA).

Functionality was evaluated by the collection of fractions of the mobile phase at the outlet of the device during washing and elution. Fluorescence signal was measured by Qubit bench-top fluorometer.
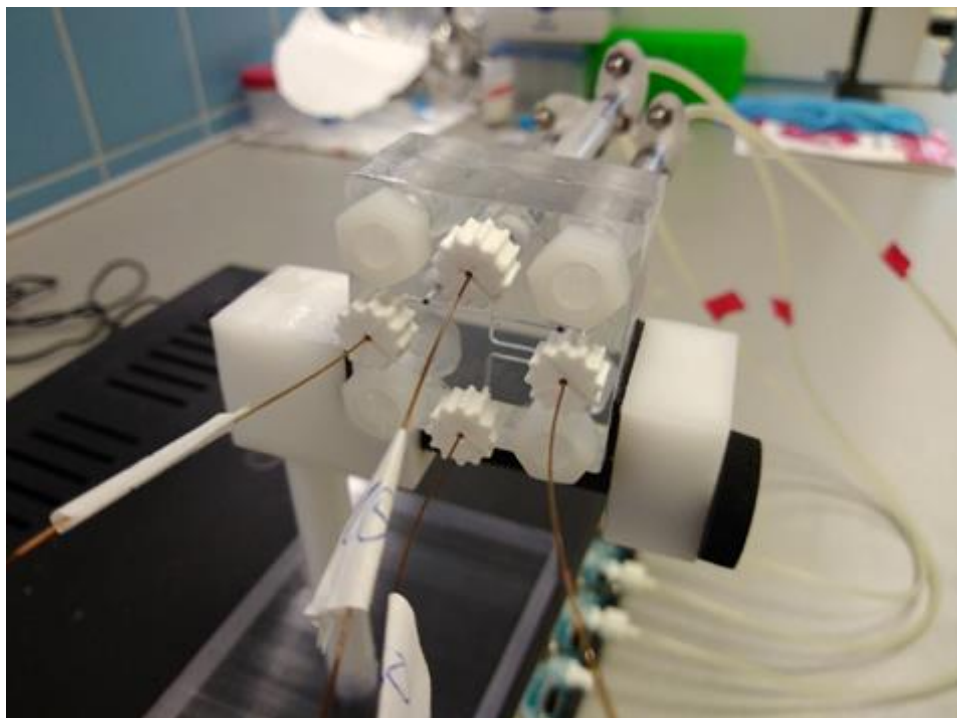

Fig. 1 **A view of the device.** Packed beads can be seen inside the loop in the center.

Results and Discussion

This report shows preliminary experiments utilizing fluorescent-labelled standards to ascertain functionality of the device. The data show significant spike in the signal in the elution fraction of the concanavalin which is not present in the corresponding fraction of the BSA.

Conclusion

The packed column formed inside the microfluidic chip is able to fulfill its role in affinity capture. At least in the setting of the system of RNase (s) – concanavalin (aq) the column shows very little non-specific interaction with the BSA control.

Acknowledgement

P37   EVALUATION OF EXTRACTION PROCEDURES FOR ISOLATION OF SELECTED BIOGENIC AMINES FROM BIOLOGICAL SAMPLES BEFORE ANALYSIS BY CAPILLARY ELECTROPHORESIS

Ilona Olędzka[1], Natalia Miękus-Purwin[1,2], Piotr Kowalski[1], Alina Plenis[1], Marta Rudnicka[1], Natalia Kossakowska[1], Tomasz Bączek[1]

[1]*Department of Pharmaceutical Chemistry, Medical University of Gdańsk, Hallera 107, 80-416 Gdańsk, Poland, ilona@gumed.edu.pl*

[2]*University of Gdańsk, Faculty of Biology, Department of Animal and Human Physiology, Gdańsk, Poland*

Summary

The following work describes extractions and analysis of seven biogenic amines: HVA, VMA, MHPG, DHPG, DOPAC, metanephrine and normethanephrine, using three extraction methods. In the experiments extraction efficiency and the possibility of enrichment of the analytes was assessed by solid phase extraction (SPE), solid phase microextraction (SPME) and dispersive liquid-liquid microextraction (DLLME). As a result of the conducted experiments, it was found that it is impossible to find universal and effective method for such a wide group of analytes. Potentially the most effective method of isolation was SPME type extraction, using DVB fibers and methanol used as desorbent. This method in combination with micellar electrokinetic capillary chromatography as a separation technique can be an efficient tool in the analysis of these biogenic amines in real clinical samples, after full validation of the method.

Introduction

Catecholamines, also called biogenic amines are organic substances which play important role is the transmission of signals between nerve cells. They are presented in human body fluids such as blood, urine and cerebrospinal fluid [1,2]. The most important role of catecholamines as neurotransmitters is to transfer signals between neurons by stimulating or inhibiting the appropriate receptors. The elevated levels of catecholamines in the blood can be directly related to stress caused by both environmental and psychological factors. Characteristic effects of catecholamine action s and products of their metabolism is increased blood pressure, high glucose level and accelerated heart rate. A disorder of catecholamines in the body can lead to many neurological, endocrine, psychiatric and cardiovascular diseases. For this reason the monitoring of their level in the body is very helpful from clinical point of view.

Experimental

In this work the experiments using three extraction techniques to isolation seven biogenic amines such as HVA, VMA, MHPG, DHPG, DOPAC, metanephrine (M) and normethanephrine (MN) from research samples were tested and evaluated. The dispersive liquid-liquid microextraction (DLLME) with ethanol as dispersion agent and dichloromethane as extraction phase were investigated. Next, three types of extraction columns with hydrophilic-hydrophobic filling (HLB), polar (CN) and non-polar (C18) filling were used to test the effectiveness of procedures based on SPE extraction. Methanol, dichloromethane, hexane, acetone and a mixture of acetonitrile-methanol (50:50, v/v) were used as eluents. Solid-phase microextraction (SPME) was used as the third technique. In the experiments, a semimanual apparatus was used in which non-polar C18 fibers and hydrophilic-hydrophobic DVB fibers were used as the solid phase. The extraction procedure from the water sample consisted of several stages: conditioning the fiber with a mixture of water and methanol (50:50, v/v), sorption and desorption of analytes from fiber. Between the stages, the fibers were rinsed with deionized water to limit the transfer of possible interfering substances or impurities.

To assess the extraction efficiency and enrichment factor (EF) capillary electrophoresis as separation technique was used. CE system (P/ACE MDQ Capillary Electrophoresis System) was equipped with an autosampler, a diode array detector (DAD), a temperature control device, and a data acquisition system supplied by the manufacturer (32 Karat 8.0). The CE optimized parameters were as follows: uncoated fused silica capillary (75 µm i.d. 60.2 cm length); UV, λ = 200 nm; hydrodynamic injection time 15 s; applied voltage 22 kV; temperature 25.0 ($\pm$0.1) °C. Adequate rinsing the capillary ensured the reproducibility of the analyses. The first step was rinsing the capillary with 0.1 M NaOH for 1 min under the pressure of 50 psi and subsequently with Milli-Q water for 1 min under the pressure of 50 psi between each run. Background electrolyte (BGE) consists of 5 mM sodium tetraborate decahydrate, 50 mM SDS, 15 % (v/v) MeOH, 150 mM boric acid.

The results of the analyzes after each extraction were compared with the results obtained for the analysis of the standard solution containing all analytes at concentration 10 µg/mL, and then the extraction efficiency (R) and the enrichment factor (EF) were calculated after the isolation process for each of the analytes. The extraction efficiency (R) was expressed as recovery of analyte. Due to the fact that during the extraction step these procedures were not yet validated at this stage of the research, the response of apparatus (peak height) were used to determine the EF.

Results and Discussion

The effective use of separation techniques in qualitative and quantitative analysis requires proper sample preparation step. Therefore, the most optimal extraction parameters of analytes of interest from the research material should be selected. Moreover, an additional analytical challenge is the necessity of simultaneously isolating a larger group of analytes that differ in their physicochemical properties [3]. Unfortunately, there is no universal extraction method,

and the choice of technique always constitutes a compromise between the degree of isolation of compounds from the matrix and the efficiency of the sample purification.

In this study isolation of 7 mentioned biogenic amines from biological samples by using various extraction approaches (DLLME, SPE, SPME) were carried out. For each technique, both the extraction efficiency (R) and enrichment factor (EF) were evaluated. In the case of DLLME, the effect of dichloromethane as the extraction phase and ethanol as the desorbing phase on the extraction efficiency of selected biogenic amines was checked. Despite that the DLLME is characterized by low reagent consumption and less time-consuming, but this procedure showed low efficiency for all the analyzed biogenic amines.

The SPE with C18 columns and the ACN-methanol mixture (50:50, v/v) used as an elution solvent proved the most effective isolation conditions for DHPG, VMA, HVA, M and DOPAC.

Potentially the most effective method of isolation selected biogenic amines was SPME with a DVB coated fibres and methanol used as a desorbent. For six tested amines, EF were obtained in the range from 1.11 to 6, for one analyte (DHPG) the extraction yield was 72%. In the case of the SPME technique with the C18 and the desorbing mixture composed of ACN-methanol (50:50, v/v), a high EF, close to 3-fold, for metanephrine was obtained.

Conclusion

As a results of conducted study the SPME extraction technique with a DVB-type of fibres coating and methanol as a desorbent was selected as the most effective method for the isolation of seven biogenic amines from biological samples. Next, this method in combination with micellar-electrokinetic capillary chromatography as a separation technique can be selected for further experiments as an efficient tool in the analysis of mentioned biogenic amines in biological samples after full validation of the method.

Acknowledgement

Reference

[1] Miękus, N., Kowalski, P., Olędzka, I., Plenis, A., Bień, E., Miękus, A., Krawczyk, M., Adamkiewicz-Drożyńska, E., Bączek, T., J. Chromatogr. B, 2015, 1003, 27-30.
[2] Miękus, N., Olędzka, I., Plenis, A., Kowalski, P., Bień, E., Miękus, A., Krawczyk, M.A., Adamkiewicz-Drożyńska, E., Bączek, T., J. Chromatogr. B, 2016, 1036-1037, 114-123.

[3] Miękus, N., Olędzka, I., Kossakowska, N., Plenis, A., Kowalski, P., Prahl, A., Bączek, T., Talanta 2018, 186, 119-123

P38 OPTIMIZING VOLTAMMETRIC ANALYSIS OF SUDAN I AT PYROLYTIC GRAPHITE ELECTRODES IN AQUEOUS MEDIA: TOWARDS DEVELOPMENT OF ELECTROCHEMICAL ASSAY FOR ACTIVITY OF HYDROXYLASE ENZYMES

Anna Ondráčková[1], Karolina Schwarzová-Pecková[1,2], Miroslav Fojta[1]

[1]*Central European Institute of Technology, Masaryk University, Kamenice 753/5, CZ-625 00 Brno, Czech Republic*

[2]*Charles University, Faculty of Science, Department of Analytical Chemistry, UNESCO Laboratory of Environmental Electrochemistry, Hlavova 8, CZ-128 43, Prague 2, Czech Republic*

Summary

Sudan I is an azo dye belonging to category 3 carcinogens. In organisms it is transformed by microsomal hydroxylation system involving cytochrome P450. The dye is electrochemically active due to presence of reducible azo group and oxidizable phenolic moiety. In this work we study voltammetric behavior of Sudan I at basal plane pyrolytic graphite electrode (PGE). We observed well developed signals in both cathodic ad anodic regions due to primary reduction or oxidation of the dye, as well as analytically useful signals attributable to products of these processes. Moreover, Sudan I as well as products of its electrochemical transformations are strongly adsorbed at the PGE, making it possible to analyze small volume samples using a simple *ex situ* voltammetry.

Introduction

The Sudan dyes are a group of azo compounds used to color various industrial products, including solvents, oils, fats, waxes etc. Sudan I, 1-(Phenyldiazenyl)naphthalene-2-ol, is an intensely orange-red azo dye that has been adopted for coloring (besides products mentioned above) various foods, such as spices. However, the use of Sudan I in foods is now banned in many countries, because Sudan I has been classified as category 3 carcinogen by the International Agency for Research on Cancer (IARC).
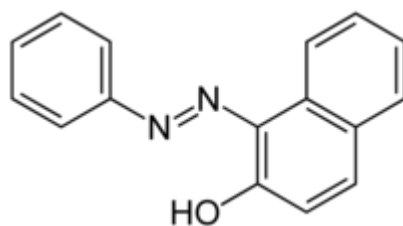
In mammalian organisms, Sudan I is metabolized by the microsomal detoxifying system with a central role of cytochrome P450 (CYP) hydroxylation activity. Numerous studies (e.g., [1-3]) have been devoted to biochemical mechanisms of the hydroxylation reactions, analysis of products and involvement of different CYP isoforms.

Electrochemical methods have been applied to determine Sudan I in relevant matrices, with particular attention paid to analysis of food samples [4-8]. Due to the presence of suitable functional groups, the dye can be detected either via oxidation of the phenolic group, or via reduction of the azo group. In addition, these primary conversions result in formation of other electrochemically active moieties. Four-electron reduction of the azo group results in splitting of the Sudan I molecule to give aniline and an ortho-quinoneimine reversible redox system [9]. Oxidation of the naphthol moiety is based on one-electron, one-proton loss forming a naphtoxy radical, possibly followed by further oxidation to corresponding napthoxy cation. Following chemical transformations of these species, e.g., coupling reactions leading to polymer formation or addition of water (hydroxyl) leading to formation of quinonic species is expected, similarly as for other phenolic compounds [10].

In this work we focus on (a) an improvement of electrochemical detection of Sudan I via more detailed knowledge about processes taking place at the pyrolytic graphite electrode and (b) establishing conditions favorable for distinction of products of Sudan I hydroxylation formed upon action of the CYP enzymes.

Experimental

Cyclic voltammetry (CV; scan rate 1 V s^{-1}) was carried out using AUTOLAB potentiostat made by Eco Chemie driven by GPES software. All measurements were performed in the three-electrode setup with basal plane PGE as working electrode, Ag|AgCl (3 mol L^{-1} KCl) as a reference electrode and platinum wire as an auxiliary electrode. Argon was used for removing oxygen from studied solutions (3 min). Stock solution of Sudan I was prepared in nonaqueous ethanol at the concentration of 5 mmol L^{-1} and stored at +3° C in dark. The volume of the measured solutions was 3 mL, final concentration of Sudan I 5 μmol L^{-1}. For *ex situ* measurements, 4 μl of Sudan I solution (c = 10 μmol L^{-1}) was applied on the PGE surface. After 3 min the surface was washed in buffer solution and consequently transferred to supporting electrolyte for measurement. Britton – Robinson buffer pH 1.0, 7.0, and 10.0 was used for this purpose.

Results and Discussion

Electrochemical behavior of Sudan I was studied using CV at the basal plane pyrolytic graphite electrode. Owing to sufficiently wide potential window, both reduction (azo group) and oxidation (phenol) of the dye could be performed at the same electrode. Figure 1A shows CV of Sudan I measured with initial potential (Ei) 0 V, the first anodic scan to +0.25 V, followed by repeated cycles between +0.25 and –1.0 V. The strong signal at the first negative scan (black curve; peak potential about –0.8 V) corresponds to irreversible reduction of the azo group to two amines (aniline and 1-amino naphthalene-2-ol). The latter substance is oxidized in anodic scan to corresponding quinoneimine giving the quasireversible pair (II) centered around 0 V. Strikingly, no peaks are observed in the latter region unless the irreversible reduction of the azo moiety takes place.
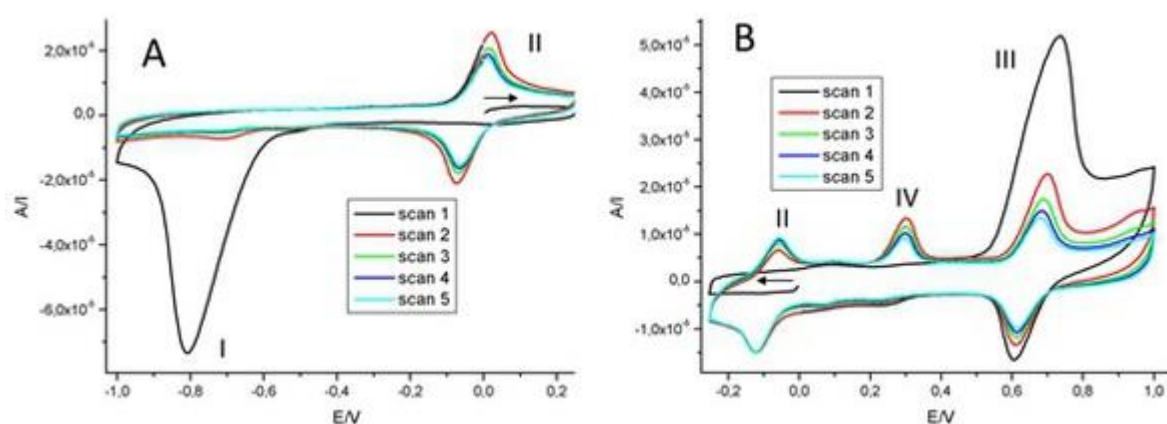

Fig. 1. Cyclic voltammograms of 5 μmol L^{-1} Sudan I. (A) Initial potential 0 V, positive vertex potential +0.25 V, negative vertex potential -1.0 V. (B) Initial potential 0 V, negative vertex potential –0.25 V, positive vertex potential +1.0 V. Initial scan directions are indicated by arrows. Measured in Britton-Robinson buffer, pH 7.0, scan rate 1 V s^{-1}.

When analogous CV experiments are performed with Ei = 0 V, the first cathodic scan to –0.25 V followed by cycling between -0.25 and +1.0 V, a well-developed anodic peak is observed close to +0.7 V (Fig. 1B, peak III). This signal can be attributed to oxidation of the phenolic hydroxyl group. In following potential cycles, two quasireversible pairs appeared, one centered around +0.65 V (suggesting a reversible process in the region of phenol oxidation, presumably due to the presence of an quinone/hydroquinone system resulting from oxidation of the phenolic moiety) and the other close to -0.05 V (i.e., slightly more negative than observed after reduction of the azo group, Fig. 1A). Again, the latter redox pair was not detected without the primary oxidation process having taken place (black curve). In addition, an anodic signal (peak IV) appeared around +0.3 V in the second and next potential cycles. Peak IV disappeared when more positive vertex potentials (such as +1.2 V) were used.

Results of our experiments indicated a strong adsorption of Sudan I, as well as its reduction or oxidation products, at the PGE surface. For example, irreversible reduction peak I is well developed only in the first potential scan, while the quasireversible quinoneimine/1-amino

naphthalene-2-ol pair is remarkably stable during repeated potential cycling (Fig. 1A). Similar stability of voltammetric signals was observed in the anodic region as well (Fig. 1B). Moreover, the Sudan I itself was observed to accumulate efficiently at the PGE surface. Adsorption of the dye at the electrode was so strong that even resisted medium exchange and allowed measurements, in both cathodic and anodic regions, in *ex situ* mode (i.e., in blank background electrolyte with the analyte adsorbed at the electrode). On one hand this property is advantageous in voltammetric analysis of small samples when selective strong adsorption of analytes can be utilized to isolate them from reaction mixtures. By contrast, strong adsorption of the products may complicate electrode renewal e.g., in liquid flow methods. Our ongoing studies are oriented towards selection of proper electrodes for specific purposes. Basal plane PGE, used in here presented experiments, is known to adsorb efficiently aromatic compounds [11]. On the other hand, when absence of strong adsorption is preferred, boron doped diamond electrodes may be the ones of choice [11, 12].

Conclusion

Sudan I gives well-developed voltammetric signals at the PGE in both negative and positive potential regions. Reduction of the azo group or oxidation of phenolic hydroxyl group leads to formation of electrochemically active species giving distinct electrochemical signals. Some of them can be, in a controlled way, switched on/off to increase selectivity of Sudan I detection. Based on these data we anticipate that hydroxylation products of the dye will give specific voltammetric responses and analogical approaches will allow their identification and resolution in mixtures. Sudan I as well as products of its electrochemical transformations are strongly adsorbed at the PGE surfaces. Electrochemical properties of Sudan I hydroxylation products and behavior of the dye at electrode surfaces exhibiting weaker adsorption are matter of our ongoing studies.

Acknowledgement

Reference

[1] Martinek, V., Stiborova, M., in: Cytochromes P450, Biochemistry, Biophysics and Drug Metabolism (Anzenbacher, P. Hudecek, J., eds.), 13th International Conference on Cytochromes P450, Jun 29-jul 03, 2003, Prague, Czech Republic; p. 235-240.

[2] Stiborova, M., Martinek, V., Rydlova, H., Hodek, P., Frei, E., Cancer Res. 2002, 62, 5678-5684.

[3] Stiborova, M., Martinek, V., Rydlova, H., Koblas, T., Hodek, P., Cancer Lett. 2005, 220, 145-154.

[4] Chailapakul, O., Wonsawat, W., Siangproh, W., Grudpan, K., Zhao, Y. F., Zhu, Z. W., Food Chem. 2008, 109, 876-882.

[5] Li, B. L., Luo, J. H., Luo, H. Q., Li, N. B., Food Chem. 2015, 173, 594-599.

[6] Li, J. H., Feng, H. B., Li, J., Feng, Y. L., Zhang, Y. Q., Jiang, J. B., Qian, D., Electrochim. Acta 2015, 167, 226-236.

[7] Li, L., Liu, X. H., Lu, J. J., Liu, Y. L., Lu, X. Q., Analytical Methods 2015, 7, 6595-6601.

[8] Mao, Y. X., Fan, Q. N., Li, J. J., Yu, L. L., Qu, L. B., Sens. Actuator B-Chem. 2014, 203, 759-765.

[9] Yang, D. X., Zhu, L. D., Jiang, X. Y., J. Electroanal. Chem. 2010, 640, 17-22.

[10] Zhu, X. P., Shi, S. Y., Wei, J. J., Lv, F. X., Zhao, H. Z., Kong, J. T., He, Q., Ni, J. R., Environ. Sci. Technol. 2007, 41, 6541-6546.

[11] Hasoň, S., Daňhel, A., Schwarzová-Pecková, K., Fojta, M., Carbon Electrodes in Electrochemical Analysis of Biomolecules and Bioactive Substances: Roles of Surface Structures and Chemical Groups. In Nanotechnology and Biosensors, Nikolelis, D. P.; Nikoleli, G.-P., Eds. Elsevier Inc.: Amsterdam, Oxford, Cambridge, 2018; pp 51-111.

[12] Vosahlova, J., Kolacna, L., Danhel, A., Fischer, J., Balintova, J., Hocek, M., Schwarzova-Peckova, K., Fojta, M., J. Electroanal. Chem. 2018, 821, 111-120.

P39   HEXAHISTIDINE-BASED TAG FOR CAPILLARY ELECTROPHORESIS-MASS SPECTROMETRY ANALYSIS OF OLIGOSACCHARIDES AND N-LINKED GLYCANS

Jan Partyka, **Jana Krenkova, Richard Cmelik, Frantisek Foret**

Institute of Analytical Chemistry of the CAS, v. v. i., Brno, Czech Republic, partyka@iach.cz

Summary

Various basic amino acids and peptides were studied as an alternative labels for capillary electrophoresis-mass spectrometry analysis of oligosaccharides. The hexahistidine-based label with big number of positive charges allowed to use effective and sensitive CE-MS analysis in positive ion mode both neutral and acidic glycans.

Introduction

Glycosylation, the most common post-translational modification of proteins, plays important roles in biological systems. Functions of glycans include structural components, solubility and stability of proteins, cell-cell and cell-matrix interactions and modulating signaling pathways. Glycom is dynamic and physiological changes can change the collection of glycans.

The analysis of glycans usually includes the derivatization step which ensures improvement of separation and detection properties of the analyte. The attached label can introduce a charge into neutral molecules, enhance sensitivity of used detection technique and change hydrophilic properties to hydrophobic. The most commonly used labels are neutral or negatively charged molecules (2-aminopyridine, 2-aminobenzamide, 2-aminobenzoic acid, 8-aminopyrene-1,3,6-trisulfonate). We tested hexahistidine-based label which can be easily protonated under mild acidic conditions and thus it provides high number of positive charges. The use of this label enables migration of glycans as cations in the capillary zone electrophoresis and sensitive detection by the mass spectrometry in the positive ion mode.

Experimental

All the experiments are detaily described in our published article [1]. Briefly, 10 mL of oligosaccharides in water (1 mmol/L) were mixed with 10 mL of hydrazinoacetyl-GHHHHHHG-OH (100 mmol/L) and 30 mL of a sodium borate buffer (400 mmol/L, pH 8.5). The reaction mixture was incubated at 55 °C for 20 h. Finally, the mixture was diluted with 100 mL of 0.5% formic acid, desalted by HyperSep Hypercarb SPE column and lyophilized.

CE-MS analyses were performed on an Agilent 7100 CE system (Agilent Technologies, Walbronn, Germany) coupled to a maXis impact ESI-TOF MS (Bruker Daltonics, Bremen, Germany) via a liquid junction based CE-MS interface. The CE separations were performed in the uncoated or LPAA-coated fused silica capillaries. 100 mmol/L acetic acid or 1 mol/L formic acid served as background electrolytes and spray liquids.

Results and Discussion

We have studied various basic amino acids and peptides for improvement of CE-MS analysis of oligosaccharides in the positive ion mode. The oligosaccharide standards (isomaltotriose, maltotetraose, maltopentaose, maltohexaose and maltoheptaose) were labeled via reductive amination (Fig. 1A). The all basic amino acids (histidine, lysine and arginine) and peptides with different number of histidines introduced positive charges into a molecule of saccharide and enabled sufficient separation by capillary electrophoresis. The migration times of tagged oligosaccharides were decreased with increasing number of positive charges provided by the label. The highest velocity was observed at oligosaccharides labeled by tag with six histidines in the structure. Oligosacharide standards labeled by this hexahistidine label migrated approximately two times faster than the standards labeled by histidine alone.
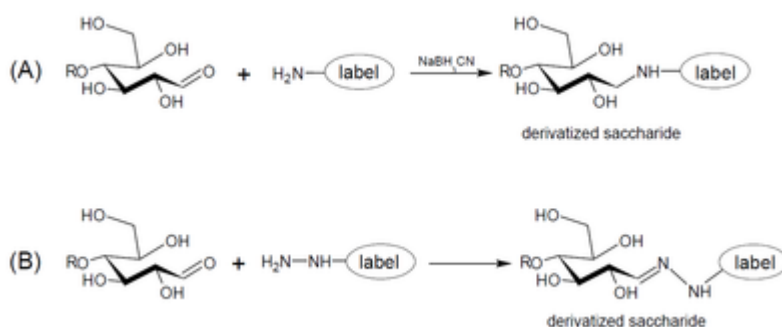
Fig. 1. (A) Reductive amination, (B) hydrazone formation.

We have also tested more complex samples such as N-linked glycans released by an enzyme PNGase F from ribonuclease B and fetuin. The labeling of N-linked glycans via reductive amination was problematic and several different products was observed [2]. Therefore, the labeling of N-linked glycans by hexahistidine-based tag was finally performed via hydrazone formation under alkaline conditions (Fig. 1B). The labeling by hydrazinoacetyl-GHHHHHHG-OH allows efficient CE separation of neutral glycans from ribonuclease B as well as acidic mono-, di-, tri- and tetra-sialylated glycans from fetuin (Fig. 2).
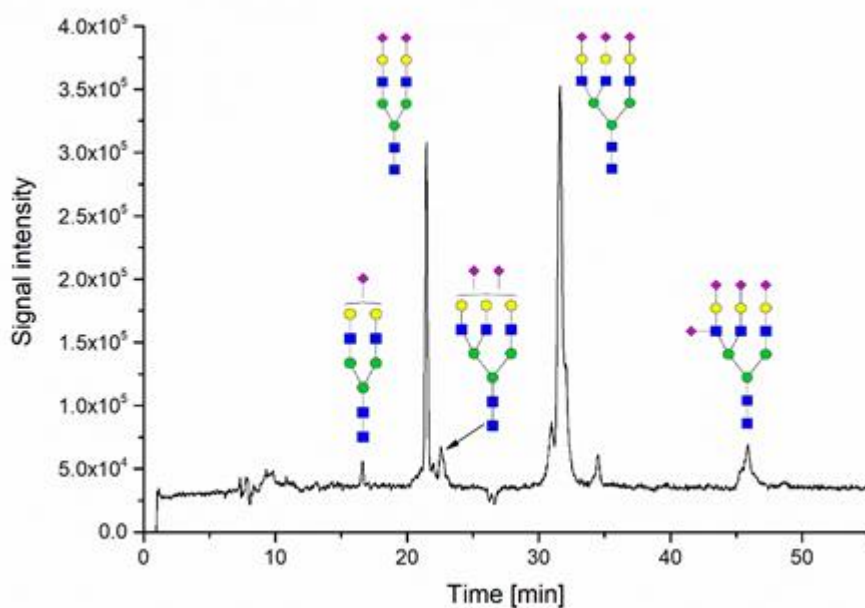
Fig. 2. CE-MS analysis of acidic N-linked glycans from fetuin labeled by hydrazinoacetyl-GHHHHHHG-OH. CE conditions: LPAA coated capillary (75 µm ID, 75 cm), BGE: 100 mmol/L aceticacid, injection: 50 mbar, 30 s.

Conclusion

The various basic amino acids and peptides were studied for labeling of oligosaccharides. The labeling of both neutral nad acidic N-linked glycans by hydrazinoacetyl-GHHHHHHG-OH via hydrazone formation enables efficient CE separation and sensitive MS detection in the positive ion mode.

Acknowledgement

P40   SPECIATION ANALYSIS OF As AND Hg IN BIOLOGICAL MATERIAL

Inga Petry-Podgórska[1], Tomáš Matoušek[1], Michaela Migašová[2], Veronika Zemanová[3], Milan Pavlík[3], Jan Kratzer[1], Daniela Pavlíková[4]

[1]*Institute of Analytical Chemistry CAS, v.v.i., Brno, Czech Republic, podgorska@iach.cz*

[2]*Department of Analytical Chemistry, Faculty of Science, Charles University, Prague, Czech Republic*

[3]*Institute of Experimental Botany CAS, Prague, Czech Republic*

[4]*Faculty of Agrobiology, Food and Natural Resources, Czech University of Life Sciences, Praha, Czech Republic*

Summary

This work was focused on an analysis of arsenic in selected plants and mercury in hair. A combination of HPLC and ICP-MS was used for analysis of biological tissues extracts. The speciation analysis of low molecular arsenic and mercury species like inorganic iAs^{3+} and iAs^{5+}, methylarsenic and dimethylarsenic forms was carried out with hydride generation (HG) technique, arsenic peptides and inorganic mercury (iHg^{2+}) and its methylated form (MHg^+) - with reverse phase (RP) chromatography and detected by ICP-MS.

Introduction

Every living organism is subjected to an influence of arsenic and mercury coming from food, water and the environment. Presence and speciation analysis of these toxic elements in plants and animals have been monitored using developed analytical methods. An anion exchange chromatography or hydride generation (HG) technique connected with ICP-MS are the typical analytical choices. Unfortunately, the two first techniques are not suitable for separation of arsenic-peptide compounds that are present in living organisms. A reverse phase chromatography enables to separate arsenic-peptide complexes and also inorganic mercury and its alkylated forms.

One of the aims of this work was to focus on the determination of arsenic accumulation in three ferns (*Pteris cretica* var. Albo-lineata, *Pteris cretica* var. Parkerii and *Pteris straminea*). The goal was to establish the total arsenic content in ferns using HG-ICP-MS technique and quantify arsenic species using HPLC and ICP-MS. The separation on the C18 reverse phase commonly is carried out with gradient elution. It is known that the content of the organic solvent introduced to plasma strongly affects the intensity of the arsenic signal [1]. In order to avoid this effect the LC method was developed to separate arsenospieces in the isocratic mode followed by short gradient jump to elute more hydrophobic components of the extracts. We

have tested the method using a mixture of arsenic complexes with glutathione (AsGS) which is a common metallic ions chelator in most of the living organisms.

Hair is a biological material consisting of polypeptide chains of keratin arranged into filaments. It is also used as a "memory stick" of a state of an organism. That is why it is one of the samples chosen for monitoring of chronic exposure. There are lots of procedures developed to dissolve efficiently hair [2]. The main problem is the possible occurrence of matrix-dependent alkylation and de-alkylation reactions during the sample preparation procedure. This causes erroneous determination of the particular mercury species. Mainly Hg^{2+} and $MeHg^+$ are detected in hair and the ratio is strongly connected to the extracting step. As different treatments may give contrasting results we decided to test the influence of several parameters such as extraction solution, temperature, and sample amount on the result.

Experimental

HPLC and ICP-MS: 1260 Infinity Quaternary LC System (Agilent Technologies) was used for separation of arsenic and mercury species and 7700 Series ICP-MS (Agilent Technologies) was used for detection of analyte. Detailed conditions of the HPLC-ICP-MS analysis are gathered in the table below.

HPLC	Plants	Hair

• Column:
 • Mobile phase:
 	
 • Flow rate:
 • Injection volume:
 • Column temp.:
 • Gradient:
	• Aeris 3.6u XB-C18 250 x 2.10 mm
	 • A: 0.1% formic acid,
	   B: 0.1% FA, 80% acetonitrile,
	 • 0.25 ml/min.,
	 • injection volumes: 5-100 ml,
	 • 4°C,
	 • 0-15min. 5%B, 18-20min. 60%B, 22-30min. 5%B.
		• Zorbax Eclipse XDB-C18 4.6 x 150mm 5-Micron,
		 • A: 0.5g/L of L-cys and L- cys x HCl, pH 2.3,
		   B: methanol,
		 • 1 ml/min.,
		 • injection volumes: 5-100 ml,
		 • 21°C,
		 • 0-1min. 2.50%B, 1-3min 50%B, 3-4min. 50-2%B, 6min. 2%B.

ICP-MS	• Torch injector ID: 1.5 mm; Power: 1600W, • Carrier gas: Ar 0.6 l/min ; Dilution gas: Ar 0.25 l/min; Nebulizer pump: 0,2 rps, • Collision cell: 3.5 ml/min for As, no gas for Hg, • Internal standard: 200 μg/l Te in 2% HNO₃; Monitored m/z: 75As and 201, 202Hg; 125Te, • Signal integration carried out manually using Mass Hunter software.	

Plant samples: Selected ferns (*Pteris cretica* L. var. Albo-lineata, *Pteris cretica* L. var. Parkerii, *Pteris straminea* Mett. ex Baker) have been treated with 20 mg As/kg, 100 mg As/kg and 250 mg As/kg of soil for 90 days. Samples of fronds and roots have been collected and subjected to extraction. Approximately 100 mg of the sample was soaked in 1 ml of 0.1% formic acid in water. The sample was kept at 1 ºC and vortexed 5 times within hour for 15 seconds. The extract was filtered with syringe filter (0.45 mm PTFE) and analysed immediately.

Hair samples: Hair certified reference material (CRM) was used for the analysis (GBW07601a, SwanLeaf, Australia) with certified total Hg content of 670±100 mg/kg Hg. A mass of 10-100 mg of the sample was soaked in the tested solutions for given period of time. The extract was subsequently filtered through a syringe filter (0.45 mm PTFE) and/or centrifuged if needed to separate microparticles and analysed immediately.

Calibrations were carried out with 100 μg/l iAs^{3+} and 10 μg/l Hg^{2+} in mobile phases A. Various injection volumes were applied: 20 μl of blanks (mobile phases A), 5, 10, 25, 50, 75μl of iAs^{3+} and 1, 2, 5, 10, 25μl of iHg^{2+} standard solutions;

Results and Discussion

A series of extractions and chromatographic separations were carried out to establish the degree of arsenic accumulation in selected ferns. We observed an elution of series fractions containing arsenic species within 15 minutes of isocratic separation (at 5% mobile phase B) and significant signal of a fraction eluting with around 30 % of acetonitrile. Small organic arsenic compounds eluted within four minutes and were could not be separated under this conditions. The arsenic-peptide complexes are minor As species (less than 35%) found in the plant extracts. Comparing retention times of the fractions with the arsenic-glutathione ones we noticed that only *Pteris cretica* var. Parkerii extract may contain As(GS)$_3$ complex (Fig. 1). The other signals were quantified but unidentified. Their determination will be carried out using ESI-MS. The total content of arsenic measured using two different methods: HG-ICP-MS and LC-ICP-MS were quite consistent. We observed that the *Pteris cretica* var. Albo-lineata is the most efficient arsenic accumulator as having been treated with just 20 mg As per 1kg soil and it gathered 282 ng/g of the element in fronds. Much smaller concentration of arsenic (38.2 ng/g) was observed in the roots even after treatment with 250 mg/kg of As. The other two ferns have much lower capacity for storage of arsenic. The maximum concentrations of total As content obtained are 35.73 ng/g in fronds of *Pteris cretica* var. Parkerii (250 mg/kg As treatment) and 10.03 ng/g in roots of *Pteris straminea* (100 mg/kg As treatment).

Several solutions have been tested to assess efficiency of the extraction (Fig. 2) and risk of changes in speciation analysis from CRM as a model sample. Only total Hg content is certified in this CRM. However, extraction with 2M HCl at room temperature is known to extract selectively only MeHg$^+$ (3) with extraction yields close to 100%. Between 200 and 220 ng/g of MeHg$^+$ was found under these conditions whereas only about 60 ng/g of iHg^{2+}, i.e. 10-15% of expected 470 ng/g iHg^{2+}, was co-extracted. The cysteine buffer, commonly used for effective extraction of Hg species from samples of marine origin (4), was found to be insufficient. The highest extraction yields 69-83 % were reached using 1M NaOH and 5M HNO$_3$ (Fig.2). Nevertheless, the latter one seems to influence the speciation analysis significantly causing 66% de-alkylation of MeHg$^+$.
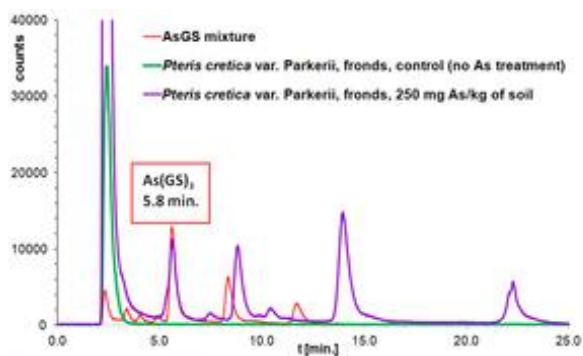
Fig. 1. Chromatographic separation of an extract of *Pteris cretica* var. Parkerii grown for 90 days in 250 mg arsenic per 1kg soil.
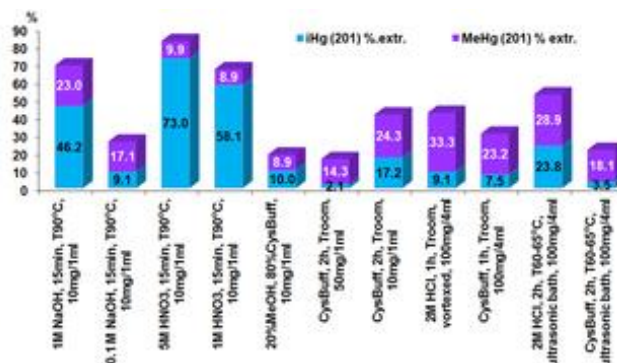
Fig. 2. The extraction yields of iHg^{2+} and MeHg$^+$ obtained under various condition.

Conclusion

The HPLC-ICP-MS combination enables quantification of particular eluted fraction of the plant extract. Unfortunately, the ICP is not able to identify the compounds in the separated mixture unless a known standards are available. On the other hand the ESI is designed to determine the structure and molecular weight of an anlyte but cannot be used for quantification unless derivatisation techniques are applied. A combination of ICP and ESI can give a full picture of arsenic specie arising during accumulation in plants.The results considering mercury are preliminary. The 2M HCl (for MeHg$^+$ determination) and 1M NaOH extraction procedures will be further tested on an IAEA-086 CRM in which MeHg^{2+} level is certified. Fast and user-friendly approach to Hg speciation analysis in hair will be tested in near future. It will be based on total Hg determination by AMA-254 (solid sampling, result in 5 min) and selective MeHg^{2+} extraction by 2M HCl with subsequent detection by cold vapour generation atomic absorption spectrometry (CV-AAS). Conditions for MeHg$^+$ generation were also optimized within this study (0.3 M HCl, 0.5% NaBH4, 25 ml/min Ar, 500 °C atomization temperature, LOD 0,2 ng/g MeHg$^+$).

Acknowledgement

Reference

[1] Bluemlein, K., Raab, A., Meharg, A.A., Charnock, J.M., Feldman, J., Anal. Bioanal. Chem. 2008, 390, 1739-1751.

[2] Horvath, A. L., The Scientific Worl Journal 2009, 9, 255-271.

[3] Čejchanová Čejchanová V., Spěváčková, V., Kratzer, K., Wranová, K., Spěváček, V. and Beneš, B., Biol. Trace Elem. Res. 2008, 121, 97–105.

[4] Sannac, S., Chen, Y.H., Wahlen, R. and McCurdy E. Application Note, 2012, Agilent Technologies, Manchester, UK

P41   DEVELOPMENT AND VALIDATION OF LC METHOD FOR THE DETERMINATION OF EPIRUBICIN IN HUMAN PLASMA AND URINE. APPLICATION TO A DRUG MONITORING

Alina Plenis[1], **Natalia Treder**[1], **Olga Maliszewska**[1], **Piotr Kowalski**[1], **Ilona Olędzka**[1], **Natalia Miękus**[1,2], **Ewa Bień**[3], **Małgorzata Anna Krawczyk**[3], **Elżbieta Adamkiewicz-Drożyńska**[3], **Tomasz Bączek**[1]

[1]*Department of Pharmaceutical Chemistry, Medical University of Gdańsk, Gdańsk, Poland,*
aplenis@gumed.edu.pl

[2]*Department of Animal and Human Physiology, University of Gdańsk, Gdańsk, Poland*

[3]*Department of Pediatrics, Hematology and Oncology, Medical University Gdansk, Gdańsk, Poland*

Summary

A simple, rapid, reliable and sensitive liquid chromatography with fluorescence detection (LC-FL) for the determination of epirubicin in human plasma and urine samples was developed and validated. The LC analysis was carried out after solid-phase extraction procedure (SPE) with a hydrophilic-lipophilic balance (HLB) cartridges, and with daunorubicin hydrochloride used as the internal standard. The limits of detection and quantification for DOX were 0.5 and 1 ng/mL in both biological fluids, respectively. The usefulness of the proposed SPE-LC-FL technique as an interesting alternative analytical tool in pharmacokinetic and clinical investigations was confirmed during the drug monitoring in pediatric cancer patient treated with epirubicin.

Introduction

Epirubicin hydrochloride, an anthracycline glycoside antibiotic, is widely used in the treatment of various cancers, including leukemias, Hodgkin's disease, Kaposi's sarcoma, malignant lymphoma as well as ovarian, breast and lung cancers. Epirubicin can be used alone or in combination with other anticancer drugs in many cancer therapeutic protocols for adults and children [1,2]. However, the clinical use of epirubicin is limited by many serious side effects such as the risk of cardiomyopathy with congestive heart failure, vomiting, nausea, myelosupression and mucositis. Therefore, it is necessary to monitor the concentration levels of this anticancer drug in human plasma and urine samples to avoid adverse effects and improve the effectiveness of chemotherapy.

The aim of the present work was to develop an uncomplicated, accurate and sensitive method for quantification of epirubicin in human plasma and urine, which could be useful in clinical study and drug monitoring.

Experimental

Epirubicin hydrochloride and daunorubicin hydrochloride (internal standard, IS), following solid-phase extraction using a hydrophilic-lipophilic balance (HLB) cartridges, were separated on a Synergi Hydro column with mobile phase consisting of 40 mM phosphate buffer (pH 4.1) and acetonitrile (69:31, *v/v*). The column temperature was set at 30ºC, while the flow rate of the mobile phase was 1 mL/min. Fluorescence (FL) detection was performed at the excitation wavelength of 497 nm and the emission wavelength of 557 nm. The method was validated according to the FDA and ICH requirements.

Results and Discussion

In the study, rapid and sensitive LC method with FL detection for the quantification of epirubicin in human plasma and urine was developed. Thus, a lot of liquid-liquid extraction (LLE) procedures and solid-phase extraction (SPE) were tested. Among them, the SPE with Supel Select HLB cartridge and the mixture of dichloromethane:2-propanol:methanol (2:1:1, *v/v/v*) for the elution of epirubicin and IS was selected as the most effective.

Next, to determine optimal LC conditions for epirubicin in human plasma urine and various analytical columns and mobile phase compositions were tested. Among them, the Synergi Hydro column (150 mm x 4.6 mm, 4 μm) column and the mixture of 40 mM phosphate buffer (pH 4.1) and acetonitrile (69:31, *v/v*) at the flow-rate of 1 ml/min was chosen as optimal. The LC analysis at 30ºC was chosen as a good compromise between shorter retention times and effective peak separation whereas the highest epirubicin peak signal values were observed while the excitation wavelength and excitation wavelengths were respectively 497 and 557 nm. Thus, these parameters were selected as the most optimal for further epirubicin analyzes by LC-FL technique.

Next, the developed SPE-LC-FD method was validated for selectivity, linearity, sensitivity, accuracy and precision, and extraction recovery. The linearity was confirmed over the concentration range of 1-1500 ng/mL for epirubicin in plasma and 1-10000 ng/mL for urine samples, respectively. In both cases, the limit of detection (LOD) and the limit of quantification (LOQ) was 0.5 and 1 ng/mL, respectively. The intra- and inter-day precisions were less than 9.57% while the accuracies were in the range of 92.1-108.8% and 93.6-108.3% for doxorubicin in plasma and urine, respectively. The percentage of recovery of anthracycline was 98.9 for urine and 93.5% for plasma.

The validation data confirm that the developed LC-FD method fulfills the FDA and ICH validation requirements and could be applied in clinical studies. Finally, this LC-FL technique was successfully used to monitoring of drug in a cancer child treated with epirubicin, for whom the drug at 150 mg/m^2 was given by a 6-hour infusion.

Conclusion

The proposed LC-FL method in the isocratic mode is sensitive, robust and specific allowing reliable drug quantification in plasma and urine samples. This methodology is time-saving and economical; furthermore, it is suitable for analyzing large numbers of plasma and urine samples for drug monitoring, pharmacokinetic and biomedical investigations. The utility of the proposed LC-FL method was demonstrated through its application to monitoring of epirubicin in a pediatric cancer patient.

Conclusion

[1] Plenis, A., Frolow, A., Rekowska, N., Olędzka, I., Kowalski, P., Bień, E., Krawczyk, A.M, Adamkiewicz-Drożyńska, E., Bączek, T. Chromatographia 2016, 79, 861-873.

[2] Maliszewska, O., Plenis, A., Olędzka, I., Kowalski, P., Miękus, N., Bień, E., Krawczyk, M.A., Adamkiewicz-Drożyńska, E., Bączek, T., J. Pharm. Biomed. Anal. 2018, 158, 376-385.

P42 ARDUINO-BASED PRESSURE-DRIVEN FLOW CONTROLLER FOR DROPLET MICROFLUIDICS

Jan Prikryl, Jana Krivankova, Antonin Hlavacek

Institute of Analytical Chemistry of the Czech Academy of Sciences, Veveri 967/97 602 00 Brno, prikryl@iach.cz

Summary

Droplet-based microfluidic systems bear significant value in an extremely wide range of applications due to its remarkable advantages, nevertheless, their technical demands on precise flow control are high. Here, we present lab-built Arduino-based flow controller fulfilling needs of droplet microfluidics to easily and effectively automate the system. As an additional required accessory, CNC-milled component for vials pressurizing was presented.

Introduction

Droplet-based microfluidics has rapidly emerged as important technology opening up new experimental possibilities in high-throughput screening and diagnostics with rapid measurements on strictly defined and small samples. Production of droplets from immiscible liquids allows spectrum of operations performed on a chip, or thanks to exceptional droplets stability even off a chip, including reagent addition, droplets fusion or division, incubation, sorting etc.

Nevertheless, droplet microfluidics requires high-precision flow control to ensure precise conditions in droplet formation and reagent additions. Routine usage of syringe pumps embedded with stepper motors is not the best option because of flow fluctuations, therefore pressure-driven flow is preferred choice.

In a complex system, where several liquids have to be manipulated, flow control system appears complicated and in case of commercial solution also remarkably expensive. In such area, lab-built equipment has emerging increasingly important. Interesting way to automate lab processes are open source computer hardware provided by Arduino project. Such boards are equipped with digital inputs and outputs, analog inputs and pulse-width-modulated (PWM) analog outputs.

Here, we present lab-built PC-controlled 6-channel pressure regulator based on electropneumatic converters driven by Arduino board including CNC-milled caps allowing pressurizing of tubes or microtubes to induce liquid flow in droplet microfluidics.

Experimental

Computer numerical control (CNC) machining was used for fabrication of duralumin tube and microtube caps and all plastic parts necessary to assemble whole system using an inexpensive CNC router. The pressure controller equipped with 6 pressure output channels consists of Arduino UNO board (Arduino S.r.l., Italy), 6 units of 12-bit digital-to-analog converter (DAC) MCP4921-E/P (Microchip Technology Inc., USA), 6 units of electropneumatic converter ITV0010-2N with input voltage 0-5 V and output pressure 0-1 bar (SMC Corporation, Japan) and power supplies.

Specially designed duralumin caps were equipped with special plastic CapTite connector (LabSmith, Inc., USA) sealed by polydimethylsiloxane foil with thickness 0.5 mm allowing air-tight connection of capillary by miniature ferrule. Air pressure was connected to the cap by frequently used push-in fittings.

Results and Discussion

The first part of the system is multichannel pressure regulator based on SMC electropneumatic converter that could be controled by Arduino board directly. However, Arduino boards are equipped only with PWM analog output providing pulsed output, therefore we have chosen usage of external DAC. Every Arduino user can profit from supplier support and huge community of users around Arduino project. Therefore, communication between Arduino and external DAC was easily established thanks to support of SPI protocol of serial communication by both manufacturers and lot of examples presented on web. Analog output of DAC was used as an input signal of electropneumatic converter to adjust desired pressure. Communication of Arduino with PC was ensured through standard serial communication via USB and was arranged by custom-built JAVA program. Whole system depiction is in Fig. 1.
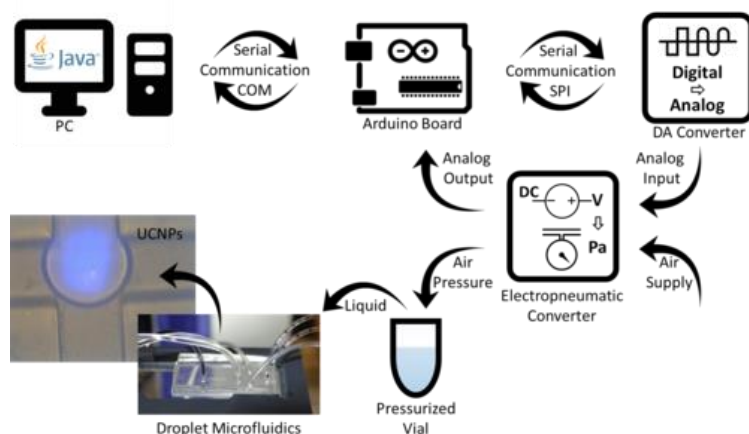

Fig. 1. Schema of control principle with key parts in consecutive order: PC with JAVA graphical user interface, Arduino board controlling digital-to-analog converter, electropneumatic converter, pressurized vial, microfluidic chip producing droplets containing photon-upconversion nanoparticles (UCNPs).

SMC pressure regulators were placed into a lab-made housing together with Arduino board, DACs and power supplies. All pressure outputs were brought onto the front panel to ensure clear arrangement (Fig. 2). Housing was designed to be extendable up to ten channels.
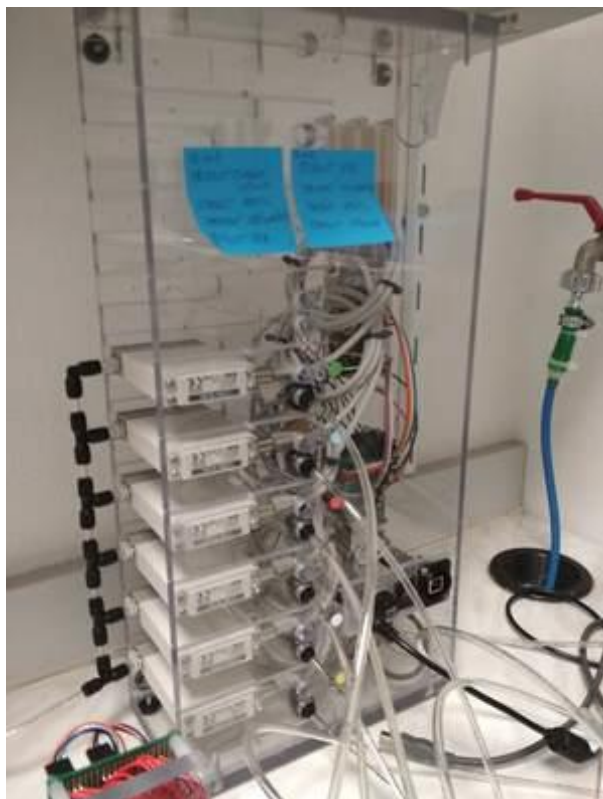
Fig. 2. Arduino-based pressure control system.

The second part of the system is pressurizing of a vial filled with desired liquid. The special duralumin cap was designed to use CapTite fitting for connection of capillary and push-in fitting to connect pressurized air. Microtubes (2 ml) were fixed into the cap by bottom part locked by screws and sealed by nitrile rubber o-ring. Tubes (15 ml) were directly screwed into the cap thread and sealed by o-ring. This ensemble ensures air-tight connection of capillary and air tubing. Caps could be placed in a rack stand (Fig. 3, left) or equipped by magnet to allow user-friendly positioning around microfluidic chip (Fig. 3, right).
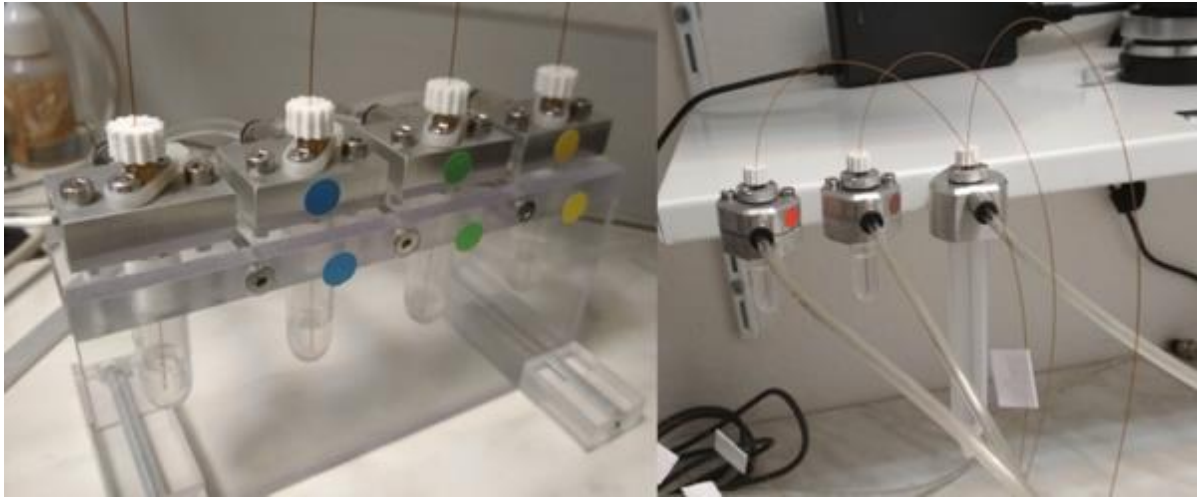
Fig. 3. Pressurized vials: microtubes (2 ml and 15 ml) in a rack stand (left) and magnetically mount on a shelf (right).

Conclusion

Open-hardware projects, such as Arduino together with CNC milling technology allow to easily and effectively automate lab processes and construct custom-built systems completely fulfilling special demands. We presented completely custom-built flow control system for droplet microfluidics allowing full computer control.

Acknowledgement

P43 CAPILLARY ELECTROPHORETIC METHOD WITH FLUORESCENCE DETECTION AS A PROMISING TOOL FOR SCREENING OF BETA-SECRETASE INHIBITORS

Roman Řemínek, Jan Schejbal, Zdeněk Glatz

Department of Biochemistry, Faculty of Science, Masaryk University, Kamenice 5, 62500 Brno, Czech Republic, roman.reminek@gmail.com

Summary

Alzheimer's disease (AD) represents the most common cause of dementia. According to amyloid cascade hypothesis, pathogenesis of the disease could be slowed down or even stopped by inhibition of beta-secretase (BACE). Capillary electrophoretic (CE) methods are regarded as a promising tool for enzyme assays. A CE method with fluorescence detection for screening of potential BACE inhibitors was therefore introduced.

Introduction

AD represents a severe neurodegenerative disorder characterized by progressive memory and cognitive functions impairment, with evolution to dementia and eventually death. Worldwide, it accounts for about 34 million cases and its prevalence rapidly increases [1]. Recent studies suggest beta-secretase (BACE), an aspartic-acid protease playing a key role in the development of neurotoxic amyloid plagues in the patient's brain tissue, as a promising druggable target to slow down or even stop the progression of AD [2]. Screenings of BACE inhibitors are commonly performed by using systems based on Förster resonance energy transfer (FRET); however, the information gathered from these assays may be negatively affected by non-specific interferences with measured signal leading to the risk of false positive/negative results and need of data confirmation by further tests [3]. For this reason the main aim of the presented study was to develop a method for activity studies of BACE based on capillary electrophoresis (CE) with fluorescence detection. Separation of reaction products increases the assay sensitivity by reducing the background noise and diminishes the risk of interaction with other sample components.

Experimental

An Agilent 7100 CE System equipped with a Picometrics Zetalif LEDIF detector was used to perform all analyses. The bare 75 μm id (375 μm od) fused-silica capillary was of 66 cm total length (45 cm effective length) and BGE was composed of 45 mM SDS prepared in 65 mM sodium tetraborate buffer (pH 9.2). Separations were accomplished by application of 30 kV

(positive polarity) in the capillary thermostated at 25 °C. The analyte was monitored at excitation/emission = 490 nm/520 nm. Data was acquired and peak areas were determined using the ChemStation software. The capillary was rinsed with 0.1 M NaOH for 1 min, deionized water for 1 min, and BGE for 2 min before every analysis. This procedure was sufficient to ensure good method repeatability despite sample containing the enzyme and substrate and products peptides was directly injected into the capillary.

All solutions of enzyme and standards of the QXL$^®$ 520/ HiLyte^{TM} Fluor 488 FRET substrate and HiLyte^{TM} 488 reaction product obtained from commercially available SensoLyte$^®$ 520 beta-secretase assay kit were prepared in the incubation buffer consisting of 50 mM sodium acetate (pH 4.25). The enzyme at the final concentration of 100 U/mL and substrate at a respective concentration were incubated in a thermomixer for 90 min at 37 °C and 650 rpm. After it, the reaction was terminated by 10fold dilution with 40 mM NaOH. The samples were stored on ice prior the analysis.

Results and Discussion

The method development, validation, and the final approving were accomplished using model BACE's reaction with QXL$^®$ 520/ HiLyte^{TM} Fluor 488 FRET substrate. The capillary id (50 and 75 µm), BGE composition (ammonium acetate, sodium tetraborate), its pH range of 4.5–9.2, concentration (30–100 mM), and SDS concentration (10–160 mM), respectively, separation voltage range of 24–30 kV, capillary temperature range of 15–35 °C, sample injection time (3–33 s), and various rinsing procedures (50% acetic acid, acetonitrile, 0.1 M NaOH, deionized water) were tested in order to achieve a repeatable separation of fluorescently labelled components of the reaction mixture. A typical electropherogram obtained with the optimized method is shown in Fig. 1.
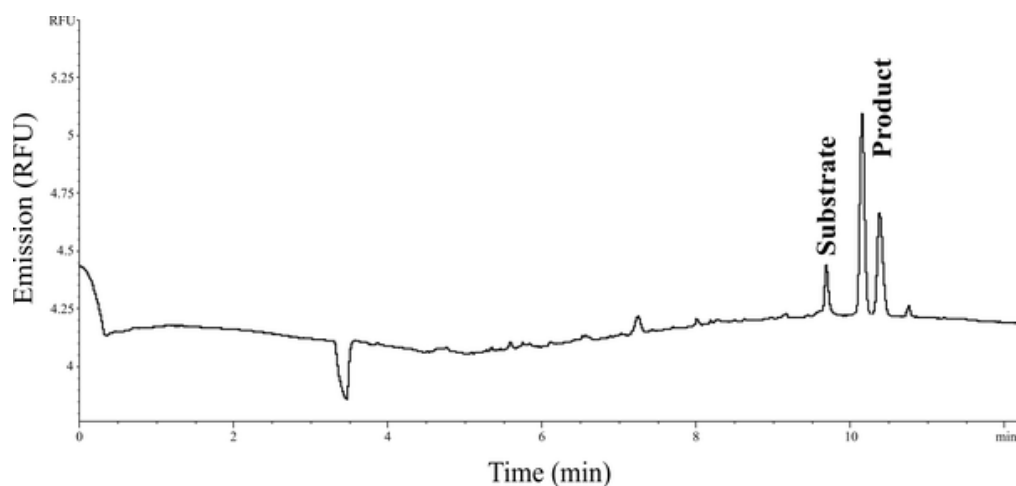

Fig. 1. The typical electropherogram obtained using the final method. Sample: 100 U/mL BACE incubated with 100 µM substrate (QXL™ 520/ HiLyte Fluor™ 488 FRET peptide) at 37 °C for 90 min and then diluted 10fold with 40 mM NaOH. The reaction product (HiLyte™ 488-EVNL peptide) was detected at excitation/emission = 490 nm/520 nm. Other incubation and separation conditions were as described in the Experimental part.

After the optimization was finished, the final method was partially validated. The resulting values of the selected parameters are summarized in Tab. 1.

RSD of migration time (n = 6)	0.52 %
RSD of peak area (n = 6)	5.13 %
Linearity range	1 – 400 nM
R^2 of calibration curve	0.9992
Accuracy (30 nM, n = 6)	+3.10 %
LOD (S/N = 3)	0.3 nM
LOQ (S/N = 10)	1 nM
Recovery (n = 6)	98.55 – 106.32 %

Tab. 1. Summary of the final method validation.

Basic kinetic and inhibition parameters of the BACE's reaction with FRET substrate and KTEEISEVN-[Statine]-VAEF used as a probe inhibitor were determined in order to confirm the practical applicability of developed method. Apparent value of Michaelis-Menten constant $K_m = 36.2 \pm 8.47$ μM was obtained from the dependence of reaction rate on substrate concentrations (1–200 μM). Value of half-maximal inhibitory concentration (IC_{50}) was established from the dependency of remaining BACE activity on inhibitor concentrations using one-site competition model (see Fig. 2). Apparent values of inhibitory constant (K_i) were calculated using equation of Cheng and Prusoff expressed as $K_i = IC_{50} / (1 + [S] / K_m)$ [4].
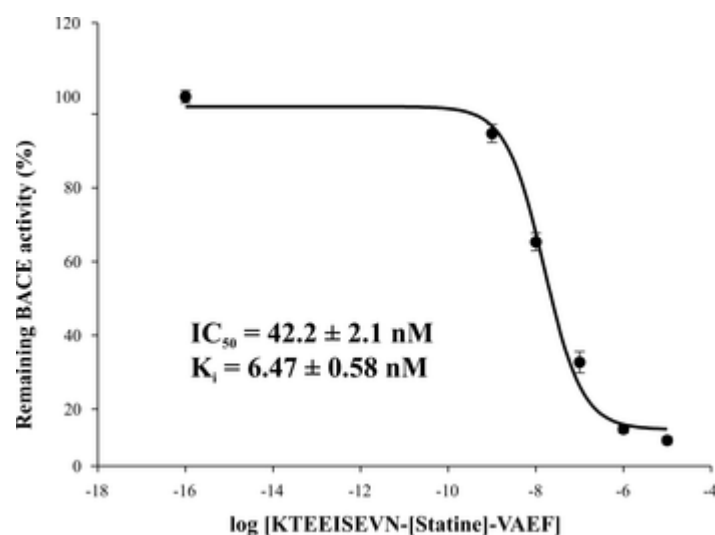

Fig. 2. The remaining BACE activity vs. concentration of KTEEISEVN-[Statine]-VAEF plotted with one-site competition model.

Conclusion

A CE method with fluorescence detection for studies of BACE activity was developed. The obtained values of basic kinetic and inhibition parameters were in a good agreement with literature data established using FRET-based assays in the microtiter plate format [3,5]. Contrary to these systems, separation of the reaction product from other sample components enables monitoring of the distinct analytical signal and thus significantly reduces risk of false positive/negative results given by non-specific interactions already described in previous studies [3,6]. Together with minuscule sample consumption, high degree of automatization, and possible application of multi-capillary systems, it makes CE favorable analytical technique for BACE inhibitor screenings.

Acknowledgement

Reference

[1] Association, A. s., Alzheimer's & Dementia 2018, 14, 367–429.

[2] Vassar, R., Kuhn, P.H., Haass, C., Kennedy, M.E., Rajendran, L., Wong, P.C., Lichtenthaler, S.F., J. Neurochem. 2014, 130, 4–28.

[3] Mancini, F., De Simone, A., Andrisano, V., Anal. Bioanal. Chem. 2011, 400, 1979–1996.

[4] Cheng, Y., Prusoff, W.H., Biochem. Pharmacol. 1973, 22, 3099–3108.

[5] Grüniger-Leitch, F., Schlatter, D., Küng, E., Nelböck, P., Döbeli, H., J. Biol. Chem. 2002, 277, 4687–4693.

[6] Schejbal, J., Slezáčková, L., Řemínek, R., Glatz, Z., J. Chromatogr. A 2017, 1487, 235–241.

P44   RAPID FABRICATION OF MICROEXTRACTION DEVICES FOR DIRECT DETERMINATION OF BASIC DRUGS IN DRIED BLOOD SPOTS

Lenka Ryšavá[1,2], Jan Přikryl[2], Miloš Dvořák[2], Zdeňka Malá[2], Pavel Kubáň[2]

[1]*Institute of Food Science and Biotechnology, Faculty of Chemistry, Brno University of Technology, Purkyňova 118, 61200 Brno, Czech Republic, rysava@iach.cz*

[2]*Institute of Analytical Chemistry of the Czech Academy of Sciences, Veveří 97, 602 00 Brno, Czech Republic*

Summary

A 3D-printed cutter was designed for rapid fabrication of supported liquid membrane (SLM) extraction devices compatible with injection system of commercial capillary electrophoresis (CE) instrument. Low cost and single use microextraction devices were fabricated from polypropylene micropipette tips with high precision (dimension variances $\leq$ 3% RSD). Practical applicability of the microextraction devices was examined by in-line coupling of SLM extractions to CE for direct analysis of four model basic drugs in dried blood spot extracts. Excellent repeatability of the hyphenated technique was achieved (RSD $\leq$ 7.6%), transfer of analytes across the SLM ranged from 23 to 73% and limits of detection were as low as 0.07 µg/mL.

Introduction

Direct coupling of extraction and analytical technique is not a trivial task and the extraction and the analytical steps are often performed off-line [1,2]. Despite the reported difficulties, different approaches were described for on-line coupling of membrane extractions to separation methods [3]. These hyphenated systems were, however, usually highly complex and additional instrumentation was required. Recently, a simple approach for direct coupling of supported liquid membrane (SLM) extraction to capillary electrophoresis (CE) was presented [4], which uses standard CE instrument and consumables.

In this contribution, SLM-CE hyphenation is further simplified by development of a 3D-printed device, which enables precise and rapid fabrication of SLM microextraction devices fully compatible with injection system of a commercial CE instrument. Practical applicability is demonstrated on direct SLM-CE analyses of model basic drugs in dried blood spot samples.

Experimental

Chemicals, reagents and dried blood spot (DBS) samples

All chemicals were of reagent grade and were purchased from Sigma (Steinheim, Germany), Lach-Ner (Neratovice, Czech Republic), and Fluka (Buchs, Switzerland). Deionized (DI) water was prepared by water purification system G7749 (Miele, Gütersloh, Germany). Stock solution of physiological saline (150 mM NaCl) was prepared in DI water. Stock solutions of four basic drugs: nortriptyline, papaverine, haloperidol and loperamide (1 mg/mL) were diluted with pure methanol and standard solutions of the drugs were prepared from these stock solutions. Working solutions of HCl were prepared from concentrated (37%) HCl. Optimum background electrolyte solution for CE of basic drugs consisted of 15 mM NaH_2PO_4 and 15 mM o-H_3PO_4, pH 2.23. 1-Ethyl-2-nitrobenzene (ENB) was used for impregnation of SLMs. Human DBS samples (10 µL of capillary blood) were obtained from volunteers at the Institute of Analytical Chemistry and were collected on Whatman 903[TM] (GE Healthcare Ltd, Cardiff, UK) collection cards. DBS drying time was 2 hours.

CE

A 7100 CE instrument (Agilent Technologies, Waldbronn, Germany) was operated at a potential of +25 kV applied at the injection side of the separation capillary and analytes were detected at 200 nm. CE analyses were performed in 75/375 µm (ID/OD) fused silica capillary with L_{tot} 45 cm and L_{eff} 36.8 cm (Polymicro Technologies, Phoenix, AZ, USA). Other instrumental details, capillary conditioning and flushing procedures and injection parameters can be found elsewhere [4].

SLM microextraction devices

Microextraction devices fully compatible with sample vials (P/N 5182-0567) of Agilent 7100 CE were prepared using a 3D-printed cutter. The cutter consisted of a bottom part with a groove for 200 µL polypropylene (PP) micropipette tip (FL Medical, Torreglia, Italy, P/N 28063) and a top part with three razor blades (0.2 mm, P/N 35020, Martor, Solingen, Germany). By pressing the bottom and the top part against each other, the tip was cut into 4 pieces, resulting into acceptor and donor unit with lengths of 7 and 11 mm, respectively. Each microextraction device consisted of the acceptor and the donor unit, which were separated by a flat sheet PP membrane (Celgard® 2500; Celgard LLC, Charlotte, NC, USA). The 3D-printed cutter, micropipette tip and parts of the microextraction device are shown in Figure 1. The size of circular PP membrane was 9 mm and was cut with a cork borer. The membrane was impregnated with 1 µL of ENB to form the SLM just before extraction. 20 µL of donor solution and 10 µL of acceptor solution were pipetted into donor and acceptor unit, respectively, and the device was placed in a stainless-steel compression spring; for additional details see [5].

Transfer of analyte across SLM (in %) was calculated as a concentration of the analyte injected from phase interface between SLM and acceptor solution divided by original concentration of the analyte in donor solution [5].
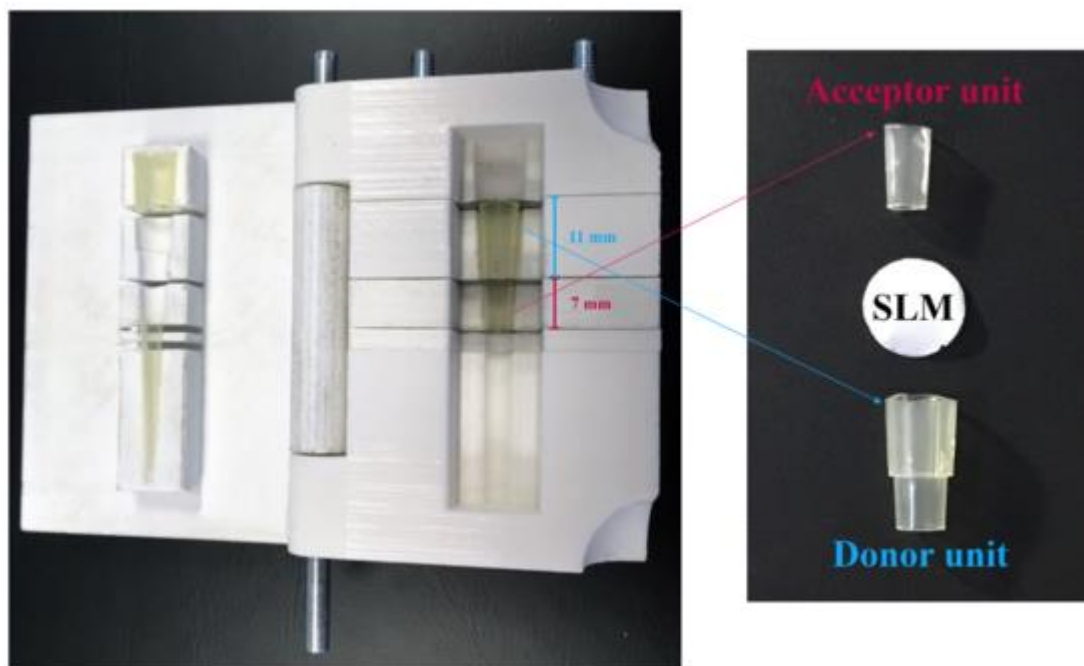
Figure 1. 3D-printed cutter, micropipette tip, microextraction units and SLM.

Results and Discussion

Each extraction device was prepared by cutting a new micropipette tip using the 3D-printed cutter. Dimensions of the two units were measured by a digital calliper and repeatability (RSD, *n = 20*) of the units' size was better than 3%. The performance of the microextraction devices in-line coupled to CE was examined by SLM extractions of four model basic drugs from DBS samples. The selected SLM extraction conditions were 10 mM NaOH as donor phase and 10 mM HCl as acceptor phase. Transfer of analytes was investigated for extraction time 19 min, which ensured extraction equilibrium [5]. The DBS were dissolved in 8-fold (v/v) excess of 10 mM NaOH and extracted as blank samples (no spiking with the drugs). No analytical signals were detected demonstrating that the four drugs were not present in DBS samples or were at concentrations below the method limit of detection (LOD). Subsequently, the alkaline DBS extracts were spiked with 1 μg/mL of the four basic drugs and the drugs were extracted from 7 unique microextraction devices. Repeatability of the hyphenated SLM-CE-UV method was 3.1 – 7.6% (RSD, *n = 7*), transfer of the drugs from donor solution to the phase interface ranged from 23 to 73% and LODs were between 0.07 and 0.5 μg/mL.

Conclusion

3D-printing was applied to develop a cutter for rapid and repeatable fabrication of microextraction devices suitable for direct coupling of SLM extractions to CE analyses. The microextraction devices are made of standard PP micropipette tips, are cheap and disposable and thus eliminate carry-over effects in analyses of complex biological samples. Constant dimensions of the devices ensure repeatable analytical performance of the hyphenated SLM-CE-UV system in analyses of model basic drugs in complex, such as, DBS

samples. Application of these devices might be of particular interest in analysis of complex samples for the following reasons: (i) device disposability, (ii) high analytical repeatability, (iii) automation of the entire extraction and analytical process in commercial CE and (iv) minimum manipulation with biological samples enabling rapid "sample in – answer out" procedures.

Acknowledgement

Reference

[1] Snow, N. H., J. Chromatogr. A 2000, 885, 445–455.

[2] Pedersen-Bjergaard, S., Rasmussen, K.E., Halvorsen, T. G., J. Chromatogr. A 2000, 902, 91–105.

[3] Jönsson, J. A., Mathiasson, L., TrAC 1999, 18, 318-325.

[4] Pantůčková, P., Kubáň, P., Boček, P., J. Chromatogr. A 2015, 1389, 1–7.

[5] Pantůčková, P., Kubáň, P., J. Chromatogr. A 2017, 1519, 137–144.

P45 N-GLYCOSYLATION MODIFICATION ANALYSIS OF SEVERAL IMPORTANT SERUM GLYCOPROTEINS IN ALZHEIMER'S DISEASE

Zsuzsanna Kovács[1], Balázs Reider[1], Dániel Sárközy[1], András Guttman[1,2]

[1]*Horvath Csaba Laboratory of Bioseparation Sciences, Research Center for Molecular Medicine, Faculty of Medicine, University of Debrecen, Debrecen, Hungary*

[2]*MTA-PE Translational Glycomics Research Group, Research Institute for Biomolecular and Chemical Engineering, University of Pannonia, Veszprem, Hungary*

Summary

Alzheimer's disease, one of the most common neurodegenerative diseases, affects at least 30 million people worldwide. Currently very LITTLE information is available about its pathomechanism, especially the role of glycosylation modification of key proteins. It was recently published that the amyloid precursor protein (APP), the tau protein and their metabolites are probably responsible for the pathological changes, and their glycosylation changes during Alzheimer's disease (both O- and N-glycosylation). In our preliminary experiment, the total serum N-glycan profiles of Alzheimer's disease patients were investigated. We applied our earlier developed sample preparation method including the triple internal standard based glyco-database search approach. Compared to the healthy control, we found quantitative differences in both the sialylated and the neutral N-glycan structures, and detected a new peak in case of the Alzheimer's disease samples.

Introduction

Alzheimer's disease (AD) is a serious neurodegenerative disease affecting a large number of people worldwide. Currently there are only symptomatic managements are available, but the medical field makes efforts to cure the disease. Unfortunately, we still have only little knowledge about its pathomechanism, especially the role of pathological post-translational glycosylation modification of proteins [1]. ER stress has been implicated in the development of amyotrophic lateral sclerosis, Parkinson's, Alzheimer's and prion disease [2]. The brains of the patients showed sporadic Parkinson's and AD accumulate an S-nirtosylated version of protein disulphide isomerase, which inhibited its activity, leading to energy deficiency and finally to increased cell death. There are two further proteins behind the pathological changes in Alzheimer's, one of the amyloid precursor protein (APP) [3] , and the other the tau protein [4] and their metabolites, whose glycosylation alters during AD (O- and N-glycosylation). Tau is abundantly phosphorylated in the early stages of brain development, but throughout adult life it is extensively O-GlcNAcylated, while phosphorylation decreases. One of the normal functions of O-GlcNac is to cover phosphorylation sites to shut them off. Most of the tau protein involved in the pathology of AD is altered by O-GlcNAcs [5, 6]. There is little information

about the N-glycosylation of proteins involved in AD. Our research group developed an N-glycan releasing method for AD patient samples and analyzed total serum sample N-glycome of healthy control and AD patients with capillary electrophoresis.

Experimental

Serum samples: Serum samples were collected at the Psychiatric Clinic (University of Debrecen, Hungary) with the Ethical permission (6058-13/2018/EÜIG) from AD and healthy controls using clot activator containing serum tubes (BD, Franklin Lakes, NJ). The collected blood samples were centrifuged at 7500 x g for 30 min and the serum fractions were stored at –70°C until further processing.

N-Glycan release and fluorophore labeling: One microliter of serum from each patient samples were diluted by 10 µL of HPLC grade water then 1 µL of denaturing buffer was added followed by incubation at 65°C for 10 min. The reaction mixture was filtered through 10 kDa spin-filters at 11 270 x g for 10 min. The samples were then digested in situ on the filters by the addition of 29 µL of NaHCO3 buffer (20 mM, pH 7.0) and 1 µL of PNGase F, followed by incubation at 37°C overnight. The released N-glycans were centrifuged though 10 kDa spinfilters at 7500 x g for 10 min and dried in SpeedVac prior to the fluorophore labeling step. 6 µL of 20 mM 8-aminopyrene-1,3,6-trisulfonic acid in 15% acetic acid and 2 µL of NaCNBH3 (1 M in THF) were added to the dry pellet and incubated at 37°C overnight. The labeled samples were purified with CleanSeq magnetic beads.

Capillary electrophoresis: A P/ACE MDQ System was used to perform all capillary electrophoresis analyses. The separations were monitored by LIF detection using a 488 nm Ar-ion laser with a 520 nm emission filter. Fifty centimeters effective length (60 cm total) 50 µm id NCHO capillaries were employed with the NCHO separation gel buffer system for the analysis. The 32 Karat software was used for data acquisition and processing.

Results and Discussion

During a pilot test we analyzed the total serum N-Glycomes of AD patients and healthy controls. Structural elucidation of these carbohydrates was based on their calculated GU values following the triple internal standard approach of Jarvas et al. in conjunction with searching the NIBRT database (https://glycobase.nibrt.ie) and previously published literature data. As one can observe, the neutral to sialo structure ratio significantly decreased in AD patients compared to the control. Furthermore, a new peak appeared, which was not detected in the healthy control.

Conclusion

- In our preliminary experiment, the total serum N-glycan profiles of an Alzheimer's disease patient was compared to a healthy control.

- Compared to the healthy control, we found quantitative differences in both the sialylated and the neutral N-glycan structures.

- Furthermore, a new peak (F(6)A2[6]BG(4)1S(6)1) was detected in the serum of the AD patient

- Our joint FR-HU research team plans to investigate more samples to underpin these preliminary findings.

Acknowledgement

Reference

[1] Dos Santos Picanco, L. C., Ozela, P. F., de Fatima de Brito Brito, M., Pinheiro, A. A., Padilha, E. C., Braga, F. S., de Paula da Silva, C. H. T., Dos Santos, C. B. R., Rosa, J. M. C., da Silva Hage-Melim, L. I., Current medicinal chemistry 2018, 25, 3141-3159.
[2] in: rd, Varki, A., Cummings, R. D., Esko, J. D., Stanley, P., Hart, G. W., Aebi, M., Darvill, A. G., Kinoshita, T., Packer, N. H., Prestegard, J. H., Schnaar, R. L., Seeberger, P. H. (Eds.), Essentials of Glycobiology, Cold Spring Harbor (NY) 2015.
[3] Pena-Bautista, C., Baquero, M., Vento, M., Chafer-Pericas, C., Current neuropharmacology 2018.
[4] Ismail, T., Kanapathipillai, M., Journal of peptide science : an official publication of the European Peptide Society 2018, e3125.
[5] Zhu, Y., Shan, X., Yuzwa, S. A., Vocadlo, D. J., The Journal of biological chemistry 2014, 289, 34472-34481.
[6] Yuzwa, S. A., Vocadlo, D. J., Chemical Society reviews 2014, 43, 6839-6858.

P46 ENANTIOSEPARATION AND ESTIMATION OF RACEMIZATION BARRIERS OF SELECTED HELQUATS AND THEIR DERIVATIVES BY CAPILLARY ELECTROPHORESIS USING SULFATED CYCLODEXTRINS AS CHIRAL SELECTORS

Petra Sázelová, Dušan Koval, Lukáš Severa, Paul E. Reyes-Gutiérrez, Michael Jirásek, Filip Teplý, Václav Kašička

Institute of Organic Chemistry and Biochemistry of the CAS, Flemingovo nám. 2, 166 10 Prague 6, Czech Republic, sazelova@uochb.cas.cz

Summary

Anionic highly sulfated β- and γ-cyclodextrins (S-CDs) and single-isomer heptakis-(2,3-diacetyl-6-sulfato)-β-CD (14Ac-7S-β-CD) were used for chiral separation of [5], [6] and [7]-ring helquats and helquat styryl dyes by capillary electrophoresis (CE) in the background electrolyte composed of 22 mM NaOH/35 mM H_3PO_4, pH 2.4. The CE method was applied for monitoring of racemization of eight helquats and helical dyes. Rate constant k of conversion, half-life $T_{1/2}$ of racemization, and activation Gibbs free energy $\Delta G^{\ddagger}$ of interconversion of one enantiomer into the other were calculated from the dependence of natural logarithm of enantiomeric excess (*ee*) on time using linear regression analysis.

Introduction

Helquats (helical N-heteroaromatic dications) represent structural link between helicenes and viologens [1]. They have been synthesized in a racemic form and then *P* and *M* enantiomers were prepared by various subsequent crystallizations [2]. The aim of this work was to use recently developed CE method for chiral analysis of helquats [3] for monitoring of racemization of selected helquats and helquat styryl dyes [4] and for determination of their racemization barriers, *i.e.* activation Gibbs free energy $\Delta G^{\ddagger}$.

Experimental

Racemization experiments of eight compounds dissolved in dimethyl sulfoxide (DMSO) were performed at temperature range 61–120°C. Samples for CE analyses taken every 20–30 min were analyzed in Beckman-Coulter MDQ (fused silica capillary 50/370 µm, id/od and 29.5/39.5 cm, effective/total length, with inner hydroxypropylcellulose coating, 22°C) using BGE 22/35 mM NaOH/ H_3PO_4, pH 2.4, containing highly sulfated 1.5% (m/v) γ-S-CD or 6 mM S-β-CD, or single-isomer 6 mM 14Ac-7S-β-CD. Applied voltage was constant, -11.4 kV, and current was at range 26–37 µA. Analytes were detected by UV absorbance at 200 nm. Data

were treated using Clarity data station. Enantiocomposition was determined from the ratio of the corrected (migration times normalized) peak areas of the separated enantiomers.

Results and Discussion

CE records of monitoring racemization process are shown in Figure 1A. The enantiomeric excess (*ee*) of (*M*)-enantiomer decays by the first order kinetics with rate constant $2k$:

$$ee_M = ee^0_M \cdot e^{-2kt} \,,$$

where ee^0_M is the initial enantiomeric excess of (*M*)-enantiomer. The natural logarithm of ee_M was plotted against time. Using linear regression analysis (see Figure 1B and 2), rate constant $2k$ was calculated. From this value, half-life $T_{1/2}$ of racemization and activation Gibbs free energy $\Delta G^{\ddagger}$ were calculated according to eqs: $T_{1/2} = (\ln 2) / 2k$, and

$$\Delta G^{\neq} = -RT \ln \frac{kh}{k_B T}$$

where R = 8.314472 J·K^{-1}·mol^{-1} is the gas constant, T is the termodynamic temperature (in K), k is the rate constant obtained from the measurement, h = 6.62606896 × 10^{-34} J·s is the Planck's constant, and k_B = 1.3806504 × 10^{-23} J·K^{-1} is the Boltzmann constant). Results for compounds **1–8**, whose structures are shown in Figure 1B and 2 are summarized in Table 1.
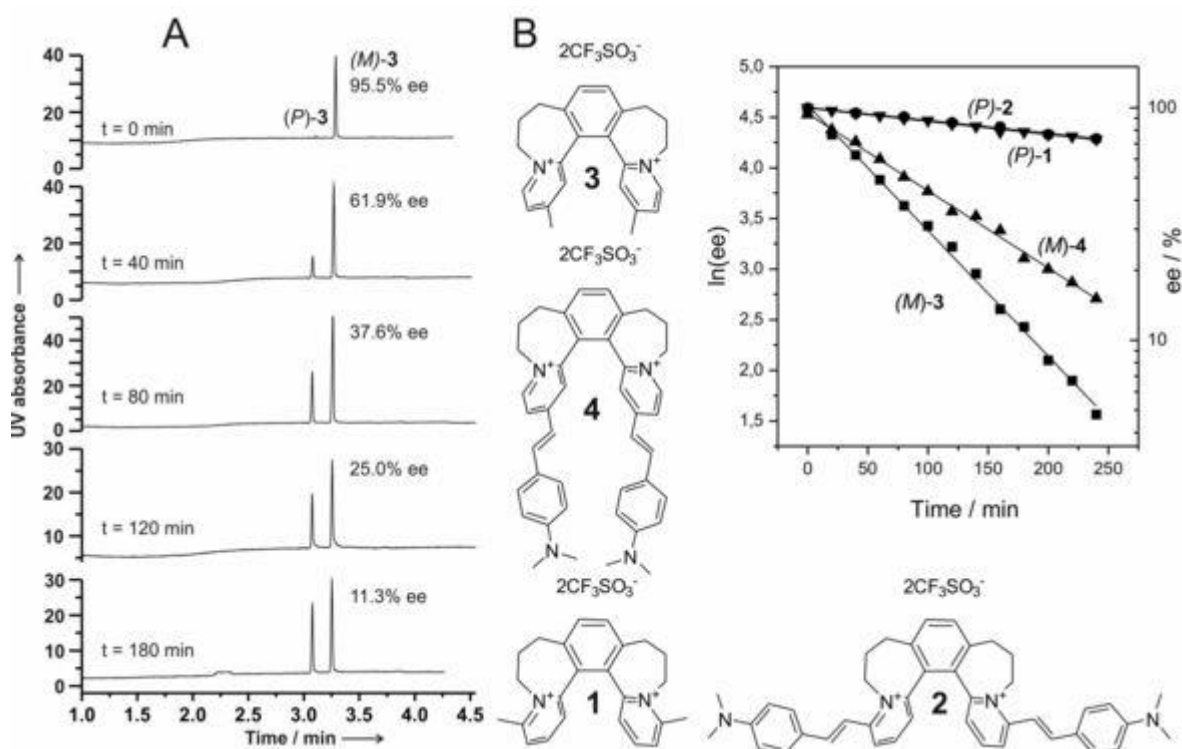

Figure 1. (A) CE records from the individual composition analyses during racemization of (*M*)-**3** in DMSO at 61°C; (B) Dependence of natural logarithm of enantiomeric excess ln(*ee*) on time as determined by CE for compounds **1–4**.
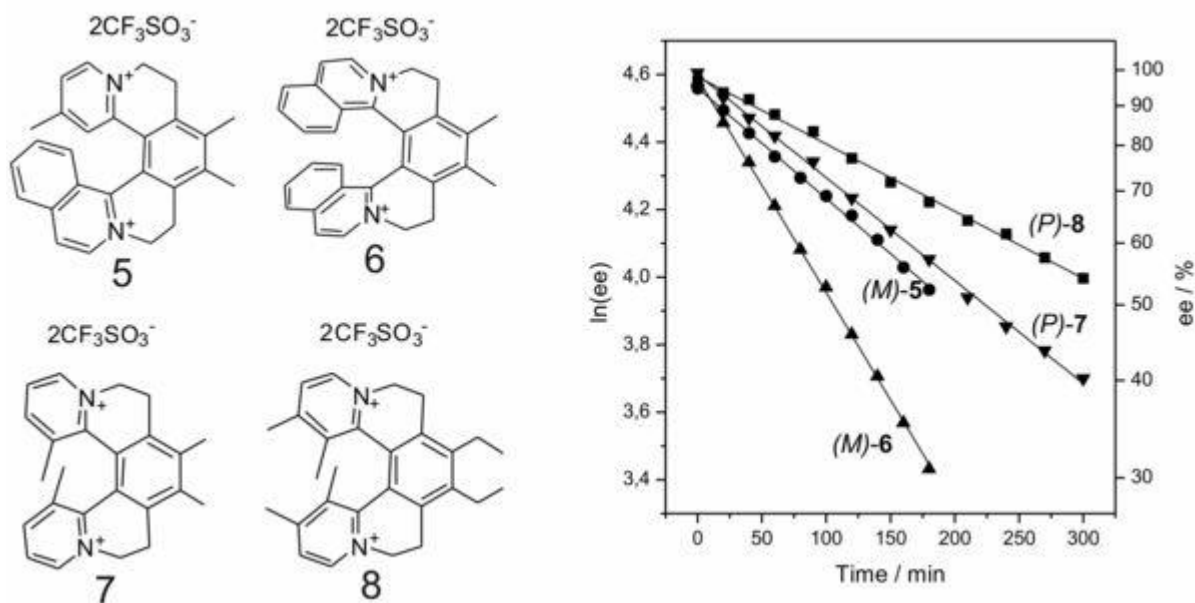
Figure 2. Dependence of natural logarithm of enantiomeric excess ln(*ee*) on time as determined by CE for compounds **5**–**8**.

Table 1. Calculated rate constants, *k*, and half-lives, $T_{1/2}$, of racemization, and activation Gibbs free energy $\Delta G^\ddagger$ of interconversion of compounds **1**–**8**.

Comp.	Chiral selector	Racem. temp. [°C]	Rate constant $k *10^5$ [s^{-1}]	Half-life $T_{1/2}$	Gibbs free energy $\Delta G^\ddagger$ [kJ mol^{-1}]
(*P*)-**1**	1.5 % S-γ-CD	66	1.06	9 h	115.7
(*P*)-**2**	1.5 % S-γ-CD	66	1.08	8h 50 min	115.5
(*M*)-**3**	1.5 % S-γ-CD	61	10.33	56 min	107.7
(*M*)-**4**	1.5 % S-γ-CD	62	6.35	1h 30 min	109.3
(*M*)-**5**	6 mM S-β-CD	120	2.72	3h 32 min	131.6
(*M*)-**6**	6 mM 14Ac-7S-β-CD	120	5.29	1h 49 min	129.4
(*P*)-**7**	6 mM 14Ac-7S-β-CD	108	2.54	3h 47 min	127.7
(*P*)-**8**	6 mM S-β-CD	108	1.66	5h 48 min	129.0

Conclusion

CE is a powerful method for monitoring of interconversion of one enantiomer into the other. Rate constants *k* of conversion, half-lives $T_{1/2}$ of racemization, and activation Gibbs free energy $\Delta G^\ddagger$ were calculated from dependence of natural logarithm of enantiomeric excess (*ee*) on time using linear regression analysis.

Dimethyl helquat **1** and its styryl dye, compound **2**, show nearly the same parameters of racemization.

Dimethyl helquat **3**, and its styryl dye, compound **4**, show lower Gibbs free energy $\Delta G^{\ddagger}$ in comparison with their positional isomers, compounds **1** and **2**.

Surprisingly, [7]-ring helquat, (*M*)-**6**, has got a lower racemization barrier than [6]-ring helquat, (*M*)-**5**.

Tetramethyl helquat, (*P*)-**7**, has got a lower racemization barrier than tetramethyldiethyl helquat, (*P*)-**8**.

Acknowledgement

Reference

[1] Adriaenssens, L., Severa, L., Šálová, T. et al., Chem.-Eur. J. 2009, 15, 1072-1076.
[2] Vávra, J., Severa, L., Švec, P. et al., Eur. J. Org. Chem. 2012, 489-499.
[3] Koval, D., Severa, L., Adriaenssens, L. et al., Electrophoresis 2011, 32, 2683-2692.
[4] Reyes-Gutiérrez, P.E., Jirásek, M., Severa, L. et al., Chem. Commun. 2015, 51, 1583-1586.

P47   MAXIMIZING EFFICIENCY OF FIELD-AMPLIFIED ELECTROKINETIC INJECTION OF WEAK BASES FOR ENANTIOSELECTIVE CAPILLARY ELECTROPHORESIS WITH SULFATED CYCLODEXTRINS

Jozef Šesták[1], Wolfgang Thormann[2]

[1]*Institute of Analytical Chemistry of the Czech Academy of Sciences, Brno, Czechia*

[2]*University of Bern, Clinical Pharmacology Laboratory, Institute for Infectious Diseases, Bern, Switzerland*

Summary

The optimal conditions for field-amplified electrokinetic injection of cations followed by their separation based on the stereoselective interaction with sulfated cyclodextrins are discussed. Results show that addition of a short water plug together with a short plug free of cyclodextrins and with a buffer concentration similar to the BGE greatly increase the injection efficiency.

Introduction

Field-amplified sample injection (FASI) [1] encompasses electrokinetic injection and stacking of analytes from a low conductivity sample into the BGE at the head of the capillary. High efficient and repeatable FASI requires introduction of a short water plug into the column prior to analyte injection [2]. Enantioselective capillary electrophoresis is based on differential enantiomer complexation with a chiral selector and/or differences in the mobilities of the formed complexes. Addition of a water plug was found to provide unsatisfactory results when the BGE contains negatively charged selectors [3, 4]. A selector free buffer plug has to be used instead [4, 5]. Data presented in this contribution document the effect of complexation within the buffer plug during electrokinetic injection and help to understand the underlying processes such that the water plug can be used for high efficient FASI when negatively charged selectors are used [6].

Experimental

Experiments were performed with the PrinCE 560 CE system (Prince Technologies, Emmen, The Netherlands). UV 2000 (Spectra-Physics, Santa Clara, CA, USA) set to 210 nm was used for detection. Computer simulations were executed with the SIMUL5complex (downloaded from http://echmet.natur.cuni.cz/download). Racemic methadone was selected as a model compound, multiple isomer sulfated β-cyclodextrin (S-β-CD, from Sigma-Aldrich) as chiral selector and phosphate buffers (pH 6.3) for the BGE and the buffer plug. EOF was not

considered in simulations and suppressed in experiments by using polyacrylamide-coated 50 μm I.D. fused-silica capillary of 90 cm total (35 cm effective) length. Instrument temperature was set to 25 °C. Injection was performed at 5 μA, and separations were executed at 20 μA together with a net buffer flow (0.1 mm/s) towards the detector. 10-mm water and buffer plugs were injected at 1 mm/s. Additional experiments with methadone, EDDP, and romifidine were executed on a P/ACE MDQ (Beckman Coulter) that was equipped with an uncoated 50 μm I.D. fused-silica capillary of 45 cm total (35 cm effective) length and detection at 200 nm. Phosphate buffer (pH 3) with HS-γ-CD (Beckman-Coulter) as chiral selector was employed as BGE.

Results and Discussion

Fig. 1A shows that only the S enantiomer of methadone is detected when the BGE comprises 50 mM phosphate buffer and 0.3% (w/v) of S-β-CD and a 10-mm long plug of 10 mM phosphate is used. The efficiency of R enantiomer injection is greatly increased, when phosphate concentration in the plug is increased to 50 mM (Fig. 1B), when phosphate concentration in the BGE is increased to 100 mM (Fig. 1C), when the concentration of S-β-CD in the BGE is 0.1% (w/v) (Fig. 1D), when the injection time is 15 s (Fig. 1E), or when the buffer plug length is 50 mm (Fig. 1F).
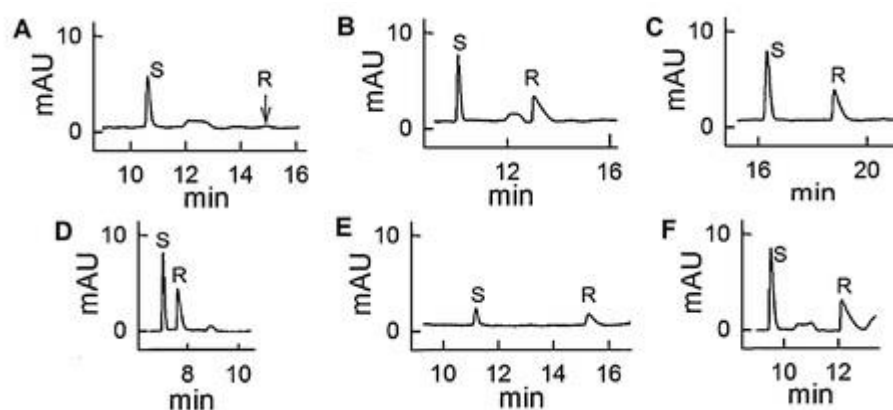
Fig. 1. Separation of methadone enantiomers at 20 μA after FASI at 5 μA; If not stated otherwise, the buffer plug length was 10 mm, the BGE comprised 50 mM phosphate (pH 6.3) and 0.3% (w/v) of S-β-CD and the injection time was 60 s. (A) Buffer plug comprised 10 mM phosphate (pH 6.3). (B) Buffer plug comprised 50 mM phosphate (pH 6.3). (C) BGE comprised 100 mM phosphate (pH 6.3). (D) BGE comprised 0.1% (w/v) of S-β-CD. (E) Injection time was 15 s. (F) Buffer plug length was 50 mm. Data are from [6].

Fig. 2 displays simulations when the BGE comprises 50 mM phosphate (pH 6.3) and 0.34% w/v S-β-CD. Fig. 2A shows that methadone and S-β-CD may interact within the 10 mM phosphate buffer plug already after 30 seconds of injection while with 50 mM phosphate buffer plug (Fig. 2B) the methadone and S-β-CD remains separated for longer injection time. R-methadone is thus not detected in Fig. 1A but appears in Fig. 1B and 1E. Data of Fig. 2 further show that the ionic strength within the buffer plug is lower than that of BGE. The complexation

constants for this conditions are believed to be higher [7] than those valid for the BGE and used for simulation. Thus predicted injection and separation of both enantiomers displayed in Fig. 2A doesn´t agree with experimental data of Fig. 1A.
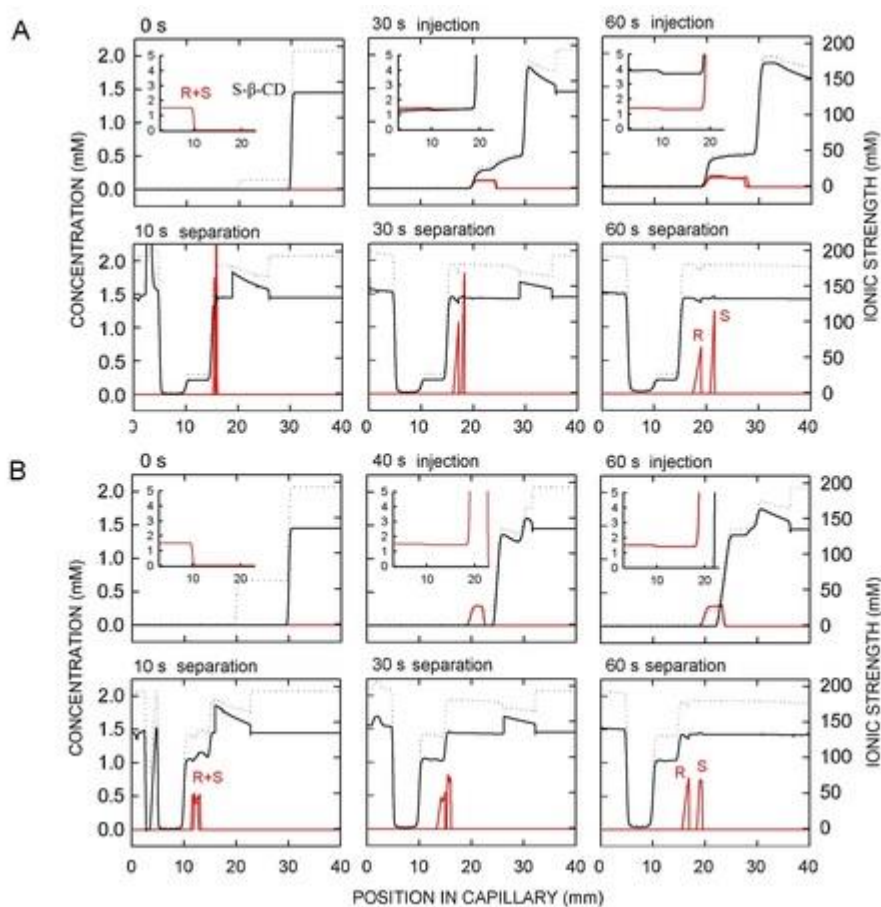

Fig. 2. Simulation of methadone enantiomers field-amplified electrokinetic injection (upper panels) and separation after 60 s injection (lower panels). Configuration contains (A) a 10 mM phosphate buffer plug, or (B) a 50 mM phosphate buffer plug. Panels include the concentrations of methadone enantiomers (red lines, left axis), the concentration of S-β-CD (black line, left axis) and the ionic strength (dotted line, right axis). y-axis scale of inserts is in μM. Data calculated for 25 °C, 50 μm I.D. capillary, 5 μA and 20 μA for injection and separation, respectively. The cathode is to the right. Data are from [6].

Results of Fig. 1 and 2 indicate, that concentration of buffer within the buffer plug which is close to that of BGE prevents analyte-ligand interaction during injection such that injection time can be extended. In this case however, addition of water plug between high conductivity buffer plug and low conductivity sample is required.

Fig. 3 displays separation of D-(+)-norephedrine, romifidine, S-methadone, R-methadone, R-EDDP, and S-EDDP employing a BGE composed of 100 mM phosphate (pH 3.0) and 0.12% (w/v) of HS-γ-CD. The optimal injection time at 8 kV with a 20-mm long plug of 50 mM phosphate was 15 s (Fig. 3A). With addition of a 10-mm water plug, and the phosphate

concentration in the buffer plug increased to 100 mM, the injection time can be extended to 30 s (Fig. 3B), which makes injection much more efficient.
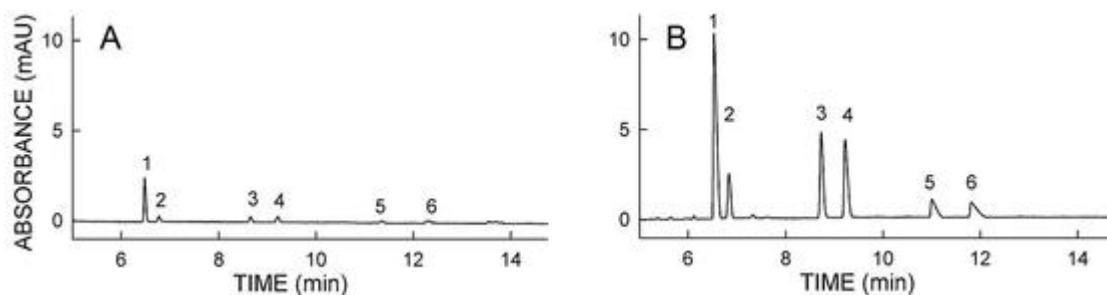
Fig. 3. Separation of methadone and EDDP enantiomers in presence of romifidine and D-(+)-norephedrine. Injection and separation voltage was 8 and 20 kV, respectively. Buffer plug length was 20 mm, BGE comprised 100 mM phosphate (pH 3) and 0.12% (w/v) of HS-γ-CD. (A) Buffer plug comprised 50 mM phosphate buffer (pH 3), injection time was 15 s. (B) 10-mm water plug was introduced prior injection, buffer plug comprised 100 mM phosphate buffer (pH 3), injection time was 30 s. Key: 1: D-(+)-norephedrine, 2: romifidine, 3: S-methadone, 4: R-methadone, 5: R-EDDP, 6: S-EDDP. Data are from [6].

Conclusion

The optimal conditions for field-amplified electrokinetic injection of cations followed by their separation based on the stereoselective interaction with sulfated cyclodextrins were elucidated. Computer simulations visualized that the buffer plug free of sulfated cyclodextrins creates a spacer between cationic analytes and negatively charged chiral selector during injection and that the injection time can be extended via use of a high conductivity buffer plug. Furthermore, the use of a short water plug together with a high buffer concentration in buffer plug greatly increase the FASI efficiency.

Acknowledgement

Reference

[1] Chien, R.L., Burgi, D.S., J. Chromatogr. A 1991, 559, 141-152.
[2] Šesták, J., Thormann, W., J. Chromatogr. A 2017, 1502, 51-61.
[3] Huang, L., et al., Electrophoresis 2008, 29, 3588-3594.
[4] Theurillat, R., et al., Electrophoresis 2016, 37, 1129-1138.
[5] Schappler, J., et al.,Electrophoresis 2008, 29, 2193-2202.
[6] Šesták, J., et al., J. Chromatogr. A 2018, 1558, 85-95.
[7] Mikkonen, S., et al., Electrophoresis 2018, 39, 770-778.

P48   DETERMINATION OF BINDING CONSTANTS OF HUMAN INSULIN COMPLEXES WITH SEROTONIN, DOPAMINE, ARGININE, AND PHENOL BY PRESSURE ASSISTED PARTIAL FILLING AFFINITY CAPILLARY ELECTROPHORESIS

<u>Veronika Šolínová</u>, Lenka Žáková, Jiří Jiráček, Václav Kašička

Institute of Organic Chemistry and Biochemistry of the Czech Academy of Sciences, Flemingovo n. 542/2, 166 10 Prague 6, Czechia

Summary

A new method, pressure assisted partial filling affinity capillary electrophoresis (PF-ACE), has been developed to study noncovalent interactions of the hexamer of human insulin (HI) with cationic ligands, such as phenolic neurotransmitters serotonin and dopamine, and amino acid arginine, or with anionic ligand phenol, in alkaline aqueous solutions. The apparent binding constants, K_b, of the HI-ligand complexes were determined from the dependence of the effective migration time changes of the above ligands on the variable zone lengths of HI dissolved in the background electrolyte (BGE) and hydrodynamically introduced into the bare fused silica capillary close to the UV detector. The HI interactions with the above ligands were found to be moderately strong, with K_b values in the range 385-1314 L/mol.

Introduction

Human insulin (HI) is one of the key protein hormones controlling metabolism, growth, and ageing [1]. Its malfunction causes diabetes, some types of cancer, and Alzheimer`s disease. HI is a 51-amino acid protein consisting of two disulfide-linked chains. Affinity capillary electrophoresis (ACE) refers to the methods, where analyte reversibly interacts with one or more components of the BGE while it is driven through the capillary by the force of electric field [2]. It offers several benefits, such as high separation efficiency, mass sensitivity, and presence of interacting compounds in a free solution with easy control of their concentrations.

The aim of this work was to apply PF-ACE method for investigation of noncovalent molecular interactions of HI with basic phenolic neurotransmitters serotonin and dopamine, basic amino acid L-arginine, and very weakly acidic phenol. The strength of these interactions was characterized by the apparent binding constants of the respective complexes.

Experimental

ACE experiments were carried out in Agilent CE7100 analyzer (Agilent, Waldbronn, Germany), equipped with photodiode array UV-vis detector set at 200 and 260 nm, and with the internally uncoated fused silica capillary, total/effective length 480/395 mm, id/od 50/375 mm with outer polyimide coating (Polymicro Technologies, Phoenix, AZ, USA). Capillary temperature was set to 22°C and sample carousel was cooled to 20°C by external water bath.

Results and Discussion

The experimental conditions were selected with respect to the acid-base and electromigration properties of the studied interacting compounds. Study of HI interactions with cationic ligands, dopamine, serotonin and arginine, was performed in the BGE 1, 40/40 mM Tris/tricine, pH 8.1. In this BGE, HI moved with anionic effective mobility -13.6×10^{-9} $m^2V^{-1}s^{-1}$, whereas serotonin, dopamine and arginine migrated with cationic effective mobilities in the range $(18.6\text{-}21.3) \times 10^{-9}$ $m^2V^{-1}s^{-1}$. The electroosmotic flow (EOF) mobility in this BGE was strongly cationic (52.0×10^{-9} $m^2V^{-1}s^{-1}$). Under these conditions, both the cationic ligands and the anionic receptor (HI) would be fast transported in cathodic direction to the detector and the receptor would leave the capillary earlier than the ligand could pass through its zone. This problem was solved by compensation of the strong EOF by the hydrodynamic counter flow induced by the external pressure at cathodic capillary end (see Figure 1A).
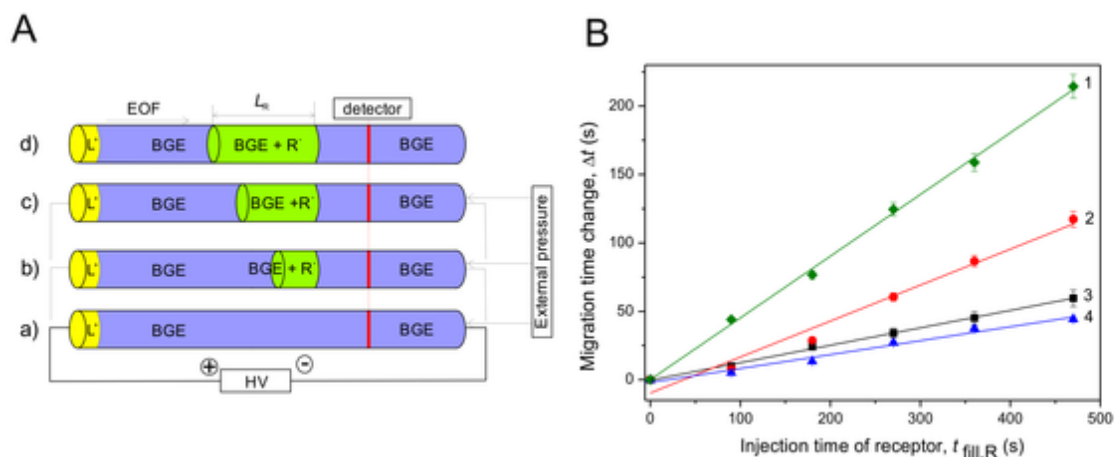
Fig. 1 A) The scheme of the arrangement of PF-ACE experiments. a) Ligand (L^+) and receptor (R^-) zones positions in the capillary at the beginning and (b-d) during the experiment with applied separation voltage and low external pressure decreasing the strong cathodic EOF and ensuring receptor migration to anode. L_R, is the variable zone length of injected HI. B) The dependence of the change of the effective migration times of ligands, Δt, on the injection time of HI in the capillary, $t_{fill,R}$. (1) Phenol in BGE 2; (2) Dopamine in BGE 1; (3) Serotonin in BGE 1; (4) Arginine in BGE 1.

In the BGE 1, pH 8.1, phenol migrated as an anion with very low mobility around -0.5×10^{-9} $m^2V^{-1}s^{-1}$, which was insufficient for its separation from the EOF marker. Hence, for investigation of HI-phenol interactions, the BGE with higher pH, particularly BGE 2, 25/34 mM NaOH/tricine, pH 8.5, was used. In this BGE, the effective mobility of HI was -14.5×10^{-9} $m^2V^{-1}s^{-1}$ and the effective mobility of phenol increased to -1.5×10^{-9} $m^2V^{-1}s^{-1}$, which was sufficient for its baseline separation from the peak of the EOF marker. In the BGE 2, the high cationic EOF mobility 58.0×10^{-9} $m^2V^{-1}s^{-1}$ was reduced to the value 10.0×10^{-9} $m^2V^{-1}s^{-1}$ by hydrodynamic counter flow induced by 60 mbar pressure at capillary outlet end.

In the PF-ACE experiments, 0.1 mM hexamer of HI dissolved in the BGE containing 0.2 mM Zn^{2+} ions was introduced into the capillary close to the detector window as a zone of variable lengths by applying external pressure 48.3 mbar at anodic capillary end for the time intervals 0, 90, 180, 270, 360, and 470 s, respectively. The records of PF-ACE experiments of the cationic ligand serotonin applied as analyte and HI applied as receptor zone of variable lengths inside the capillary in the BGE1 are depicted in Figure 2A and records of analogous PF-ACE experiments with anionic ligand phenol and HI in the BGE 2 are shown in Fig. 2B.
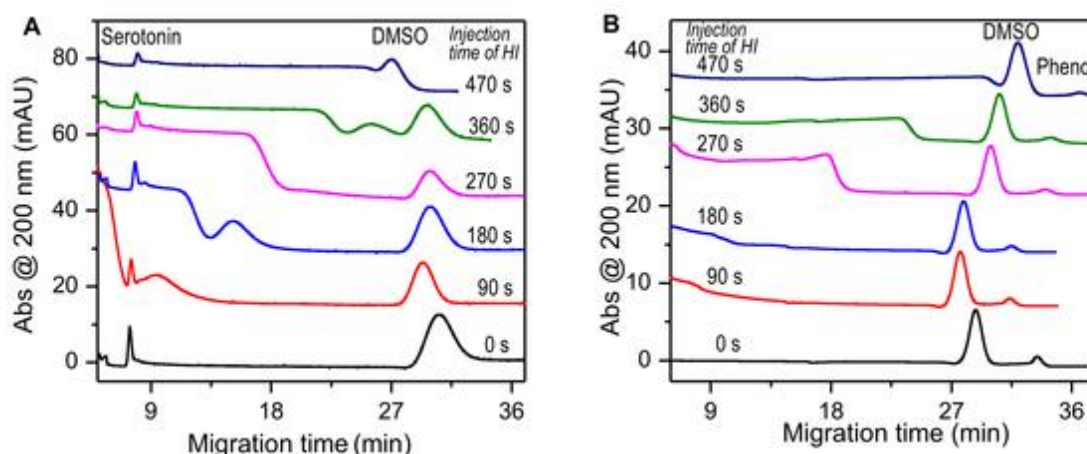
Fig. 2 Electropherograms demonstrating noncovalent interactions of ligands with HI. The receptor (HI) zone in the BGE was injected for 0-470 s close to the UV detector with low pressure of 48.3 mbar. (A) 0.1 mM serotonin in BGE 1; (B) 0.1 mM phenol in BGE 2.

Nilsson et al. [3] derived that using the PF-ACE method, the apparent binding constant, K_b, of the receptor-ligand complex can be determined from the linear dependence of the change of the migration time of the ligand, Δt, on the length of the receptor zones inside the capillary expressed by the filling time of their introduction to the capillary, $t_{fill,R}$, according to the equation

$$\Delta t = K_b \frac{c_R t_0}{t_{fill,det}} t_{fill,R}$$

where t_0 is the migration times of the ligand in the absence of the receptor (HI in our case) in the BGE, c_R is the receptor concentration, and $t_{fill,det}$ is the filling time of the capillary till the detector. Linear regression analysis of the dependences of the migration time changes of the ligands on the length of the receptor (HI) zones in the capillary (see Figure 1B) provided the binding constants of these complexes. This way obtained apparent binding constants of the HI complexes with all four ligands are presented in Table 1.

Table 1 Apparent binding constants, K_b, of the HI-ligand complexes, their standard (SD) and relative standard (RSD) deviations, and the effective mobilities of the ligands in the absence of the HI zone ($m_{eff,0}$) and in the presence of the longest HI zone (388 mm) inside the capillary (m_{eff}).

Ligand	BGE no.	$K_b \pm SD$ (L/mol)	RSD (%)	$m_{eff,0} \pm SD$ ($10^{-9}\,m^2V^{-1}s^{-1}$)	$m_{eff} \pm SD$ ($10^{-9}\,m^2V^{-1}s^{-1}$)
Serotonin	BGE 1	540 ± 11	2.7	21.29 ± 0.16	18.39 ± 0.08
Dopamine	BGE 1	970 ± 70	7.2	18.56 ± 0.09	14.60 ± 0.02
Arginine	BGE 1	385 ± 26	6.7	19.03 ± 0.02	17.22 ± 0.00
Phenol	BGE 2	1314 ± 29	2.2	-1.47 ± 0.00	-1.05 ± 0.01

Conclusion

The pressure assisted PF-ACE proved to be a suitable method for investigation of noncovalent interactions between hexamer of HI and cationic ligands, serotonin, dopamine and arginine or anionic ligand phenol. Pressure assistance was necessary to reduce the high EOF velocity in alkaline BGEs to the values ensuring opposite migration of both cationic and anionic ligands and receptor and resulting migration of both cationic and anionic ligands in cationic direction and their detection by UV-detector at cathodic capillary end. HI interactions with the above ligands were found to be moderately strong with binding constants in the range 385-1314 L/mol. From the above four ligands, phenol was the strongest binder of insulin whereas the strongly basic amino acid arginine formed with HI the weakest complex.

Acknowledgement

Reference

[1] Cohen P., Nature Reviews Molecular Cell Biology 2006, 7, 867-873.
[2] Heegaard N. H. H., Electrophoresis 2009, 30, S229-S239.
[3] Nilsson M., et al., Electrophoresis 2004, 25, 1829-1836.

P49 DYNAMICS OF REST-TRF2 INTERACTIONS AND THE FATE OF NEURAL CANCER CELLS

Martin Stojaspal, **Tomas Janovic, Pavel Veverka, Ctirad Hofr**

LifeB, Molecular Complexes of Chomatin CEITEC, Masaryk University, Brno 625 00, Czech Republic, 376043@mail.muni.cz

Summary

Glioblastomas (GBM) are the most frequent brain tumors in adults. No efficient treatment of GMB has been developed so far. The median maximum survival rate of glioblastoma-suffering patients is 12 months. The Repressor Element-1 Silencing Transcription factor (REST), also known as Neuron-Restrictive Silencing Factor (NRSF) is a transcriptional repressor recognized as a negative regulator of many genes, mainly neuronal. REST is usually expressed in non-neuronal tissues and stem cells, wherein it suppresses neuronal differentiation. REST is also present in differentiated neurons during the postnatal brain development and in normal aging, where it promotes neuroprotection by repressing genes involved in oxidative stress. But what makes REST so interesting? REST is crucial for self-renewal of cancer stem cell and brain tumor cells such as GBM. Shelterin protein TRF2 protects REST against proteasomal degradation, facilitates the physiological self-renewal of neural progenitor cells and the pathological uncontrolled proliferation of cancer cells. Identification of the interacting regions and following disruption of TRF2-REST interaction targets REST for proteasomal degradation. This could be the way how we can inhibit cancer stem cells and whole GLM tumor proliferation. In our initial studies we used FLIM-FRET (Fluorescence Lifetime Imaging Microscopy – Fluorescence Resonance Energy Transfer), PLA (proximity ligation assay) and pull-down assay to determine interacting regions of REST and TRF2.

Introduction

Telomeres are located at the ends of linear eukaryotic chromosomes. Telomeres comprise telomeric proteins and tandem arrays of DNA that differs across the species. Telomeric DNA usually contain single-stranded 3′ G-rich overhangs. These single-stranded regions invade the double-stranded telomeric DNA forming a stable secondary structure called telomere loop (T-loop) [1]. Proteins that specifically bind telomeric DNA stabilize T-loop to prevent unwanted DNA degradation, recombination or fusion of chromosomal ends. Additionally, T-loop avoids the recognition of the telomeres as a target region of the DNA damage repair machinery [2].

Due to incomplete DNA replication, telomeres shorten during each cell cycle. Telomerase is a ribonucleoprotein complex with RNA dependent DNA polymerase activity that can prevent telomere shortening by adding new telomeric DNA repeats. Telomerase is active in fast

dividing stem cells, germ cells and also in cancer cells. Telomerase is composed of two main parts: the telomerase reverse transcriptase (TERT) and telomerase RNA (TR). TR serves as a template for de novo synthesis of telomeric repeats, meanwhile TERT adds telomeric repeats at telomere ends [3, 4]. The reverse transcriptase function of telomerase is directly controlled by a protein complex called shelterin. Shelterin plays an essential role in the structure and dynamics of the telomeres because it binds in a sequence-specific manner to the telomeric DNA and regulates the telomerase access to DNA.

Human shelterin complex (Figure 1) contains six proteins: TRF1, TRF2, POT1, TIN2, TPP1 and RAP1. TRF1 and TRF2 specifically interact with double-stranded telomeric DNA and TIN2 protein. Furthermore, TRF2 forms a subcomplex with protein RAP1. TIN2 binds TPP1/POT1 heterodimer and thus bridges telomeric dsDNA and ssDNA of telomeric overhang. POT1 is a single-stranded DNA binding protein, which interacts with the telomeric G-rich overhang [5].

Figure 1: TRF2 plays a key role within shelterin protein complex that protects telomeric DNA and regulates telomerase access and activity on telomeres. TRF2 is highlighted in red (lablifeb.org, update 8/2018).

TRF2 plays central role in T-loop formation which protects sterically telomeres against damage, chromosomal fusion or DNA repair machinery. Protein TRF2 (Figure 2A) contains central TRFH (TRF homology) domain that mediates homodimerization. TRFH domains of TRF1 and TRF2 share 66% homology and do not form heterodimers [6]. The N-terminal part of TRF2 protein is basic and mostly composed of glycine and arginine and therefore it is also called GAR domain (glycine and arginine rich) [7]. Loss of GAR domain disrupts T-loop formation resulting in large deletions and shortened telomeres [8]. Importantly, C-terminal Myb domain is responsible for precise DNA-binding of TRF2 to the double-stranded 5′-

TTAGGG-3′ telomeric [9]. TRF2 has non-telomeric functions as well. TRF2 protects essential transcription factor REST from polyubiquitination and proteasomal degradation.
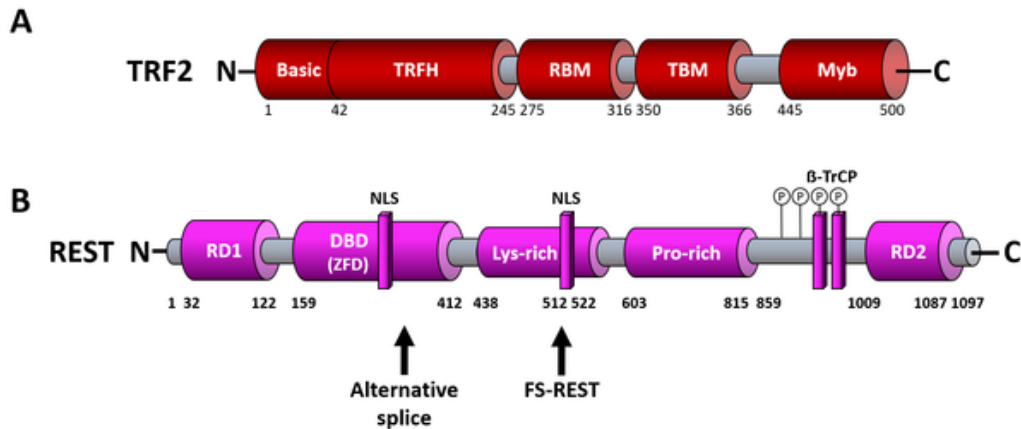

Figure 2: TRF2 and REST domain structure. A) TRF2 contains N-terminal basic domain (GAR), C-terminal DNA-binding Myb domain, TRFH dimerization domain; RBM–Rap1 binding motif, TIN2-binding motif TBM. B) REST consist of two repressor domains (RD1, RD2), DNA binding domain, lysine and proline rich regions and two β-TrCP binding sites. Arrows indicate truncated forms of REST that are associated with small-cell lung cancer and neuroblastoma (alternative splicing) or colon cancer resulting from a frameshift (FS-REST).

REST, also known as NRSF, is a master repressor of neural genes in non-neural cells. REST has N-terminal and C-terminal recruitment domains (RD1 and RD2) that serve as scaffolds for formation of diverse gene repressor complexes. The DNA binding domain is followed by lysine- and proline-rich domains and two β-TrCP binding sites (Figure 2B). Alternative splicing or frameshift leads to truncated forms of REST that are associated with diseases such as small-cell lung cancer and neuroblastoma or colon cancer [10].

REST is a DNA-binding protein that recognize RE1 sequence, scattered throughout human genome with consensus sequence 5„-NNCAGCACCNNGCACAGNNNC-3" [11, 12]. RE1 is found mostly in the promoters of genes associated with the neuronal differentiation. REST target genes are connected to cell maintenance, communication and neural developmental signaling pathways [13].

Interestingly, REST serves as a tumor suppressor in non-neuronal cancers, but in neural tumors, REST plays an oncogenic role. REST is important for self-renewal of GSCs (glioblastoma-derived stem-like cells) [14]. GSCs are derived from glioblastoma multiforme tumors, the most common and the most malignant primary brain tumors in adults. High levels of REST were correlated with lower apoptotic and higher invasive properties of GSCs produced in tumors. This makes REST protein an important factor in GSC-mediated tumorigenesis. It is known that TRF2 binds to and stabilizes REST, thereby preventing its degradation, whereas activity of the ubiquitin E3 ligase SCFb-TrCP accelerates proteasomal degradation of REST [15]. Thus TRF2 binding plays an essential role in REST protection. Dissociation of REST-TRF2 complexes

results in ubiquitin-proteasomal degradation of REST and expression of REST target genes. After REST downregulation, GSCs stop dividing and acquire several phenotypic properties of differentiated neuron. Thus, in addition to protecting telomeres, TRF2 possesses an essential role in stabilization of REST that is required for controlling neural tumor and stem cell fate.

Experimental

In our study, we used pull-down assay to determine a physical interaction between TRF2 and REST. Protein of our interest – REST (bait) was tagged and captured on an immobilized affinity ligand specific for the tag thereby interacting partner – TRF2 (prey) can be co-purified. Obtained protein mixtures are analyzed by SDS electrophoresis.

To confirm the interaction between TRF2 and REST in cells, we carried combined FLIM-FRET (Fluorescence Lifetime Imaging Microscopy – Fluorescence Resonance Energy Transfer) measurements and PLA (proximity ligation assay). For FRET experiments, the potential binding partners are labeled with spectrally distinct fluorophores (GFP_TRF2 and mCherry_REST) in such a way that the emission spectrum of the donor molecule overlaps the excitation spectrum of the acceptor molecule. If both interaction partners are in close proximity (situation when they are interacting), the excited donor can transfer its energy to the acceptor. In turn, the acceptor emits a fluorescence photon and the fluorescence lifetime of the donor molecule decreases. FLIM-FRET provides information about fluorescence lifetime of the donor that shorten when FRET occurs.

PLA otherwise is a method based on immunofluorescence, where proteins of our interest are detected using specific primary antibodies from two different species. Secondary antibodies carry DNA probes that creates DNA circles. Afterwards rolling circle amplification is used to increase the amount of DNA that is detected using sequence specific fluorescence probes.
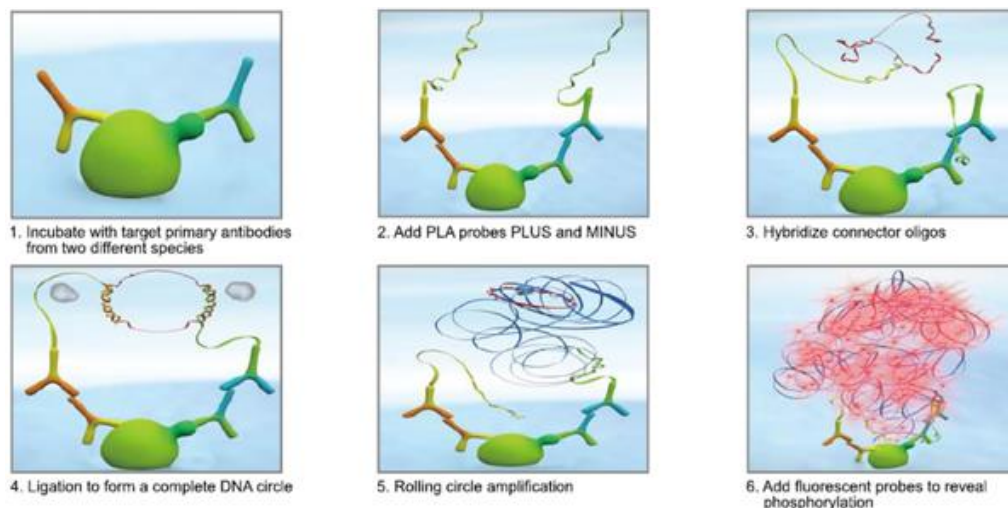

Figure 3. Principle of proximity ligation assay (taken from abnova.com).

Results and Discussion

We wanted to observe the interaction of TRF2 and REST and define their interacting regions. To do so, we transiently transfected HEK293T cells by plasmid containing fluorescent protein GFP conjugated with TRF2 and mCherry with REST. After optimization, we found out that plasmid ratio should be 1:1,5 (GFP:mCherry) to get maximum amount of double-transfected cells. Cells transfected by donor only was used as a negative control. A positive control contained fused GFP and mCherry. Fresh cells were prepared for FLIM-FRET measurements that were performed next day. When we compared data between interaction and negative control, the significant decrease in fluorescence lifetime was detected. Our FLIM-FRET measurements suggest that significant amount of REST and TRF2 all molecules are interacting, because we could see significant shift towards positive control lifetime (Figure 4).
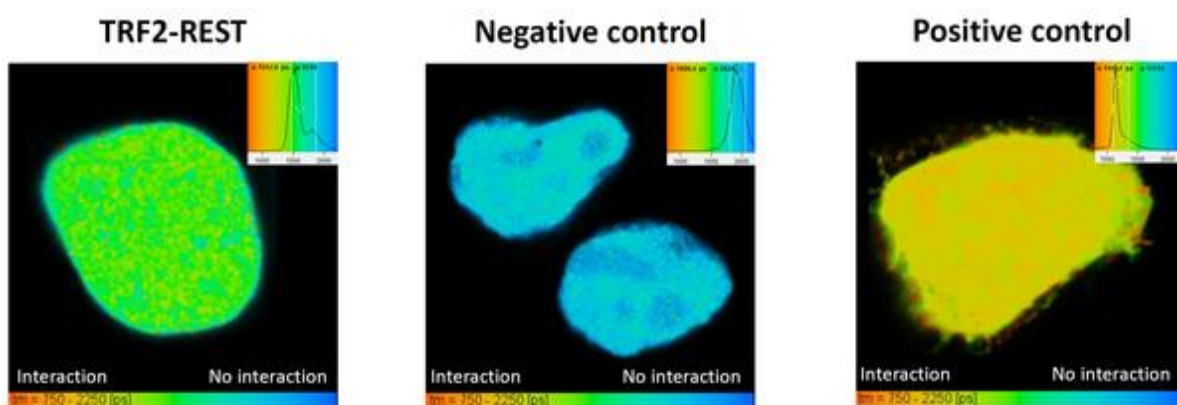
Figure 4. FLIM-FRET result. Decrease of fluorescence lifetime after double-transfection by GFP_TRF2 and mCherry_REST suggest the interaction between TRF2 and REST.

For PLA we used U251 cells on pre-treated cover slips and then continue according to the protocol provided by the manufacturer of the PLA kit (Duolink). To specifically detect TRF2-REST interaction, the primary antibody against TRF2 and REST were used. To simulate lower level of TRF2, we treated cells by anticancer cisplatin, as the formation of double-strand breaks on DNA by cisplatin causes efflux of TRF2 protein to damage sites and lower the level of TRF2 that are available for interaction. As you can see in figure 5, cisplatin induced reduction in TRF2-REST interaction spots is obvious. Our results of PLA support FLIM-FRET results and demonstrate the interaction between TRF2 and REST in cells.
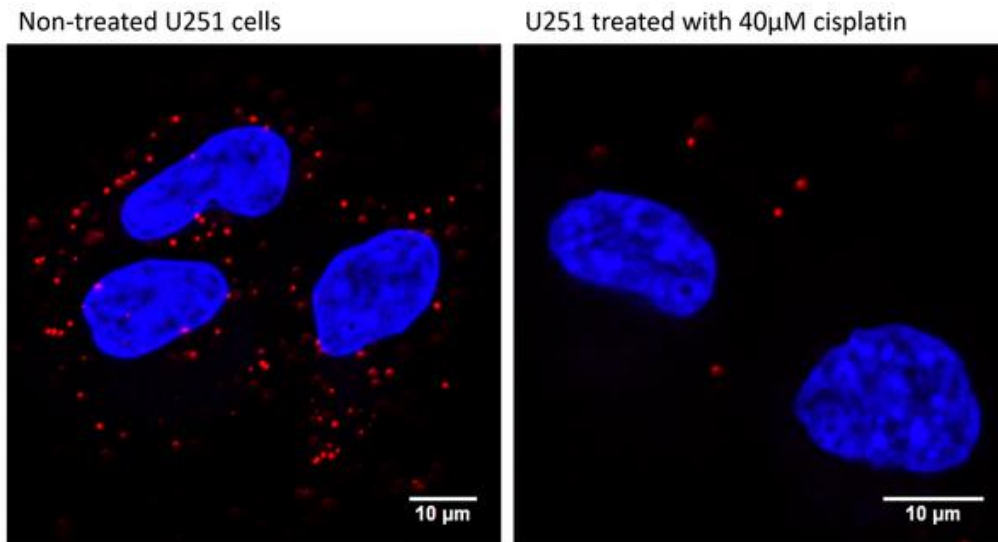
Figure 5. Proximity ligation assay suggest the interaction between TRF2 and REST. Interacting signals ("red dots") are diminished after cis-platin addition.

We used pull-down assay to detect interaction of TRF2 and REST in vitro. We double-transfected HEK293T cells by GFP_TRF2 and different variants of REST in pTriEx4 vector, containing his tag, which was used to purify REST proteins from a cell lysate. As a positive control we used REST full-length that should bind TRF2 according to our previous results. Truncated variants of REST were designed to preserve main functional domains of REST. REST_RD1 contains recruitment domain 1 and DNA binding zinc finger motif. REST_LINK contains unstructured lysine- and proline-rich regions and REST_RD2 comprises phosphodegron and recruitment domain 2. After purification of REST proteins, we detected TRF2 presence in both, REST_RD1 and REST_RD2 by SDS-PAGE and following western blot (Figure 6). These results suggest that both recruitment domains are involved in interaction with TRF2.
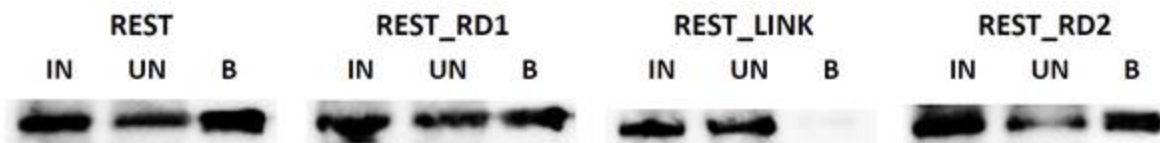
Figure 6. Pull down assay – TRF2 and variants of REST. REST full-length was used as a positive control. Input (IN) is the cell lysate with both proteins, unbound (UN) fraction contains TRF2 even in case of interaction suggesting higher expression and amount of TRF2. Bound (B) fraction contains TRF2 only in case of interaction that we can see in REST_RD1 and REST_RD2.

Conclusion

Our PLA and FLIM-FRET studies confirmed direct interaction between full-length REST and TRF2. FLIM-FRET in cells that were double-transfected using plasmids for GFP_TRF2 and mCherry_REST, showed lower lifetime of fluorescent protein GFP in comparison with

negative controls (cells transfected by single plasmid for GFP-tagged TRF2). PLA showed lower amount of interacting "dots" after addition of cis-platin, which creates double-strand DNA breaks thus it decreases TRF2 molecules that are available for interaction with REST.

Pull-down assay focused on interaction of TRF1 with truncated variants of REST. We observe interaction only in RD1 and RD2 regions of REST, suggesting that recruitment domains of REST are responsible for the interaction with TRF2.

Acknowledgement

Reference

[1] Griffith, J. D. et al. Cell 1999, 97, 503–514

[2] Cimino-Reale, G. Nucleic Acids Res. 2001, 29, 35e–35

[3] Cohen, S. B. et al. Science 2007, 315, 1850–1853

[4] Zvereva, M. I., Shcherbakova, D. M. & Dontsova, O. A. Biochem. Biokhimiia 2010, 75, 1563–1583

[5] de Lange, T. Genes Dev. 2005, 19, 2100–2110

[6] Fairall, L., Chapman, L., Moss, H., de Lange, T. & Rhodes, D. Mol. Cell 2001, 8, 351–361

[7] Broccoli, D., Smogorzewska, A., Chong, L. & de Lange, T. Nat. Genet. 1997, 17, 231–235

[8] Wang, R. C., Smogorzewska, A. & de Lange, T. Cell 2004, 119, 355–368

[9] Hanaoka, S., Nagadoi, A. & Nishimura, Y. Protein Sci. Publ. Protein Soc. 2005, 14, 119–130

[10] Weissman, A. M. Cancer Cell 2008, 13, 381–383

[11] Schoenherr, C. J., Paquette, A. J. & Anderson, D. J. Proc. Natl. Acad. Sci. U. S. A. 1996, 93, 9881–9886

[12] Abrajano, J. J. et al. PloS One 2009, 4, e7936

[13] Kamal, M. M. et al. Stem Cells Dayt. Ohio 2012, 30, 405–414

[14] Chen, H., Farkas, E. R. & Webb, W. W. Methods Cell Biol. 2008, 89, 3–35

[15] Zhang, P. et al. Trends Neurosci. 2009, 32, 559–65.

P50 A NEW EVALUATION OF COMBINED ANTITUMOR EFFECTS OF NATURAL AND SYNTHETIC NUCLEAR RETINOID RECEPTOR LIGANDS IN HUMAN BREAST CARCINOMA CELLS

Dana Strouhalová[1], Markéta Laštovičková[1], Pavel Bobál[2], Dana Macejová[3], Barbora Mosná[3], Julius Brtko[3], Janette Bobálová[1]

[1]*Institute of Analytical Chemistry of the CAS, v. v. i., Brno, Czech Republic*

[2]*Department of Chemical Drugs, Faculty of Pharmacy, University of Veterinary and Pharmaceutical Sciences Brno, Brno, Czech Republic*

[3]*Institute of Experimental Endocrinology, BMC, Slovak Academy of Sciences, Bratislava, Slovak Republic*

Summary

This work represents the study of the effects of biologically active ligands of nuclear retinoid X receptors, triorganotin compounds, on proteomic profile of MDA-MB-231 cells. We focused primarily on tributyl/phenyltin derivatives that suggest the combined antitumor effect when they are used with natural nuclear retinoid receptor ligand all-trans retinoic acid (ATRA). Proteomic strategies connected to PDQuest evaluation were applied in this study. Some specific proteins with tumor process association were chosen for more detail study. Our findings indicate that selected triorganotins derivatives resulted to significantly reduced level of studied proteins belonging to metabolic pathway or to other cellular processes as apoptosis or epithelial–mesenchymal transition. In the case of vimentin, the key protein of EMT process, the silencing was set up by triorganotin compounds and significantly enhanced by combination with ATRA. This additive effect on downregulation can result from the potential engagement of RXR/RAR heterodimer, considering co-addition of both partner ligands of mentioned heterodimer to the treatment.

Introduction

Nuclear retinoic acid receptors (RARs) and nuclear retinoid X receptors (RXRs) are retinoid/rexinoid inducible transcription factors. In response to retinoid binding, RAR/RXR heterodimers undergo conformational changes and activate the transcription of specific gene networks, through binding to specific DNA response elements [1,2]. In addition, their presence in the organism together with other biologically active ligands is essential for many important functions, so they play an important role in embryonic development, reproduction and apoptosis.

Retinoids as well as rexinoids are either natural or synthetic compounds related to retinoic acids (RAs) that act through interaction with two basic types of nuclear receptors belonging to the nuclear receptor superfamily: all-trans RA receptors and retinoid X receptors as retinoid-inducible transcription factors [3,4]. Retinoids are known to inhibit carcinogenesis, suppress tumor growth, induce tumor cell differentiation and invasion in a variety of tissues. They are considered to be promising anti-cancer drugs for a variety types of cancer [5, 6].

Experimental

Cell culture

The MDA-MB-231 cell line was obtained from the HPACC (Health Protection Agency Culture Collections, Salisbury, U.K.), grown and passaged routinely. Cells were seeded in Petri dishes (Sarstedt, Germany) in Dulbecco´s modified Eagle´s medium (DMEM) supplemented with 10% fetal bovine serum (FBS), glutamine and antibiotics (penicillin/ streptomycin, gentamicin) and cultured at 37°C in humidified atmosphere of 5 % CO_2. The cells were treated for 48 h either with 10 µmol/L all-trans retinoic acid (ATRA), 100 nmol/L triorganotin derivatives individually, or with their combination. Control cells were incubated with particular concentration of ethanol. After incubation, the cell lysis was made according to an instruction manual of the RIPA (Radio-Immunoprecipitation Assay) buffer. Protein concentrations were assessed using the Lowry assay.

2D SDS-PAGE

2D-PAGE was performed using ReadyPrep 2D Starter Kit, ReadyStrip IPG strips 7 cm, pH 3 – 10 nonlinear and 4 – 20 % Mini-Protean TGX gel (Bio-Rad, CA, USA). The protein visualization was carried out using Coomassie Brilliant Blue G 250 dye.

In-gel digestion

The protein spots were excised from the gel and digested with trypsin overnight at 37°C. The resulting tryptic peptides were extracted from the gel by 0.1% trifluoroacetic acid (TFA) and acetonitrile (1:1, v/v). For mass spectrometric analyses, the extracts were purified by ZipTip C18 (Millipore).

Mass spectrometry and database searching

MALDI MS experiments in positive ion reflectron mode were performed on AB SCIEX TOF/TOF™ 5800 System (AB SCIEX, USA). Acquired mass spectra were processed using 4000 Series Explorer software and the data were submitted to the Mascot database searching. Protein identifications were assigned using the Swissprot database with taxonomy restriction to Homo sapiens.

Results and Discussion

All proteins of our interest were strongly affected by triorganotin chloride or isothiocyanate derivatives (Fig.1- upper) treatment (downregulated or completely reduced). Generally, observed proteins suppression was increased caused by combined treatment what confirmed the synergistically enhanced effect of both nuclear retinoid receptor ligands. All these proteins have been described as overexpressed within the breast tumor cells, so the silencing of these proteins indicates the promising opportunity for further research. Among all proteins we found, the greatest attention was paid to vimentin (Fig.1- lower), which is a key element regulating the expression of the EMT-related transcription factors. Our experiments indicate that the vimentin silencing seems to be of the promising value and suitable for the further more detail study. Since, the vimentin represents one of the main factors connected with poor prognosis in triple negative breast cancer, study of VIME expression changes could be useful as a potential therapy target.

Used proteomic techniques in combination with mass spectrometry confirmed the ability for analysis and identification of proteins originated from a complex biological material.

Conclusion

In conclusion, the data based on the proteomic approach was able to give us an overview on the expression changes of specific proteins which seem to be suitable markers for evaluation of the potential effect of organotin compounds in cancer treatment. Regarding to fact that used organotin compounds are ligands for RXR receptor and ATRA is natural ligand for RAR receptor, we decided to apply the combination of both treatments to prove potential additive effect.

Acknowledgement

P51 ELECTROMAGNET FOR CAPTURE OF MAGNETIC BEADS FROM LARGE VOLUME INTO MICROFLUIDIC CHAMBRE CHIP

Zuzana Svobodova[1,2], Rudolf Kupčík[1], Denisa Smělá[1], Jakub Roupec[3], Ondřej Macháček[3], Lucie Nováková[2], Zuzana Bilkova[1]

[1]*Department of Biological and Biochemical Sciences, Faculty of Chemical Technology, University of Pardubice, Studentska 573, 532 10 Pardubice, Czech Republic, Zuzana.Bilkova@upce.cz*

[2]*Faculty of Pharmacy in Hradec Kralove, Charles University Prague, Heyrovskeho 1203, 500 05 Hradec Kralove, Czech Republic*

[3]*Institute of Machine and Industrial Design, Faculty of Mechanical Engineering, Brno University of Technology, Technicka 2896/2, 616 69 Brno, Czech Republic*

Summary

Immunomagnetic separation is method of choice besides filtration or centrifugation when a bioanalyte is to be specifically isolated form a larger volume. Here, home-made electromagnet with special, optimized construction, to fit to the microfluidic rhombic chip is presented. The experiments show how to capture 1 mg of superparamagnetic beads (SMB) from 20 mL syringe into 120 µL chamber in microfluidic chip. The captured beads can be easily transported to another microfluidic device for subsequent analysis. Various flow rates were tested and SMB were collected firstly from a phosphate buffer and subsequently from a cow's milk sample.

Introduction

The microfluidic approach was included in many areas of analytical chemistry bringing new insight and technologies. The immunomagnetic separations (IMS) are one of them [1]. In this method, the superparamagnetic beads (SMB) are conjugated to e.g. specific antibodies. Such biofunctionalized SMB are added to a heterogeneous suspension to bind to the desired target (bacterial or mammal cells, cell lysates compounds, viruses, proteins, nucleic acids, etc.) [2-4] and from a complex composed of SMB and target. A magnet is used to immobilize the complex SMB–target against the vessel wall, and the remainder of the material is removed. Washing steps to remove food material and other microorganisms are easily performed while the SMB–target complex is retained. The target then can be detected using conventional immunoassays, pipetting or streaking on to agar or other culture media, or by using nucleic acid-based methodologies, as the magnetic particles do not interfere with other methods of detection [5]. In certain application is necessary to collect the target from larger volume (50 mL) of heterogeneous suspension, e.g. for isolation of subcellular structures from cell lysate or capture bacteria from food samples [6]. A permanent magnets surrounding the tube are usually applied

and 10-50 min incubation is required to separate all SMB with the captured target depending on the matrix. Then, the SMB are removed from the magnet manually collected into lower volume using a pipette and then again permanent magnet is used for capture, the liquid is discarded and resuspended in desired volume. Here, an easy technique based on microfluidic principles is applied to IMS with the aim to collect the SMB from 20 mL volume inside the chamber of microfluidic chip.

Experimental

2.1 The electromagnet was home-made on FME VUT in Brno from pure ferrum with trademark Behanit which C-shaped body was twisted around with a copper wire. In the aperture of behanit material, the microfluidic rhombic chamber chip was inserted and the coil was connected to power supply (Fig. 1A). The part of the magnet that surrounds the microfluidic chip was designed with the aim to maximize the capture SMB from the liquid samples. The dimensions (width and depth) and number of grooves on the magnet were based on findings from finite element method (FEM): magnetostatic analysis.

2.2 The microfluidic rhombic chamber chip contains two microfluidic chambers (120 μl volume, hydrophilized) with two inlets and two outlets, the dimensions are mentioned in Fig. 1B. The microfluidic chip was purchased from Microfluidic ChipShop (Jena, DE).

2.3 The reservoir of the sample could be syringe of various sizes (1-50 mL) that syringe tip fits to the inlet of the μchip. The liquid suspension (mixture of sample and 1 mg SMB from ProMAGTM-COOH, size 0.746 μm) passed through the microfluidic chamber using home-made syringe pump filled with the air. The compression of the air creates a pressure that push the suspension inside the microchip chamber. The gas syringe pump work in flow range 1–7 mL/min.
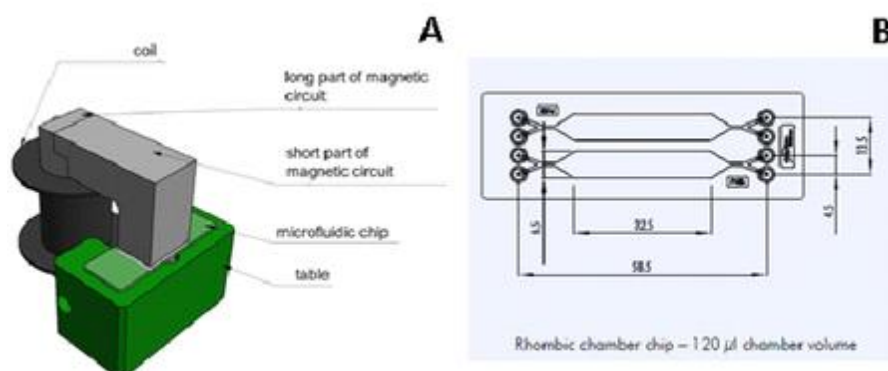

Fig. 1 (A) Scheme of home-made electromagnet from behanit with microfluidic chip (B) Scheme of Rhombic chamber chip with 120 μL.

Results and Discussion

The SMB were dispersed in 20 mL of phosphate buffer and/or of undiluted cow´s milk. Various flow rates were tested. At 5 mL/min some SMB leakage was observed but at 3 mL/min the

whole amount of SMB was captured inside the chip chamber. If 20 mL of sample is used the analyte is finally captured into 120 µL and is concentrated 167 times. In case of cow´s milk the optimal flow rate was determined as 2 mL/min. The capture was compared with a manual application with 20 mL tube and MagnetoPURE-Macro from Chemicell (DE) which was able to separate SMB from milk in 30 min (Table1).

Table 1 Comparison of permanent magnet (MagnetoPure-Macro, Chemicell, DE) and the electromagnet

	Permanent magnet + tube	Electromagnet + µ chip
SMB separation time	30 min	7-10 min
SMB volume reduction	From 20 mL to 1 ml	From 20 mL to 120 µL

Fig. 2 Captured 1 mg of SMB in phosphate buffer in rhombic chamber chip (120 µL volume, 6 cm long) using special electromagnet.

Conclusion

The combination of specially designed electromagnet, SMB and microfluidic chip presents a system that is able to capture such small amount as 1 mg of SMB from 20 mL of phosphate buffer or from cow´s milk in 10 min. Moreover, the SMB can be transfered from the chamber to a subsequent microfluidic chip for another analysis, e.g. for PCR analysis, to be performed online. This could help to the automation of detection system e.g. for food and/or cell analysis. Thus, the manual handling with SMB could be omitted.

Acknowledgement

Reference

[1] O. Olsvik, T. Popovic, E. Skjerve, K.S. Cudjoe, E. Hornes, J. Ugelstad, M. Uhlén, Clinical Microbiology Review 1994, 7(1), 43-54.

[2] Q. Chen, J. Lin, C. Gan, Y. Wang, D. Wang, Y. Xiong, W. Lai, Y. Li, M. Wang, Biosensors and Bioelectronics 2015, 74, 504-511.

[3] D.J. Wright, P.A. Chapman, C.A. Siddons, Epidemiology and Infection 1994, 113(1), 31-39.

[4] C. Clarke, J. Titley, S. Davies, M. J O'Hare, Epithelial cell biology 1994, 3(1), 38-46.

[5] J.W. Austin, F.J. Pagotto, MICROBIOLOGY | Detection of Foodborne Pathogens and their Toxins, in: B. Caballero (Ed.), Encyclopedia of Food Sciences and Nutrition, Academic Press, Oxford, 2003, pp. 3886-3892.

[6] J.W.-F. Law, N.-S. Ab Mutalib, K.-G. Chan, L.-H. Lee, Frontiers in Microbiology 2015, 5(770), 1-19.

P52   PRECONCENTRATION STRATEGIES FOR APTS LABELED CARBOHYDRATE CE-LIF ANALYSIS

Robert Farsang[1], Balazs Reider[1], Mate Szarka[1], Gabor Jarvas[1], Andras Guttman[1,2]

[1]*Translational Glycomics Research Group, MUKKI, University of Pannonia, Veszprem, Hungary, szarkamatthew@gmail.com*

[2]*Horvath Csaba Laboratory of Bioseparation Sciences, Research Center for Molecular Medicine, Faculty of Medicine, University of Debrecen, Debrecen, Hungary*

Summary

Capillary electrophoresis (CE) offers unique selectivity and separation efficiency and because of the small dimensions, only a small amount of sample (several nL) is required for the analysis. However, this represents some drawbacks of CE with very diluted samples. To address this issue, various techniques have been developed to increase the amount of the injected sample, but these methods often show limited efficiency or complex setup. In this poster we present three alternative approaches to preconcentrate APTS labeled sugars inside the capillary prior to CE separation: 1) making the capillary glass wall porous to conduct electricity; 2) sealing the capillary by a metallic plug; 3) agarose embedded amine surface microparticle mediated solid-phase extraction (SPE).

Introduction

Due to its excellent selectivity and separation efficiency, capillary electrophoresis successfully competes with HPLC for carbohydrate analysis. CE features an important advantage as capable to differentiate oligosaccharides based on their molecular shape – even if the mass to charge ratios of two analytes are the same – thus readily separates linkage and positional isomers. Applying laser-induced fluorescence detection (LIF) makes CE a robust tool offering rapid analysis with high resolution and excellent reproducibility. In addition, CE requires only nanoliter sample amounts to be injected for full structural analysis, compared to other techniques that need microliter quantities for the same. However, this advantage can turn into a handicap due to the limitation of the injected amount of low concentration sample components.

Preconcentrating the analytes from their sample matrix could be the most comfortable solution for resolving this issue. This can be carried out by injecting large amounts of sample and subsequently narrowing the sample zone prior to separation. Numerous sample-stacking methods have been developed based on manipulating these two operations, e.g. field-enhanced sample stacking (FESS) [1], large-volume sample stacking (LVSS) [2], transient ITP [3] and

dynamic pH-junction [4], all widely implemented. However, these techniques often show limited enrichment factors and can lead to biased injection. In this work, we present three individual approaches for in-line preconcentration of APTS labeled oligosaccharides inside a bare fused-silica capillary. In every instances the analytes are concentrated electrokinetically into a small sample plug. These methods are based on either etching the capillary wall to as thin as 5 μm, which can conduct electricity [5], sealing the capillary end by a metallic plug and applying a special solid-phase extraction section in the capillary.

Experimental

Acetic acid, lithium acetate, hydrogen fluoride, sodium bicarbonate was from Sigma-Aldrich (St. Louis, MO, USA). MetaPhor® agarose was from Cambrex (Rockland, ME, USA) SiMAG-Amino magnetic microbeads were from Chemicell (Berlin, Germany), the OP70 low melting point (70°C) alloy was from Metalloglobus (Budapest, Hungary).

Etched capillary: The polyimide coating of a 40 cm bare fused-silica capillary was mechanically removed in 0.5 mm ID circle at 10 cm from the inlet end and was etched by hydrogen-fluoride. The resistance across two electrodes was measured to monitor the progress of the etching using a regular multimeter. The resistance between the two electrodes was >220 MΩ, but as the etching progressed, it dropped until entering the range of <220 MΩ. At this point, the HF was neutralized with a saturated sodium bicarbonate solution and the capillary was washed with water to remove the excess salt. Finally, the capillary was filled by water to detect any leaks at the etched section.

Sealed capillary: The inlet end of a 40 cm bare fused-silica capillary was sealed by low melting point (70°C) alloy. Initially, the capillary was filled by 25 mM LiAc solution, then the inlet end was immersed into the molten alloy and quickly cooled down to solidify the metal. Finally, the capillary was checked for electric conductance.

Agarose embedded amine microbeads: The storage buffer was removed from 50 μl of SiMAG-amino microbeads using a magnetic separator. The microparticles were taken up in 50 μl water then 2 mg agarose was added. The mixture was heated up to 95°C, vortexed and cooled down to room temperature. The inlet end of a 30 cm bare fused-silica capillary was filled by 25 mM LiAc buffer (pH 6.6). The inlet end of the capillary was pushed into the agarose embedded amine microbeads twice to introduce and approximately 4 mm long agarose plug into the capillary.

Analysis: A P/ACE MDQ system (SCIEX) was used for all capillary electrophoresis analyses, equipped with an LIF detector (λex=488 nm / λem=520 nm). Capillary columns: EZ-CE cartridge (SCIEX) – 20 cm effective length (30 cm total, 50 μm I.D.) bare fused-silica capillary. Separation matrix: 25 mM LiAc buffer (pH 6.6). Separation temperature: 25°C. Applied electric field (E): 500 V/cm.

Results and Discussion

As it was published by Whitt et al, tapering a capillary wall down to 5 μm resulted in conducting electricity through the porous glass. To follow this idea, we etched a bare fused-silica capillary 10 cm from the inlet end and immersed the porous part into the background electrolyte (25 mM LiAc). By dipping the inlet end of the capillary into a sample vial and closing the circuit between the sample vial and the electrolyte around the porous wall the electrophoretic process initiates inside the capillary leading to the migration of all charged species towards the etched capillary wall. However, larger analytes such as APTS labeled oligosaccharides cannot pass through the glass wall, therefore get enriched against the porous glass surface. After the pre-concentration step, the circuit is simply closed between the inlet and outlet ends of the capillary and CE separation started. This method can be automated by simply switching between the electrodes and the setting is easily reusable numerous times. Please note that the thin capillary wall makes the system fragile. Application this setting into the P/ACE MDQ also needed some modification in the capillary cartridge (Table 1).

In the second approach, we sealed the inlet end of the capillary by a low melting point (70°C) alloy plug, which was used as an electrode itself. The outlet end of the capillary was dipped into the sample vial and the circuit was closed between the inlet and outlet end. This made the charged analytes migrating towards the metal seal and enriched at the surface of the alloy. After the pre-concentration step, the polarity was switched and the CE separation was conducted normally. Preparation of this sealing was easy, but the separation media had to be pre-filled before assembly. This made it essential to use below 100°C melting point alloy for sealing to prevent the vaporization of water inside the capillary. Unfortunately, applying high voltage to the capillary lead to gas formation on the surface of the metal seal, which can break the electric circuit. Despite of the durable setup and easy application, this method was not suitable for automation because after every separation the system had to be taken apart and reassembled again (Table 1).

The third preconcentration method applied was solid-phase extraction based. Similarly, to a related method [6], a simple and reusable technique was developed suitable for full automation. The agarose embedded amine surface microbeads acted as a plug inside the capillary, which can be introduced by simply dipping the inlet end of the column into the solidified agarose block. This plug then retains the negatively charged sample components, therefore the analytes can be enriched on the surface of the microparticles and then eluted by the injection of an anionic solution with higher ionic strengths. After CE separation, the agarose plug can be simply pressurized out and the capillary refilled. This setup is durable and easy to re-assemble also suitable for automation (Table 1).

Conclusion

Numerous preconcentration techniques have been developed for analyte enrichment in CE, but despite their easy implementation, these methods often suffered limited efficiency. Here we presented three alternative approaches for pre-concentration of APTS labeled oligosaccharides

prior to CE-LIF analysis. These methods were compared by the complexity of their preparation, use and suitability for automation. According to our results, the agarose embedded amine surface microparticle based solid-phase extraction was the most efficient technique.

Acknowledgement

Reference

[1] C. X. Zhang; W. Thormann, Anal. Chem. 1996, 68, 2523-2532.

[2] R.-L. Chien; D. S. Burgi, Anal. Chem. 1992, 64, 489A-496A

[3] Z. Malá; P. Gebauer; P. Boček, Electrophoresis 2013, 34, 19–28.

[4] A. A. Kazarian; E. F. Hilder; M. C. Breadmore, J. Sep. Sci. 2011, 34, 2800-2821.

[5] J. T. Whitt; M. Moini, Anal. Chem. 2003, 75, 2188-2191

[6] K. Jooß; J. Sommer; S.-C. Bunz; C. Neusüß, Electrophoresis, 2014, 35, 1236–1243.

P53   SEPARATION AND DETERMINATION OF ACTIVE PHARMACEUTICAL INGREDIENT AND EXCIPIENTS BY MICROCHIP ELECTROPHORESIS

Peter Troška, Marián Masár

Department of Analytical Chemistry, Faculty of Natural Sciences, Comenius University in Bratislava, Bratislava, Slovak Republic, peter.troska@uniba.sk

Summary

The use of microchip electrophoresis (MCE) has attracted growing interest in recent years. MCE is simple and fast miniaturized analytical technique suitable for the analysis of small sample volumes. In this study, MCE has been used for simultaneous separation and determination of excipients (methylparaben, propylparaben and erythrosine) and for determination of active pharmaceutical ingredient (diclofenac) in various pharmaceutical preparations. The developed methods allowed fast (< 13 min total analysis time), reproducible ($\leq 4.1\%$ RSD of migration times and 0.3–5.7% RSD of peak areas) and sensitive (0.2–2.0 mg/L limits of detection) determinations of studied analytes in real pharmaceutical products with easy sample handling (centrifugation and dilution sample pretreatment steps).

Introduction

Pharmaceutical dosage forms are consisted of active pharmaceutical ingredient (API) and various excipients. The ideal excipients must be able to fulfill the important functions, i.e. dose, stability and release of API from the formulation [1]. Excipients are considered inert substances and can be classified in various categories such as bulk filler, sweeteners, flavoring agents, coloring agents, preservatives, surfactants, binding agents, lubricants, etc. Determination of these compounds is important in term of quality control of pharmaceutical products. In recent years, several studies have been published on the use of capillary electrophoresis (CE) for the determination of the excipients [2].

APIs have been also determined in pharmaceuticals using CE [3]. In addition to use of conventional CE methods, there is an obvious interest in applying microchip electrophoresis (MCE) to the analysis of pharmaceutical samples [4]. MCE analyzes are more favorable than CE because they are considerably faster; they achieve higher separation efficiency and, in particular, reduce overall costs associated with chemical consumption and waste production.

The aim of this work was to develop simple and fast miniaturized analytical methods for the determination (i) excipients (methylparaben, propylparaben and erythrosine) and (ii) API (diclofenac as non-steroidal anti-inflammatory drug) in pharmaceutical preparations on

microchip with conductivity detection. Zone electrophoresis (ZE) was used for simultaneous separation and determination of excipients, while online combination of isotachophoresis (ITP) with ZE was favored for the determination of API.

Experimental

ZE separations of studied excipients and ITP-ZE determination of diclofenac were carried out on the microchip with coupled channels and conductivity detection (IonChip 3.0, Merck, Darmstadt, Germany). MCE analyzer consisted of electrolyte and electronic unit [5]. MicroCE Win software, version 2.4 was used for monitoring the analysis as well as for collecting the data from conductivity detectors and their evaluation.

Chemicals used for the preparation of electrolyte solutions and stock solution of model samples were obtained from Sigma-Aldrich (Steinheim, Germany) and Fluka (Buchs, Switzerland). Samples of pharmaceutical preparations (Veral, Glimbax, Gastrotuss, Paxeladine and Brufen) were purchased in local pharmacy. Sample pretreatment included only centrifugation and appropriate dilution.

Results and Discussion

The optimal conditions for separation of studied excipients, i.e. preservatives methylparaben and propylparaben and dye erythrosine on microchip were achieved in a background electrolyte (BGE) with pH 9.8. Complete resolution of the analytes was achieved by complexing agent β-cyclodextrin which was added to the BGE (Fig. 1). Adsorption of the analytes on the walls of a poly(methylmethacrylate) microchip was suppressed by adding of 1 mmol/L sulfate to the injected sample.

The limit of detection (LOD) for the excipients ranged from 0.2 to 2.0 mg/L. High repeatability of the migration times of the analytes in model ($< 2.9\%$ RSD) and real ($< 4.1\%$ RSD) samples were reached under suppressed electroosmotic flow on the microchip. Peak areas of the analytes in all analyzed samples were characterized by RSDs in the range 0.4–5.7%. The developed ZE method was applied to the analysis of three pharmaceutical samples (Gastrotuss, Paxeladine and Brufen) with recoveries of analytes in the range 86–97%. The electropherogram from ZE analysis of pharmaceutical syrup Paxeladine is shown in Fig. 1.
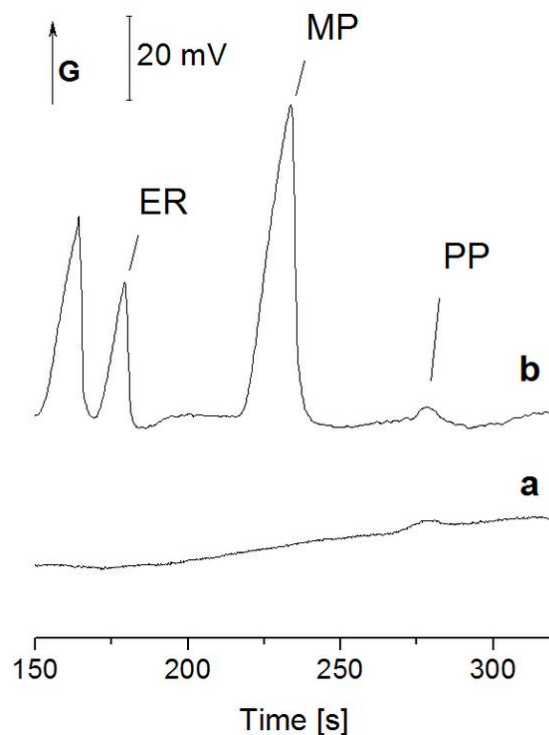
Fig. 1. ZE separation of excipients in pharmaceutical preparation on the microchip. Injected sample: (a) 10% BGE (a blank run); (b) 10-times diluted Paxeladine with 1 mmol/L sulfate in 10% BGE. Driving current was stabilized at 30 μA in the first separation channel. ER - erythrosine, MP - methylparaben, PP - propylparaben, G - conductivity.

The determination of API diclofenac in pharmaceutical preparations was performed by online ITP-ZE combination on the microchip. ITP was realized in first separation channel on microchip. Leading electrolyte at pH 6.5 and terminating electrolyte (TE) at pH 7.4 with TES as a terminating anion were used. BGE at pH 7.0 was favored for ZE separation which was performed in second channel of microchip. Data in Fig. 2 were acquired from the conductivity sensor placed at the end of the second channel.

Intra-day repeatability of diclofenac in model samples calculated on three concentration levels gave RSD for peak areas in the range 0.3–3.1%. RSD values of migration time of the analyte were within 0.4%. The LOD was estimated at 1.4 mg/L. Recoveries of diclofenac in two analyzed pharmaceutical samples (Veral and Glimbax,) were in range 96–99%. Electropherogram in Fig. 2 show the ITP-ZE analysis of pharmaceutical preparation Veral.
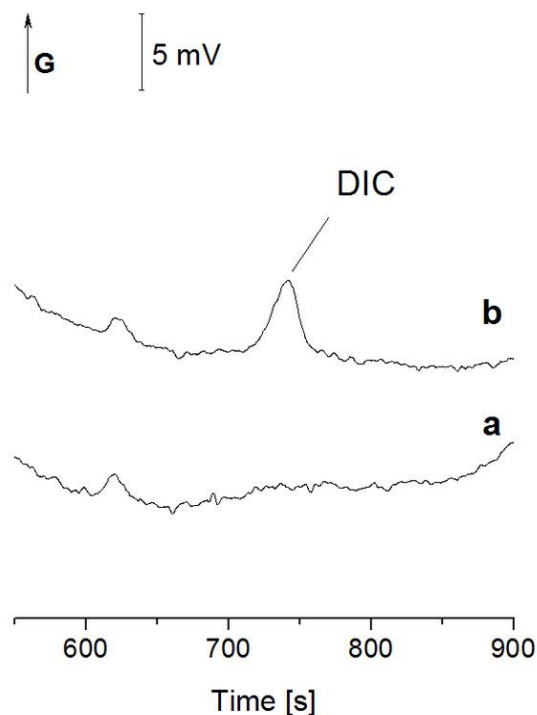
Fig. 2. ITP-ZE analysis of pharmaceutical preparation for a content of diclofenac on the microchip. Injected sample: (a) 10% TE (a blank run), (b) Veral in 10% TE. Concentration of diclofenac in pharmaceutical preparation was ca. 20 mg/L. Driving current was stabilized at 20 μA in the first separation channel and at 25 μA in the second separation channel. DIC - diclofenac, G - conductivity.

Conclusion

The simple and fast miniaturized electrophoretic methods performed on the microchip with conductivity detection have been developed for simultaneous separation and determination of three excipients and determination of API in various pharmaceutical formulations. Only minimum pretreatment steps including centrifugation and appropriate sample dilution prior to the MCE analysis were needed. The developed MCE methods can be used as a good alternative for routine drug analysis and quality control.

Acknowledgement

Reference

[1] Fathima, N., Mamatha, T., Qureshi, H.K., Anitha, N., Venkateswara Rao, J., J. App. Pharm. Sci. 2011, 1, 66-71.

[2] Corrêa de Carvalho, R., Pereira Netto, A.D., Marques, F.F.D.C., Microchem. J. 2014, 117, 214-219.

[3] Podar, A., Suciu, Ş., Oprean, R., Farmacia 2016, 64, 159-170.

[4] Nuchtavorn, N., Suntornsuk, W., Lunte, S.M., Suntornsuk, L., J. Pharm. Biomed. Anal. 2015, 113, 72-96.

[5] Hradski, J., Chorváthová, M.D., Bodor, R., Sabo, M., Matejčík, Š., Masár, M., Anal. Bioanal. Chem. 2016, 408, 8669-8679.

P54   NOVEL ELECTROPHORETIC ACETONITRILE-BASED SAMPLE STACKING FOR SENSITIVE MONITORING OF DIFFERENT KINDS OF PHARMACEUTICALS IN BLOOD PLASMA

Petr Tůma

Charles University, Third Faculty of Medicine, Department of Hygiene,
petr.tuma@lf3.cuni.cz

Summary

Four completely new electrophoretic methods were developed for the sensitive determination of commonly used pharmaceuticals in human or rat plasma. All determinations are coupled with the novel kind of acetonitrile based sample stacking. All methods are characterised by a low limit of detection and simple sample pretreatment: i) the antiepileptic drug perampanel is determined in the background electrolyte 50 mM chloroacetic acid (pH 2.15), LOD 0.008 µM; ii) the antibiotic ceftazimide is determined in 50 mM chloroacetic acid dissolved in 20% MeOH (pH 2.32), LOD 0.08 µM; iii) the antimicrobial agent pentamidine is determined in 100 mM acetic acid/Tris (pH 4.7), LOD 0.03 µM; iv) the antidiabetic drug metformin is determined in 2.0 M acetic acid (pH 2.15), LOD 0.03 µM.

Introduction

Quantitative measurements of the drug in small sample volumes obtained from humans or other living organisms must be carried out using microanalytical techniques that are capable of reproducibly while working with several microliters of body fluid taken sequentially from the studied object [1]. In addition, body fluids represent a very complicated matrix, for whose analysis is necessary to use an effective separation technique of drug substance from the other components of the biological sample prior the detection. All these preconditions are satisfied by the capillary electrophoresis (CE). The main disadvantage of CE, which limits its broader use in bioanalysis, consists in its low concentration sensitivity combined with the commonest UV/Vis photometric detection or contactless conductivity detection (C^4D) that varies at the level of $10^{-5} - 10^{-6}$ M. However, for pharmacological purposes, it is often necessary to determine plasmatic levels of drug at micromolar to submicromolar concentration levels. This unfavourable state of affairs can be relatively easily overcome by an implementation of on-line preconcentration technique, so called stacking.

Experimental

All electrophoretic measurements were carried out using the Agilent 7100 Capillary Electrophoretic System (Agilent Technologies, Waldbronn, Germany) equipped with three independent detectors, which detection cells are placed directly in the electrophoretic cassette maintained at a constant temperature of 25 °C. CE separations were performed in fused-silica capillaries (Composite Metal Services, UK) with outer diameter 363 µm and minimal length 31.5 cm (35 cm in combination with fluorescence detector). All capillaries are i) dynamically coated by INST-coating solution [2], or ii) permanent hydroxypropyl cellulose coating made in laboratory [3] is implement to reduce the EOF. All chemicals are of analytical grade of purity and deionized water is use for preparation of BGE and other solutions. Optimized experimental conditions are briefly summarized here and the detailed description is provided in original papers:

i) Determination of the antiepileptic drug perampanel is performed in background electrolyte (BGE) consisted from 50 mM chloroacetic acid with addition of 0.5% *m/v* polyvinylalcohol (pH 2.15) [4]. Separation is performed in 50 µm capillary under application of voltage +30 kV. Human serum samples (25 µL) treated by the addition of acetonitrile (ACN) in a ratio of 1:3 v/v were hydrodynamically injected into the capillary by pressure 50 mbar for 120 s that corresponded to the length (129 mm) of the sample zone. A fluorescence detector with a broad excitation filter (240 - 400 nm) and an emission filter (495 nm) was used for visualisation of the native fluorescence of perampanel; a fluorescence detector ARGOS 250 B (Flux Instrument, Switzerland) [5].

ii) The monitoring of the antibiotic ceftazidime in human blood was made in optimized BGE composed of 50 mM chloroacetic acid + 20% *v/v* methanol + 0.5% *v/v* INST coating solution [6]. The separation in 25 µm capillary was controlled by a maximum voltage of + 30 kV and the movement of the analyte was accelerated by a pressure of 50 mbar. 33.3 µL of plasma sample was deproteinized by 100 µL of acidified ACN with 0.01 M HCl. Samples were injected by a pressure impulse of 100 mbar for a period of 30 s (5.4% of the total length of the capillary). UV radiation absorbing ceftazimide is monitored by diod-array detector at selective wave length equalled 260 nm.

iii) The anti-microbial agent pentamidine is separated in the 50 µm capillary coated with covalently bound hydroxypropyl cellulose; the BGE was 100 mM acetic acid/Tris at pH 4.7; voltage +15 kV [7]. 12.5 µL of plasma treated by the addition of ACN in a ratio of 1:3 *v/v* was injected into the capillary by pressure of 50 mbar for 120 s that correspond to 28.3 % of the capillary length. UV absorbing pentamidine with two benzene rings is visualized by diod-array detector at selective length 260 nm.

iv) The determination of metformin, that is routine used for treatment of patients suffering from type II diabetes mellitus, was performed in 50 µm INST-coated capillary in 2.0 M acetic acid (pH 2.15) as BGE under voltage of +20 kV [8]. 100 µL of human serum is treated by 300 µL of ACN acidified with 0.01 M HCl and consequently injected into the capillary by pressure 50 mbar for 20 s, corresponding to a sample zone with a length of 22.9 mm. The UV-Vis radiation

non-absorbing metformin was detected by contactless conductivity detector worked at frequency 1 MHz [9].

Results and Discussion

Here is described an effective stacking technique, which certainly need not be useful for only this specific kind of drug substances, but has more general applications, as we demonstrated in the determination of neurotransmitters [10] or branched chain amino acids [11]. Detailed instructions follow for performance of a novel ACN based sample stacking:

i) Plasma or some other body fluid with high NaCl content is diluted with ACN in a ratio from 1:3 to 1:5 *v/v*. The addition of ACN not only deproteinization the biological sample, but also reduces its electrical conductivity for stacking process. The treated sample is then injected hydrodynamically into a capillary with zone length of 1 to 100% of the total length of the capillary.

ii) Then the electrophoretic stacking is turned on by application of the separation voltage with simultaneous forcing of the ACN zone out of the capillary. The voltage is gradually increased linearly over a time equal to 90% of the time used for injecting the sample. The ACN zone is forced out of the capillary by constant negative pressure of the same magnitude as the injection pressure, in the opposite direction. The time employed for forcing out ACN equals 110% of the injection time. The pressure impulse prolonged by 10 %, which is used for forcing ACN out of the capillary compared with the impulse for injection of the sample, is intentional and ensured complete forcing of all the ACN out of the capillary. A sharper increase in the separation voltage over a time is by 10 % shorter than the injection time and ensures rapid migration of the analyte from the sample zone and prevents its loss during forcing out ACN. However, the proposed times can differ from one application to the next; nonetheless, in general it holds that: a) the pressure impulse used for forcing out should be longer than the impulse used for injecting the sample; b) the maximum separation voltage should be attained before ACN is forced out of the capillary.

iii) The actual stacking can be explained that drug substances migrates faster in the sample zone with suppressed conductivity than in the BGE zone and its concentration is thus increased at the ACN/BGE boundary. In addition, the conditions for transient isotachophoresis are met as a result of the presence of sodium ions from the biological solution; sodium ions take on the role of leading electrolyte and the slowly migrating analyte accumulates at its rear boundary. Suitable conditions for temporary isotachophoresis occur very frequently because most cationogenic analytes have lower mobility compared to sodium ions. The entire process is depicted schematically in Fig. 1.
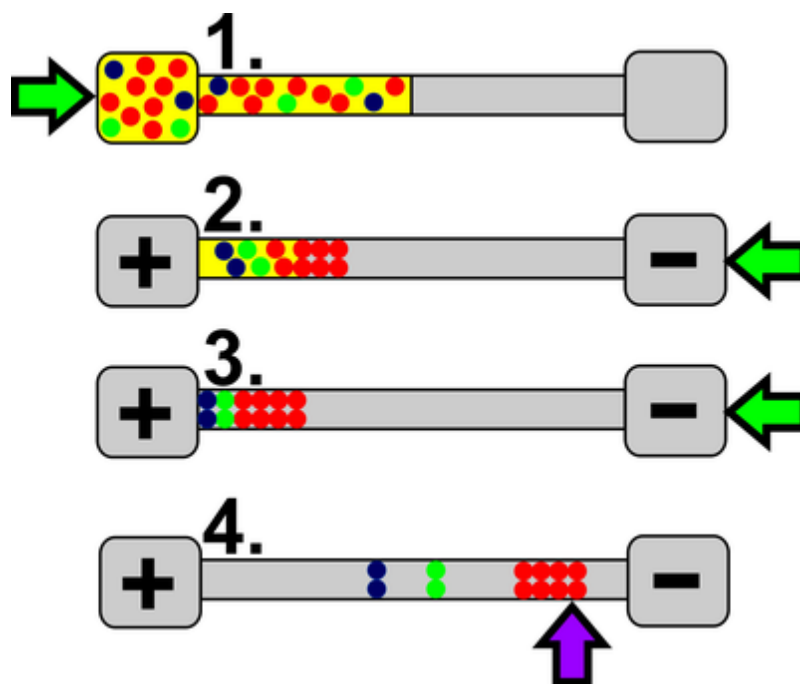
Fig. 1 ACN stacking of clinical samples: 1. Large volume sample injection into separation capillary by pressure; 2. Focusing of the ions in the sample zone by the electric field with simultaneous forcing of the ACN zone out of the capillary by pressure application into terminal vial; 3. Finalization of sample stacking; 4. Electrophoretic separation of stacked sample zone. Color differentiation: analytes (blue and green), sodium (red), ACN (yellow), BGE (grey), pressure (green - arrow), detection (purple - arrow).

The main separation characteristic of developed CE methods are summarized in Table 1 and illustrative separation of human or rat plasma sample are documented in Fig. 2.

Table 1

The main separation characteristic of developed methods

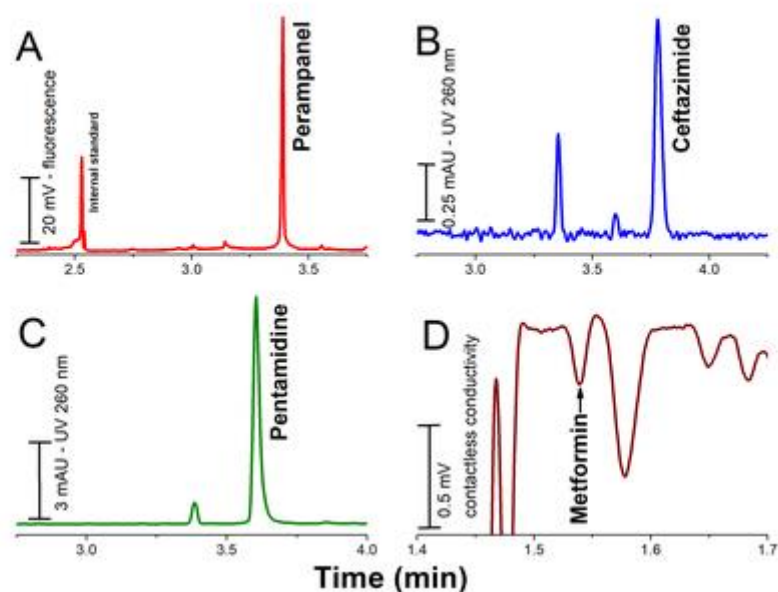| Analyte	BGE	Capillary - length (cm)/id (µm)	Injection length, mm	Detection	LOD, µM
Perampanel	50 mM chloroacetic acid, pH 2.15	35/50	129	fluorescence	0.008
Ceftazimide	50 mM chloroacetic acid in 20% MeOH, pH 2.32	31.5/25	86	UV	0.8
Pentamidine	100 mM acetic acid/Tris, pH 4.7	31.5/50	89	UV	0.03
Metformin	2.0 M acetic acid, pH 2.15	31.5/50	23	conductivity	0.03

Fig. 2 Illustrative electropherograms, A – CE/fluorescence determination of antiepileptic drug perampanel in human plasma (241 ng/mL); B – CE/UV determination of antibiotic drug ceftazidime in human plasma (6 µg/mL); C – CE/UV determination of antimicrobial agent pentamidine in rat plasma (14.2 µM); D – CE/contactless conductivity determination of antidiabetic drug metformin in human plasma (4.4 µM).

Conclusion

CE constitutes a very strong instrument for monitoring different kind of drugs in the complex clinical matrix. Low requirements on the amount of clinical sample and its simple treatment also permit performance of pharmacological experiments on small laboratory organisms. High sensitivity of the determination characterised by low LOD can be attained using the application of the novel kind of ACN based sample stacking. This stacking requires suppression of the conductivity of the clinical sample by addition of ACN, simultaneous application of the separation field and hydrodynamic pressure during the separation with effective suppression of the electroosmotic flow.

Acknowledgement

Reference

[1] Nandi, P., Lunte, S. M., Anal. Chim. Acta 2009, 651, 1-14.
[2] Tůma, P., J. Sep. Sci. 2014, 37, 1026-1032.
[3] Shen, Y. F., Smith, R. D., J. Microcolumn Sep. 2000, 12, 135-141.
[4] Tůma, P., Bursová, M., Sommerová, B., Horsley, R., Čabala, R., Hložek, T., J. Pharm. Biomed. Anal. 2018, 160, 368-373.

[5] Tůma, P., Opekar, F., Analytical Separation Science, Wiley-VCH Verlag GmbH & Co. KGaA 2015.

[6] Tůma, P., Jaček, M., Fejfarová, V., Polák, J., Anal. Chim. Acta 2016, 942, 139-145.

[7] Tůma, P., Heneberg, P., Vaculín, Š., Koval, D., Electrophoresis 2018, 39, in press.

[8] Tůma, P., J. Chromatogr. A 2014, 1345, 207-211.

[9] Tůma, P., J. Sep. Sci. 2017, 40, 940-947.

[10] Tůma, P., Šustková-Fišerová, M., Opekar, F., Pavlíček, V., Málková, K., J. Chromatogr. A 2013, 1303, 94-99.

[11] Tůma, P., Gojda, J., Electrophoresis 2015, 36, 1969-1975.

P55 SURFACE ENHANCED RAMAN SPECTROSCOPY: DETECTION PLATFORMS FOR SAMPLE ANALYSIS WITH AND WITHOUT ELECTROPHORETIC SEPARATION

Anna Tycova[1,2], **Jan Prikryl**[1], **Frantisek Foret**[1], **Detlev Belder**[2]

[1]Institute of Analytical Chemistry of the CAS, v. v. i., Brno, Czech Republic, tycova@iach.cz

[2]Institute of Analytical Chemistry, University of Leipzig, Leipzig, Germany

Summary

In this work we present two platforms of relatively simple construction for user-friendly sample detection via surface enhanced Raman spectroscopy (SERS). The first platform is designed for direct sample analysis and deals with hydrophilic spots array within a hydrophobic surface. The second presented platform aims on analysis of samples of higher complexity requiring separation step prior the detection. This is achived via microfluidic electrophoretic device with online SERS detection.

Introduction

Surface enhanced Raman spectroscopy (SERS) belongs among fast developing tools for definite identification and quantification of analyte [1]. The SERS signal has origin in inelastic scattering of photons interacting with investigated molecule changing its rotational-vibrational states. Although the inelastic scattering is in comparison to other spectral phenomena very rare, its intensity can be significantly increased if the analysed molecules are in close proximity of the surface of metal nanostructures.

The SERS provides spectral bands of relatively narrow profile. Thus, in some cases more analytes might be identified from a single spectrum. However, separation is vital for more complicated mixtures or in case of presence of interfering agents.

In this work, two devices with SERS detection of relatively simple construction are presented. A platform for data collection from sample droplets (offline detection) and a device for efficient sample separation via microfluidic capillary electrophoresis (online detection) are introduced. The potential of both approaches is shown on the example of analysis of riboflavin from food samples.

Experimental

A platform for off-line SERS spectra measurement was fabricated from a microscopic glass slide. After plasma activation, the glass was exposed for 5 minutes to vapours of trichloro(1H,1H,2H,2H-perfluorooctyl)silane (Sigma Aldrich, USA) and baked on a hot-plate (10 min, 110°C) achieving stable and strongly hydrophobic surface. This surface was removed on several places via sand blasting using a metal mask with holes of 1 mm diameter. The diameter of the sand was within the range of 20-60 µm and was introduced to the glass surface at pressure of 2.4 bar. This way a hydrophilic array of 91 spots was created particularly suited for SERS analysis of polar (i.e. water-based) samples (Fig. 1). The whole fabrication process did not take more than 20 minutes.
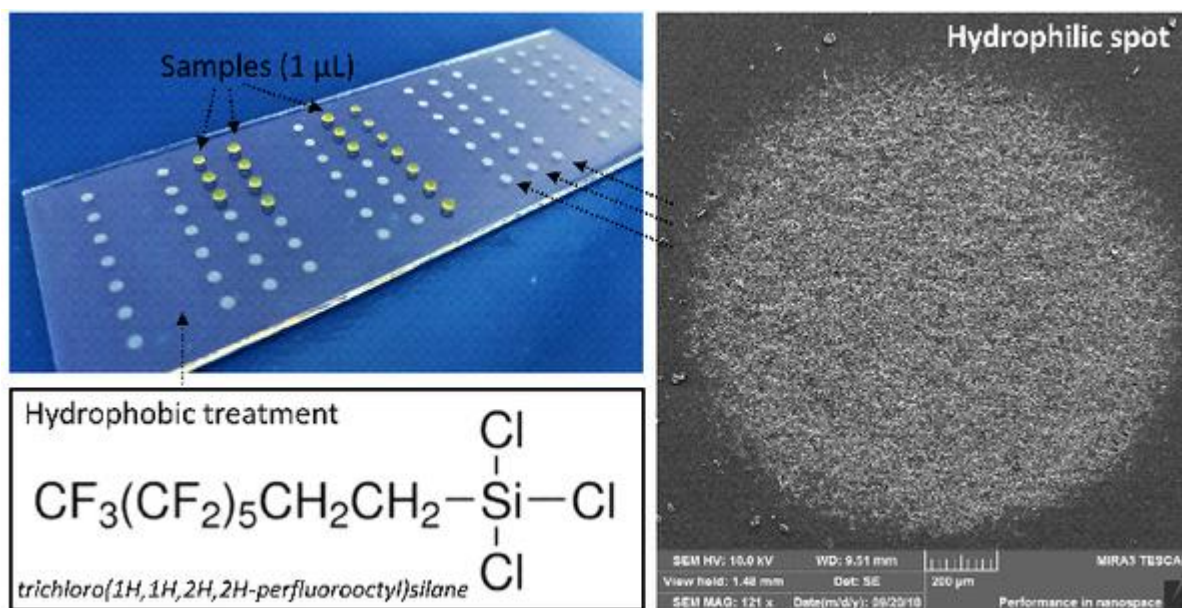
Fig. 1: A glass platform used for collection of water-based samples.

The chip for microfluidic capillary electrophoresis (MCE) with online SERS detection was prepared from glass slides by standard wet etching procedure in detail described elsewhere [2]. The channel dimensions were 30×110 and 30×210 µm before and after the dosing unit, respectively (Fig. 2A). The sample was loaded via pinched injection and analysed using voltage conditions given in Fig. 2B. A solution of 20 mM 3-(N-morpholino)propanesulfonic acid (MOPS) of pH = 6.5 acted as a BGE.

The SERS experiments were conducted on an IX-71 epifluorescence microscope (Olympus, Japan), which was part of a modular confocal Raman system using laser of 473 nm (50 mW, Cobolt, Sweden). The accumulation time was set on 250 ms. The silver nanoparticles were synthetized via reduction of silver nitrate with sodium citrate according to the standard Lee-Meisel protocol. The absorption spectra of nanoparticles provided λmax = 430 nm and FWHM of 150 nm.

Riboflavin was analysed from two food samples (pudding and barbeque sauce), in both acting as a food colorant. The vanilla pudding (Dr. Oetker, Germany) and American barbeque sauce (J.H. Heinz, Germany) was dissolved in concentration of 0.5 mg/mL and 1 mg/mL in 5 mM NaOH and centrifuged. The supernatant was before analysis filtered through 0.22 µm filter.

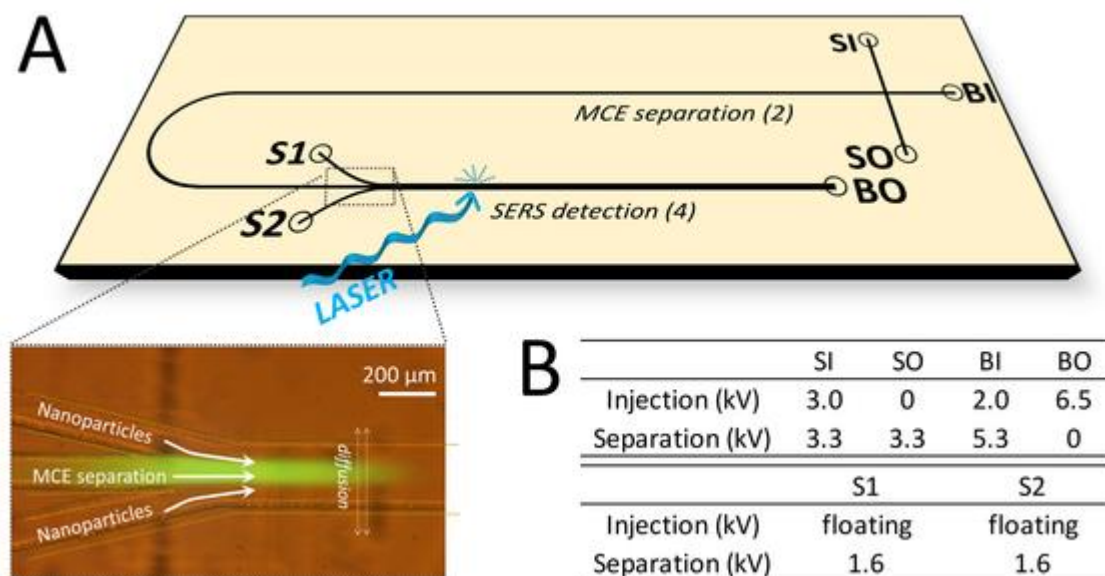Fig. 2: A - Design of MCE-SERS device with dosing unit located 90 mm after the injection cross. B - Voltage conditions for sample injection and separation. BI - BGE inlet, BO - BGE outlet, SI - sample inlet, SO - sample outlet, S1 and S2 - side channels 1 and 2.

Results and Discussion

The SERS signal can be collected directly from a sample in cases, where no interfering agents are present in a sample. Besides experimental simplicity, offline arrangement brings possibility to increase time for signal accumulation improving S/N ratio.

Here, we present a simple platform for measurement of samples from droplets of 1 µL volume. The platform is based on an array of hydrophilic spots (approximate diameter of 1.4 mm) within a silanized hydrophobic area. This approach minimizes droplet spreading and helps to unify SERS signal. The platform has a disposable character decreasing the risk of memory effect. One row consists of seven spots aimed for repeated analysis of one sample to obtained data unbiased of possible signal fluctuation. However, the design can be easily adjusted for a particular application – e.g. to fit the dimensions for multichannel pipetting.

This platform has great potential if no separation is necessary and/or when only minimal volume of sample is available. Analysis of riboflavin from a vanilla pudding demonstrate such a case. After simple pre-treatment the sample was mixed with concentrated silver nanoparticles (3.2 mg/mL of silver) and easily measured from a droplet (Fig. 3A).

However, for samples of higher complexity a separation would be requested to achieve removal of interference agents. Microfluidic capillary electrophoresis represents a very fast and efficient separation method particularly suited for separation of charged entities. However, nanoparticles needed for Raman signal enhancement can negatively influence the separation process. To avoid this, a dosing structure was designed, where two side channels joined the separation channel in the distance of 90 mm from the injection cross (see Fig. 2A). These channels supplied colloid (3.2 mg/mL of silver) into separated zones. Thus, the separation and detection process was decoupled. In online mode, there is necessary to consider the time of signal accumulation. The long time would result in improved S/N ratio; however, the separation peak would be significantly deformed due to insufficient amount of data points (Fig. 3C).
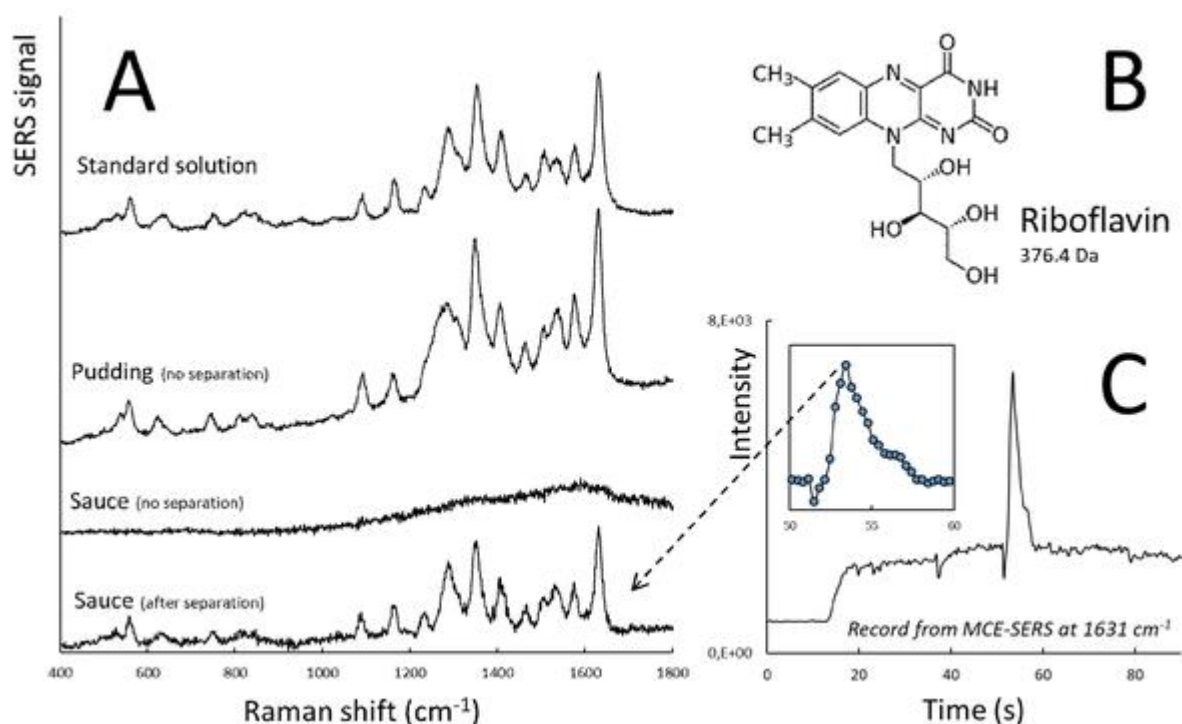
Fig. 3: A - Various samples containing riboflavin analysed from a droplet or online as a zone after MCE separation. B - Structure of riboflavin. C - MCE-SERS record of analysis of barbeque sauce. The inserted window shows frequency of data points.

The strategy of sample separation was used for analysis of riboflavin from a barbeque sauce. The importance of separation is depicted in the Fig. 3A. No reasonable signal from unseparated sample was obtained due to strong interference of chlorides, presented in the sauce. On contrary, the MCE-SERS was able to remove chlorides easily revealing clear riboflavin spectrum.

Conclusion

Two various approaches towards SERS detection were in this work presented. Whereas platform with hydrophilic spots array represents user-friendly strategy for direct analysis of

sample without prior separation, microfluidic electrophoretic chip is a promising tool for in-time detection.

Acknowledgement

Reference

[1] Xi, W. J., Shrestha, B. K., Haes, A. J., Anal. Chem. 2018, 90, 128-143.
[2] Tycova, A., Gerhardt, R. F., Belder, D., J. Chromatogr. A 2018, 1541, 39-46.

P56 PURIFICATION OF HUMAN TELOMERASE TEN DOMAIN AND ITS INTERACTION PARTNER TPP1

Pavel Veverka, **Martin Stojaspal, Tomas Janovic, Ctirad Hofr**

LifeB (Chromatin Molecular Complexes, CEITEC and Functional Genomics and Proteomics, National Centre for Biomolecular Research, Faculty of Science, Masaryk University, Brno, Czech Republic), pavel.veverka@ceitec.muni.cz

Summary

The telomerase adds telomeric repeats to chromosome ends to act against telomere shortening. Telomerase activation contributes to the immortality of cancer cells. Therefore, telomerase inhibition is an attractive target for cancer therapy. In this study we show initial results of preparation of recombinant construct of TEN domain from human telomerase and human protein TPP1 from shelterin complex, which is responsible for telomerase recruitment to telomeres and promotion of an effective DNA synthesis.

Introduction

Every cell division leads to duplication of its DNA. However polymerase cannot replicate very ends of chromosomes. This leads to telomeric DNA shortening during every replication. Human telomeres consist of tandem TTAGGG repeats and associated proteins. In normal cells, approximately 100 bases of telomeric DNA are lost during every cell division [1]. Telomeres shorten in most somatic cells with age and the shortening to a certain length leads to senescence and cell death via apoptosis. Telomeres in fast dividing cells such as cancer cells, stem cells, and germline cells do not shorten with progressive divisions. It is due to the activity of the enzyme called telomerase. Telomerase is usually inactive in somatic cells. However, cancer cells show usually high activity of telomerase [2] (Scheme 1A). Telomerase contributes to the immortality of cancer cells. Thus, the controlled suppression of telomerase activity in cancer cells would contribute to the more efficient defeat of tumour growth [3, 4]. Therefore, telomerase inhibition is an attractive target for cancer therapy.

Telomerase

Telomerase is an enzyme that extends telomeric DNA by adding short nucleotide repeats at the 3'- ends of chromosomes. Human telomerase contains two essential subunits: telomerase reverse transcriptase catalytic subunit (hTERT), and a functional telomerase RNA (hTR) (Scheme 2) [5], which serves as a template for telomeric repeats amplifications. The telomerase N-terminal domain (TEN-domain) participates in the catalysis of telomeric repeat addition [6]. The TEN-domain of telomerase has been proposed to mediate recruitment to telomeres [7].

Recent study showed structural data of the catalytic core of telomerase using cryo-electron microscopy [8].
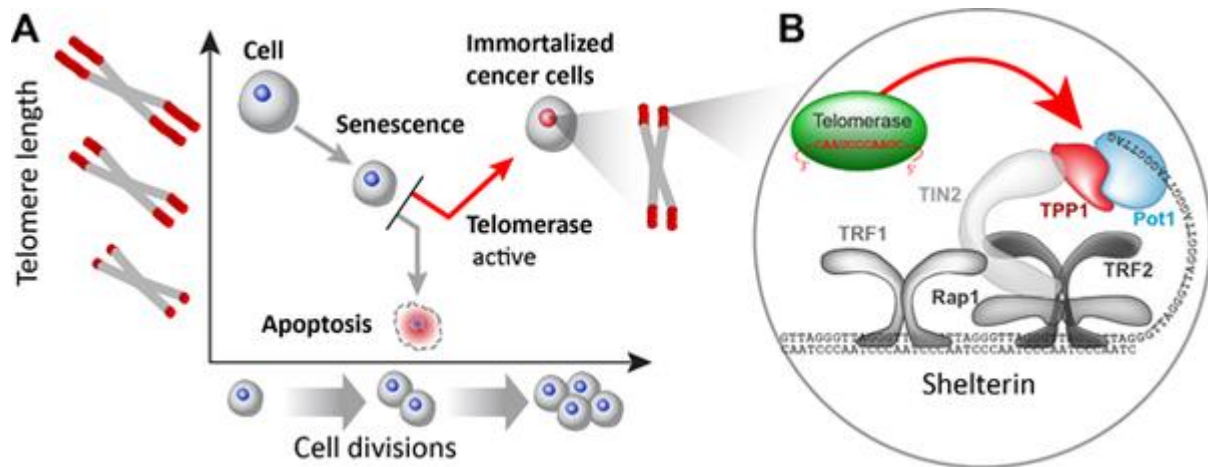

Scheme 1: (A) Telomerase prevents natural shortening of chromosome ends and contributes to the immortalization of cancer cells. Telomeres shorten after each round of cell division. Active telomerase revert cell aging process and contributes to immortalization of cancer cells. (B) Shelterin protein complex binds telomeric DNA and regulates telomerase access to ends of chromosomal DNA. TPP1-Pot1 heterodimer directly interacts with telomerase and affects telomerase activity and processivity.

Shelterin complex

Telomerase access to chromosome ends is regulated by shelterin protein complex (Scheme 1B). Shelterin consists of six unique telomere-specific proteins that associate with the telomeric regions to protect chromosome ends from recombination, end-joining reactions, and degradation [9]. In this study, we are also interested in telomere interaction partner TPP1, which forms heterodimer with protein Pot1. This heterodimer binds the telomeric single-stranded DNA tail [10]. Importantly, TPP1 has been found to recruits telomerase to telomeres and promote high-processivity DNA synthesis [11].

The most recent studies performed on cancer cell lines strongly encourage the development of new cancer therapies that involve selective inhibition of telomerase recruitment and telomerase activity.

Telomere maintenance is crucial for the proliferation of all dividing cells in the human body (including stem cells and cancer cells) [8]. Telomeres elongation is promoted via TPP1 from shelterin complex. There is no published structural in vitro study about interaction between hTPP1 and TEN domain of human telomerase. To describe this interaction in vitro we need both interaction partners. In this study, we describe recombinant preparation of human hTERT-TEN domain and its partner hTPP1.
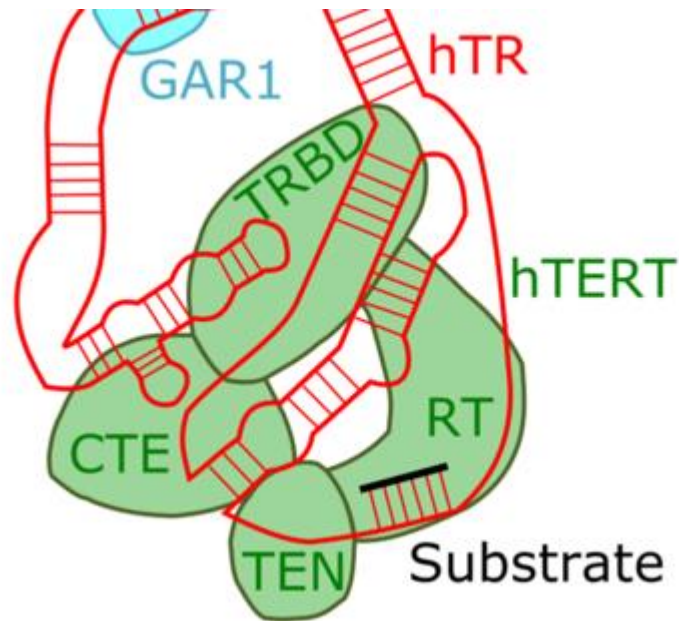
Scheme 2: Schematic of telomerase subunit catalytic core arrangements. hTR - RNA subunit of telomerase interconnects whole hTERT. Adapted from [8].

Experimental

Cloning, expression and purification of hTPP1

For interaction studies was prepared recombinant human TPP1 protein with an N-terminal deletion: TPP1(89-544). It was used because the 87 N-terminal residues of TPP1 are functionally dispensable in human [12]. For simplicity, we hereafter use TPP1 to represent TPP1(89-544) unless stated otherwise.

TPP1 was cloned into pRbxKan5_X105 vector with 6xHistidine purification tag and rubredoxine tag for better stability and solubility. Expression was done in Escherichia coli BL21(DE3)RIPL in Luria-Bertani medium at 37° C until A600 reached 0.5. The protein expression was initiated by addition of IPTG (isopropyl-β-D-thiogalactopyranoside) to a final concentration of 0.5 mM. The cells were cultured for 3 h at 15° C

after induction. Cells were harvested by centrifugation at 8000 g for 8 min at room temperature. Pellet was dissolved in Lysis buffer containing 50 mM sodium phosphate, pH 8.0, 500 mM NaCl, 10 mM Imidasole, 0.5% Tween-20, 10% glycerol along with protease inhibitor cocktail cOmplete tablets EDTA-free (Roche). The cell suspension was sonicated for 3 min of process time with 1 s pulse and 2 s of cooling on ice (Misonix). Cell supernatant was collected after centrifugation at 20 000 g, 4° C for 1 h and filtrated with 0.45 um filters. Chromatographic column with Talon resin was pre-equilibrated with Lysis buffer. Protein of our interest was eluted at 300 mM imidazole in the same buffer without Tween-20.

After elution was added HRV3C protease to remove purification tags. Cleavage was perform overnight at 4° C. Protein of desire was separated using size exclusion chromatography with

HiLoad 16/600 column containing Superdex200 pg (GE Healthcare Life Sciences) and resolved using 50 mM sodium phosphate buffer pH 7.0 with 800 mM NaCl.

Protein was concentrated and the buffer was exchanged to 50 mM sodium phosphate pH 7.0 and 150 mM NaCl by ultrafiltration (Amicon 3K/30K, Millipore).

The concentration of purified proteins was determined by Bradford assay. We evaluated protein purity by SDS-polyacrylamide gels stained by Bio-Safe Coomassie G 250 (Bio-Rad). Western blotting, using monoclonal Anti-polyHistidine antibody produced in mouse and Fc-specific Anti-Mouse IgG-peroxidase antibody produced in goat (Sigma Aldrich), confirmed the presence of the tagged protein of our interest. Quantitative mass spectrometry analyses confirmed appropriate purity of the obtained protein for further studies.

Cloning, expression and purification of hTERT-TEN

In case of hTERT-TEN domain was prepared so far in 14 different constructs. As candidates were selected from N-terminal part first 179, 185 and 200 amino acids from human telomerase coding DNA sequence. Cloning into plasmid for bacterial expression was done with original unoptimized and later codon optimised (Biomatik) human telomerase TEN domain DNA sequence. Protein of interest had several combination of expression tags on N- or C-terminal. Expression and purification was carry out in Escherichia coli BL21(DE3)RIPL with same conditions as described TPP1 above.

We have also performed expression in insect cells Spodoptera frugipera SF9 using baculovirus expression system. Desired protein DNA was cloned into pFastBac vector suitable for recombinant reaction. This plasmid is suitable for bac-to-bac system (Thermofisher). Expression was done at 1L or 2L of Insect-XPRESS medium with L-Gln (Lonza) after initial viral budding. Recombinant protein is produced, when infection occurs in the cell culture. When viability dropped below 80 % cells were harvested by centrifugation at 1500 g for 20 min at room temperature.

Purification of TEN domain was performed via many different steps and conditions. As buffering agents were used: PIPES pH 6.1, PIPES pH 7.5, HEPES pH 7.5, MOPS pH 7.5, Phosphate pH 6.0 or Phosphate pH 8.0 in combination with 0%, 5% or 10% glycerol. Concentration of NaCl were 500 mM or 800 mM. 15mM imidazole was added when purification was perform through 6xHis tag.

Cells (from bacteria or insect cells) were resuspended in selected buffer with addition of 1 mM PMSF (phenylmethane sulfonyl fluoride), 1 mM Benzamide and 2 mM DTT (Dithiothreitol) with protease inhibitor cocktail cOmplete tablets EDTA-free. The cell suspension was sonicated for 4 min of process time with 1 s pulse and 3 s while cooling on ice. Soluble fraction was separated via centrifugation at 20 000 g (for bacterial cells lysate) or 50 000 g (for insect cells lysate), 4° C for 1 h and filtrated with 0.45 µm filters. Chromatography column with sorbent Talon or Amylose resin was pre-equilibrated with selected buffer.

Tag removal was done in solution after elution (300 mM imidazole (6xHis tag) or 10 mM maltose (MBP tag)) or with protein still bounded to chromatography resin. HRV3C protease (MBP tagged variant) or UlpI protease (SUMO tagged variant) was used to cleave out tags with incubation at 4° C (2 h, 4h or overnight). As final step were performed ionic exchange chromatography (also tried with heparin columns) and size exclusion chromatography with selected buffers with lower salt concentration.

Results and Discussion

We have successfully prepared recombinant hTPP1 from bacterial expression.

In case of TEN domain is very hard to prepare soluble recombinant peptide without solubility and stability expression tags. Codon optimized expression in E. coli doesn't work, as 99 % of desired protein is in insoluble fraction according to previous study [13]. They used in the end variant with expression tag and performed experiment with tag itself as negative control. In the beginning, we used unoptimized DNA sequence of TEN domain but we have obtained no observable expression in E. coli.

Subsequently, we have successfully prepared soluble form of codon optimised TEN domain fused with SUMO tag for better solubility together with 6xHis tag on its N-terminal part. We have encountered unspecific cleavage ability of UlpI SUMO protease. First 16 amino acids were missing after cleavage according to mass spectrometry analysis. After tag cleavage, TEN domain coagulated immediately. It is probably because SUMO tag can significantly increase solubility of recombinant proteins and after cleavage the solubility of TEN is low.

We have also used insect cells and baculovirus expression systems. Only soluble construct from prepared constructs was the one with N-terminal MBP tag + 6xHis. Tag cleavage was carried out via HRV3C sequence specific protease. Unfortunately, after tag cleavage, TEN domain remained bound to MBP tag. Small part of TEN domain around 10 % was immediately coagulated probably because its basic nature – isoelectric point for TEN domain alone is 10.6 and constructs with MBP tag + TEN domain has isoelectric point around 7.2. We have also tried many buffers with different pH to avoid this coagulation due to rapid isoelectric point change – but so far without success.

We have been preparing constructs for mammalian cells expression of TEN domain. We believe that it may overcome previous expression troubles. We plan to carry out co-expression with hTR of telomerase to increase TEN domain stability after expression tags cleavage.

Another planed approach is to perform basic experiments with still interconnected stability and solubility purification tags and perform negative control with these tags without TEN domain, as was showed in previous study [13].

Conclusion

In this initial study, we showed successful hTPP1 purification steps. In case of TEN domain of human telomerase we are still searching for soluble and active recombinantly prepared peptide. So far, we have done many optimization steps without major success. We have selected two working constructs: one with SUMO tag for bacterial expression and another one with MBP for insect cell expression. In both cases TEN domain is immediately coagulated after cleavage of solubility improving tags. We believe that it is important to share with scientific community our experience with rather problematic preparation of human telomerase TEN domain.

Acknowledgement

Reference

[1] Harley, C. B., Futcher, A. B., Greider, C. W., Nature 1990, 345(6274), 458-60.

[2] Borah, S., Cech, T. R. at al., Science 2015, 347(6225), 1006-10.

[3] Shay, J. W., Wright, W. E., FEBS Lett. 2010, 584(17), 3819-25.

[4] D'Souza, Y., Chu, T. W. et al., Mol Biol Cell. 2013, 24(9), 1469–1479.

[5] Greider, C. W., Blackburn, E. H., Nature 1989, 337(6205), 331-7.

[6] Wu, R. A., Collins, K., EMBO J. 2014, 33(8), 921-35.

[7] Armbruster, B. N. et al., Mol Cell Biol. 2004, 24(8), 3552-61.

[8] Nguyen, T. H. D. et al., Nature 2018, 557(7704), 190-195.

[9] Wu, L. et al., Cell 2006, 126(1), 49-62.

[10] Baumann, P., Cech, T. R., Science 2001, 292(5519), 1171-5.

[11] Abreu, E., Aritonovska, E. et al., Mol Cell Biol 2010, 30(12), 2971-82.

[12] Wang, F. et al., Nature 2007, 445(7127), 506–510.

[13] Sealey, D. C. F., Harrington, L. A., Nucleic Acids Res. 2010, 38(6), 2019–2035.

P57   EPITACHOPHORETIC SEPARATION AND CONCENTRATION OF LARGE VOLUME SAMPLES

Ivona Voráčová[1], František Foret[1], Vladimíra Datinská[1,2], Jakub Novotný[1], Pantea Gheibi[2], Jan Berka[2], Yann Astier[2]

[1]*Czech Academy of Sciences, Institute of Analytical Chemistry, Brno, Czech Republic*

[2]*Roche Sequencing Solutions, Inc., Pleasanton, USA*

Summary

There has been a growing interest in developing isotachophoretic protocols for concentration and purification of DNA as an alternative to the solid phase extraction protocols of DNA preparation. Also concentration of DNA from large volume samples is required. We have developed a new device suitable for separation, concentration and collection of ions from several milliliter sample volumes into microliter fractions. We have used a discontinuous electrolyte system comprising of the leading and terminating electrolytes utilized for concentration of samples containing DNA fragments. The method is simple, fast with high concentration factor and without extensive surface interactions

Introduction

Recently, concentration and purification of biomolecules such as nucleic acids (NAs) [1], proteins, peptides, metabolites [2] and small organic ions from complex matrix (e.g. blood, plasma, urine, saliva, water and soil extract) and large sample volumes are requested and widely studied. There are many clinical and diagnostic applications requiring pure and high quality NAs for various downstream analytical methods such as next-generation sequencing, quantitative PCR and microarrays. For example, the analysis of cell-free DNA extracted from whole blood and plasma is now widely applied to areas as a non-invasive prenatal testing and the classification of cancer sub-types to inform appropriate therapies [3-6].

Isotachophoresis has emerged as an alternative to the solid phase extraction protocols for quantitative, easy-to-automate, and gentle NA extraction from various sample types. While some of the first published experiments described agarose filled tubes for ITP concentration of DNA sample, most of the recent papers focus on a microfluidic scale [1].

To address the large volume sample capacity we have designed a new device with the circular design of separation channel. The new circular design is able to focus sample volumes up to several milliliters. Whereas the migration velocity of moving boundary and also widths of analyte zones in steady state is not constant we introduce term epitachophoresis for this mode of migration.

Experimental

The newly designed device (Figure 1) was machined from Ertacetal® (Quadrant Plastic Composites GmbH, Lotte, Germany). The wire ring electrode (1 mm diameter stainless steel wire; radius of 55 mm) was attached on the edge of the circular separation compartment. The sample volume was defined by the space between the ring electrode and an agarose stabilized leading electrolyte disk (radius of 35 mm). Thus, the applicable sample volume was 5.7 ml for every mm of its height. The second electrode was placed in the leading electrolyte reservoir on the side of the device.
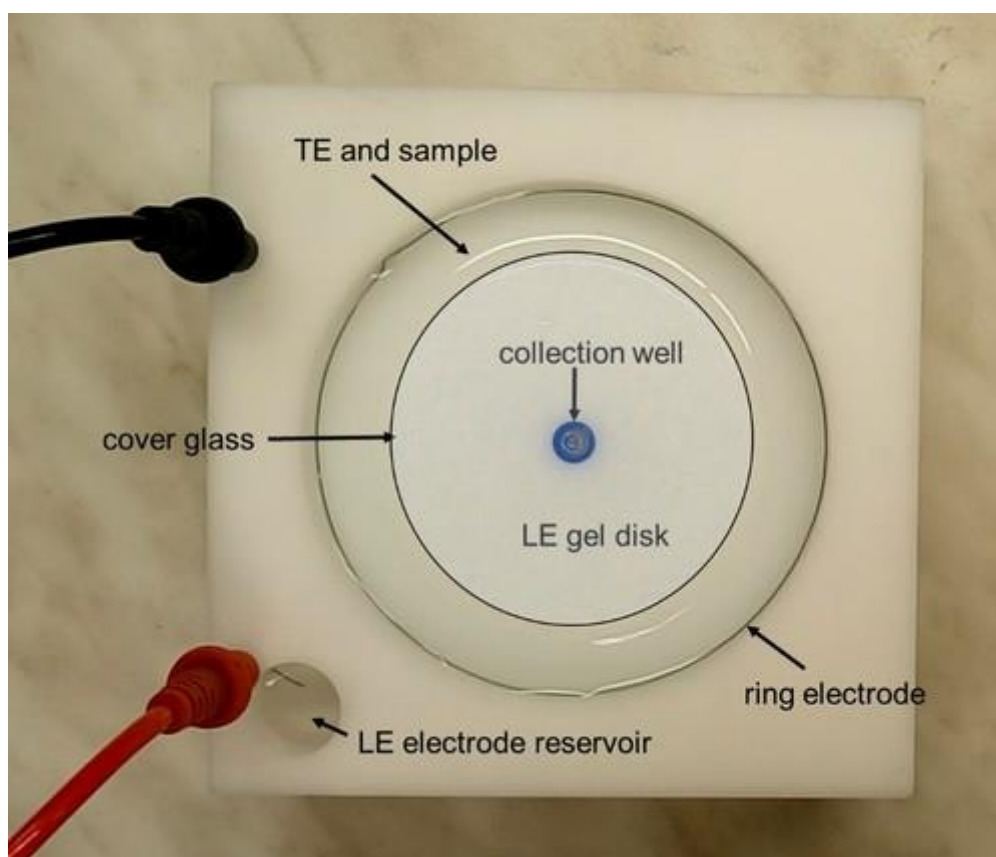
Fig. 1. The device machined from Ertacetal® and its internal structure including the collection membrane cup inserted into the collection well.

For every analysis a half cut plastic vial with a semipermeable membrane (Slide-A-Lyzer™ MINI Dialysis Units 2000 Da MWCO, Thermo Fisher Scientific, USA) was inserted into the central collection well. Next a 0.3% agarose gel disk (70 mm diameter, 4 mm thick) was prepared in 20mM leading electrolyte (HCl-Histidine; pH 6.25), positioned in the center of the device and covered by a 75x1 mm round glass plate also having a center 8 mm hole to avoid bubble accumulation. The sample solution in the terminating electrolyte (10mM TAPS-TRIS, pH 8.30) was applied by a syringe into the space between the gel disk and ring electrode. The polarity of the electric current was selected so that anionic sample components migrated from the ring electrode towards the collection well in the device center. After the focused sample zone entered the collection cup the electric current was turned off and sample pipetted out for

further use. Power supply PowerPac 3000 (BioRad) was run at constant power mode at 2 W. Analysis took approximately 1 hour.

Results and Discussion

Low molecular weight dsDNA ladder (11 fragments from 25 bp to 766 bp from New England BioLabs, USA) was used for experimental testing of proposed device. Nucleic acid fluorescence stain (SYBR™ Gold, in DMSO from Invitrogen, Carlsbad, CA, USA) was used for visualization of DNA ladder during the analysis. The Figure 2 documents the separation recorded at chosen time intervals. The first two pictures demonstrate the formation of the DNA zone on the gel edge. Gradual acceleration of the zone velocity is obvious in last sixteen minutes of analysis. Finally, TE buffer and gel were removed, the central piston was moved to an upper position and the sample was collected from the dialysis unit cup. Collected fractions were further analyzed using the chip CGE-LIF instrument Agilent 2100 Bioanalyzer (Agilent, Santa Clara, CA, United States). Bioanalyzer separation records in the the Fig. 3 show analyses of samples of DNA ladder (standard) and from collected sample documenting that the size distribution of the collected DNA fragments remained the same as in the injected sample. As a result, the sample injected from 15 mL of TE buffer was concentrated to the volume of 200 μl. It should be noted that the volume of the migrating DNA zone prior to entering the collection cup was much smaller (~3 μl) and the final fraction concentration depends mainly on the volume of the collection vial. According to the fluorimetric analysis, it corresponds to the concentration factor of 52 with ~80% recovery.
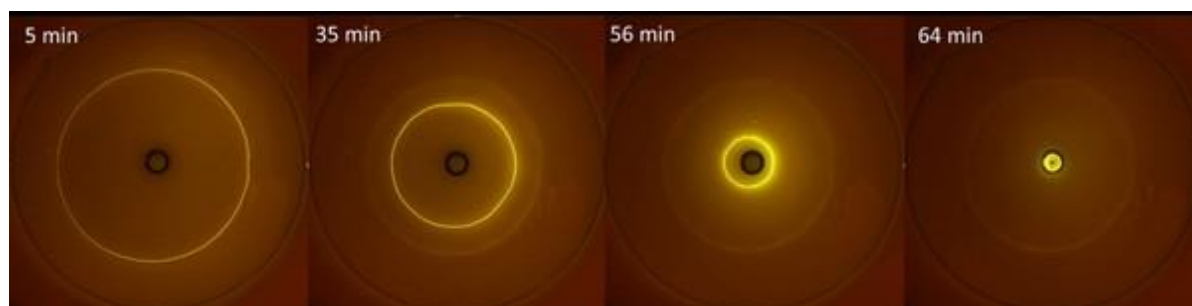

Figure 2: Focusing of a DNA ladder labeled by SYBR gold, LE: 20 ml of agarose gel 0.3% in 20mM HCl/HIS 6.2. TE: 10mM TAPS/TRIS pH 8.30. Sample: 2.5 μg of DNA ladder dissolved in 15 ml of TE. Constant power 2 W.
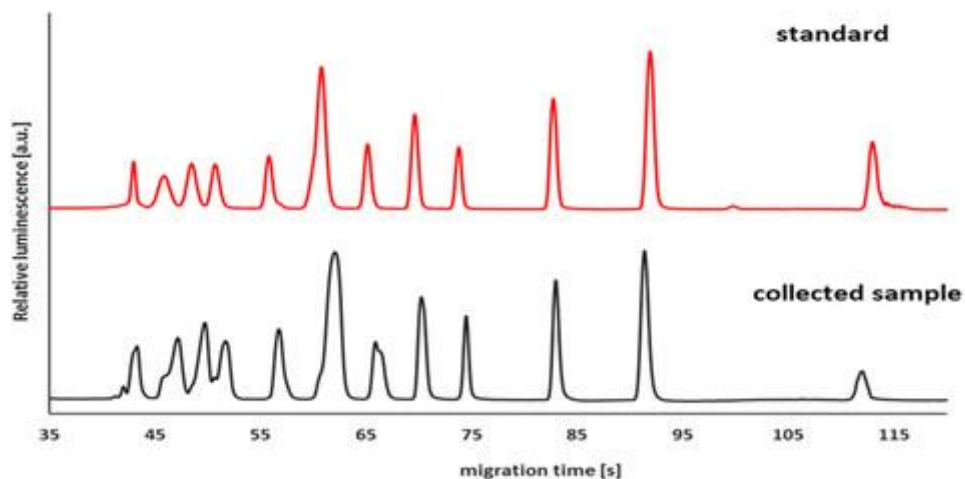
Figure 3: Separation records of DNA ladder from Bioanalyzer. Standard: 2.5 µg of DNA ladder dissolved in 200 µl of water, Collected sample: 2.5 µg of DNA ladder dissolved in 15 ml of TE, focused by circular epitachophoretic device to 270 µl

Conclusion

We designed and fabricated a new device based on moving boundary electrophoresis principle, suitable for focusing of large sample volumes (up to 15 milliliters). The device provides high recovery and concentrates the DNA in a microliter volume collection cup for easy recovery for further use. Compared to the solid phase DNA extraction methods the electrodriven separation is simple, fast with high concentration factor and without extensive surface interactions. In a non-sieving separation media all DNA fragments can be focused in one zone.

Acknowledgement

Reference

[1] Datinská, V., Voráčová, I., Schlecht, U., Berka, J., Foret, F., J Sep Sci 2018, 41, 236-247.

[2] Wang, C. C., Chiou, S. S., Wu, S. M., Electrophoresis 2005, 26, 2637-2642.

[3] Allison, M., Nat Biotechnol 2013, 31, 595-601.

[4] Wan, J. C. M., Massie, C., Garcia-Corbacho, J., Mouliere, F., Brenton, J. D., Caldas, C., Pacey, S., Baird, R., Rosenfeld, N., Nat Rev Cancer 2017, 17, 223-238.

[5] Underhill, H. R., Kitzman, J. O., Hellwig, S., Welker, N. C., Daza, R., Baker, D. N., Gligorich, K. M., Rostomily, R. C., Bronner, M. P., Shendure, J., Plos Genet 2016, 12.

[6] Snyder, M. W., Kircher, M., Hill, A. J., Daza, R. M., Shendure, J., Cell 2016, 164, 57-68.

P58 TEMPERATURE-PROGRAMED MICRO-HPLC ANALYSIS OF FATTY ACID METHYL ESTERS WITH APCI-MS DETECTION

Vladimír Vrkoslav[1], Barbora Rumlová[1,2], Josef Cvačka[1,2]

[1]*Institute of Organic Chemistry and Biochemistry of the Czech Academy of Sciences, Prague 6, Czech Republic, Vrkoslav@uochb.cas.cz*

[2]*Department of Analytical Chemistry, Faculty of Science, Charles University in Prague, Prague 2, Czech Republic*

Summary

HPLC/APCI-MS analysis at microliters-per-minute flow rates was optimized for separation of fatty acid methyl esters (FAMEs). HPLC C18 column with an internal diameter of 0.3 mm and isocratic elution using 99.9 % acetonitrile and 0.1% formic acid were employed. Standard APCI ion source was suitable for detection of FAMEs at 10 µl/min flow rate with the detection limit of micrograms-per-milliliter. APCI-MS spectra with predominant $[M + H]^+$ molecular adducts were observed. The main advantage of micro-flow measurements is the possibility of using a temperature gradient, which significantly reduces retention times of FAMEs with longer aliphatic chain. The significant reduction of solvent consumption is also an important economic and environmental advantage. The positions of double bonds in FAME chains were established using acetonitrile-related adducts and tandem mass spectrometry. The optimized method was applied for analysis of FAMEs in triacylglycerol fraction of black currant seeds oil.

Introduction

Fatty acid methyl esters (FAMEs) are mostly analyzed by gas chromatography with flame ionization or mass spectrometry detection. The HPLC method offers double bond localization or analysis of very long chain FAMEs [1-4]. In this work, HPLC was scaled down to take advantages of miniaturized separation systems like the low sample and solvent consumption, higher sensitivity, and column temperature programming. Temperature-programmed HPLC can be easier used with narrow columns at low flow rates because the thermal capacity of the solvent and the wide diameter of the normal bore columns do not allow fast equilibration of separation temperature without a special equipment [5, 6]. The temperature acts in a similar way as the gradient of the mobile phase composition. It brings many advantages including enhanced resolution, increased sensitivity or shorter retention times [5]. Atmospheric pressure chemical ionization - mass spectrometry (APCI-MS) has been used previously for detection of FAMEs [1, 2]. The conventional APCI ion sources are constructed for high flow rates, typically

0.1 - 3 ml/min and APCI detection of FAMEs at microliter-per-minute flow rates has not been demonstrated yet.

In this work, an isocratic HPLC/APCI-MS method for FAMEs originally developed for the conventional column and 0.7 ml/min mobile phase flow [2] was optimized for capillary column operated at 10 µl/min flow rate of the mobile phase. The column temperature gradient was used to improve chromatographic separation. To the best of our knowledge, this is the first demonstration of HPLC/APCI-MS of lipids at very low flow rate realized using a standard, commercial APCI source.

Experimental

The micro HPLC system was assembled from dual sample size internal volume injector VICI CI4W.06 (VICI AG International), Teledyne ISCO M65 manual valve gradient pump, Zorbax SB-C18 HPLC column (0.3 mm × 150 mm, 3.5mm; Agilent), column thermostat of Accela autosampler (Thermo Fisher Scientific), and LCQ Fleet mass spectrometer (Thermo Fisher Scientific). The separation was performed isocratically using acetonitrile with 0.1 % of formic acid. The 37 Component FAME Mix (Supelco) was used for optimization of chromatography. LCQ Fleet mass spectrometer was equipped with standard APCI source set as follows: The capillary temperature 300 °C, the capillary voltage 25.5 V, tube lens voltages 80 V, vaporizer temperature 180 °C, sheath gas flow rate 40 arbitrary units, auxiliary gases 5 arbitrary units. The temperature program was realized by the abrupt change of the temperature from 5 °C to 50 °C in the 6th min of the HPLC run. The temperature slowly increased and the final value (50 °C) was reached at 13 min. The detection limits were calculated from calibration curves as a signal corresponding S/N=3. The calibration curve was constructed for methyl linoleate measured in selected reaction monitoring mode (SRM). The molecular adduct $[M + H]^+$ at m/z 295 was fragmented by the normalization collision energy of 30% and the signal intensity of the most intense fragment m/z 263 was recorded. Collision induct dissociation (CID) spectra of $[M + C_3H_5N]^{+\bullet}$ were used for double bond localization [2,7]. Black currant seeds oil FAMEs were obtained from triacylglycerols according to the workflow published previously [8].

Results and Discussion

The micro-HPLC/APCI-MS method was based on an isocratic method published earlier [2]. A standard APCI ion source was operated at the flow rate of 10 µl/min and the vaporizer temperature of 180 °C. The temperature was substantially lower than the values typically used for APCI (above 300 °C). The reason was to prevent evaporation of the mobile phase already in the fused silica capillary of the nebulizer and thus prevent the formation of gas bubbles causing excessive baseline noise. Narrow and symmetric peaks with good retention time reproducibility were achieved at 25 °C using acetonitrile with 0.1 % formic acid as a mobile phase (Figure 1a). The elution order was found to depend on the number of carbons and double bonds in aliphatic chain of the analytes. As expected, the retention times increased with the number of carbon atoms and decreased with the number of double bond. APCI-MS spectra showed mostly $[M + H]^+$ molecular adducts. To achieve chromatographic resolution of isobaric

FAMEs, the separation was run at 5 °C. Such a low column temperature made it possible to separate *cis/trans* isomers almost to baseline. Unfortunately, the retention times significantly increased, which caused peak broadening and poor signal to noise ratios (S/N) for some FAMEs (Figure 1b). The capillary column offered us to use temperature-programed chromatography. The total analysis time of unsaturated FAMEs was shortened from 30 min to 13 min, and the S/N significantly increased (Figure 1c). FAME 18:2n-6 gave detection limit of 3.02 µg/ml. The analysis of an equimolar mixture of FAMEs with 18 carbon atoms and up to 3 double bonds revealed almost the same response factor of unsaturated C18 FAMEs. Saturated FAME 18:0 provided about $5 \times$ lower intensity of $[M+H]^+$ than unsaturated species with the same chain length. Nevertheless, saturated FAMEs showed abundant acetonitrile adduct $[M + 40]^+$, which can be used for their sensitive detection.
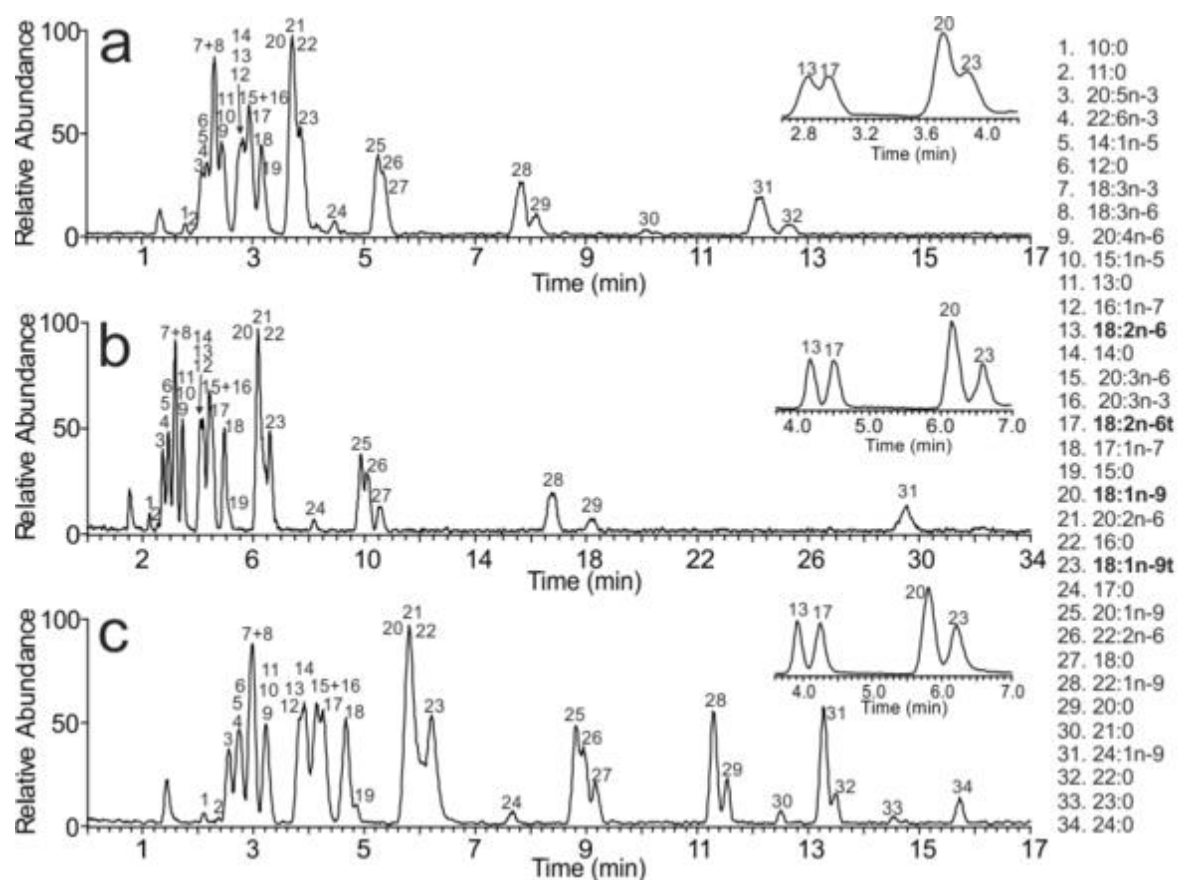

Figure. 1 Micro-HPLC/APCI-MS base peak chromatograms of 37 Component FAME Mix (Supelco) obtained at the column temperature set to a) 25°C, b) 5°C and c) at temperature program 0.00 -6.00 min, 5°C; 6.01-40.00 min, 50°C; isomers with all-*trans* double bonds are marked with "t", unmarked isomers are *cis*.

The optimized method was applied to FAMEs from black currant seeds oil. Mostly unsaturated fatty acids with sixteen, eighteen and twenty carbons were identified based on their molecular adducts $[M + H]^+$ (Figure 2a). Their retention times were consistent with the retention times of standards in Supelco 37 FAMEs mix. The double bond positional isomers could not be determined from full scan MS data (Figure 2b). Therefore, the double bond positions were

established using CID of $[M + C_3H_5N]^{+\bullet}$ [2]. Based on the abundant diagnostic fragments α and ω, we were able to identify coeluted isomers 18:3n-6 and 18:3n-3 (Figure 2c). In addition, FAMEs 18:4n-3, 18:3n-6, 18:3n-3, 18:2n-6, 18:1n-9, 16:0, 20:1n-9 and 18:0 were identified in the sample, which is in accordance with literature [8].
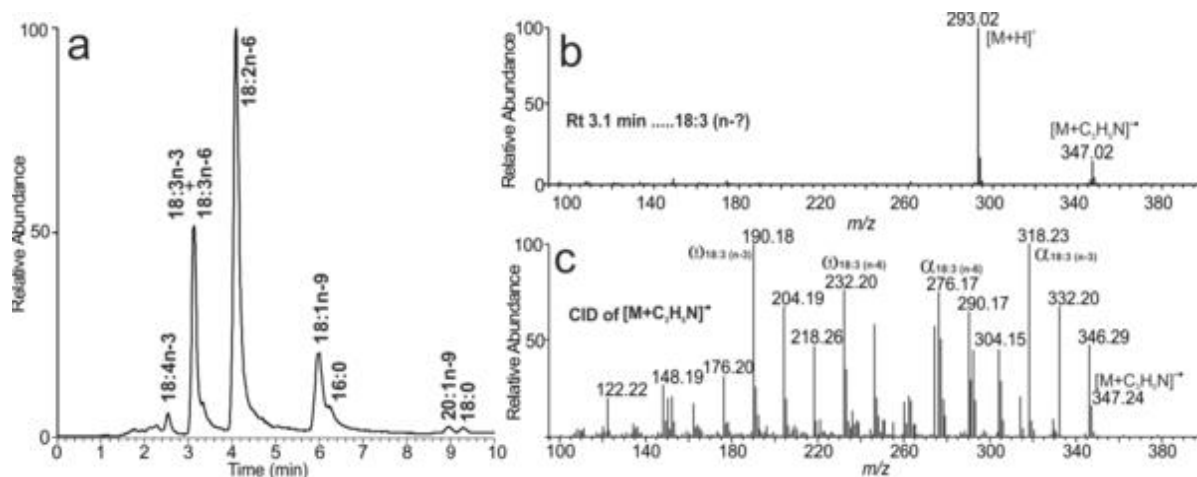

Figure 2. a) Micro-HPLC/APCI-MS basepeak chromatogram of FAMEs from triacylglycerol fraction of black currant oil. b) MS spectrum of the peak at tR = 3.1 min. c) MS/MS spectrum of molecular adduct $[M + C_3H_5N]^{+\bullet}$ of peak at t_R = 3.1 min.

Conclusion

Temperature programmed micro-HPLC with APCI-MS detection was found to be a powerful technique for analyzing FAMEs. The method is faster and more sensitive when compared to the method without temperature programming. APCI-MS with commercial high-flow source can be used at the flow rate of 10 μl/min with the detection limit of unsaturated FAMEs in units of μg/ml.

Acknowledgement

Reference

[1] Rezanka, T., Biochem. Syst. Ecol. 2000, 28, 847-856.

[2] Vrkoslav, V., Cvacka, J., J. Chromatogr. A 2012, 1259, 244-250.

[3] Sehat, N., Rickert, R., Mossoba, M. M., Kramer, J. K. G., Yurawecz, M. P., Roach, J. A. G., Adlof, R. O., Morehouse, K. M., Fritsche, J., Eulitz, K. D., Steinhart, H., Ku, Y., Lipids 1999, 34, 407-413.

[4] Nikolovadamyanova, B., Herslof, B. G., Christie, W. W, J. Chromatogr. 1992, 609, 133-140.

[5] Vanhoenacker, G., Sandra, P., Anal. Bioanal. Chem. 2008, 390, 245-248.

[6] Teutenberg, T., Anal. Chim. Acta 2009, 643, 1-12.

[7] Vrkoslav, V., Hakova, M., Peckova, K., Urbanova, K., Cvacka, J.,. Anal. Chem. 2011, 83, 2978-2986.

[8] Vacek, M., Zarevucka, M., Wimmer, Z., Stransky, K., Koutek, B., Mackova, M., Demnerova, K., Enzyme Microb. Technol. 2000, 27, 531-536.

P59   GREEN-SYNTHESIZED SILVER NANOPARTICLES AND FOOD PROTECTION

Bozena Hosnedlova[1], Michaela Docekalova[2], Branislav Ruttkay-Nedecky[3], Mojmir Baron[1], Rene Kizek[2,3], Carlos Fernandez[4], <u>Jiri Sochor</u>[1]

[1]*Mendel University in Brno, Faculty of Horticulture, Department of Viticulture and Enology, Lednice, Czech Republic*

[2]*Department of Research and Development, Prevention Medicals, s.r.o., Butovice, Studénka, Czech Republic*

[3]*University of Veterinary and Pharmaceutical Sciences Brno, Pharmaceutical Faculty, Brno, Czech Republic*

[4]*Robert Gordon University, School of Pharmacy and Life Sciences, Aberdeen, United Kingdom*

Introduction

Nanotechnology is used in many fields. In food science, it can be practically applied in all areas, including agriculture, food processing, security, packaging, nutrition, and neutraceuticals [1] (Figure 1).

Nanotechnology can improve the quality of food products - their palatability, nutritional value, health aspects, but also can create completely new foods, new food packaging and storage methods [1]. Given the growing consumer demand for the longer shelf life of fresh food and the need to protect food from food-borne diseases, the development of antimicrobial food packaging has been necessary. One of the highly efficient methods is the use of embedded metal nanoparticles. Especially silver nanoparticles (AgNPs) or nanosilver evince antimicrobial, antiviral, antifungal, and anti-yeasts activities and can be combined with both non-degradable and edible polymers for active food packaging [2]. In addition to improving the taste of the food, nanotechnological processes can also be applied to improve food structure, reduce fat content or encapsulate nutrients such as vitamins, thereby minimizing product degradability during long-term storage [3].

Traditionally AgNPs were prepared only by physical and chemical methods [4]. However, chemical synthesis often results in toxic effects induced by the rest of chemicals on the surface of nanoparticles, which significantly limits use for medical and food purposes [4,5]. This problem could be eliminated when using nanoparticle biosynthesis through green synthesis [4,6], creating the NPs more biocompatible [7].

Green synthesis represents cheaper routes for nanoparticles synthesis, and it includes use of microbial enzymes and plant extracts. Green synthesis is more cost-effective than chemical and

physical methods, environment friendly, easily scaled up for large scale synthesis and in this method there is no need to use high pressure, energy, temperature and toxic chemicals [8].

Jose-Yacaman et al. [9] first reported the formation of AgNPs by living plants. Very recently green AgNPs have been synthesized using various natural products like green tea (Camellia sinensis) [10], neem (Azadirachta indica) leaf broth [11], natural rubber [12], starch [13], aloe vera plant extract [14] etc.

The techniques of green synthesis include polysaccharide method, Tollens method, irradiation method, biological method, and polyoxometalates method [15].
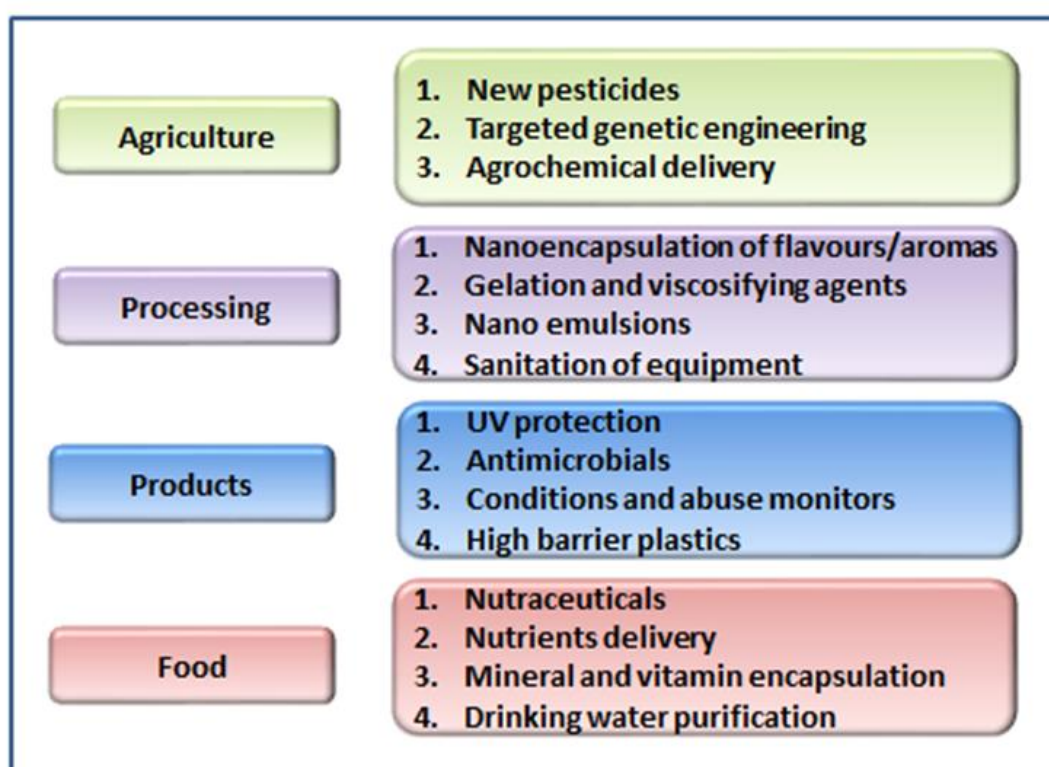

Figure 1 The use of nanotechnology in food science. Adapted from [1].

Conclusion

AgNPs produced by green synthesis offer many advantages over those produced chemically, especially due to the absence of chemicals used in their preparation, and they can be used in food processing as well as antimicrobial food packaging materials.

Acknowledgement

Reference

[1] Chung I-M, Rajakumar G, Gomathi T, Park S-K, Kim S-H, Thiruvengadam M. Nanotechnology for human food: advances and perspective. Frontiers in Life Science. 2017;10(1):63-72.

[2] Carbone M, Donia DT, Sabbatella G, Antiochia R. Silver nanoparticles in polymeric matrices for fresh food packaging. Journal of King Saud University-Science. 2016;28(4):273-279.

[3] Sekhon BS. Food nanotechnology–an overview. Nanotechnology, science and applications. 2010;3:1.

[4] Ramya M, Subapriya MS. Green synthesis of silver nanoparticles. Int J Pharm Med Biol Sci. 2012;1(1):54-61.

[5] Parashar UK, Saxena PS, Srivastava A. Bioinspired synthesis of silver nanoparticles. Digest Journal of Nanomaterials & Biostructures (DJNB). 2009;4(1).

[6] Begum NA, Mondal S, Basu S, Laskar RA, Mandal D. Biogenic synthesis of Au and Ag nanoparticles using aqueous solutions of Black Tea leaf extracts. Colloids and surfaces B: Biointerfaces. 2009;71(1):113-118.

[7] Bar H, Bhui DK, Sahoo GP, Sarkar P, De SP, Misra A. Green synthesis of silver nanoparticles using latex of Jatropha curcas. Colloids and surfaces A: Physicochemical and engineering aspects. 2009;339(1-3):134-139.

[8] Forough M, FAHADI K. Biological and green synthesis of silver nanoparticles. Turkish journal of engineering and environmental sciences. 2011;34(4):281-287.

[9] Gardea-Torresdey JL, Gomez E, Peralta-Videa JR, Parsons JG, Troiani H, Jose-Yacaman M. Alfalfa sprouts: a natural source for the synthesis of silver nanoparticles. Langmuir. 2003;19(4):1357-1361.

[10] Vilchis-Nestor AR, Sánchez-Mendieta V, Camacho-López MA, Gómez-Espinosa RM, Camacho-López MA, Arenas-Alatorre JA. Solventless synthesis and optical properties of Au and Ag nanoparticles using Camellia sinensis extract. Materials Letters. 2008;62(17-18):3103-3105.

[11] Shankar SS, Rai A, Ahmad A, Sastry M. Rapid synthesis of Au, Ag, and bimetallic Au core–Ag shell nanoparticles using Neem (Azadirachta indica) leaf broth. Journal of colloid and interface science. 2004;275(2):496-502.

[12] Bakar NA, Ismail J, Bakar MA. Synthesis and characterization of silver nanoparticles in natural rubber. Materials Chemistry and Physics. 2007;104(2-3):276-283.

[13] Vigneshwaran N, Nachane R, Balasubramanya R, Varadarajan P. A novel one-pot 'green'synthesis of stable silver nanoparticles using soluble starch. Carbohydrate research. 2006;341(12):2012-2018.

[14] Chandran SP, Chaudhary M, Pasricha R, Ahmad A, Sastry M. Synthesis of gold nanotriangles and silver nanoparticles using Aloevera plant extract. Biotechnology progress. 2006;22(2):577-583.

[15] Sharma VK, Yngard RA, Lin Y. Silver nanoparticles: green synthesis and their antimicrobial activities. Advances in colloid and interface science. 2009;145(1-2):83-96.

P60 LEAD DETERMINATION IN DRIED BLOOD SPOTS USING DLTV ICP MS

Martin Ďurč[1], Marek Stiborek[1,2], Viktor Kanický[1,2], Jan Preisler[1,2]

[1]*Department of Chemistry, Masaryk University, Brno, Czech Republic,*
451045@mail.muni.cz

[2]*CEITEC– Central European Institute of Technology, Masaryk University, Brno, Czech Republic*

Summary

This paper deals with the use of the technique of diode laser thermal vaporization inductively coupled plasma mass spectrometry (DLTV ICP MS) and its compatibility with the dried blood spot (DBS) sampling method. Blood samples were applied to a special DBS card or office paper, which played a role of a DLTV substrate. DBS card offers a limited space, therefore the minimum number of blood samples required for determination of lead in the blood was investigated. This was achieved by reducing the number of standard additions and its repetitions with regard to the precise and accurate determination. To increase precision of determination the effect of internal standard ^{209}Bi was also examined.

Introduction

Lead toxicity

Lead is still one of the most used toxic heavy metals, so monitoring its amount is important in the human population. Most lead in a body is found in the blood, namely 95 to 98 % of lead in the human body is found in erythrocytes. Physiological lead concentration in blood is ~ 10-50 μg L^{-1} for children and females and 30-70 μg L^{-1} for men and old people in the Czech Republic. But even concentrations below 100 μg L^{-1} may have a negative impact on human organisms [1]. Depending on the concentration of this substance in the blood, poisoning may occur - leading to anemia, encephalitis, and even death [2].

DLTV

The ink printed on the substrate plays an important role when introducing the sample into ICP MS. Conventional black ink from the printer absorbs light at a wavelength 808 nm of the applied laser. Absorbed energy causes pyrolysis of the substrate and aerosol formation. During the vaporization of the sample, the burning does not occur due to the atmosphere of the inert carrier gas present. The aerosol is removed from the ablation cell and transported using He carrier gas into mass spectrometer [3].
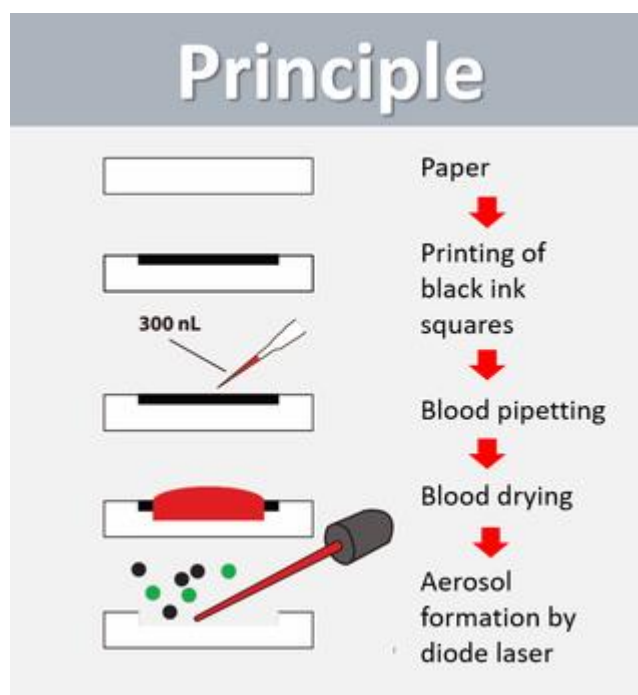
Fig.1 Principle of DLTV

Experimental

The first step consists of printing the black ink squares on the surface of substrate (office paper or DBS sample card). Secondly, the standard additions of lead with final concentrations of 50, 100, 500 µg L^{-1} and an internal standard of ^{209}Bi (200 µg L^{-1}) were added to a blood sample to reduce matrix effects and to improve accuracy and precision of the analysis. Next step, pipetting of blood as well as lead standards, is a critical step in the preparation of samples. The depositing of the samples had to be very precise and repeatable. After the samples were prepared, they were introduced into inductively coupled plasma mass spectrometer (ICP MS) using an ablation system equipped with a DLTV apparatus under optimized conditions.

Results and Discussion

During the method optimization, we concluded that the most intensive signals are achieved by complete vaporization of the ink and only partial vaporization of the substrate. The substrate used in DBS sample card is designed to absorb as large sample volume as possible. This means that ink and sample soak into DBS sample card which prevents efficient vaporization of the sample and lowers signal intensities. Therefore, the use of regular office paper is advantageous. In this case, the ink and sample do not soak into the paper but remain mostly on its surface leading to vaporization of both ink and sample.

Finally, we found out that even one standard addition (50 or 100 µg L^{-1}) is sufficient for accurate determination of lead in whole human blood (RSD under 10 %). However, we suggest using two internal additions and thus reduce requirements on a pipetting precision compared to using a single standard addition.

Conclusion

Experiments have shown that accurate and precise determination of lead in blood is possible with a single addition of lead standard (50 or 100 µg L^{-1}) in three replicates which overcomes matrix effects. Simple sample preparation and determination accuracy (RSD up to 10 %) has confirmed possible use in practice. However, it was found that bismuth is not a suitable internal standard was and a special DBS sampling card is not compatible with the DLTV method.

Acknowledgement

Reference

[1]   P. Foltynova, V. Kanicky and J. Preisler, Analytical Chemistry, 2012, 84, 2268- 2274.

[2]   A. A. Moncrieff, G. E. Roberts, A. D. Patrick, O. P. Koumides, A. G. C. Renwick and B. E. Clayton, Archives of Disease in Childhood, 1964, 39, 1-8.

[3]   M. Ďurč, Bachelor Thesis, Masaryk University, 2018.

P61　DETECTION OF MONOCLONAL FREE LIGHT CHAINS (FLC) BY VARIOUS LABORATORY METHODS

Pavlína Kušnierová[1,2], David Zeman[1,2], Kamila Revendová[3], Ondřej Dlouhý[4]

[1] *Department of Biomedical Sciences, Faculty of Medicine, University of Ostrava, Ostrava, Czech Republic, pavlina.kusnierova@fno.cz*

[2] *Institute of Laboratory Diagnostics, University Hospital Ostrava, Ostrava, Czech Republic*

[3] *Faculty of Medicine, University of Ostrava, Ostrava, Czech Republic*

[4] *Department of Physics, Faculty of Natural Sciences, University of Ostrava, Ostrava, Czech Republic*

Summary

Background and Aims. The aim of the study is determination of free light chains in patients with abnormal kappa free/lambda free ratio (FLC ratio) by various quantitative methods and assessment of characteristic of small abnormal protein bands (monoclonal bands or oligoclonal bands) by immunofixation electrophoresis (IMF) and isoelectric focusing followed by affinity immunoblotting (IEF/AIB).

Methods. 20 serum samples were examined. Serum FLC levels were determined using an immunoturbidimetry and an enzyme-linked immunosorbent assay, the monoclonal or oligoclonal bands of free light chains were examined by immunofixation electrophoresis and isoelectric focusing followed by affinity immunoblotting.

Results. No statistically significant correlation was found between the individual FLC ratios using the Passing-Bablok regression. A statistically significant dependence was found between FLC ratio Sebia and FLC ratio SPA using the nonparametric Spearman's correlation coefficient ($rs = 0.666$, $p = 0.001$). Kappa statistic evaluated a moderate conformity between the FLC ratio Sebia and immunofixation electrophoresis (kappa = 0.468), no conformity between FLC ratio SPA and FLC ratio Sebia (kappa = 0.000).

Conclusion. The Binding Site diagnostic kit provides false positives of FLC ratios. It will be necessary to revise the reference limits for the respective free light chains and the FLC ratio on a larger set of data.

Introduction

The current classification of monoclonal gammopathies (MG) defines the monoclonal gammapathy of free light chain with an abnormal FLC ratio (99% reference interval 0.26-1.65)

at increased concentration of the relevant FLC type. In our previous studies involving neurological patients without other signs indicative of MG, the abnormal FLC ratio was found in approximately 11.7%, but only in one case it was associated with the finding of monoclonal FLC by IEF/AIB detection [1,2].

We believe that the reference intervals for FLC and especially for the FLC ratio need to be revised. We also assume that the current MG classification of free light chains leads to a significant percentage of false positives and needs to be clarified. In case of confirmation of our hypothesis in a prospective study, we will propose the introduction of IEF/AIB as a "decision" method in case of a negative finding of immunofixation electrophoresis in routine practice.

Experimental

The study have been approved by the Ostrava University Hospital Ethics Committee (reference number 13/2018). In the initial phase of this study we examined 20 serum samples. FLCs were measured by immunoturbidimetry assay on SPAPLUS with Freelite Kappa SPAPLUS kit and Freelite Lambda SPAPLUS kit (FLC SPA), (Cat. No. LK016.L.S and LK018.L.S, respectively, The Binding Site Ltd., Birmingham, UK), by enzyme-linked immunosorbent assay (ELISA) using the Sebia FLC kappa and the Sebia FLC lambda kit (FLC Sebia), (Cat. No. 5100, 5101, respectively, BioVendor-Laboratorni medicina a.s., Brno, Czech Republic) and by in-house ELISA method using polyclonal anti-free light chain antibodies and appropriately diluted Freelite Calibrators (FLC in-house), (Cat. No. A0100 and A0101, Dako, Glostrup, Denmark). To confirm monoclonality / oligoclonality we used immunofixation electrophoresis on Hydrasys 2SCAN Focusing with Hydragel 4 IF (Cat. No. 4304, BioVendor-Laboratorni medicina a.s., Brno, Czech Republic) and isoelectric focusing (IEF) in 1.2% agarose gels containing 12% sorbitol (interelectrode distance 8.5 cm, limits 200 V/cm, 100 mA, 10 W) on Multiphor II apparatus (GE Healthcare UK Ltd., Buckinghamshire, England) at 10°C for 1,200 Vh. Statistical evaluation of results was performed using MedCalc software vision 11.4 (Frank Schoonjans, Belgium).

Results and Discussion

No statistically significant correlation was found between the individual FLC ratios. The regresion relationship between these parameters was evaluated using Passing-Bablok regression, Figure 1.

Furthermore, the correlation between the individual FLC ratios was evaluated using the nonparametric Spearman's correlation coefficient. A statistically significant dependence was found between FLC ratio Sebia and FLC ratio SPA ($rs = 0.666$, $p = 0.001$), Table 1.

Kappa statistic was used to compare methods based on clinical interpretation because the methods have the different reference intervals, Table 2. No conformity was demonstrated between FLC ratio SPA and FLC ratio Sebia (kappa = 0.000). The comparison of these

qualitative results (positive / negative ratios) with the interpretation of immunofixation assay (presence / absence of monoclonal immunoglobulin) showed the moderate conformity between the FLC ratio Sebia and immunofixation electrophoresis (kappa = 0.468), Table 2.
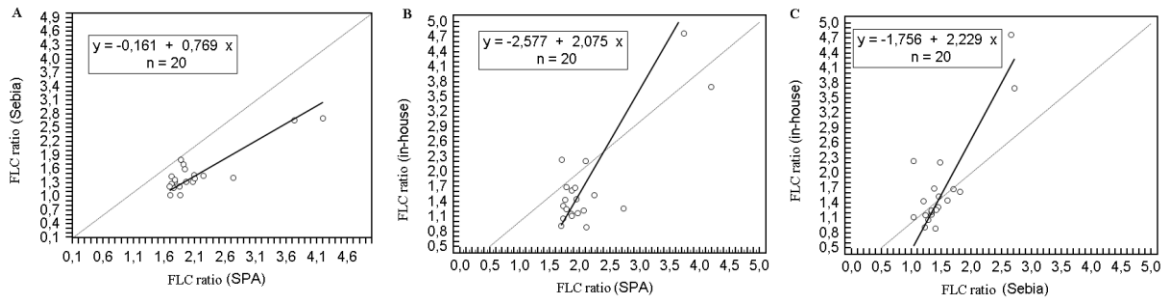

Figure 1. Correlation analysis between FLC ratio (SPA) and FLC ratio (Sebia) (A), FLC ratio (SPA) and FLC ratio (in-house) (B) and FLC ratio (Sebia) and FLC ratio (in-house) (C).

Table 1. The distribution of the correlations between the FLC ratios using the different diagnostic kits.

Methods		FLC ratio (in-house)	FLC ratio (SPA)	FLC ratio (SEBIA)
FLC ratio (in-house)	r_s		0.296	0.567
	P		0.205	0.009
FLC ratio (SPA)	r_s	0.296		0.666
	P	0.205		0.001
FLC ratio (SEBIA)	r_s	0.567	0.666	
	P	0.009	0.001	

r_s... Spearman rank correlation coefficient

Table 2. Comparison of methods based on the conformity of clinical interpretation using Kappa statistics.

	FLC ratio (SPA) vs. FLC ratio (SEBIA)	FLC ratio (Sebia) vs IMF	FLC ratio (Sebia) vs. IEF/AIB (FLC kappa)
Kappa statistics	0.000	0.468	0.286
95% CI	-	0.071 – 0.865	-0.049 – 0.620
Standard error	0.000	0.203	0.171

Conclusion

The Binding Site diagnostic kit provides false-positive results for FLC ratios thus influencing the suspicion of the monoclonal free light chain as opposed to the Sebia diagnostic kit. Immunofixation electrophoresis and isoelectric focusing followed by affinity immunoblotting have rebutted suspicion of FLC monoclonality. In the future, it will be necessary to revise the reference limits for the respective free light chains and the FLC ratio on a larger set of data.

Acknowledgement

Reference

[1] Rajkumar, S.V., Dimopoulos, M.A., Palumbo, A. et al. Lancet Oncol. 2014, 15, 538-548.
[2] Willrich, M.A.V., Murray, D.L., Kyle, R.A. Clin Biochem. 2018, 5 1, 38-47.

Sponsors

Waters

THE SCIENCE OF WHAT'S POSSIBLE.®

TESCAN

PERFORMANCE IN NANOSPACE

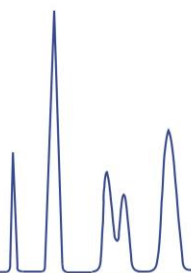pragolab

thermo
scientific

Authorized Distributor

VILLA LABECO, s.r.o.
Chrapčiakova 1, 052 01 SPIŠSKÁ NOVÁ VES, SLOVAKIA
tel.: 00421 53 44 260 32   fax : 00421 53 4298359
email: info@villalabeco.sk,   www.villalabeco.sk

CHEMAGAZÍN

MŠMT V4-Korea 8F17003